A HOLOCENE SAND BUDGET FOR THE SEASONALLY WET TROPICS REGION OF NORTH QUEENSLAND

Thesis submitted by

Ramona Imelda DALLA POZZA BAppSc (Hons) JCU

in December 2005

for the Degree of Doctor of Philosophy
in the School of Tropical Environment Studies and Geography
James Cook University

ELECTRONIC COPY

I, the undersigned, the author of this work, declare that the electronic copy of this thesis provided to the James Cook University Library, is an accurate copy of the print thesis submitted, within the limits of the technology available.

Signature   Date

STATEMENT OF ACCESS

I, the undersigned, the author of this thesis, understand that James Cook University will make this thesis available for use within the University Library and, via the Australian Digital Theses network, for use elsewhere.

I understand that, as an unpublished work, a thesis has significant protection under the Copyright Act and;

I do not wish to place any further restriction on access to this work.

R.I. Dalla Pozza

Date

STATEMENT ON SOURCES

DECLARATION

I declare that this thesis is my own work and has not been submitted in any form for another degree or diploma at any university or other institution of tertiary education. Information derived from the published or unpublished work of others has been acknowledged in the text and a list of references is given.

__________________________ ____________________
R.I. Dalla Pozza Date

ABSTRACT

The discharge of coastal streams between Bowen and Rollingstone, north Queensland is highly seasonal with ~90% of the total annual discharge typically occurring between December and April. This section of the Queensland coast is referred to as the Seasonally Wet Tropics. In this thesis the abbreviation SWT will be used to refer to the Seasonally Wet Tropics region and seasonally wet tropical systems. Most of the shorelines along this coast are dominated by sand. Previous literature suggests that seasonally wet tropics streams deliver large quantities of sand to the coast. However, little is known regarding the timeframes, pathways and dominant processes of sand delivery. A Holocene sand budget was developed for the SWT coastal zone from the studies of three SWT coastal systems: i) the Haughton River Estuary (Lat. -19.416, Long.147.126); ii) the Elliot River Estuary (Lat.-19.880, Long. 147.885) and iii) the Black River Delta (Lat. 146.651, Long. -19.178). These systems are typical examples of tropical, variable discharge rivers responding to the marked intra and inter-annual variability of the SWT weather and climate. This region is meso tidal and subject to relatively low-energy ambient wave conditions.

Conceptual models of the spatial and temporal patterns of coastal sand transfer for the Haughton and Elliot River Estuaries and the Black River Delta were developed based on historic, sedimentological, stratigraphic and hydrodynamic data. Three different sand transfer processes were observed in each system. The lack of coarse, poorly-sorted, angular sediments within the Haughton River Estuary suggests that the relative proportion of fluvial sediment supplied from the Haughton River is minor compared to the influx of marine sediment via tidal currents. Therefore, the Haughton River Estuary is tide-dominated and a sink for marine sediment. Relatively strong wave and tidal energy dominate sand transfer processes in the Elliot River Estuary, with little evidence to suggest that the Elliot River is contributing significant amounts of fluvial sand to the coast. In contrast, deposits of coarse poorly sorted sediments identified at the mouth of the Black River Delta suggested that the modern Black River exports some fluvial sand to coast, which is transported northwards by relatively strong wave energy and wave generated currents.

To interpret these findings within an evolutionary context, current estimates of fluvial sand delivery reported in the literature were extrapolated over the last 7 ka and compared with Holocene sand stored in onshore coastal deposits, nearshore and on the inner shelf. The results of the Holocene sand budget suggest an apparent deficit of ~6.5×10^8 m^3 of sand (including loss to the system via longshore drift) suggesting that seasonally wet tropics streams have not been delivering predicted volumes of sand to the coast for at least the last 1.6 ka. It is concluded that the sand derived landforms that dominate the seasonally wet tropics coast are the result of multi-cyclic processes – initiated by the landward movement of marine sand during the Holocene transgression.

ACKNOWLEDGEMENTS

Thanks are due to many people for their support and encouragement during the completion of this thesis. Firstly, my biggest thanks must be reserved for my supervisor Dr. Scott Smithers for his guidance, detailed and timely feedback, assistance in the field, perseverance and friendship. I am similarly indebted to Professor David Hopley for his invaluable advice, guidance and never failing encouragement. I am grateful to Dr Mark Mabin for his supervision and guidance in the early stages of the project. I wish to thank all staff and students at the School of Tropical Environment Studies and Geography, James Cook University who helped out along the way, especially Dr. Jonathon Luly for his assistance in the field and Associate Professor Kevin Parnell for his advice. Thank you Adella Edwards for your advice, assistance and patience in all matters cartographic, Clive Grant and Rob Scott for technical support and Jody Kreuger for assistance in the field. Many thanks must go to fellow students William Wilson, Veronica Sculac and Donna Cannon for their assistance and enthusiasm in the field.

I am grateful to the Australian Research Council, Sinclair Knight Merz and the School of Tropical Environment Studies and Geography, James Cook University for funding this project. I would particularly like to thank Dr Brett Kettle for his role in initiating the project and Dr. Frank Hoedt and James Monkavitch from Sinclair Knight Merz for fieldwork assistance. I would like to thank Peter Gibson, David Savage, Paul Prensler and Jim Waldron from the Department of Environment and Heritage and Ian Boyce, Geoff Pocock and John Mackay and Rochelle from the Department of Natural Resources and Mines for providing data and assistance.

I would like thank my fellow PhD students for their support and friendship, especially Dr. Elizabeth Dinsdale, Dr. Anna Lasko, Nadine Marshall, Ameer Abdulla and Dr. Penny Davidson.

Finally, I would like to thank my parents, sisters and brother-in-laws for their endless words of encouragement and helping me keep it all in perspective. I owe my deepest gratitude to my husband, Brendon, without his understanding, support and encouragement none of this would have been possible.

TABLE OF CONTENTS

LIST OF FIGURES

LIST OF TABLES

CHAPTER 1 - INTRODUCTION

1.1 INTRODUCTION

Sand is an important building block of this part of the north Queensland coast, with eighty-one percent of the coast between Rollingstone and Bowen composed of sand. The coastal area between Rollingstone and Bowen is significant as it has distinct climatic and marine regimes compared to neighbouring areas of north Queensland. This area is referred to in this thesis as the Seasonally Wet Tropics, abbreviated as SWT. The SWT climate can also be referred to as type 'Aw' in Köppen's (1931 as cited in Davis, 1968) widely quoted classification, which is defined as a tropical wet and dry or savanna climate with a pronounced dry season (driest month having precipitation less than 60 mm). There are other regions in north Queensland with a similar SWT (Aw) climate for example the Gulf of Carpentaria and Cape York Peninsula (Figure 1.1). However, this study will focus on the SWT coastal zone in the vicinity of Townsville between Rollingstone and Bowen.

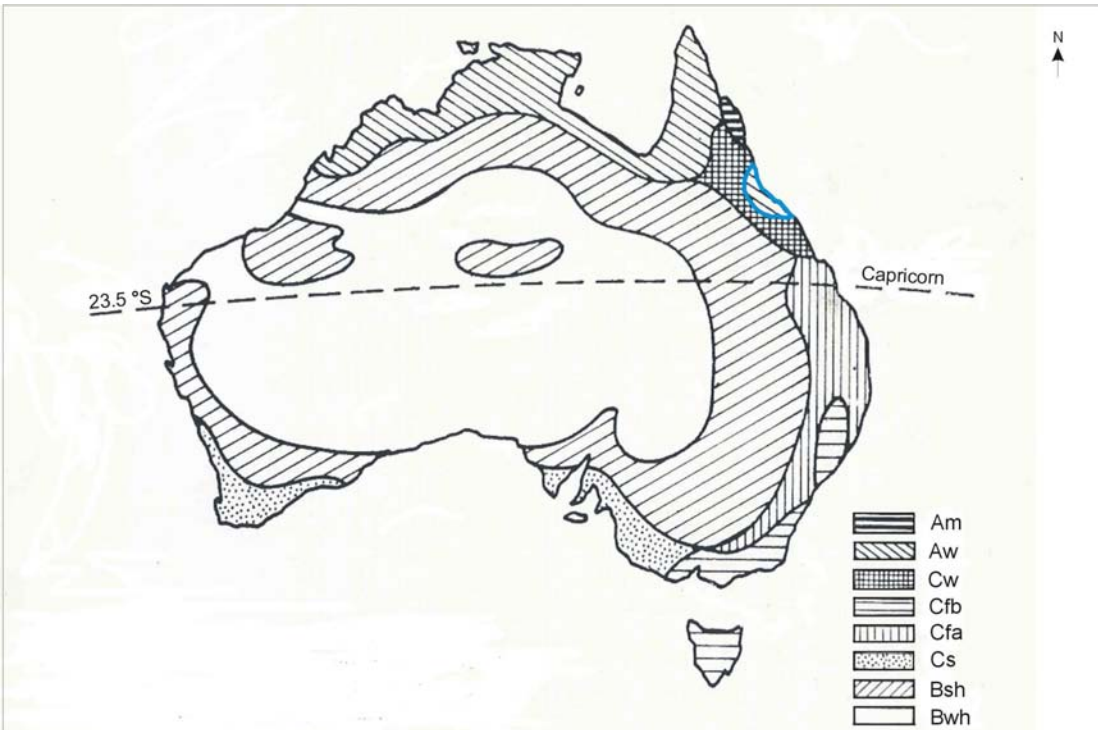

Figure 1.1 The SWT climate can also be referred to as type 'Aw' in Köppen's (1931 as cited in Davis, 1968: 230) classification of the Australian climate. The 'Aw' climate is defined as a tropical wet and dry savanna climate with a pronounced dry season (driest month having precipitation less than 60 mm). While there are other regions in north Queensland with a SWT or 'Aw' climate, this study will focus on the coastal zone in the vicinity of Townsville between Rollingstone and Bowen (indicated in blue on this map).

Early workers on the SWT coast between Rollingstone and Bowen inferred that most of the coastal sand deposits were supplied by streams draining coastal catchments (Hopley, 1970a; Holmes, 1992); classic climatic geomorphology predicts that catchments experiencing a SWT rainfall regime have amongst the highest sand yields in the world (Fournier, 1960). Thus given the localised high rates of soil erosion in SWT catchments due to variable high intensity rainfall (Yu, 1998); low vegetation cover (Neil and Yu, 1996b); relatively steep coastal rivers (~0.015) and a sand dominated coastline (~81%), it may be inferred that SWT streams supply sand to coast. This assumption is supported by extensive beach ridge plains on the SWT coast between Rollingstone and Bowen which indicate rapid coastal progradation, averaging 1 km every 1 ka since sea level stabilized at ~6 ka BP (Belperio, 1978). Also, recent empirical modelling results suggest that SWT streams are delivering even more sediment to the coast, an estimated four to fifteen times total sediment load (washload, suspended and bedload) due to post-European anthropogenic activities in catchments (GBRMPA, 2001). However, detailed studies of the Normanby River Estuary in the Cape York Peninsula, another SWT region of north Queensland, have found that rather then exporting an average of 100,000 m^3 of sand to the coast (Prosser *et al.*, 2001a), the Normanby is a net importer of marine sediment with fluvial sand being trapped in the lower estuary for at least the last 6 ka (Bryce *et al.*, 1998). In addition, widespread occurrences of exposed mangrove muds along the SWT coast indicate recent coastal retreat (Hopley, 1970a). This mismatch in the literature and current situation on the SWT coast between Rollingstone and Bowen prompts a detailed investigation of coastal sand transfer in this unique study area.

1.2 STUDY AREA

Climatic and geographic features of the SWT coast between Rollingstone and Bowen (see figure 1.2) distinguish this coastal sedimentary system from those in other parts of Australia and overseas, which dominate the literature. The region is too far south to be influenced by persistent summer monsoon systems and too far north to experience more reliable rainfall associated with surface temperate systems common to south-east Queensland (Lyons and Bonell, 1994). As a result rainfall in the SWT is extremely variable. Cyclones can produce intense falls within the region for example 305 mm fell in 2 hours on March 3, 1946 due to a cyclonic depression (Lyons and Bonell, 1994). Rainfall records from Giru, which is located within the Haughton River catchment and is considered to be representative of the SWT region between Rollingstone and Bowen, clearly illustrate the inter-annual variability of rainfall

(Figure 1.3). The mean annual rainfall is 1249 mm, standard deviation of 535 mm. The high standard deviation reflects the inter-annual variability of rainfall in the Haughton catchment. Recent monthly rainfall records from 2000 and 2001 illustrate the marked variation between years and the seasonality (Figure 1.4). Indeed, over 80% of the total yearly rainfall usually occurs between December and April. SWT streams can be described as 'extreme variable discharge rivers' which are defined as rivers where ~90% of the total annual flow occurs during the wet season usually between December and April (Fielding and Alexander, 1996).

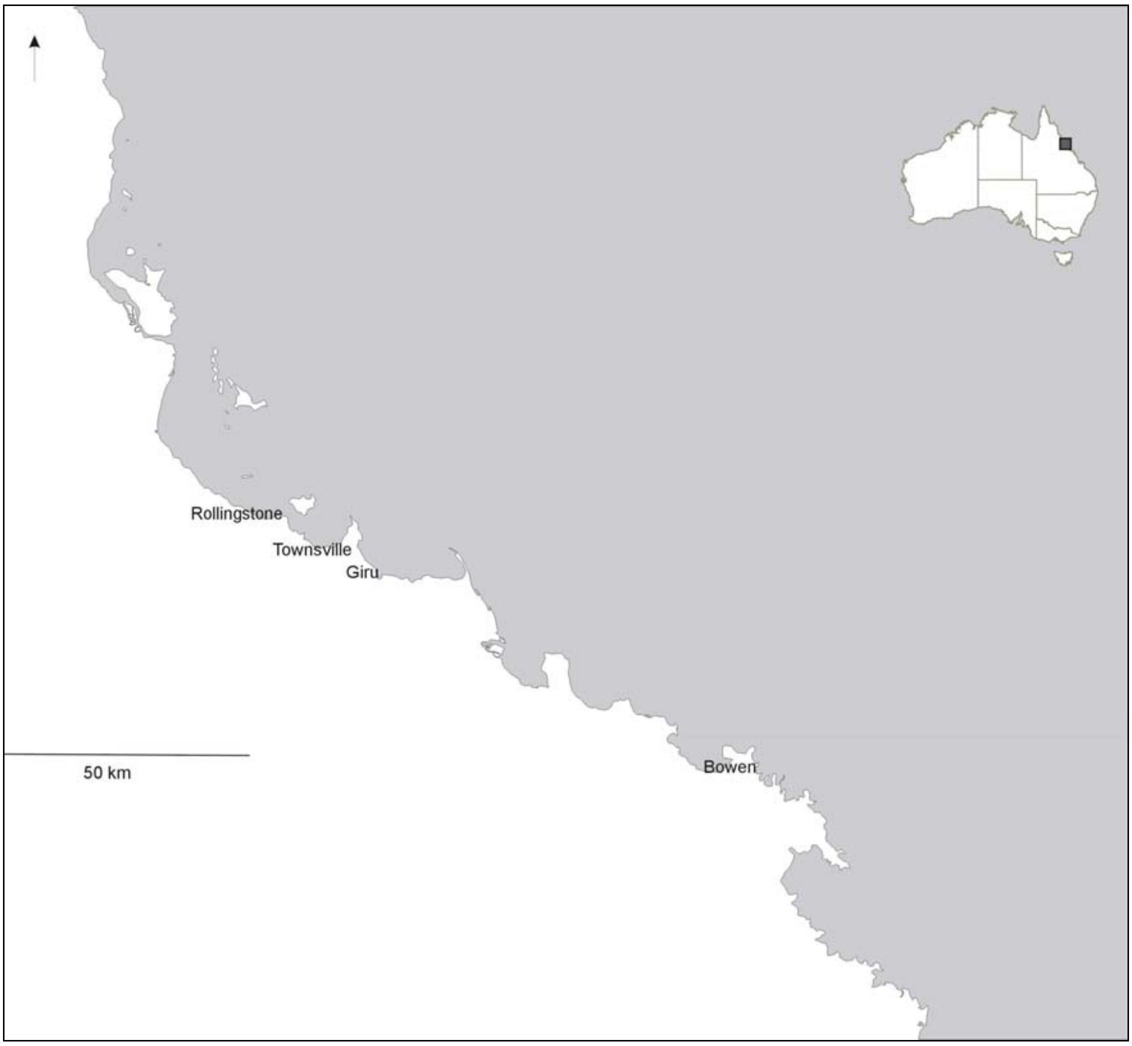

Figure 1.2. The seasonally wet tropics region of north Queensland.

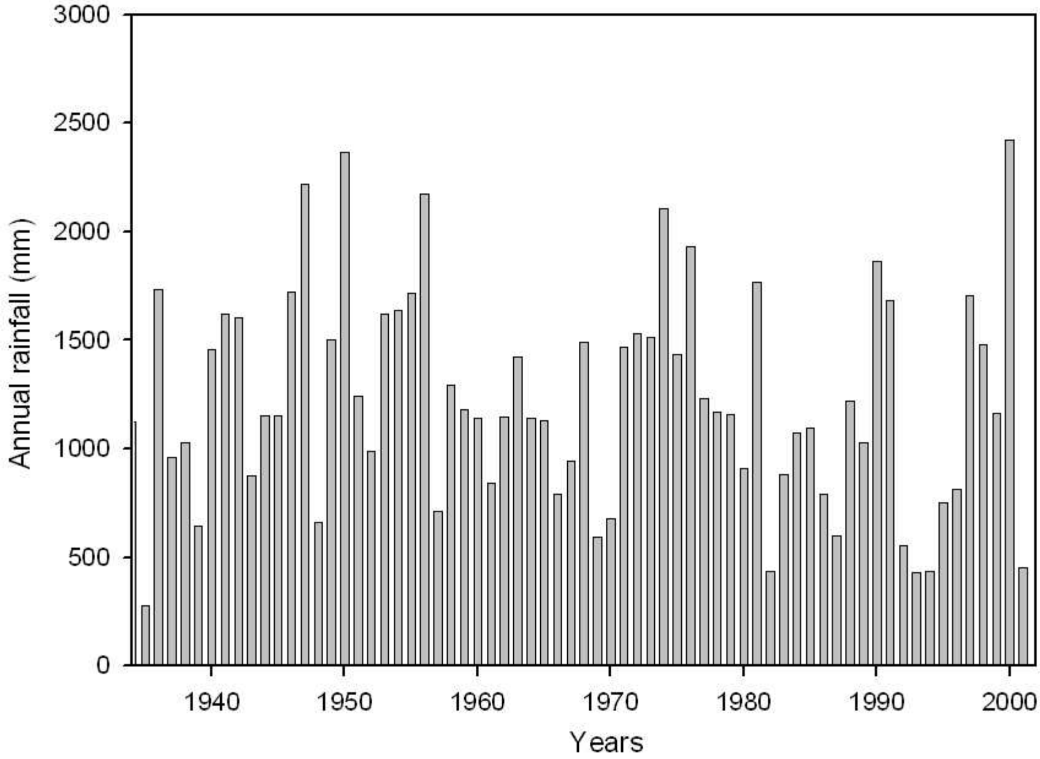

Figure 1.3. Annual rainfall totals for Giru from 1933-2001, showing inter-annual variability (Bureau of Meteorology, 2001).

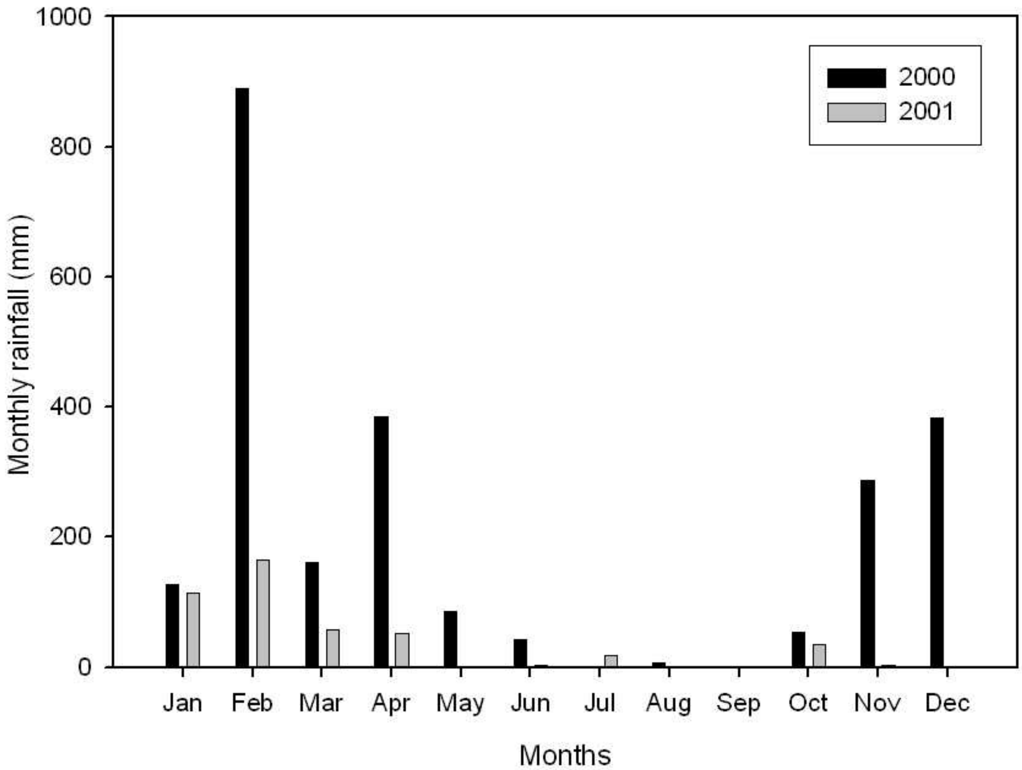

Figure 1.4. A comparison of monthly rainfall totals for Giru for 2000 and 2001, showing high seasonality and inter-annual variability (Bureau of Meteorology, 2001).

The SWT coast between Rollingstone and Bowen experiences a meso-tidal regime, with a maximum spring tide range of 3.8 m. South-easterly trade winds, averaging between 5 - 16 knots (11-20 km.h^{-1}) dominate the north Queensland coastline for most of year. However the wind observations for 9 am and 3 pm show that while south-easterly winds may dominate morning conditions, north-easterly winds develop during the afternoon. Dominant south-easterly winds are the main driving force behind wave formation. The proximity of the Great Barrier Reef to the SWT coastline limits the fetch and prevents high energy swell waves from reaching the coast, creating relatively low energy ambient wave conditions. Offshore wave rider buoy data off Cape Cleveland from 1975-1996 reveals relatively low energy ambient wave conditions; significant wave height (the highest one third of waves) is between 0.2 – 0.6 m for almost 50% of the time, with a relatively short wave period of 3 - 5 seconds (BPA, 1996b). However, strong winds associated with tropical cyclones can cause wave heights to increase by an order of magnitude. The highest significant wave height from the Cape Cleveland wave rider buoy data was 2.96 m recorded December 26, 1990 during Cyclone Joy (maximum category 2) (BPA, 1996b). The cyclone season in Australia generally extends from November to May. Between 1969 and 1997 seventeen cyclones have tracked within 100 km of the SWT coast between Rollingstone and Bowen and twelve have crossed the coast (Puotinen *et al.*, 1997). Based on almost 28 years of observations, Puotinen *et al.*(1997) have calculated that cyclones affect this coastline with an average return interval (ARI) of 1.6 years, suggesting that the SWT is one of the most cyclone-affected regions of Queensland (Puotinen *et al.*, 1997). Varying influences of fluvial, tide and wave processes over a broad range of temporal and spatial scales create a complex setting for coastal sand transfer to occur.

1.3 PREVIOUS RESEARCH

Apart from work on the Burdekin Delta by Hopley (1970a and 1970b), Belperio (1978; 1983) and Pringle (1983; 1984; 1991; 2000), few studies have looked at the fate of the coarser fraction of the fluvial sediment load in the unique climatic and low energy coastal setting of the SWT of north Queensland. Recent work in this region has focussed on the fate of suspended sediments due to their potential impact on the Great Barrier Reef (e.g. Larcombe *et al.*, 1995; Larcombe *et al.*, 1996b; Orpin *et al.*, 1999).

Previous studies of fluvial sediment delivery to the north Queensland coast have focussed on the transport of suspended sediment rather than sand (see Neil *et al.*, 2002 for a review). Studies that have focussed on sand transfer have inferred it as a proportion of the total sediment load (usually 10-20%), calculated by using sediment transport equations (e.g. Ackers and White, 1973; Belperio, 1979) or inferred transfer processes and pathways from surficial and sub-surface sediments (Hacker, 1988). Given that fine and coarse sediments have different thresholds of entrainment, transport and settling velocities (Hjulstrom, 1935) it is likely that suspended sediment (<0.02 mm) will move in the direction of the tidally average flow, while sand-sized sediment (0.02 - 2 mm) will be most affected by the highest velocities, and will move in the direction of the maximum current (Dyer, 1995). However in some cases if current velocities are sufficient very fine sand (0.02 mm) may be transported in suspension. Therefore, the examination of the fluvial – marine interface, as occurs in and around estuaries, will be an important part of this research.

The few studies that have actually measured sand transfer in SWT coastal systems are site specific and cover very limited temporal and spatial scales. For example Hopley (1980) measured sand movements around a coral cay in the Great Barrier Reef for a seven day period using sand traps and markers to measure movement over individual tidal cycles. Kana *et al.* (1999) warn that it is problematic and futile to extrapolate these small scale models over the longer term as coastal processes operate on a variety of spatial and temporal scales (see Cowell and Thom, 1994). Thus, sand transfer studies must consider the coastal sedimentary system as a whole, integrating process-based data with a geological understanding of sand sources, pathways and sinks.

1.4 HOLOCENE SAND BUDGET

Sand is such an important component of the SWT coastal zone between Bowen and Rollingstone, however little is known about the source, the spatial and temporal patterns and dominant processes of sand transfer. Temporal patterns can be as short as a tidal cycle (12 h) or as long as the Holocene transgression and stillstand (>10 ka). This study aims to quantify a Holocene sand budget for the SWT coastal zone between Bowen and Rollingstone, and link to detailed examinations of contemporary sand transport processes. The sand budget concept is shown in figure 1.5 (after Chapman *et al.*, 1982) where potential *sources* of sand, for example rivers, dunes and cliff erosion and the inner continental shelf, are indicated by solid arrows and potential *sinks* such as estuaries and longshore drift, by open arrows. Changes in sea level and streams discharging at different locations along the SWT coast during the Holocene (see Hopley, 1970a), influence the spatial distribution of sand deposits on the SWT coast. On time scales of years to millennia the linkages between the patterns and processes of coastal sand transfer in the SWT may be spatially and temporally unrelated. This sand budget defines sand as 'fluvial' and 'marine'. The initial origin of the sand is not disputed as 'fluvial' and 'marine' sand are originally derived from streams. The process of movement to the present site of delivery is the distinguishing factor; sand directly delivered to the adjacent coast by the river is termed fluvial sand, while marine sand (despite originally river-derived) is brought onshore by marine processes including waves and tides or during sea level rise (Roy *et al.*, 1980). Whilst the sand budget approach allows the quantification of sand inputs and outputs of a coastal compartment, it does not necessarily explain dominant processes and patterns of sand transfer within the compartment (Chapman *et al.*, 1982). To address this shortcoming this study will incorporate detailed process studies of individual estuaries within the SWT coastal system. The inferred source of sand to the SWT coast between Bowen and Rollingstone is SWT streams. Fluvial sediment is transported to the sea via estuaries (Dyer, 1995). Estuaries are defined as "a system which receives sediment from both fluvial and marine sources and which contains facies influenced by tide, wave and fluvial processes" (Dalrymple *et al.*, 1992:1132).

THIS IMAGE HAS BEEN REMOVED DUE TO COPYRIGHT RESTRICTIONS

Figure 1.5. Conceptual model of the inputs and sinks of a coastal sediment budget (Source Chapman *et al* ., 1982:299).

The quantification of rates of change and dominant processes for the sand budget draws on a variety of methods and information sources covering different time scales. This study includes a historical assessment of coastal change incorporating aerial photograph interpretation and photogrammetry; field data collection including surficial and sub-surface sediment sampling and measuring tidal current velocities; and applying theoretical techniques such as empirical modelling to estimate potential volumes of sand movement by fluvial, tidal and longshore processes. Detailed study of contemporary sand transfer processes in estuaries and then testing these findings against current figures of fluvial sand supply from the literature over last 7 ka will provide a holistic approach to quantifying a sand budget for the study area.

1.5 AIMS AND OBJECTIVES

This introduction has highlighted the apparent anomaly of sand delivery and sand accumulation in the SWT coastal zone between Bowen and Rollingstone. This study will address the current gap in knowledge of the spatial and temporal patterns, dominant processes and controlling factors of sand transfer in meso-tidal SWT coastal systems. The aim of this study is to quantify the coastal sand budget for the SWT between Rollingstone and Bowen within a Holocene timeframe. Specifically, the objectives are to evaluate:

- current estimates of sand supply and source to the SWT coastal zone between Rollingstone and Bowen;

- temporal and spatial patterns of sand transfer over contemporary and Holocene timeframes;

- dominant processes associated with these patterns of sand transfer;

- the relative influence of high magnitude low frequency events on sand transfer.

The research investigates these issues by incorporating geomorphological and process data to understand coastal sand transfer in SWT systems over a variety of time scales. These issues are addressed in the following eight chapters.

1.6 THESIS OUTLINE

This thesis takes the following form. The influence of fluvial sand in the evolution of the SWT coast between Rollingstone and Bowen is reviewed from the literature specific to north Queensland and SWT regions overseas. Chapter three describes and justifies the methods used to determine a Holocene sand budget in the SWT region, where conditions make fieldwork especially challenging. Conceptual models of the spatial and temporal patterns of sand transfer over contemporary timescales are presented for the three study sites. The Haughton River Estuary in chapter four; the Elliot River Estuary in chapter five; and the Black River Delta in chapter six. Chapter seven provides a big picture comparison of the results from individual study sites with a quantification of the sand budget for the SWT coast (Rollingstone - Bowen) over the last 7 ka. The major conclusions of the thesis are presented in chapter eight, together with suggestions for further study.

CHAPTER 2 – SAND TRANSFER IN THE SWT COAST

2.1 INTRODUCTION

The SWT coast between Bowen and Rollingstone, is characterised by extensive beach ridge plains, sandy beaches and sand choked inlets. Large cliffs and dunes are rare along the tropical north Queensland coast and therefore presently contribute little sediment to the beaches (Pringle, 1986). The mid and outer sections of the continental shelf adjacent to the SWT coast between Bowen and Rollingstone is dominated by carbonates associated with reefal structures (Hopley, 1986) making it an unlikely source of siliciclastic sand. Stoddart (1969) reviewed the influence of climate on geomorphology and concluded that the variability of the SWT climate (refer to chapter 1, section 1.2) has the potential to produce the highest sand yielding catchments in the world. Historically it seems that the assumption has been made that the predominance of sand along the SWT coast is a function of high sand yields derived from coastal catchments which are then transported to the coast by streams and deposited on the shoreline or in nearshore environments. From Hopley's (1970a) pioneering research of the geomorphology of the SWT coast to subsequent studies (Bird, 1971; Hopley, 1986; Pringle, 1991; Holmes, 1992) rivers, especially the Burdekin River, have been identified as the main source of sand on the SWT coast. Recently published empirical models indicate an average of 400,000 m^3 of sand is delivered to the coast by SWT rivers (notably the Burdekin, Don, Haughton, Black, Ross, Elliot) each year (GBRMPA, 2001; Prosser *et al.*, 2001a) (see chapters 7, section 7.3 for a discussion on modelling). However scarped dunes and the exposure of mangrove peat observed along the SWT coast (Hopley, 1970a) suggest that sections of the coast are presently eroding, which may indicate a reduction in fluvial sediment supply.

A large literature exists on the morphology, sedimentology and dynamics of sand bodies in the coastal zone and this is well summarised in recent books (e.g. Carter and Woodroffe, 1994; Komar, 1998). Much of this work focuses on high-energy and/or micro-tidal systems from the temperate latitudes where sand is sourced by the strong swell waves continually reworking previously deposited coastal sediments. The influence of sand supply, dominant transport processes and timeframes in the SWT which is subject to highly variable stream discharge, a meso-tidal range and relatively low energy ambient wave conditions, has received much less attention. While there has been considerable research on sediment discharge and dispersal within the SWT coast nearshore and offshore (e.g. Larcombe *et al.*, 1995; 1996b; Orpin, 1999; Orpin *et al.*, 1999; Devlin *et al.*, 2001) this work has largely concentrated on the dynamics of suspended sediment (silt and clay < 0.02 mm) rather than the fate of coarser bedload sediments (sand > 0.02 mm. The purpose of this review is to examine relevant literature from similar highly seasonal climate zones in temperate areas, and other SWT regions overseas and in Australia to determine the dominant processes of sand transfer along the SWT coast between Rollingstone and Bowen. Specifically this review will critique:

- classifications of Australian clastic coastal environments;
- classifications to accommodate the influence of the SWT climate on coastal sand transfer processes;
- the influence of low frequency high magnitude events on sand delivery to the coast;
- the Holocene evolution of SWT clastic coastal environments.

2.2 CLASSIFICATION OF CLASTIC COASTAL DEPOSTIONAL ENVIRONMENTS

Once fluvial sediment reaches the mouth of a coastal river it is subject to marine processes. This junction of a river and the sea may be referred to as an *estuary, delta, river mouth* or *inlet* (Dyer, 1995). Estuaries have been the focus of many studies - a search of the key word *estuaries* in the Ovid journal database 'Current Contents' revealed that 410 papers in 2004 were published in journals ranging from Marine Chemistry to Micropalaeontology. Estuaries are complex environments and are studied for a variety of reasons by different disciplines from biologists to geologists. Complexity creates ambiguity and conjecture in the literature regarding the exact definition and spatial and temporal boundaries of these systems prompting the use of the term *'trans-fluviomarine'* environments by some authors (e.g. Cooper, 1993). This review will follow Harris *et al.* (2002) and refer to them generally as clastic coastal depositional environments. Variations in the relative influences of river, tide and wave energy effect the geomorphology and sand transfer processes of these clastic coastal depositional environments (Dalrymple *et al.*, 1990) prompting the classification of these environments in three main ways:

1. Geomorphological;
2. Process based;

3. Morphological which includes elements of 1 & 2;

Perillo (1995) provides an excellent summary of these three classification methods.

Jennings and Bird (1967) were the first to apply a process-based classification on a regional basis to Australian clastic coastal depositional environments. Kench (1999) later applied Fairbridge's (1980) geomorphological-based classification to Australian estuaries and deltas. More recently Heap *et al.* (2001) classified Australian estuaries according to their geomorphological characteristics defined by Dalrymple *et al.*'s (1992) facies model which was constructed based on both process and evolutionary criteria. The process model uses river, tide and wave parameters; the evolutionary model uses the rate and source of sediment input, shoreline shape and rate of relative sea-level change to classify the response of delta, strandplain, tidal flat, lagoon and estuarine environments (Boyd *et al.*, 1992). Heap *et al.* (2001) extended this concept to incorporate the quantification of river, tide and river energy (see Harris *et al.*, 2002 for details) to classify environments as: tide or wave-dominated estuaries; tide or wave-dominated deltas; lagoons; strandplains; or tidal flats/tidal creeks.

Roy *et al.* (2001) used a geological framework to classify south-east Australian estuaries in terms of relative maturity - the stage in evolutionary progression. This follows on from Boyd *et al.*'s (1992) theory that estuaries are ephemeral over geological timescales, continually infilling with sediment to produce a delta (river-dominated) or a straight prograding coastline (wave/tide-dominated) (Figure 2.1). However unlike Boyd *et al.*'s (1992) classification Roy *et al.* (2001) do not distinguish between environments in terms of dominant sediment transport mechanisms, for example river, wave and tide processes. Rather, river dominance is linked to estuarine evolution to avoid being unduly influenced by river size.

None of these classification systems seem particularly suited to estuaries in the SWT. However Dalrymple *et al.*'s (1992) analysis of estuaries over evolutionary timeframes may accommodate the influence of the highly variable SWT climate.

THIS IMAGE HAS BEEN REMOVED DUE TO COPYRIGHT RESTRICTIONS

Figure 2.l The evolutionary classification of coastal sedimentary systems for Dalrymple *et al.* (1992:1132) showing the role of river, wave and tidal processes on different geomorphic settings. The relative influence of each process can change thought time as a system evolves.

2.3 SAND TRANSFER IN SWT COASTAL SYSTEMS

SWT streams are ephemeral or intermittent with highly variable discharges over seasonal and inter-annual time scales (see chapter 1, section 1.2) (Mitchell and Furnas, 1996). Long periods of drought produces low vegetation cover in the catchments and the relatively frequent occurrences of high intensity rainfall (Yu, 1998) create ideal sand-yielding conditions in the catchments. Fournier's (1960) model of sand yield potential for global climate regions suggests that the SWT region has the highest sand yielding catchments in the world. Indeed in a recent literature review of fluvial bedload supply studies, SWT streams are estimated to contribute 33% of the total fluvial sand supply for the Queensland coast (Brown and Root, 2001) Much of this literature was based on little data, with bedload delivery figures derived from extrapolation, interpolation and speculation, often from catchment erosion predictions (e.g. Fournier, 1960). Linking predictions of sediment delivery to the stream from the catchment and the volume of sediment delivered to the coast by the stream is complicated. For instance, Wasson *et al.* (1996; 1997) acknowledge that only a small percentage (~3%) of the sand estimated to be eroded from the catchment is actually delivered to the coast in Australia. Increasingly, detailed quantitative studies on individual estuaries highlight the inaccuracies of relying on these models.

As indicated in chapter 1, section 1.1, modelled estimates of sand yield to the coast in the Normanby River Estuary, located in a SWT region further north near Cape York Peninsula, do not match field studies (Bryce *et al.*, 1998). Contemporary sedimentation patterns were inferred from extensive bedform analysis, surficial sediment sampling and vibrocoring in the context of long-term sedimentation records (Bryce *et al.*, 1998). Although suspended sediments (silt and clay) being flushed out of the estuary during the wet season, the direction of net bedload transport is landward into the estuary all year round (Bryce *et al.*, 1998). Dominant flood tide currents are competent to transport sand into the estuary during spring tides (Bryce *et al.*, 1998). The net landwards transport of bedload has been documented in other SWT estuaries, for example the Salum and Casmance Rivers in Senegal, Africa (Barusseau *et al.*, 1985). However the Normanby River was classified as a delta by Heap *et al.* (2001) based on the geomorphology (protruding from the coast and sand choked mouth) and the quantification of river verses marine energy (see Harris *et al.*, 2002 for details on quantification used in Heap *et al.*, 2001),

High maximum instantaneous stream discharges associated with monsoonal and cyclonic rainfall would be considered the dominant process when compared to wave and tide energy in Harris *et al.'s* (2002) quantification, especially considering that the SWT is meso-tidal and subject to relatively low ambient wave energy. However the estimation of river power used in Harris *et al.'s* (2002) quantification did not include extreme discharge associated with flood events, but rather was based on mean annual discharge calculated from catchment area, mean annual rainfall and the runoff coefficient which was divided by the area of open water for each waterway to determine river flow (Harris *et al.,* 2002). Mean annual discharge is a misleading representation of stream flow for these extreme variable discharge streams, where discharge is event driven and episodic. Therefore the application of Heap *et al.'s* (2001) classification to clastic coastal depositional environments in the SWT is problematic, and in terms of sediment transport mechanisms even Harris *et al.* (2002) concede that fluvial sediment contributions would be mostly associated with episodic flooding events. Hence it seems that comparison of mean annual discharge with tide and wave energy would not be an accurate method for classifying estuaries and deltas in the SWT region of north Queensland due to the extremely variable nature of stream discharge. This may also explain why Harris *et al.* (2002) found that mean annual fluvial discharge does not vary significantly between deltas and estuaries in Australia. Indeed two thirds of all Australia's deltas and almost half of the prograding strand plains and tidal flats located on the north-east and Gulf of Carpentaria coasts (Harris *et al.*, 2002) are subject to highly variable seasonal and inter-annual stream flow. Therefore, the frequency and duration of storm events have more to do with the infilling of Australian coastal depositional systems by river-derived sediments than processes related to mean annual stream flow (Harris *et al.*, 2002).

2.4 FREQUENCY AND MAGNITUDE

Cyclones and associated floods are thought to control the timing and volume of terrigenous sediment delivery to the otherwise low-energy SWT coast (Bird, 1971; Woolfe *et al.*, 1998). Cyclones are categorized from one (weak) to five (severe) with the central pressure used as a measure of severity (Puotinen *et al.*, 1997). Cyclones have a two fold effect: 1. Intense rainfall events which cause the streams to flood; and 2. Strong winds which can increase wave heights by an order of magnitude. For simplicity, the fluvial and marine impacts of cyclones on SWT sandy coasts are examined separately.

2.4.1 FLUVIAL PROCESSES

The relative size of a flood can be defined in terms of recurrence intervals derived from maximum instantaneous discharges derived from stream gauge data (Wolman and Miller, 1960). Types of floods discussed in the fluvial literature include:

- Frequent/minor floods (ARI 1-2 or <5 years) (Wolman and Miller, 1960);

- Major floods (ARI 20-30 years) (Bryce *et al.*, 1998);

- Extreme/catastrophic floods (ARI 50-100 years) (Wolman and Miller, 1960) (ARI 30 years) (Cooper, 1990; Erskine, 1996; Coppus and Imeson, 2002);

- Rare/cataclysmic/extraordinary floods (ARI > 500 years) (Baker and Costa, 1987) (ARI 100-1000 years) (Osterkamp and Coasta, 1987; Osterkamp and Friedman, 2000). Sometimes the term 'catastrophic' is used to describe these types of floods as well.

Major or extreme floods (i.e. events which are orders of magnitude greater than the so-called 'annual flood') are usually referred to as 'exceptional' by geomorphologists, but these events are not so exceptional in the SWT (Fielding and Alexander, 1996). SWT streams can be described as 'extreme variable discharge streams' – which are characterised by floods where discharge increases by two to four orders of magnitude typically in less than 24 hours, in response to seasonal but erratic rainfall (Fielding and Alexander, 1996). Often floods with the largest maximum instantaneous discharge values do not produce the greatest stream power or shear stresses, indicating that the duration of the flood is also an important factor in sediment transport (Baker and Costa, 1987). Indeed Costa and O'Connor's (1995) theory of geomorphically effective floods is very applicable to the SWT. SWT stream reach high maximum instantaneous discharges for short periods (less than a few days) (Fielding and Alexander, 1996); limiting the ability of the stream to do geomorphic work.

Much of the previous research that has examined the relative importance of extreme or catastrophic events and more ordinary events in terms of their geomorphic effectiveness has occurred in temperate regions of North America (Wolman and Miller, 1960; Magilligan *et al.*, 1998). Wolman and Miller (1960) found that more frequent flood events (1-2 years and less than 5 years) do more geomorphic work and thus generally have greater geomorphic effectiveness compared to extreme or catastrophic events (50 – 100 years). Therefore the greatest part of total sediment load was removed from discharge basins during the period of record carried by small – moderate floods (Wolman and Miller, 1960). Magilligan *et al.* (1998) demonstrated the poor relationship between flood magnitude and geomorphic impact, concluding that an extreme flood in the Upper Mississippi River did not have a major impact on sand transfer.

Research in semi-arid environments of South America fails to support Wolman and Miller's (1960) theory suggesting that ideas developed for temperate streams are not always applicable in other environments. Rainfall in semi-arid areas occurs in high intensity summer storms and like SWT environments these high magnitude low frequency events are assumed to dominate sediment transport processes (Coppus and Imeson, 2002). Coppus and Imeson's (2002) research in a semi-arid valley in southern Bolivia, suggests that extreme events (1:30 year flood event) have more of an impact in terms of soil erosion and sediment transport than the majority of smaller flood events that play a minor role (Coppus and Imeson, 2002).

Research in other SWT regions from overseas also provides little support to Wolman and Miller's (1960) theory. Cooper (1990) suggests that catastrophic flood events play an important role in estuarine sedimentation in SWT estuaries in South Africa. A 120-150 year flood in 1987 in the Mgeni River flushed out sand and gravel which had been stored in the estuary since 1917, when the last catastrophic flood event occurred (Cooper, 1990). Cooper (1990) proposes that the increased stability of instream bars by permanent vegetation in regulated river-dominated systems, has increased the importance of high magnitude floods. Greater floods are now required to cause significant morphological change and transport of coarse sediment downstream (Cooper, 1990). Cooper (2002) recognizes a difference in the impact of floods on estuaries depending whether they are river or tide-dominated. Cooper (2002) also suggests that floods are important to re-activating coastal sediments in tide-dominated estuaries but they do not require floods as large as in river-dominated estuaries. Significant sand transfer also occurs during minor floods because the sand is sourced from coastal bars and barriers in tidal dominated estuaries rather than from inchannel fluvial bars. This realization prompted this thesis to examine a range of estuary types in the SWT.

It is often assumed that high magnitude low frequency events control influence over the delivery of fluvial sediment to the SWT coast of north Queensland (Bird, 1971; Woolfe *et al.*, 1998), however recent research suggests otherwise. Bryce *et al.*'s (1998) study of the Normanby River in a SWT region of far north Queensland found that fluvial sediment has been trapped in the estuary for the last 6 ka, most likely because the channel capacity of the Normanby River decreases downstream. A major flood (ARI >1:30 y) has a maximum discharge an order of magnitude greater than the bankfull capacity of the channel which means that only a small proportion (~5%) of water will travel in the channel and the rest will flow overbank (Bryce *et al.*, 1998). Modelling in the Normanby River Estuary suggests that a flood (ARI >50 y) transports 6,000-32,000 t of sand which is equivalent to four months to one year of transport into the estuary by tidal currents (Bryce *et al.*, 1998). Thus high magnitude low frequency events have little influence over sand transfer processes in this example of a tide-dominated SWT estuary.

There are examples where extreme events dominate sedimentation. For instance, the Pioneer River Estuary in Mackay north Queensland, although not technically in the SWT region has been classed as an extreme variable discharge river. Investigations of the Pioneer River have associated the transport of coarse bedload sediment with flash flood flows caused by exceptionally heavy rainfall events. Following 530 mm of rainfall in 5 hours flood flows transport very coarse bedload made up of sand, gravel and even cobbles up to 250 mm long into the estuary (Hacker, 1988). These apparent differences demonstrate the diversity of north Queensland estuaries and highlight the need for more detailed investigation of SWT coastal systems.

2.4.2 MARINE PROCESSES

The relatively frequent occurrence of cyclones (ARI 1.6 years) (Poutnien *et al.*, 1997) in an otherwise low-energy marine environment, as in the SWT of north Queensland, prompts an evaluation of the influence of cyclones on redistributing coastal sediment compared to ambient conditions. The frequency versus magnitude debate is common in coastal geomorphology literature, for example whether the beach ridges are a result of storms or ambient processes has been fiercely debated in the past (see section 2.5 for a discussion).

Insights are gained by examining examples from micro-tidal low-energy coasts of north America A study of beach volume changes along the Texas coast reveals that the impact of storms on sand dispersal and shoreline movement covers spatial scales of kilometres and temporal scales of decades (Morton *et al.*, 1995). This area of coast, San Luis Pass is usually subject to low wave energy except during hurricanes that occur at a frequency of about two storms every three years (Morton *et al.*, 1995). In this micro-tidal low-energy setting ambient conditions are too weak to transfer sand between beach compartments so the by-passing of sand is restricted to episodic high energy events. Therefore in this system low-frequency high-magnitude events dominate large-scale sand transfer (Morton *et al.*, 1995).

Work along the north Queensland coast has also shown storm deposits that have remained a feature in the Whitsundays (Heap *et al.*, 1999) and in Halifax Bay (Kirsch and Larcombe, 1999). Heap *et al.* (1999) discovered evidence of storm-dominated sedimentation in the protected basin in the Nara Inlet, Whitsundays that has remained because the ambient wave and tide conditions are too weak to rework the cyclone deposited sediments. Similarly, very large dunes composed of gravely-sand that were discovered in Halifax Bay could have only been deposited during a cyclonic event. The ambient conditions were too weak to rework the coarse sediments so the features remain at a depth of 9 m in the bay (Kirsch and Larcombe, 1999). However few studies have investigated the overall influence of cyclones on sand transfer along the north Queensland coast.

Apart from these localised areas and features mentioned above, Woolfe *et al.*, (1998) suggest that cyclones have had relatively little long-term sedimentary and geomorphic expression along the north Queensland coastline. Woolfe *et al.*(1998:618) concluded that "they (cyclones) play a relatively minor role in the long-term redistribution and deposition of this sediment because of the frequency and strength of the southeast trade winds and the waves and currents induced by them". Orpin and Woolfe (1999) extended on previous work to develop a model of sediment distribution in a typical north Queensland coastal embayment. This model depicts an embayment with a net influx of sediment driven by the south-easterly driven swell waves.

Insights from other SWT regions overseas and within Australia fail to support the assumption that high-magnitude low-frequency events control the delivery of fluvial sand or its distribution along the coast. However, given that relative influence does depend on the type of estuary, characteristics of flooding and channel morphology that impact of particular events on the SWT estuaries examined in this thesis will be assessed individually and generalisations avoided. The influence of cyclones on coastal sand transfer at both contemporary and Holocene timescales on two SWT estuaries and one delta will be further examined in this thesis.

2.5 HOLOCENE EVOLUTION OF SWT CLASTIC COASTAL ENVIRONMENTS

Previous geomorphic research on the SWT mainland coast has focussed on the three main coastal depositional environments: mangroves; cheniers; and beach ridges. Extensive mangrove forests are restricted to sheltered coastlines, particularly the leeward sides of northward facing embayments where fine-grained sediment accumulates due to hydrodynamic controls (Orpin and Woolfe, 1999). Recent work on sediment transport in mangrove creeks in the SWT region suggest they are ebb-dominated (Larcombe and Ridd, 1995; Bryce, 2001; Bryce *et al.*, 2003) exporting fluvial suspended sediment to the coast.

Cheniers are ridges of coarse and predominantly shelly material. However they may be composed of terrigenous sands or gravels and form on relatively sheltered coasts (Chappell and Grindrod, 1984). In Hopley *et al.*’s (1980) summary on cheniers in north east Queensland, the exact process of chenier formation was still unclear. Features further south dated at older than 5 ka are thought to be formed during periods of low sediment supply leading to the erosion of mangrove deposits and development of a ridge from the coarser lag deposits (Cook and Polach 1977 as cited in Hopley *et al.*, 1980). However locally, Hopley (1974) had observed the emplacement of a chenier in Bowling Green Bay during Cyclone Althea in 1971. Chappell and Grindrod (1984) describe cheniers as having an ‘internal dynamic’ with the main factors affecting formation being the ability of the mangrove fringe to trap storm drifts of shelly material and mud and the availability of shell material. Thus cheniers form as the result of low frequency high energy events such as tropical cyclones provided sedimentation conditions in mangroves are suitable and there is an adequate supply of shell material. Chenier ridges are not as common as beach ridges - in the last 2 ka six times more beach ridges have formed than chenier plains in northern Australia (Chappell and Grindrod, 1984).

Beach ridges are depositional features (Otvos, 2000). A narrow fringe of beach ridges up to 5 m high composed of quartz sand, occur along the SWT coastline particularly in locations exposed to the prevailing south easterly winds (Hopley, 1980). Komar (1998) describes beach ridges as a series of long parallel ridges that were originally formed individually as a shoreline deposit. The process behind the formation of these ridges has been the source of debate in the literature over the last century (see Graham, 1993 for a good review). Graham (1993) suggests while most authors assumed that beach ridges were formed by storm waves depositing sediment above high tide there is growing support that they are formed during ambient conditions. Wheeler’s (1902 as cited in Graham, 1993) theory suggests that where an excess of sediment exists in the nearshore, waves progressively shift sediment onshore to restore equilibrium. More recent reviews from (Tanner, 1995; Taylor and Stone, 1996; Otvos, 2000) provide additional support concluding that beach ridges form where abundance of sediment exists and the offshore gradient is low and that rises in sea level have initiated their development. Indeed in Australia, where beach ridges are common along the entire east coast, it is suggested that a reduction in the rate of sea-level rise once it reached the low gradient inner shelf permitted the onshore transport of nearshore sediment (Taylor and Stone, 1996). Further debate exists over the role of fluvial sand supply in their further development.

The majority of work on the evolution of barriers and beach ridges in Australia has been on the high-energy micro-tidal NSW coast (see Wright, 1970; Roy *et al.*, 1980; Thom *et al.*, 1981; Thom and Roy, 1985; Young *et al.,* 1996). Roy *et al*.'s (1980) evolutionary model for the NSW coast show two sources of sediment: 'fluvial' (river delivered); and 'marine' (nearshore sand moved onshore). The onshore movement of marine sand during the Holocene transgression and subsequent stillstand phase led to the formation of coastal barriers and estuaries that progressively infilled with fluvial deposits. This process has been observed in the Port Stephens – Myall Lakes area in NSW, where low sediment yielding rivers have infilled behind the barrier but have remained trapped and have had little influence on coastal development (Thom *et al*., 1981). This is not the case in the Shoalhaven River Delta where the relatively high sediment yielding river has rapidly infilled the estuary behind the coastal barrier and relatively strong tidal currents have led to the intermixing of fluvial and marine sediments (Roy *et al*., 1980). Roy *et al.* (1980) suggest that the Shoalhaven River only started to supply sand to the coast and adjacent beach ridges in the last 2 ka. However Young *et al*. (1996) suggest a far more rapid infilling of the estuary supporting earlier conclusions by Wright (1970) that fluvial sand has been delivered to the barrier system since its initiation at about 6 ka. While recent work by Umitsu *et al*. (2001) suggests a more complex re-introduction of fluvial sand delivery to the coast, it essentially supports Wright (1970) and Young *et al.*'s (1996) suggestion that for the Shoalhaven River Delta unlike other NSW estuaries, fluvial sand supply has superseded the influence of marine sand in beach ridge/barrier development. A similar situation has been reported in West Africa where the duality of sand source (i.e. marine and fluvial) has fuelled the development of beach ridges. This duality exhibits a temporal pattern wherein nearshore sand supplies have been supplemented and eventually superseded by supplies from rivers (Anthony *et al*., 1996).

Studies of the coastal development of the SWT (Hopley, 1970a; Hopley and Murtha, 1975; Pringle, 1984; Pringle, 2000) and wet tropics (Bird, 1973; Graham, 1993) coasts of north Queensland have concluded that the models of coastal evolution proposed for NSW coastal barriers (Roy *et al.*, 1980; Thom *et al.*, 1981) do not apply to these northern examples. This is not surprising considering that the NSW coast is characterised by high wave energy and low sediment yielding rivers, while the north Queensland coast is subject to low wave energy and what have been regarded as high sand yielding rivers. Thus while detailed studies have only been conducted in the Barron River Delta, Cairns and the Moresby embayment, near Innisfail in the wet tropics region, they maintain Hopley's (1970a) overall view of beach ridge development. Current literature suggests that that influence of fluvial sand supersedes marine sand in the Holocene development of the SWT coast around Townsville. However, analysis of the estimated ages of SWT beach ridges reveals similarities with their southern counterparts.

Radiocarbon dates from the most seaward beach ridges in SWT region between Bowen and Rollingstone, namely the Bohle and Cape Cleveland complexes revealed ages of 2, 460 ± 80 y (GaK-1508) and 3, 460 ± 100 y, respectively (Hopley, 1970a) Thom *et al*. (1981) found a similar pattern of progradation on the NSW coast with the formerly rapid progradation around 6 ka BP ceasing at ~3-4 ka BP. This supports the theory that the beaches are initiated by sea-level rise between 10-6 ka BP. The progradation of the beach ridges would have continued after sea level stabilised ~6 ka BP. The onshore movement of excess marine sand in the nearshore would have seen the progradation continue until equilibrium was restored.

Research into the coastal development in other SWT regions of Australia, for example, the macro-tidal South Alligator and Daly River Delta's of the Northern Territory (Woodroffe *et al.*, 1989; 1993) suggest a much different evolution. The Holocene marine transgression caused the influx of marine clay, silt and fine sands into the estuaries by strong tidal currents and while some chenier ridges were formed, no beach ridges occur. There are two likely explanations: 1. Greater tidal range (macro-tidal coast > 4 m); 2. Lack of sandy sediment common to the east coast of Australia.

Historically SWT streams have been regarded as high sand yielding therefore fluvial sand is thought to be the major source of material for coastal development. This review has demonstrated similarities with the long-term evolution of estuaries further south despite differing fluvial and marine regimes, therefore questioning the relative influence of fluvial sand in the development of the SWT coast. Large scale coastal development, i.e. the progradation of beach ridges on the SWT coast, like in other parts of eastern Australian was instigated by sea level rise 10-6 ka BP and continued through the stillstand until ~3 ka BP.

2.6 CONCLUSION

This review has demonstrated the lack of research which examines the influence of fluvial sand and dominant processes associated with coastal development in the SWT region of north Queensland. The extreme variable discharges characteristic of SWT streams do not fit well into current classifications of clastic coastal environments. SWT streams are quoted in the literature as delivering significant amounts of sand to the coast, however this often based on empirical modelling rather than site specific data. The highly variable nature of discharge in SWT streams is likely to have a substantial impact on the delivery of fluvial sand to the coast which is often not considered in modelling. Analysis of current literature has revealed that the influence of high frequency low magnitude events on fluvial sediment delivery and redistribution along the coast varies according to the characteristics of flooding and channel morphology and dominate processes in the estuary. This review reveals similarities between the long-term evolution of SWT estuaries with those further south – despite differing fluvial and marine regimes. Thus, doubt exists over whether fluvial sand supply has had more of influence on SWT coastal development than marine sand. This realisation highlights the need for the detailed study of SWT estuaries to determine the role of fluvial sand in coastal development.

CHAPTER 3 – METHODOLOGICAL APPROACHES

3.1 INTRODUCTION

The SWT coastline between Rollingstone and Bowen has changed both spatially and temporally. Therefore, an understanding of its modern geomorphology needs to be based on geological processes and time frames. Changing sea level has altered the position of the coast on the continental shelf and as a result the position of river mouths has also changed. Hopley's (1983) sea level curve for the SWT is still considered most accurate given doubts over the reliability of Larcombe and Carter’s (1998) more recent sea level re-construction for the region (Hopley *et al*., 2007). Climatic changes cause variations in fluvial activity, for example Nott *et al.*, 2002 has linked climatic data with the development of alluvial fans in north Queensland. Hopley’s (1970a) detailed study of the SWT region reveals that many of the coastal features are relict. Modern processes, measured over a few tidal cycles over a couple of years and under ambient conditions in a SWT setting with high inter and intra-annual climatic variability, must be interpreted in the context of long-term geological timescales.

In order to quantify a sand budget for the SWT, studies of sand transfer over Holocene and contemporary timeframes were conducted in individual coastal systems in the SWT. The eighty-one streams between Rollingstone and Bowen were classified according to their physical characteristics (e.g. length, catchment area, slope, tidal limit and exposure to waves) to which systems would provide representative model of sand transfer processes in region. The Haughton, Elliot and Black coastal systems were considered the most appropriate because they all have the potential to deliver sand to the SWT coast under different dominant processes. For instance, the Haughton coastal system is considered to be tidally dominated, the Black wave-dominated, while the Elliot is influenced by both tidal and wave processes.

A variety of methods and data sources encompassing Holocene and contemporary timeframes were used to develop conceptual models of sand transfer in these three coastal systems which in combination provide a model of sand transfer in the SWT region. Sand movement over contemporary timeframes (from years to hours) was interpreted from aerial photograph analysis and bedform mapping in conjunction with volumes estimated from modelling equation based on tide and wave data. The textural and sorting characteristics of all three study sites were mapped to provide insight into the source of the sediment and dominate transfer processes. Stratigraphic sediment analysis and radiocarbon dating in the Haughton and Elliot estuaries established a chronology of sediment deposition over a Holocene timeframe, which provided a context to the interpretation of contemporary sand transfer processes.

This chapter begins with a description of how the study sites were selected with a detailed description of the sites included in their respective chapters (4, 5 and 6). A detailed discussion of the specific methods and justification of their appropriateness to the study will follow.

3.2 SELECTION OF STUDY SITES

3.2.1 CLASSIFICATION OF SWT COASTAL SYSTEMS

Eighty-one streams discharge into the Great Barrier Reef lagoon along the SWT coast between Rollingstone and Bowen. They range in size from the Burdekin River which is over 600 km long and drains 129, 500 km^2 down to numerous unnamed streams less than 1 km long and draining areas of less than 2 km^2. Data on the source of streams, catchment area, channel length, and percentage of estuarine channel was collated by the author from topographic maps and is detailed in Appendix A. This data was used to classify SWT coastal systems, including estuaries, deltas, tidal inlets and mangrove creeks, into five categories is shown in Table 3.1.

Table 3.1. Selected physical parameters used to classify SWT streams.

System type (Total number in SWT)	Source	Catchment Area (km^2)	Channel Length (km)	Percent estuarine channel	Fluvial Influence	Example(s)
Large complex systems (11)	Escarpment or residual hill	> 100	> 30	< 20 %	Seasonal	Burdekin River, Don River, Haughton River, Black River, Elliot River, Ross River
Small complex systems (22)	Escarpment or residual hill	20 – 99	10 – 29	< 20 %	Seasonal	Althaus Creek, Leichhardt Creek
Perennial Systems (2)	Residual hill	20 – 99	10 – 29	< 20 %	All year	Rocky Ponds Creek
Large coastal inlets (13)	Coastal plain	20 – 60	>10	> 40 %	negligible	Crocodile Creek
Small coastal inlets (33)	Coastal plain	< 20	< 10	> 75 %	negligible	Salmon Creek

Only two streams between Bowen and Rollingstone are classified as ‘perennial’ due the occurrence of natural springs. The majority of streams between Bowen and Rollingstone are intermittent due to highly variable rainfall of the SWT region. Therefore a study of sand transfer in these coastal systems would not be representative of the SWT. ‘Large and small complex systems’ are influenced by fluvial processes (though seasonal) compared to ‘large and small coastal inlets’ where fluvial processes are considered to have a negligible influence on sand transfer processes within these systems. Therefore achieve the aim of this study and quantify the coastal sand budget for the SWT between Rollingstone and Bowen, it was considered most appropriate to focus on those systems which have the greatest potential to be significant contributors of sand to the coast. Despite Pringle’s (1983; 1984) findings that distributary channels in the Burdekin Delta supply sand to the coast during major flooding, most SWT coastal inlets are no longer active distributary channels (Prosser, et al., 2001a). Consequently coastal inlets are not considered likely to contribute substantial quantities of sand to the coast and were not selected for detailed study.

Beach ridge plains adjacent to the large complex systems (Belperio, 1978; Holmes, 1992) and empirical modelling (Kinhill et al., 1993; Prosser et al., 2001a) suggest that the larger complex systems such as the Haughton, Elliot and Black Rivers have the greatest potential to deliver sand to the coast compared to the smaller complex systems such as Leichardt, Bluewater or Althaus Creeks. Therefore, the selection the study sites were refined to only include ‘large coastal systems’ which have the greatest potential to be significant contributors of sand to the coast. However, to develop a comprehensive sand transfer model for the SWT, it was essential to select ‘large coastal systems’ that were subject to varying influences of fluvial, tide and wave processes. Therefore the potential delivery and dominate processes of sand delivery to the coast in conjunction with the practical considerations such as the proximity to Townsville, availability of data and accessibility to the mouth resulted in the selection of the Haughton, the Elliot and the Black coastal systems as the focus of this study.

Despite having the potential to be a significant contributor of sand to the coast and therefore having a major influence on coastal sand transfer in the SWT, the Burdekin coastal system was not chosen as the focus of this study. At 600 km in length and draining a catchment of 129,500 km^2, the Burdekin is an order of magnitude bigger than the second and third largest systems the Don (length: 60 km; catchment area: 3985 km^2) and the Haughton Rivers (length: 90 km; catchment area: 3600 km^2) in the SWT. The vastness and complexity of this system would have limited the extent of this study to one study site rather than a representative sample of SWT systems. Also the Burdekin Delta has been widely studied when compared to other SWT systems (see Hopley, 1970b, Belperio, 1978; 1983, Pringle, 1983; 1991; 2000) and these findings were incorporated into the model of sand transfer for the SWT in chapter 8, section 8.4. Therefore while the Burdekin coastal systems is not the subject of detailed study in this thesis, it's influence on the sand transfer in the SWT is still accounted for in the resultant conceptual model.

3.3 AERIAL PHOTOGRAPH ANALYSIS

Available large scale (1: 12,000) vertical aerial photography spanning 60 years (see Appendix B) was analysed using standard photogrammetry techniques to map the evolution of the estuaries and adjacent coastlines over the recent past. Aerial photograph analysis is one of the most efficient and economical methods for understanding large-scale coastal behaviour over historical time scales (Hapke and Richmond, 2000), and is widely used by coastal geomorphologists and engineers (Harris and Jones, 1988; Pringle, 2000). Comparing sequences of large scale (e.g. 1:12,000) vertical aerial photographs taken at frequent intervals (e.g. every 5 years) over timeframes of 50-100 years gives a visual record of historical coastal evolution and rates and patterns of change. This method was the primary source of information for Pringle's extensive work (Pringle, 1983; 2000) on the Burdekin Delta, north Queensland. Aerial photograph analysis can even be used to detect smaller scale changes in the morphology of estuaries. A sediment transport model was developed for Moreton Bay (Harris and Jones, 1988) from assessing morphological changes in large-scale bedforms (sandwaves) from a series of aerial photographs over a 26-year period.

Developing historical models of coastal change and sediment transfer within estuaries has its difficulties. Aerial photographs are a snap shot of the estuary at that particular moment in time and may represent atypical conditions or morphologies (Stafford and Langfelder, 1971; Smith and Zarillo, 1990). For instance, a photograph that was taken immediately after a storm may show unusual bedforms that lasted only a few days before the ambient conditions returned. Fixed time lapses between aerial surveys, for example Beach Protection Authority (BPA) photographs taken at five years intervals, may also result in an inaccurate interpretation of the transport processes in the estuary. Comparing the position of the coastline recorded in historical aerial photography is the most common way to estimate rates of coastal erosion and/or accretion. The accuracy and precision of aerial photographic measurements is limited by difficulties in locating coastline position (Smith and Zarillo, 1990; Thieler and Danforth, 1994). This problem has previously received little attention in coastal geomorphology literature (Galgano and Douglas, 2000), prompting calls to establish a precise and consistent method among coastal researchers. Current techniques fail to provide an adequate basis for quantifying the many errors inherent in mapping the coastline from aerial photographs which range from image space distortion on the aerial photographs due to the lack of precise ground control points through to using small scale photographs (> 1: 20,000) (see Thieler and Danforth, 1994 for a good discussion). Coastline position is most frequently taken as the wet/dry line on the beach assumed to be the high water line (after Dolan *et al.*, 1980; Crowell *et al.*, 1991) as it is easily identified on aerial photographs by the colour difference between wet and dry sand (Thieler and Danforth, 1994). The high water line has its limitations as the indicator of coastline position especially on low sloping beaches where the position of the wet/dry line due to wave, tide or wind effects can range over several tens of metres (Thieler and Danforth, 1994). Therefore in this study the use of the high water line as the indicator of coastline position is made more robust as it is commonly associated with another coastline indicator, the vegetation line i.e. the seaward limit of coastal vegetation. While a lack of ground control points at all three study sites reduced the precision of coastline change measurements, error was minimised by using large scale (1:12,000) photographs.

Aerial photographic data was used to determine coastal change by mapping coastline positions at the time of the photographs and comparing linear measurements of changing coastline position. To develop an illustrative map of changing coastline position aerial photographs were scanned at high resolution (600 dots per inch) and imported into Corel Draw 9.0 graphics program. The photographs were orientated until they lined up with permanent features on an overlayed digital topographic (1:25,000) map. The position of the coastline for each photograph was heads up digitized using a different colour for each year. The resultant maps provide a useful visual record of the changing position of the coastline, however more precise and accurate techniques were derived from linear measurements taken directly from the aerial photographs. A line was drawn between two permanent features identified throughout the photograph record and on topographic maps, for example easily identified features on Pleistocene beach ridges. Transects (~250 m apart) were drawn perpendicular to the base line allowing the distance to the high water line to be measured from the same location on each aerial photograph. Distances from baseline to coastline were measured to 0.1 of a millimetre using a planimeter. Operator’s measuring accuracy from 1:12,000 scale photography is estimated at ± 0.5 mm (Barker *et al.*, 1997; Galgano and Douglas, 2000). These figures could have been improved with more accurate ground control, however permanent survey markers are not located at the study sites. As high tide mark is used to denote the location of the coastline, there may be some differences in the height of the tide. However as the BPA photographs used are consistently taken at low tide on winter spring tides the tides error was minimised.

Sand volumes can not be accurately quantified unless photogrammetric techniques are used like integrating field survey data with the photograph data in computer models. For example, Hapke & Richmond (2000) have developed a method of producing 3D topographic models (Digital Terrain Models) and orthophotographs from digitized aerial photography. The lack of permanent survey markers at the study sites prevented the use of such techniques to give an accurate quantification of coastal change so volumes were estimated by using the average height of the coastline or bedforms (after Kidson and Manton, 1973). While this method is not considered to be as accurate as more recent developments in digital softcopy photogrammetry (e.g. Hapke and Richmond, 2000) this part of the study was limited by available data. A conservative average height of 1 m was used in the volume calculations allowing for reasonable confidence in the accuracy of volume estimates. The estimated volumes are only used to give an indication of the order of magnitude, that will be tested against modelling estimates as part of the sediment budget for the SWT between Bowen and Rollingstone (refer to Chapter 7).

3.4 SEDIMENTS

3.4.1 BEDFORMS

The morphology of estuarine sedimentary deposits is the result of the interaction between fluvial, tide and wave induced currents combined with the geometry and sedimentology of the estuary (Harris, 1988). The morphology and distribution of bedforms was observed on low spring tide on the intertidal flats of the Haughton, Elliot and Black estuaries in August 2001 by adopting similar methods used in Harris and Jones's (1988) study of bedforms in Moreton Bay, Queensland and FitzGerald *et al.*'s (2000) study in the Kennebec River Estuary, Maine U.S.A. Bedforms that were considered representative of approximately a 5 m radius of the intertidal flats were selected for detailed observation and mapped. The location of the bedform was recorded with a handheld Garmin Etrek GPS and a vertical photograph was taken. The height and wave length was measured and where the bedforms were asymmetrical the direction of the lee side was noted. Mapping of the distribution and orientation of the bedforms allowed the interpretation of patterns of sand movement within the estuaries (after Harris and Jones, 1988; Nichols, 1999).

3.4.2 SEDIMENT SAMPLING AND ANALYSIS

"Grainsize distributions are a sedimentary response to the geological processes of transport, re-suspension, deposition, mixing and sediment modification by biota and chemical mixing"(Orpin and Ridd, 1996:128). A surficial sediment sampling regime was designed for the study sites to allow the mapping and comparison of sediment facies in the upper, mid and lower estuary, offshore and on the adjacent coast. The results of the surficial sediment sampling is the basis of the conceptual model similar to the method used by Dalrymple *et al.* (1992) to develop a conceptual model of the sediment dynamics in macro-tidal estuaries. Sediment samples were collected in all three estuaries using a Van Veen grab sampler and a dredge deployed from a boat to retrieve samples off the sea and riverbeds. A small spade was used to collect samples from the dunes, beach and intertidal flats at low tide. The sample location was recorded using a hand held Garmin Etrek GPS.

The textural characteristics of sand samples were determined using standard dry sieving techniques (Lindholm, 1987) as it was considered the most efficient and cost effective method. Those samples containing fine sediment were analysed using a laser particle size analyser the Malvern Mastersizer 1000. Both sets of particle size data were analysed using the software package GRADISTAT: a grainsize distribution and statistics package for the analysis of unconsolidated sediments (Blott and Pye, 2001). While the GRADISTAT program gives the results in both methods of moments and graphical measures, only the results from the latter (graphical measures) were used in the interpretation as it is considered more likely to accurately describe the general characteristics of bulk samples (Blott and Pye, 2001). This study and many other recent studies (e.g. Anthony, 2000; Stewart *et al.*, 2000; Malvarez *et al.*, 2001) apply the same basic principles to interpret the origin and dominant transport processes of sediment from textural and sorting characteristics, together with assessments of angularity and feldspar content as Folk and Ward (1957) and Friedman (1961) did over 40 years ago. Some common relationships included linking poorly sorted, coarse sediment to fluvial environments, and well-sorted finer sand containing shells to marine environments (Folk and Ward, 1957; Friedman, 1961). Discriminant analyses, using mean grain size, sorting, skewness and kurtosis, have been successfully used for the recognition and discrimination of modern fluvial, beach and dune samples in the Burdekin Delta (Orpin, 1999).

3.5 HYDRODYNAMICS

3.5.1 WAVES

The BPA has two waverider buoys collecting offshore wave data one at Cape Cleveland (BPA, 1996b) and one at Abbot Point (BPA, 1996a). Every hour on the hour the buoy records water surface elevations which are transmitted to the receiver station on the mainland and stored in 26.62 minute intervals. In this thesis wave data is described in terms of significant wave height (H_{sig}) and the highest individual wave in the record (H_{max}). H_{sig} is the highest one third of the wave heights measured in a 26.6 minute wave record and are considered by the Bureau of Meteorology to have the most influence on wave processes (BPA, 1996b). H_{max} is reported in association with major meteorological events. As the buoys are located in deep water depths of >10m, the wave data must be manipulated using wave hind casting to provide an indication of nearshore sand transport.

Potential longshore sand transport volumes were calculated from significant deepwater wave height and wind data using equations developed by the U.S. Army Corps of Engineers (USACE, 1984). These equations form the basis of an interactive computer-based design and analysis tool called the Automated Coastal Engineering System (ACES 1.07) (Leenknecht *et al.*, 1992), which has been recently used to calculate potential longshore transport at Fox Island, U.S.A. (Miller *et al.*, 2002). Wind data (speed and direction) collected by the Bureau of Meteorology from Townsville, Ayr and Bowen recording stations were inputted into the ACES to calculate potential longshore transport volumes. Details of the calculation procedures and all results are given in Appendix C.

Wave refraction diagrams were also manually constructed from wind records to increase the applicability of the offshore waverider buoy data to nearshore sand transfer. Wave refraction maps were constructed for Abbot Bay using a template derived from King's (1972) graph illustrating the relationship between water depth, wave period and wave length. Three maps were drawn, for south easterly, easterly and north easterly winds using five second wave interval (five second wave interval is common in nearshore bays of north Queensland due to the proximity of the Great Barrier Reef) and 20 wave crest spacing. However, as the SWT region is subject to relatively low ambient wave conditions the focus of the hydrodynamic field studies was on the collection of tidal data.

3.5.2 TIDES

The most common method of collecting tide data in estuaries is to deploy a data logging S4 current meter for periods of up to a month to record ebb and flood current velocities (Bryce *et al.*, 1998). However the S4 current meters were unavailable. Therefore an alternative method had to be devised. A hand held digital flowmeter (General Oceanics model 2035) was deployed off a boat at selected sites throughout the Haughton River Estuary. This method required additional effort compared to the S4 current meter allowing detailed data collection at only one of the three study sites. However, this method provided a valuable advantage over the static S4 current meter, as variations in tidal energy in different locations of the estuary could be compared. Three sites were selected along the main estuarine channel of the Haughton representing the upper, mid and lower sections and one site on the smaller tidal channel. Current velocities were recorded every 15 minutes at 1 m above the bed and at 20%, 40% and 60% of the depth during a complete twelve-hour tidal cycle during spring and neap tides (June and July 2002 & 2003). Current velocities 1 m above the bed are most commonly used to estimate rates of bedload transport (see Larcombe and Ridd, 1995; Bryce *et al.*, 1998).

Mathematical models similar to those used to estimate fluvial sediment yield (e.g. Ackers and White, 1973) are applied to quantify bedload transport into and out of estuaries (Miles, 1991). The tidal current velocity data collected was used to model potential volumes of bedload transport into and out of the estuaries. Three bedload equations from Engelund and Hansen, (1967); Gadd *et al.*, (1978); and Hardisty, (1983) that have been previously used to model sand transport in north Queensland tidal settings (e.g. see Larcombe and Ridd, 1995; Bryce *et al.*, 1998) were applied in this study. Larcombe & Ridd (1995) compared the predictions from these equations with actual measurements of bedload transport in a tidal creek located in the SWT of north Queensland. They concluded that while there was some overestimation, overall the predictions of bedload transport were good (Larcombe and Ridd, 1995).

3.6 VIBROCORING

Estuarine evolution occurs over time scales of thousands of years and must be viewed within a context of changing environments and sea levels to interpret modern sand transfer processes and morphology (Cowell and Thom, 1994). Past estuarine conditions and dominant processes can be interpreted from the analysis of the stratigraphy and sedimentology of estuarine deposits (Nichols, 1999). Vibrocoring and radiocarbon dating is a common method of analysing estuarine deposits and formed the basis of a depositional model for the macro-tidal Alligator River Estuary in the Northern Territory (Woodroffe *et al.*, 1989). A similar strategy was applied in this study with six vibrocores retrieved from the Haughton River Estuary and four from the Elliot River Estuary (Figure 3.1). Vibrocoring was considered the most appropriate method given the shallow bathymetry in the estuary and the need to take the cores in nearshore locations where large vessels capable of taking deeper cores could not access. The cores were sub-sampled at 10-20 cm intervals and the textural and sorting characteristics were determined using the methods described in section 3.4.3. Organic material, for example mangrove peat, found in the cores and likely to be in situ was sent to Waikato University, New Zealand to be radiocarbon dated. Establishing a chronology for patterns of sedimentation aids in the interpretation of the evolution of the estuaries and dominant processes influencing sand transfer (Woodroffe *et al.*, 1989).

Figure 3.1 Vibrocoring intertidal sand flats at the Haughton River Estuary during low tide.

3.7 CONCEPTUAL MODELS

Conceptual models have been used to explain differences in the morphology and facies distribution of estuaries (e.g. Boyd *et al.*, 1992; Dalrymple *et al.*, 1992; refer to chapter 2, section 2.2). In such models the estuary is divided into a landward zone dominated by fluvial sedimentation, a seaward zone dominated by marine sedimentation and a mixed zone. The morphology and distribution of sandbodies at the estuary mouth are used to distinguish between the wave and tide dominated classifications. A number of factors can modify these models including the length of the estuary, the valley shape and stage of estuarine evolution (FitzGerald *et al.*, 2000).

Conceptual models provide an effective and efficient way of communicating and synthesising the extremely complex processes occurring in SWT coastal systems. Conceptual models can be used as part of a decision support system for environmental managers, and as a tool for comparative assessment in which a more integrative approach to the components can be applied (Ryan *et al.*, 2003). They provide a framework for organising knowledge, in order to help users understand processes and demonstrate the links between them (Ryan *et al.*, 2003). By incorporating the morphological, sedimentological and hydrodynamic data over contemporary and geological time scales a conceptual model of sand transfer was developed for SWT coastal systems. This model may assist coastal managers to consider the dynamics of coastal systems at temporal and spatial scales appropriate for decision-making.

3.8 SUMMARY

This study applies a multi-disciplinary approach integrating morphological, sedimentological and hydrodynamic data over contemporary and geological time scales to produce a conceptual model of coastal sand transfer for the SWT. A combination of aerial photo analysis and bedload modelling was used to quantify the volumes and dominant processes of sand transfer over contemporary timescales. Stratigraphic sediment analysis and radiocarbon dating established a chronology of sediment deposition over a Holocene timeframe to be incorporated in the interpretation of contemporary results. The Haughton, Elliot River Estuaries and the Black River Delta were selected for this study from a classification of all SWT coastal systems, as they were considered to have the greatest potential to deliver sand to the coast and are subject to varying influences of fluvial, tide and wave processes. Table 3.2 summaries the data collection methods used in each study site.

Table 3.2 Summary of the data collected in each study site

Study Site	Aerial photo analysis	Bedform mapping	Surfical sediment sampling	Subsurface sediment sampling	Tidal current data	Bedform sediment transport modelling	Wave sediment transport modelling	Radio-carbon dating
Haughton River Estuary	1942-2000	Yes	150 samples	6 vibrocores	Yes	Yes	Yes	Yes
Elliot River Estuary	1942-1998	Yes	95 samples	4 vibrocores	No	No	Yes	No
Black River Estuary	1942-2000	Yes	68 samples	No	No	No	Yes	No

CHAPTER 4 – THE HAUGHTON RIVER: A TIDE-DOMINATED ESTUARY

4.1 INTRODUCTION

The Haughton River Estuary (Lat. 147.126, Long. -19.416) is the largest of the three study sites and was studied in the most detail. The results of the aerial photograph analysis, sedimentological and hydrodynamic studies on the Haughton River Estuary are presented and briefly discussed here; a more detailed discussion continues in chapter seven. The results are synthesised in a conceptual model that relates contemporary processes to the existing geomorphology, to help explain the evolution of the system.

4.2 GEOMORPHOLOGY

The Haughton River Estuary is located ~30 km south of Townsville near Giru (Figure 4.1). Table 4.1 summarises the main physical attributes of the largest system within the SWT, after the Burdekin. The steep descent (0.0147) of the fluvial reach of the river the Great Escarpment (maximum height 1000 m) is contrasted by the gentle descent (0.0003) of the estuarine reach, which discharges into Bowling Green Bay. The average width of the channel along most of it is length is ~50 m, widening rapidly at the mouth to 2 km. Well developed sand bars and islands throughout the channel are indicative of the large quantities of sand originating from weathered granites and diorites of the Hervey Range and the Mount Elliot Complex (Kinhill *et al.*, 1996). The sinuosity of the channel increases from 1.4 to 2.1 about 18 km from the coast due to tidal influence. This estuarine section of the channel is flanked by about 25 km^2 of mangroves (Heap *et al.*, 2001). The Estuary is dominated by sandy sediments in the form of a large flood and/ ebb tidal delta of 9.7 km^2 (Heap *et al.*, 2001).

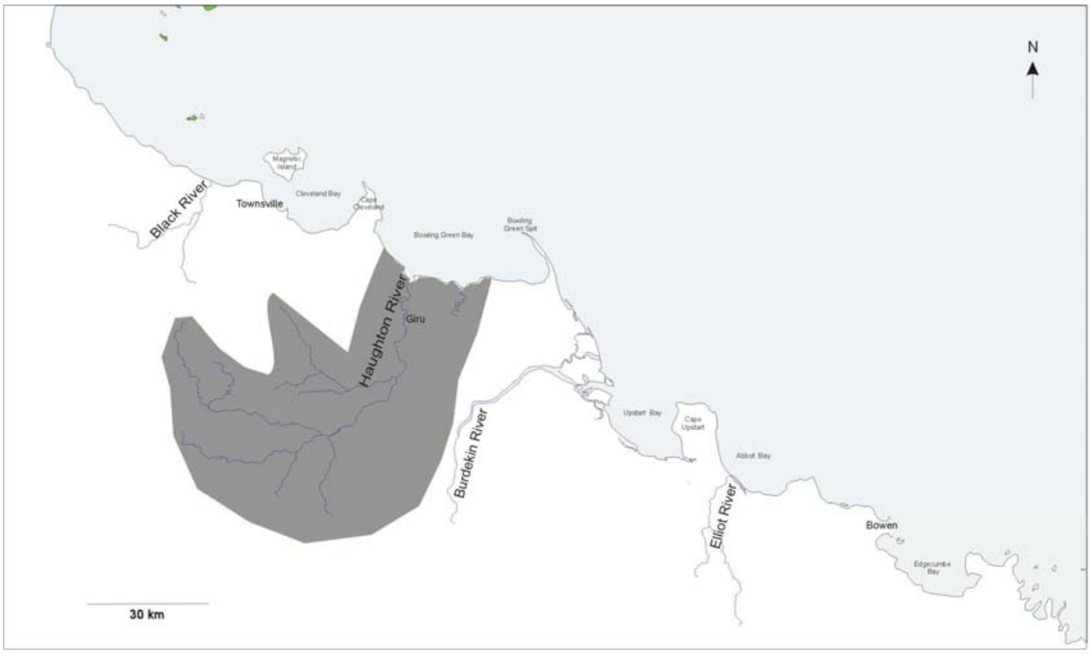

Figure 4.1 The Haughton River catchment.

Table 4.1. Physical characteristics of the Haughton River Estuary

Catchment area	3600 km^2
Channel length	90 km
Channel width	50 - 2000 m
Slope	Fluvial reach: 0.0147 Estuarine reach: 0.0003
Sinuosity	Fluvial reach: 1.4 Estuarine reach: 2.1
Percentage of channel estuarine	20%
Mean annual rainfall	1249 mm
Modifications	• 78% of catchment cleared for grazing and small areas of agriculture; • 1977 Giru Weir (AMTD 15.1 km); • 1982 Val Bird Weir (AMTD 22.7 km); • Sand extraction (>560,000 m^3 since 1984) (Kinhill *et al.*, 1996); • Altered flow due to irrigation.

The present geomorphology of the river and its estuary is the result of thousands of years of evolution and must be viewed within the context of sea level rise. Prior to 6 ka BP the Haughton River acted as a left bank distributary of the Burdekin River when it discharged into Bowling Green Bay via the Barrattas (see appendix F) (Hopley, 1970b). The large number of distributaries and lagoons in the floodplain indicate that the Haughton River has changed parts of its course many times (Kinhill *et al.*, 1996).

4.3 SETTING

The Haughton River exhibits the typical characteristics of a highly variable discharge stream (see chapter 2, section 2.4.1). Table 4.2 summarises the flow gauge data used in Figure 4.2 which illustrates the marked intra and inter-annual variability of stream flow in the Haughton River. Approximately 88% of total stream flow occurs between December and April. Discharge also varies markedly between years which is highlighted by comparing annual stream discharges as a percentage of the maximum annual flow volume for the Haughton River. Sixty-three percent of the years on record registered below a quarter of the maximum annual flow volume. Flooding in the Haughton River can be described as episodic and flashy. Figure 4.3 illustrates the rapid rise of flow reaching high maximum instantaneous discharges; however the duration of maximum flow is short, declining rapidly. For instance, the duration of a flood with an average return interval (ARI) of greater than 20 years is less than one day. Table 4.2 details downstream decreasing channel capacities, which reduce the channel's ability to convey flow (Kapitzke *et al.*, 1998). The channel capacity in the lower reaches of the Haughton River decreases by over 90%.

Table 4.2. Summary stream flow characteristics for the Haughton River Estuary (Source Kapizke, *et al.* 1998).

Gauging station	Powerline
Distance from stream mouth	33 km
Catchment area at gauging station	1735 km^2
Gauged area/catchment area	48%
Available records	1970-2001
Maximum annual flow volume	1,750,000 ML in 1991
Minimum annual flow volume	4,6000 ML in 1987
Maximum instant discharge	3964 $m^3.s^{-1}$ in January 1972
Maximum period of no flow	10 months in 1986/87
Bankfull capacity (13 km upstream of the mouth)	<400 $m^3.s^{-1}$
Outflow discharge	>3600 $m^3.s^{-1}$
Outflow (% of bankfull capacity on upper floodplain)	>90 %

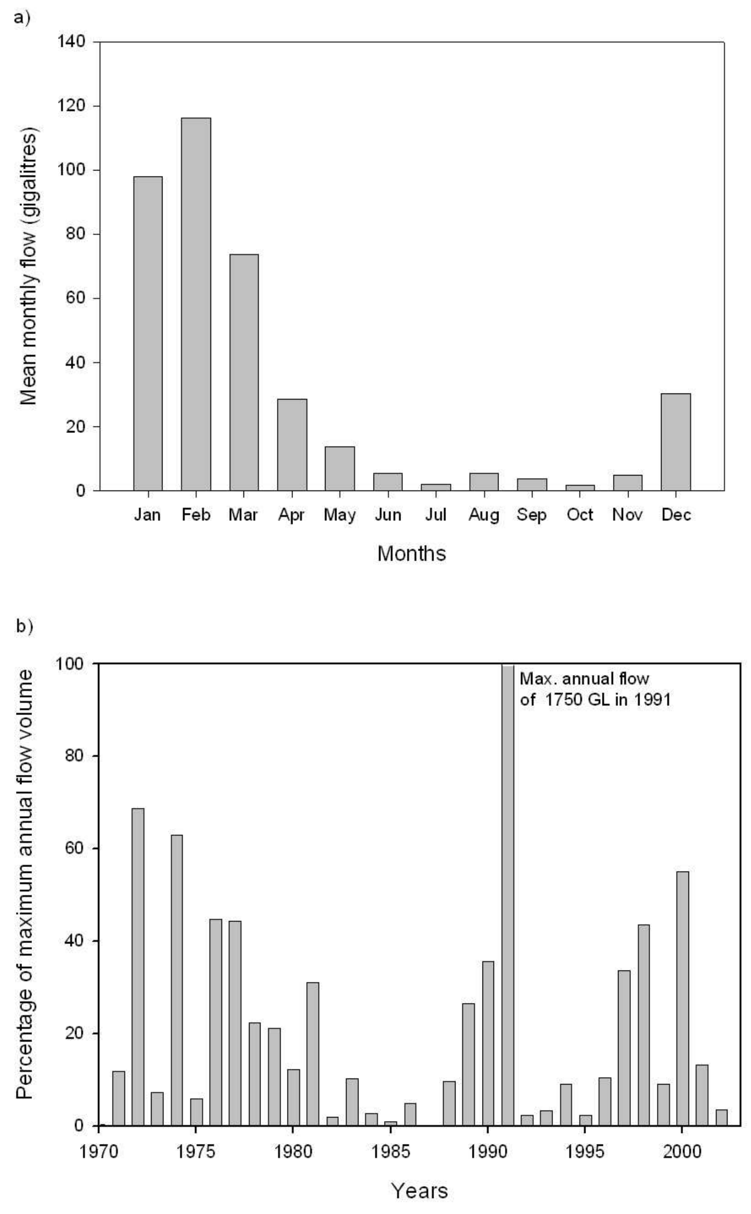

Figure 4.2 Stream flow characteristics for the Haughton River recorded at the Powerline gauge from 1970-2002 (DNR, 2002), mean monthly flow volumes (a) and annual flow volumes shown as a percentage of the maximum flow volume (b).

Waverider buoy records from off Cape Cleveland are the best data available to indicate offshore wave energy for the Haughton River Estuary. Modal significant wave height ranges from 0.2 - 0.4 m (BPA, 1996b). However it is likely that lower significant wave heights occur at the estuary mouth, given that Cape Bowling Green shelters the bay from the dominant wind driven south-easterly waves. The Haughton River Estuary experiences a diurnal meso - tidal regime with a maximum spring tide range of 3.8 m (Queensland Transport, 2003).

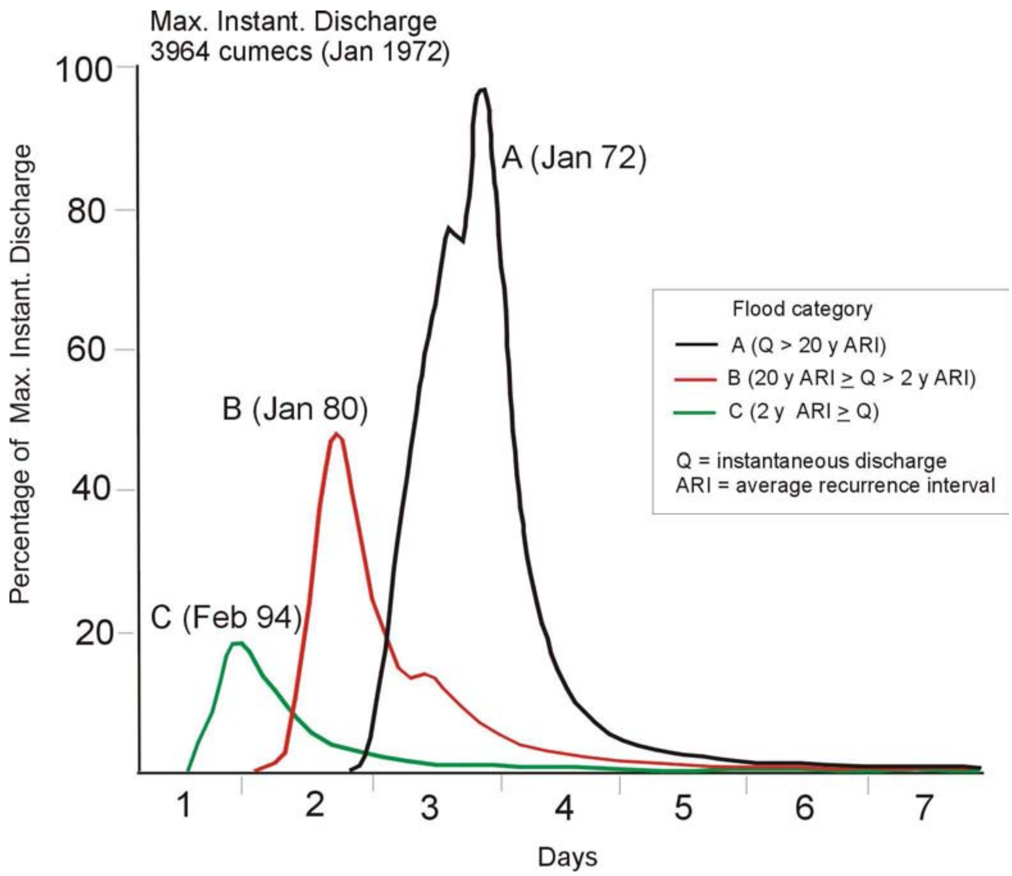

Figure 4.3 Flood hydrograph for the Haughton River reproduced from Kapitzke *et al.* (1998:42)

4.4 RESULTS

4.4.1 AERIAL PHOTOGRAPH INTERPRETATION

Analysis of aerial photographs from the last 60 years, incorporating Hopley and Rassmussen data from 1942-1995 and this study from 1952-2000 (see Appendix B), revealed a net average shoreline retreat of ~100 m on the western side of the Haughton River Estuary since 1942 (Figure 4.4). Figure 4.6 presents the linear measurements of erosion and accretion between 1974 and 1998 along the 3 km stretch of coastline on the western side of the estuary near the settlement of Cungulla (see figure 4.5 for the location of transects). Most of the transects (transects 2-5) have experienced erosion with an average of 1.2 m of shoreline retreat per year, which over 1.9 km of coast (assuming 1 m height - see chapter 3, section 3.3.1) yields 54,340 m^3 of eroded sand. However, accretion has also occurred since 1974 with transects 1, 6 and 7 prograding rapidly since 1974. Transect 6 and 7 indicate the rapid growth of a large spit orientated landward into the estuary. While transects 8 and 9 show erosion rates of 3 m and 2 m per year, respectively. Approximately 60,000 m^3 of sand has been added to the spit between 1995 and 2000. Accretion at transect 1 indicates the accumulation of sand to the south, which has been observed in the aerial photograph record migrating south approximately 300 m between 1961 and 2000. Similar volumes of erosion (54,340 m^3) and accretion (60,000 m^3) suggest that sand is contained within the Bowling Green Bay coastal compartment (see chapter 7, section 7.44).

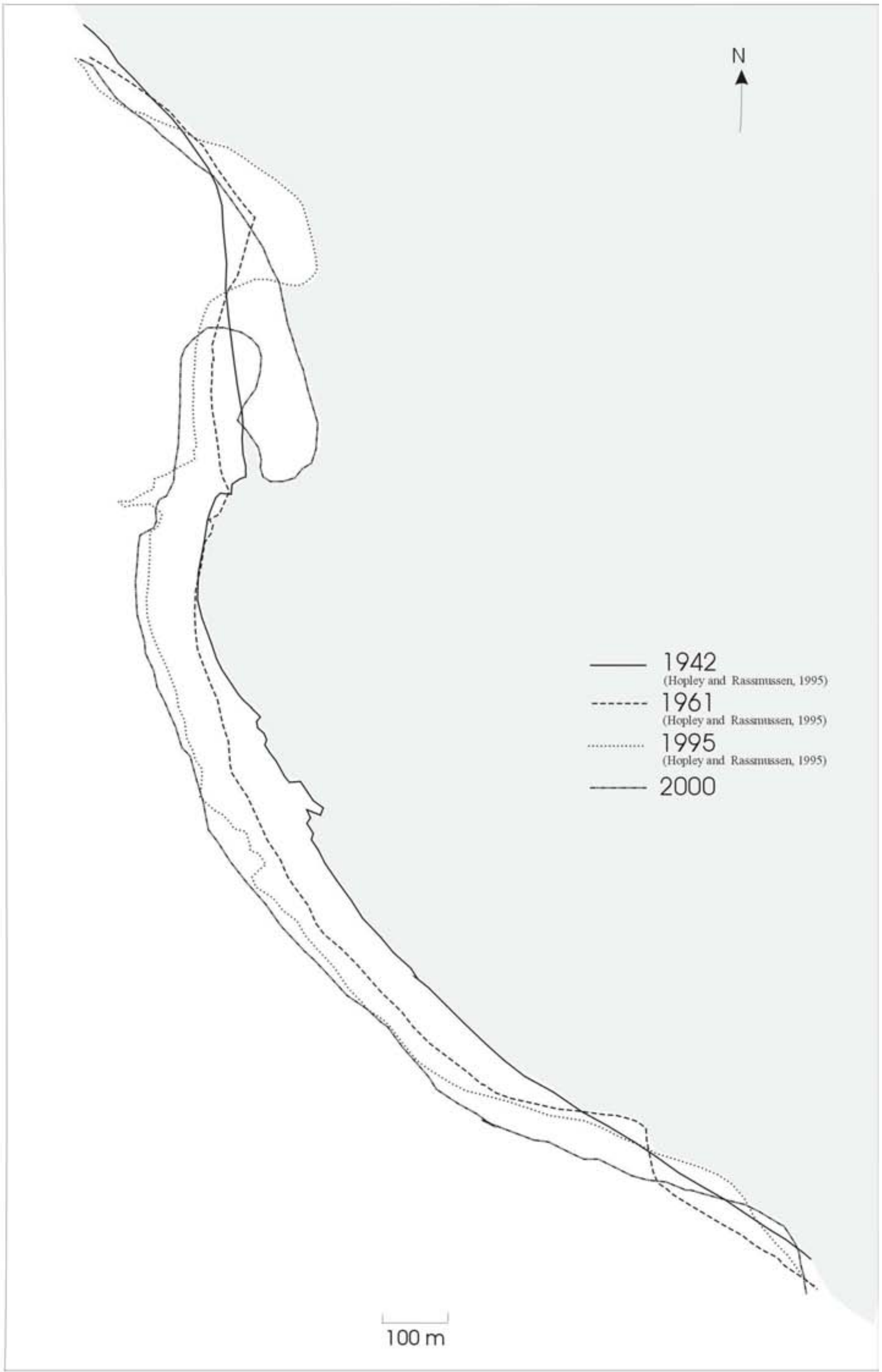

Figure 4.4 Coastal change along the western side of the Haughton River Estuary. The 1942, 1961 and 1995 shoreline position derived from Hopley and Rassmussen (1995), while the 2000 data was collected by the author (see figure 4.5 for the location of transects).

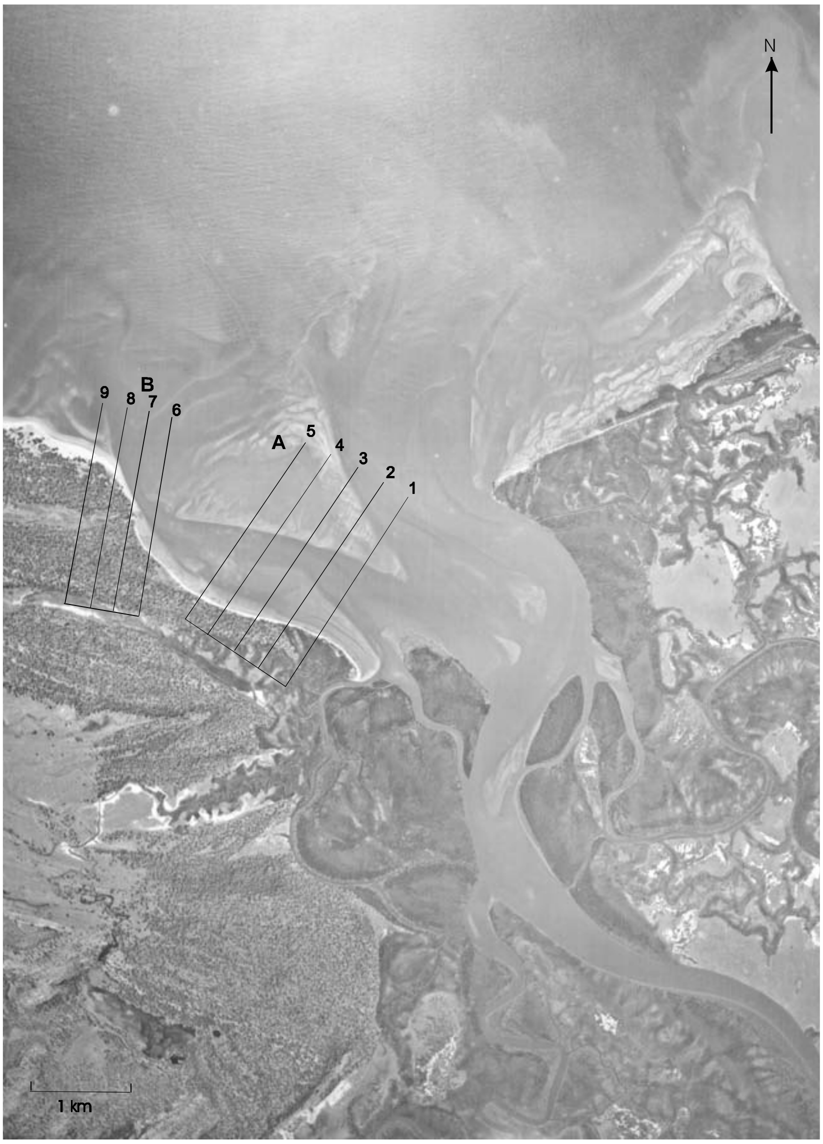

Figure 4.5 Location of transects used to measure coastal change on the western side of the Haughton River Estuary shown on the 1942 aerial photograph. A and B indicate locations of the bedforms shown in figures 4.7 and 4.8 respectively.

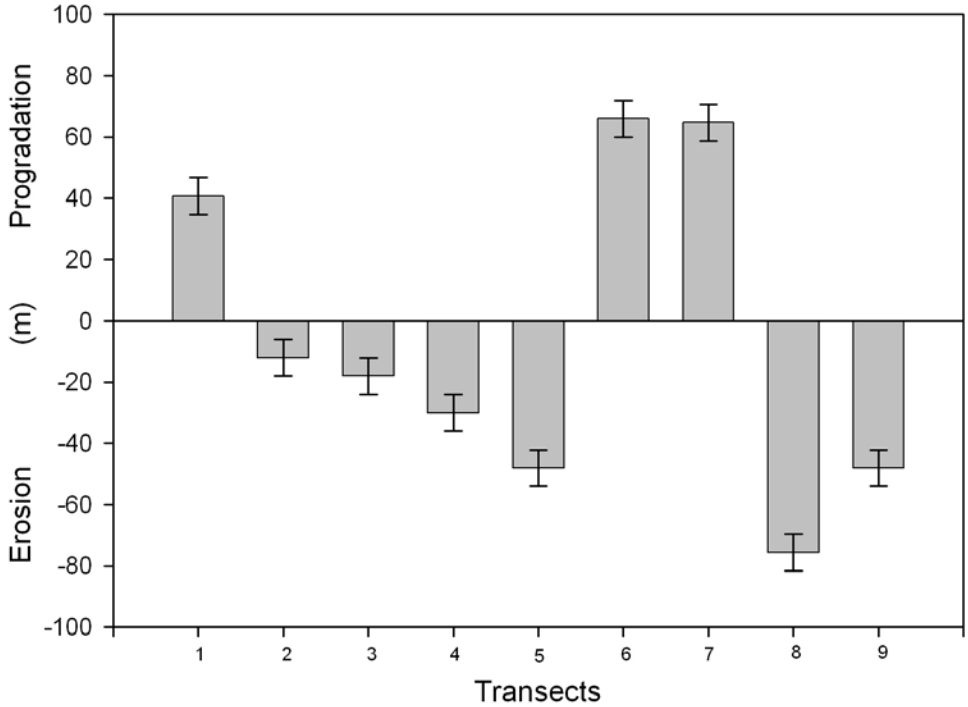

Figure 4.6 Shoreline progradation and retreat along the Haughton River Estuary measured from 1974 and 1998 aerial photographs. Standard error of measurement estimated at 6 m for 1:12,000 scale photography. (See figure 4.5 for locations of transects).

4.4.2 BEDFORMS

Bedform morphology can be used in certain setting to infer sand transport patterns and processes (see chapter 3, section 3.3.2). For example if flood tide bedforms persists for identification at low tide it suggests flood tide dominance of sand transport within the estuary (Bryce *et al.*, 1998). The most common type of bedform observed on the intertidal sand flats at low spring tides were small current ripples with an average height of 2 cm and a wavelength of 10 cm (Figure 4.7). The majority of these ripples were asymmetric, with their lee sides facing shoreward. Larger bedforms, megaripples, were observed in both the main and secondary tidal channels. These megaripples have an average height of 0.2 m and wavelength of 5 m (Figure 4.8). The lee sides of the megaripples were also orientated towards the shore. The only evidence of the outgoing tide were small current ripples (1 cm high, 5 cm wavelength) orientated towards the sea which were superimposed upon the megaripples.

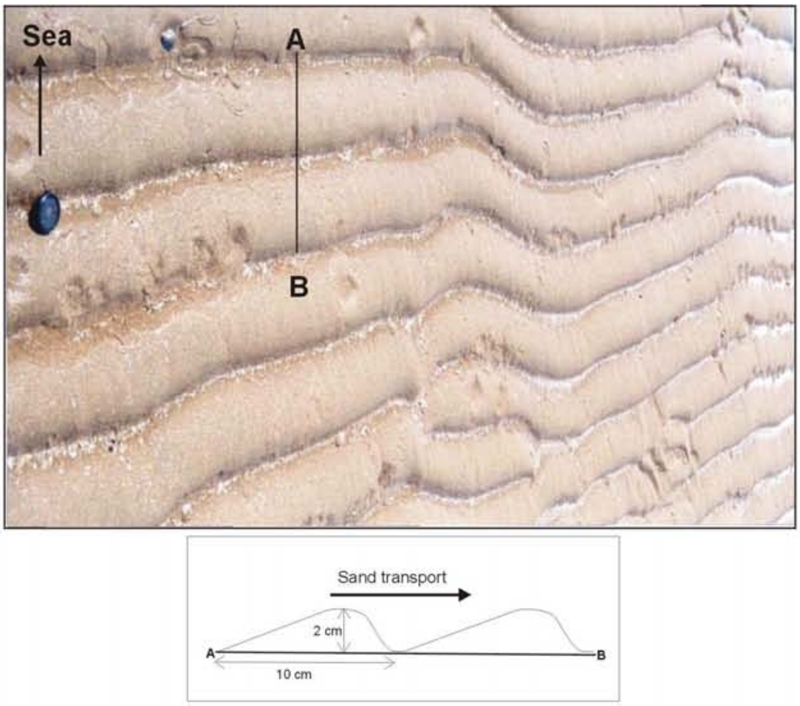

Figure 4.7. Current ripples observed at low tide at the Haughton River Estuary indicate sand transport into the estuary. Location marked as A on figure 4.5.

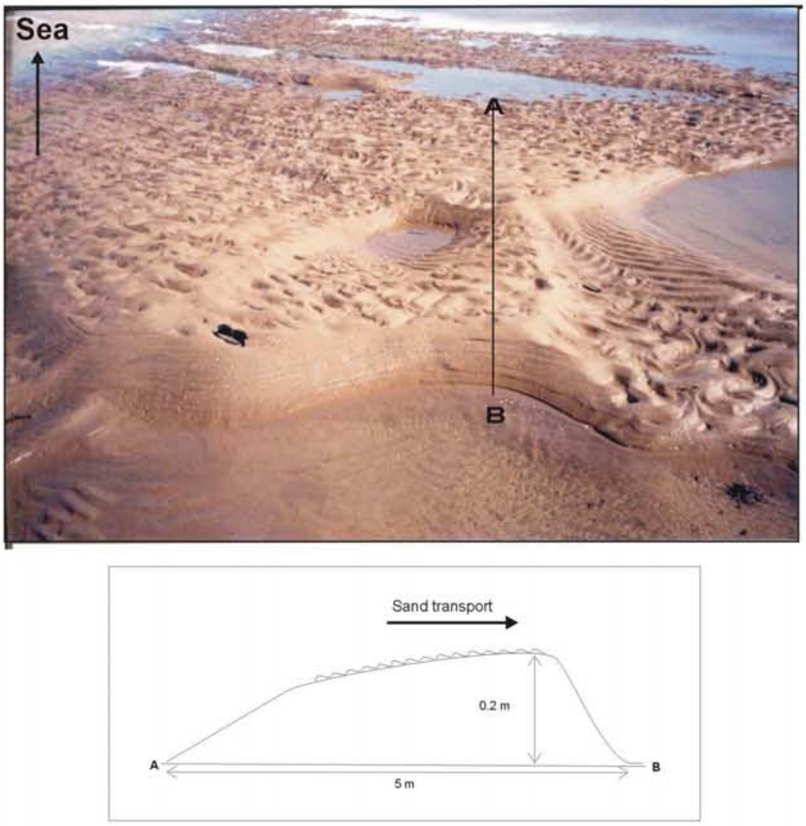

Figure 4.8. Megaripples observed at low tide at the Haughton River Estuary also indicates sand transport into the estuary. Small seaward facing current ripples occur on the crest of the megaripple. Location marked as B on figure 4.5.

4.4.3 SEDIMENTOLOGY

Over 150 surficial sediment samples and six vibrocores penetrating a maximum of 3 m below AHD were collected from the Haughton River Estuary and the adjacent coastline (see chapter 3, section 3.3.3 and 3.4.1). The locations of surficial samples and vibrocores are shown in figure 4.9 a and b. Figure 4.10 provides a summary of the results of textural analysis of the surficial samples (see Appendix D) showing the spatial distribution of sediment types. The beaches and intertidal flats are predominantly composed of well-sorted fine sand (mean grain size 0.204 mm), while well-sorted medium sand (mean grain size 0.32 mm) occurs within the tidal channels. Offshore deposits are also predominantly sandy but contain increasing proportions of silt. The only coarse, poorly sorted sediment (mean grain size 0.649 mm) was sampled from a discrete bar in the upper section of the estuarine channel.

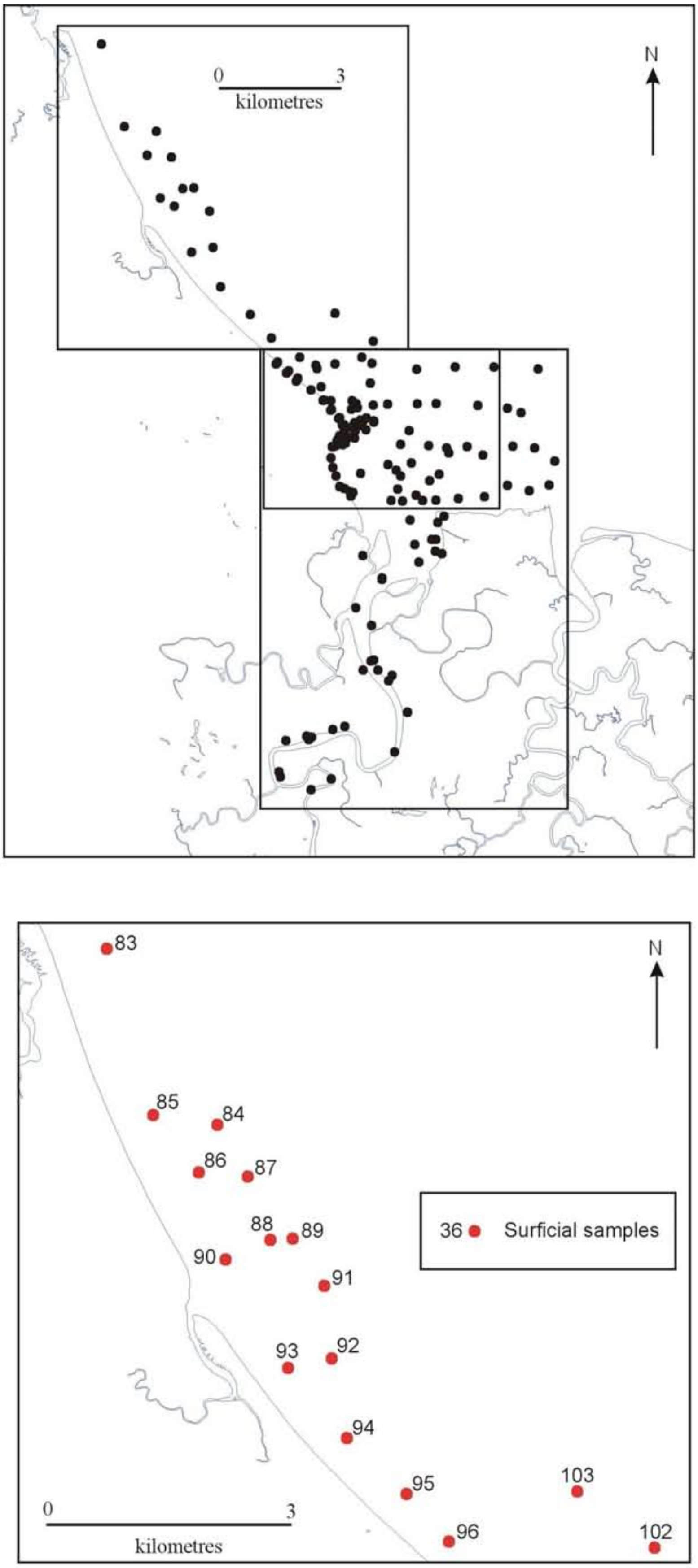

Figure 4.9 a. Locations of surficial and subsurface sediment samples taken at the Haughton River Estuary. (See Appendix D for the results of the textural analysis of samples).

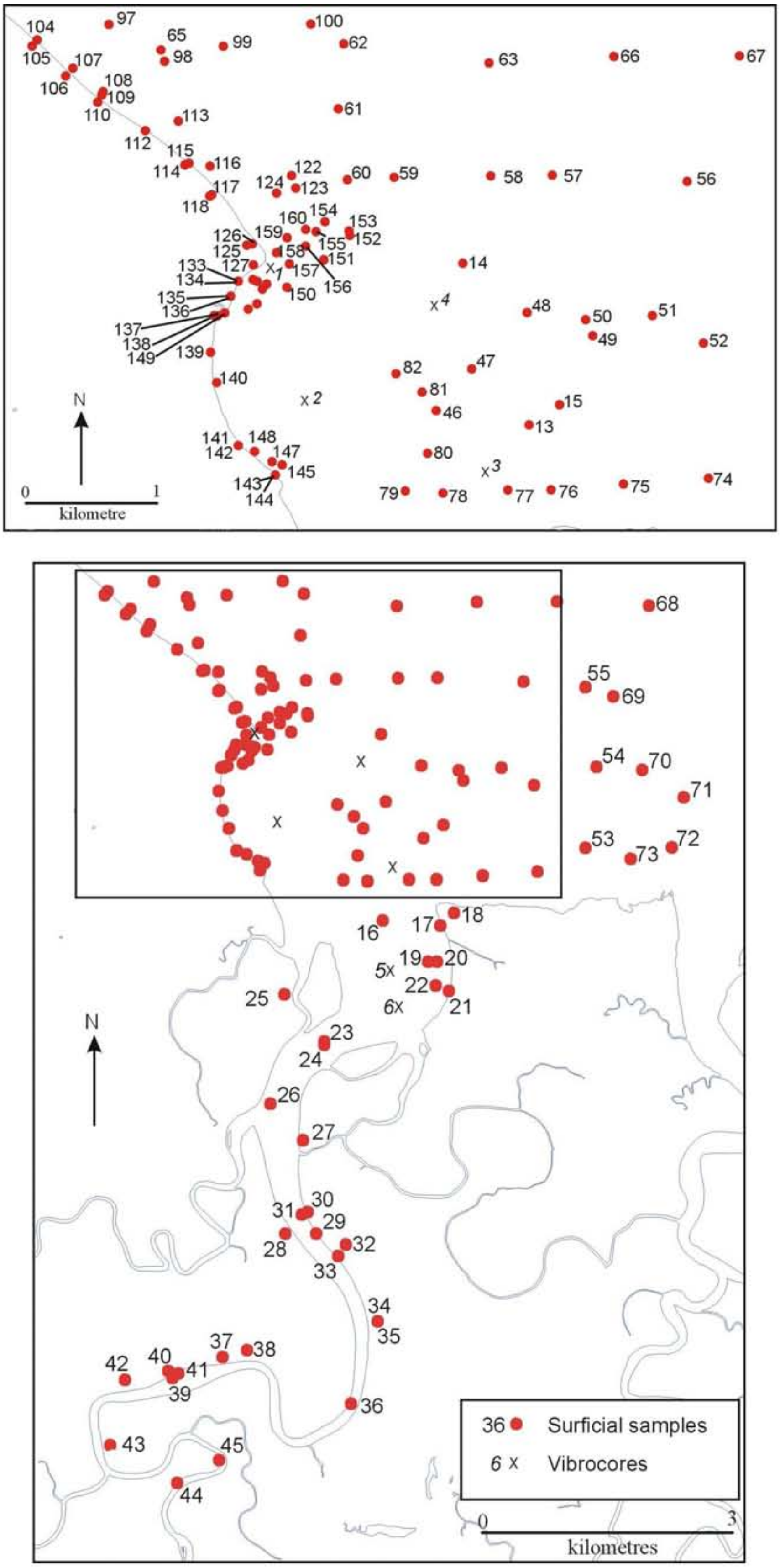

Figure 4.9 b. Locations of surficial and subsurface sediment samples taken at the Haughton River Estuary. (See Appendix D for the results of the textural analysis of samples).

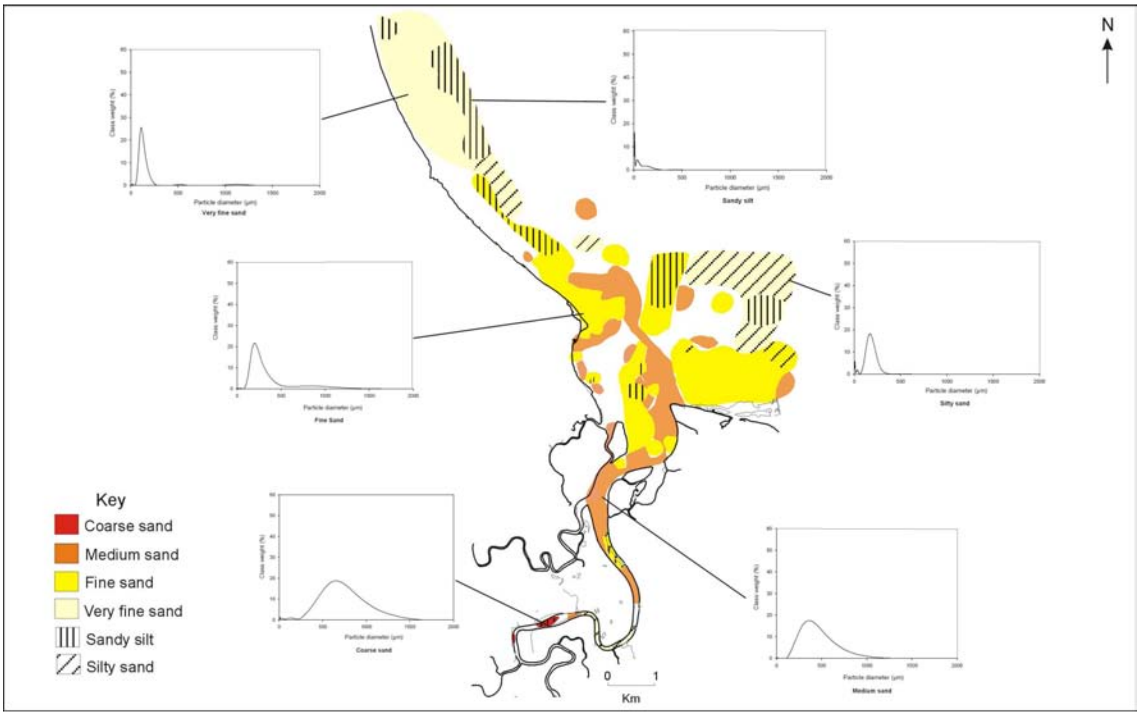

Figure 4.10. Summary of the results of textual analysis of surficial samples from the Haughton River Estuary. Histograms show the distribution of a typical example of each sediment class.

All six vibrocores had similar stratigraphies. They were predominantly composed of medium to fine sand, interspersed with silt and shell beds with occasional mud clasts. Figure 4.11 shows a cross section of the stratigraphy inferred from the estuary mouth offshore. The lack of organic material prevented a detailed chronology of sedimentation. However, mangrove peat found in HRVC 2 at 2.6 m below AHD and shells found in HRVC 4 at 0.8 m below AHD were dated (Figure 4.12). The results of conventional radiocarbon dating were 1035±105 years BP CAL (Wk10904, atmospheric data from Stuiver *et al.*, 1998; OxCal v3.5 Bronk Ramsay, 2000, see Appendix E) from mangrove peat at 2.6 m below AHD in HRVC 2 and 2378±73 years BP CAL (Wk10905, marine data from Stuiver *et al.*, 1998; Delta_R 10±7; OxCal v3.5 Bronk Ramsay, 2000, see Appendix E) from a bulk shell sample 0.8 m below AHD.

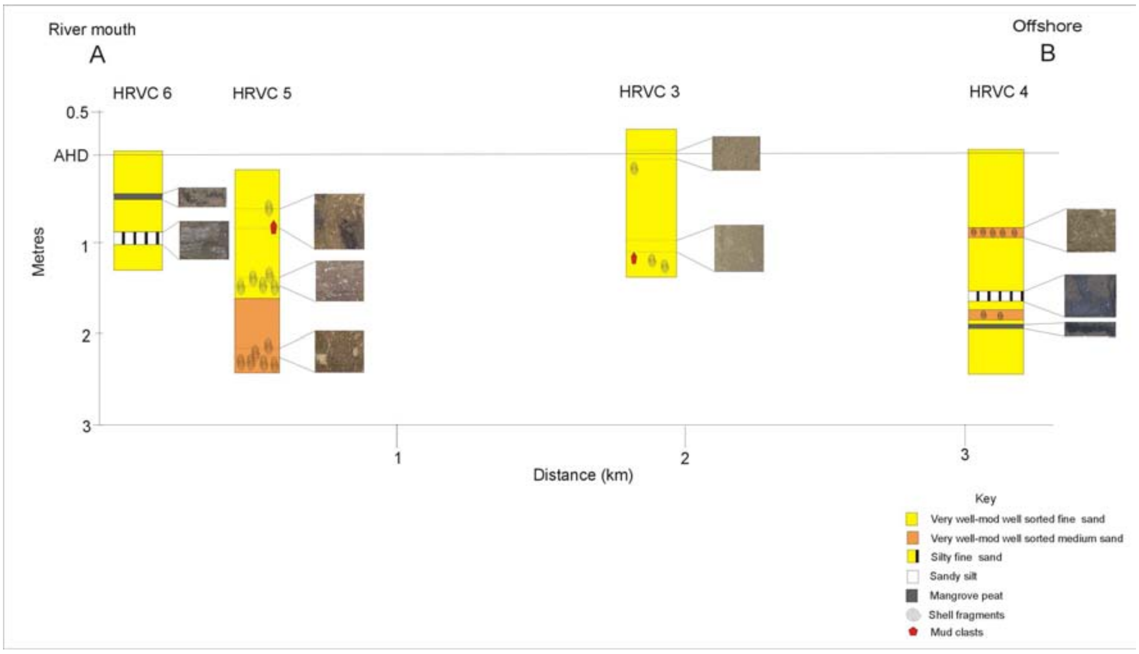

Figure 4.11. Cross-section of stratigraphy of the Haughton River Estuary including photographs of selected beds.

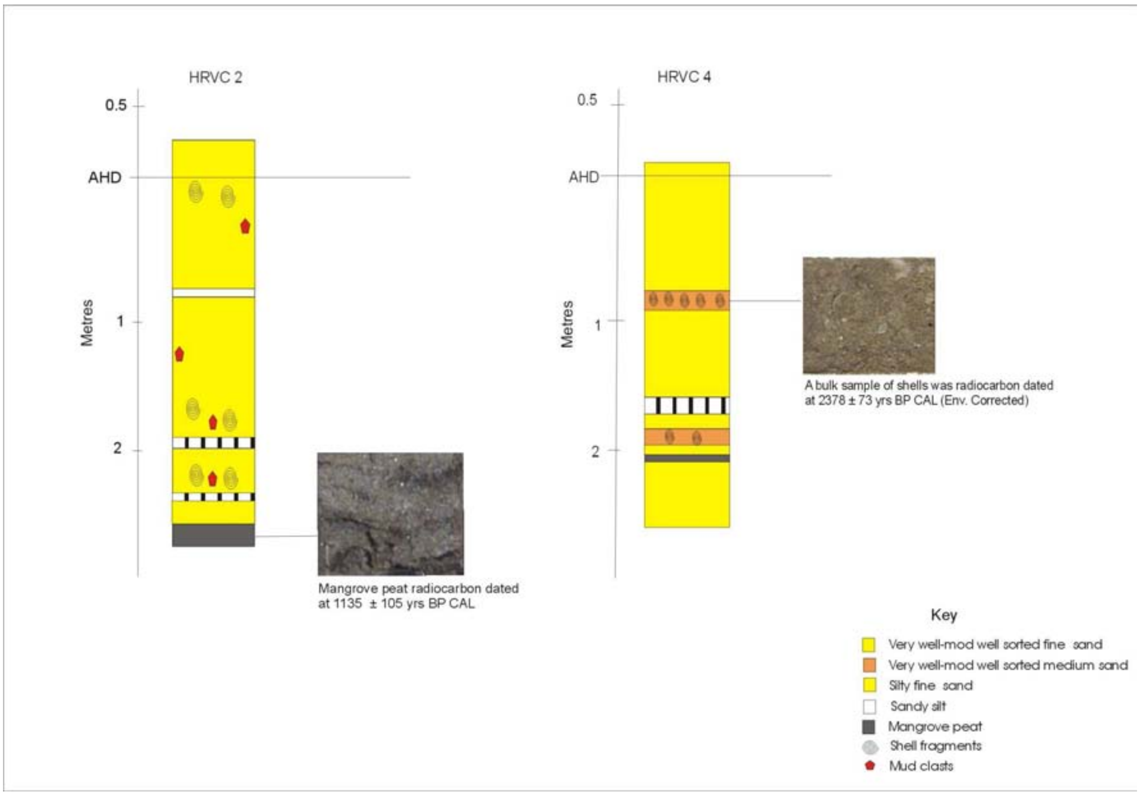

Figure 4.12. Radiocarbon dates from HRVC 2 and HRVC 4 from the Haughton River Estuary.

The textural and sorting characteristics of sediment such as grain size, sorting, skewness and kurtosis can often indicate transport processes (see chapter 3, section 3.3.2). Figure 4.13 part a-d compares subsurface, offshore, intertidal, beach and dune sediment samples according to mean grain size, sorting, skewness and kurtosis characteristics after Friedman (1961). The lack of separation of the different settings according to textural and sorting characteristics suggests that sediment has had a similar origin and transport history, despite being sampled from different locations throughout the estuary. Table 4.3 lists the textural and sorting characteristics identified in the discriminant analysis (see chapter 3, section 3.3.2) which distinguish between samples from different sedimentary environments. The closer the value to +1 or –1, the more significant the descriptive parameter is within the function. Sorting (0.863) was the most significant variable within function one. Kurtosis (0.794) was the most significant in the second function. Figure 4.14 plots the sites according to these functions i.e. sorting on the x-axis and kurtosis on the y-axis, however there is little separation of the samples according to their environment. The lack of variation of sedimentological characteristics throughout the Haughton River Estuary is further emphasised by a comparison of the different depositional environments with beach ridge sand analysed in this study and another completed over thirty years ago (Hopley, 1970a) (Table 4.4). Despite differences in their location, similar grain sizes suggests that the same amount of energy was required to transport the sediments. As sorting is a reflection of the origin and transport history of the sediment, being all fairly well sorted sands indicates substantial reworking of the sediment (Nichols, 1999). While the modern surface fine sand and that retrieved from the vibrocores have low kurtosis values the beach ridge sand has a high kurtosis value indicating a complex transport history (Hopley, 1970a). Skewness indicates the area of deposition, often dune sands are positively skewed and beach sands are negatively skewed (Hopley, 1970a) however, while most of the modern beach samples are coarsely skewed the dune and intertidal samples do not favour one skewness category.

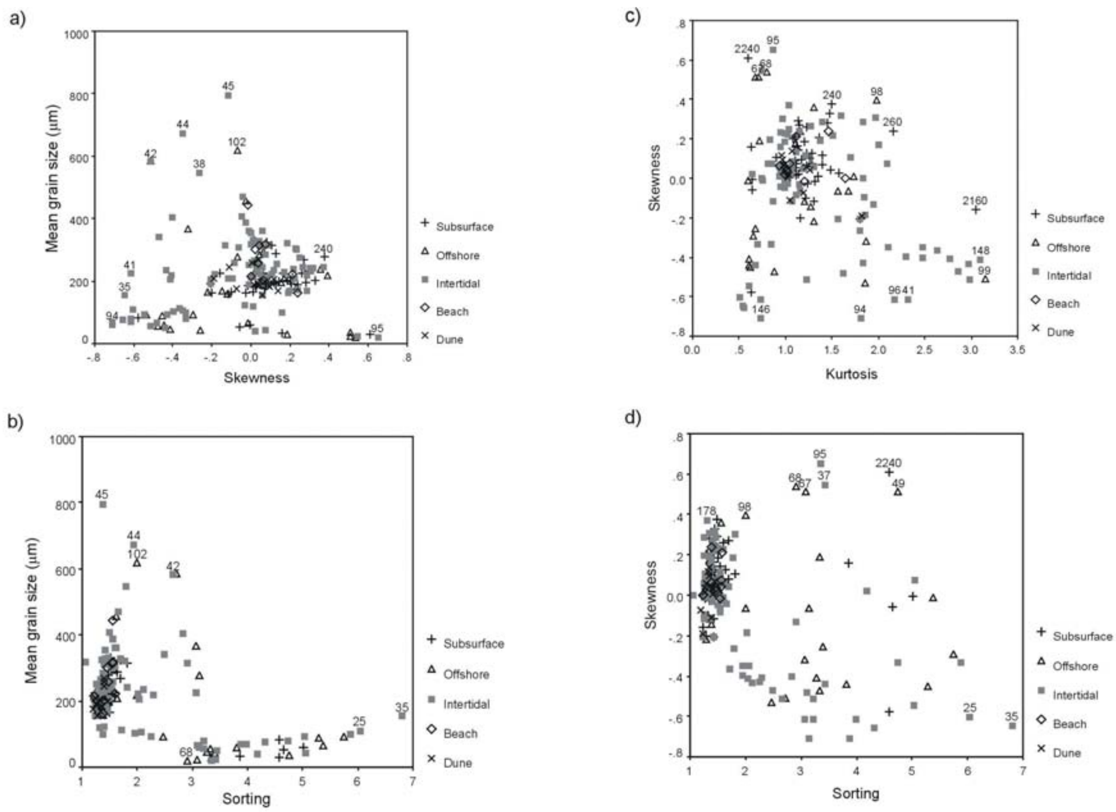

Figure 4.13 part a-d. A comparison of the surficial and subsurface sediment samples according to their mean grain size, sorting, skewness and kurtosis characteristics for the Haughton River Estuary.

Table 4.3. Structure matrix of the discriminant analysis of textural characteristics.

Variables	Function			
	1	2	3	4
Sorting	0.747*	0.487	-0.422	0.166
Kurtosis	-0.650*	0.472	0.498	0.327
Mean grain size	0.156	0.627	0.707*	0.286
Skewness	0.233	-0.214	0.511	0.800*

* indicates the largest absolute correlation between each variable and any discriminant function.

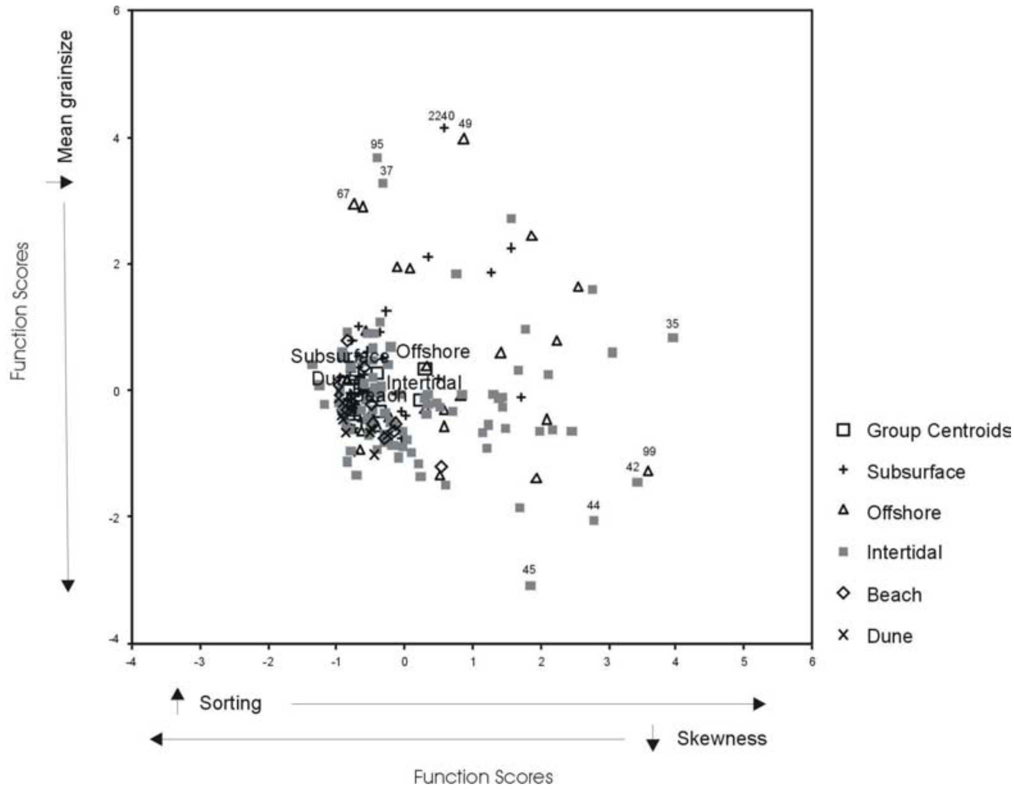

Figure 4.14. Scatter plot showing the results of the discriminant analysis using all descriptors for the Haughton River Estuary.

Table 4.4. A comparison of modern, old and beach ridge sand from the Haughton River Estuary.

Measure (Folk and Ward method)	**Modern fine sand (dune, beach, intertidal)**	**Old fine sand (Vibrocores up to 3 m deep in intertidal)**	**Beach ridges fine sand [Hopley, 1970 #50]**
Mean grain size	**Beach:** 2.376 Φ (0.195 mm) **Intertidal:** 2.250 Φ (0.213 mm) **Dune:** 2.368 Φ (0.196 mm)	2.347 Φ (0.198 mm)	2.579 Φ
Sorting	**Beach:** mod well- very well **Intertidal:** mod well- very well **Dune:** mod well- very well	0.491 Φ (0.001 mm) Well	Moderately
Skewness	**Beach:** Negative **Intertidal:** Positive, Symmetrical and Negative **Dune:** Positive, Symmetrical and Negative	-0.095 Φ Symmetrical to negative (coarse)	Negative (coarse)
Kurtosis	**Beach:** <2 **Intertidal:** <2 **Dune:** <2	0.966 – 3.049	1.466 – 12.749

4.4.4 HYDRODYNAMICS

Tidal prism calculations revealed that over 30 million cubic metres of water is exchanged during maximum spring tide (3.8 m) (Table 4.5). Cross-sectional profiles and specific data collection sites in the main and secondary tidal channels are shown in figure 4.15. For methods of tide data collection refer to chapter 3, section 3.3.4. Channel cross sections in the main channel (Sites A-C) were asymmetrical and some variation in current speed and duration was observed across the four recording sites. Figure 4.16 a-d shows the results of near bed current velocity recordings at each site during spring tidal cycles with ranges >2 m. Figure 4.17 shows field measurements of near bed tidal currents mid-estuary during a neap tide with a range of 0.8 m. The negative current velocities shown on the y-axis represents the ebb phase of the tide and the positive values the flood phase. The x-axis represents one complete tidal cycle (twelve hours). Spring tidal currents have a maximum current speed of 0.75 $m.s^{-1}$ while neap tidal currents only reach a maximum of 0.2 $m.s^{-1}$. Marked inequalities were observed in terms of the duration and maximum current velocities reached in flood and ebb phases of the tide. Data from sites A-C revealed a brief but intense flood phase lasting an average of 3 hours and reaching a maximum current speed of 0.5 $m.s^{-1}$, compared to the ebb tidal phase that lasts an average of 4.5 hours and reaches a maximum current speed of only 0.3 $m.s^{-1}$. Flood tide dominance is exacerbated in the secondary tidal channel with the flood phase lasting only 1 hour and 45 minutes and reaching a maximum current speed of 0.75 $m.s^{-1}$.

Table 4.5. Tidal prism for the Haughton River Estuary at spring and neap tides.

Tide	Tide range	Low tide water volume	High Tide water volume	Tidal Prism
Maximum spring tide	3.8 m	12,337,500 m^3	44,043,750 m^3	31,706,250 m^3
Average neap tide	1 m	12,337,500 m^3	20,681,250 m^3	8,343,750 m^3

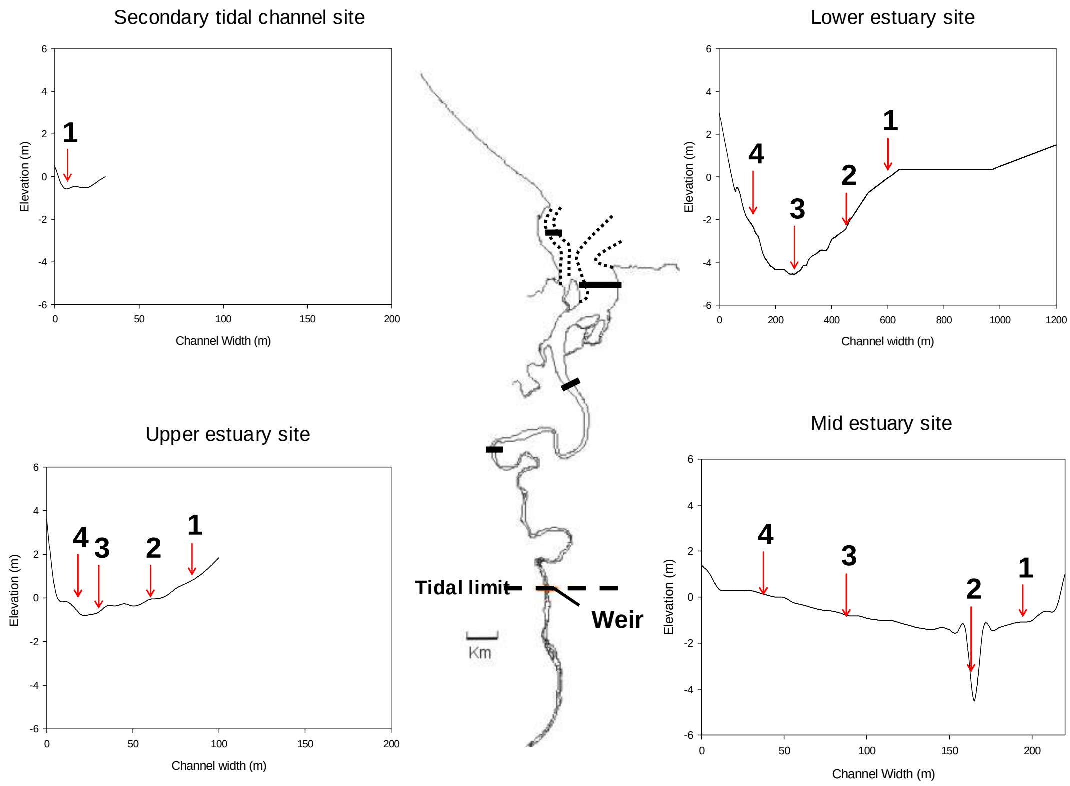

Figure 4.15. Locations and cross-sections of tidal current data collection sites, Haughton River Estuary.

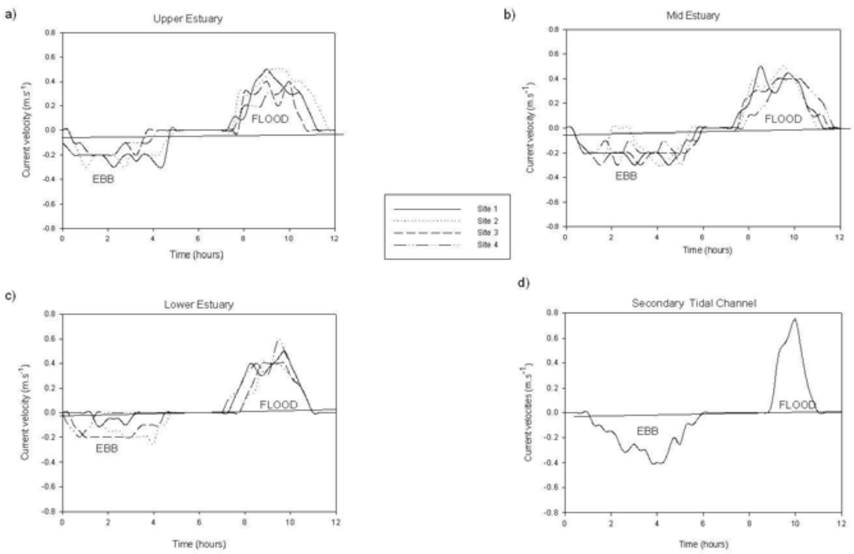

Figure 4.16 a-d. Spring tide current velocities for upper, mid and lower estuary sites and secondary tidal channel. Note: Negative current velocity values represent ebb and tide currents and positive values flood tide currents.

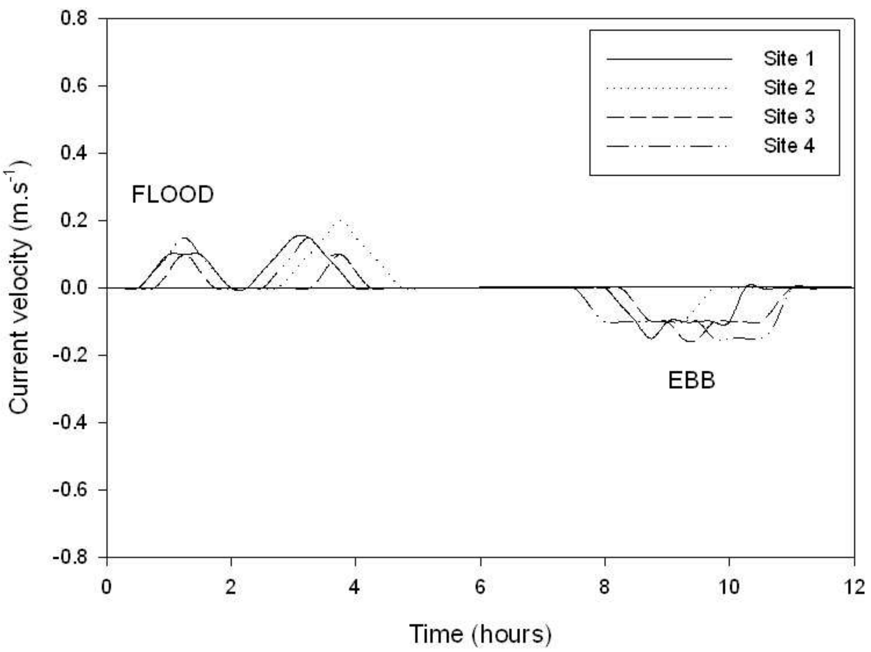

Figure 4.17. Near bed (1 m above) current velocities during a neap tide at the mid estuary site fo the Haughton River.

4.4.5 TIDAL SAND TRANSPORT MODELLING

As indicated in chapter three, section 3.3.4.2, three bedload equations (Engelund and Hansen, 1967; Gadd *et al.*, 1978; Hardisty, 1983) were used to model potential sand transport by tidal currents. Modelling of bedload transport predicts the movement for one particular grain size not the total sediment load. Equations by Gadd *et al.* (1978) and Hardisty (1983) use sediment transport thresholds from fine (0.18 mm) and medium sand (0.45 mm). The estuary is dominated by fine-medium sand with a modal grain size of 0.32 mm. As available equations do not support this exact grain size (equations support only grain sizes of 0.18 mm and 0.45 mm), the predicted volumes of fine and medium sand represent the upper and lower boundaries for transport. A sediment transport threshold of 0.16 $m.s^{-1}$ and 0.19 $m.s^{-1}$ derived from Gadd *et al.'s* (1978) equation was applied to calculate the potential volumes of fine (0.18 mm) and medium (0.45 mm) sand that could potentially be transported in and out of the estuary by tidal currents. Figure 4.18 shows that current velocities recorded during a neap tide at the mid-estuary (Site B) do not have the competency to transport fine or medium sand. Sufficient current velocities were reached during ebb and flood phases of spring tides at all four sites to transport both fine and medium sand (Figure 4.19 parts a-d). Flood tide currents during spring tides are up to five times more competent to transport fine and medium sand than ebb tidal currents, assuming a linear relationship.

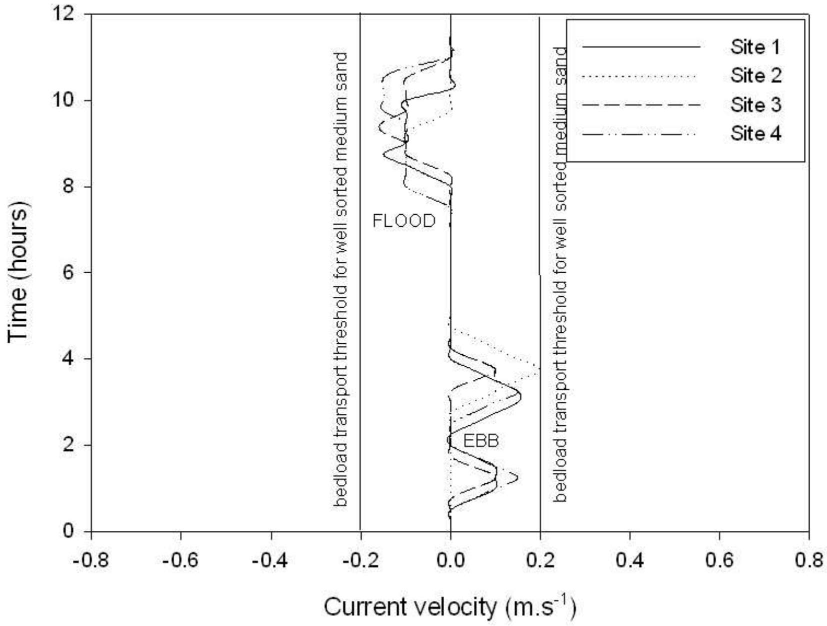

Figure 4.18. Competency of neap tide currents measured at the mid estuary site to transport bedload. Note: Negative current velocity values are flood tide currents and postive values are ebb tide currents.

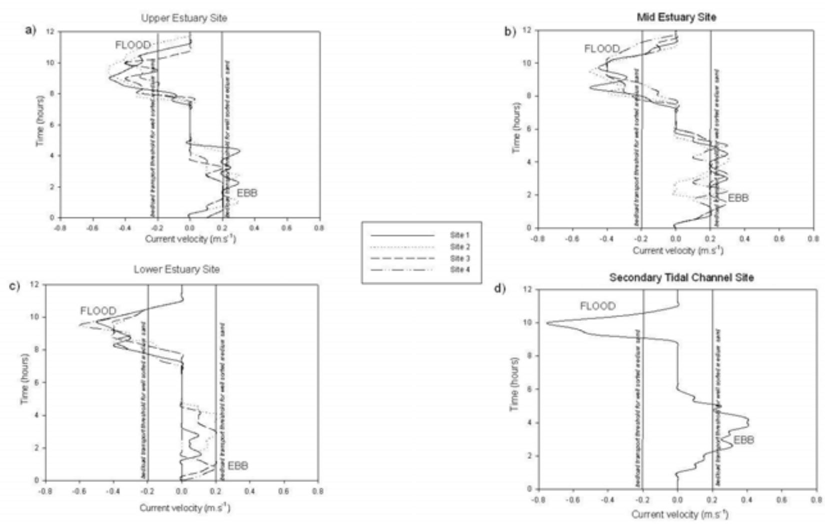

Figure 4.19 parts a-d. Competancy of spring tide currents to transport bedload for all sites. Note: Negative current velocity values are flood tide currents and positive values are ebb tide currents.

Predicted volumes of medium and fine sand potentially transported landward or seaward per spring tidal cycle using all three equations (Engelund and Hansen, 1967; Gadd *et al.*, 1978; Hardisty, 1983) are shown in figure 4.20 and 4.21. The predicted volume of medium sand does not include volumes of fine sand. Potential volumes of transport were calculated for the four recording sites across the upper, mid and lower estuary sites and secondary tidal channel and then averaged for each location. The direction of net sand transfer is clearly into the estuary due to flood tide dominance. Potentially an average of 11 times more fine sand and 18 times more medium sand is predicted to be transported into the estuary than out to sea. Figure 4.22 shows the volumes of fine and medium sand that could be potentially transported landward into the estuary per year, which ranges from 33,750 – 175,000 m^3 and 13,750 – 34,375 m^3 for fine and medium sand, respectively.

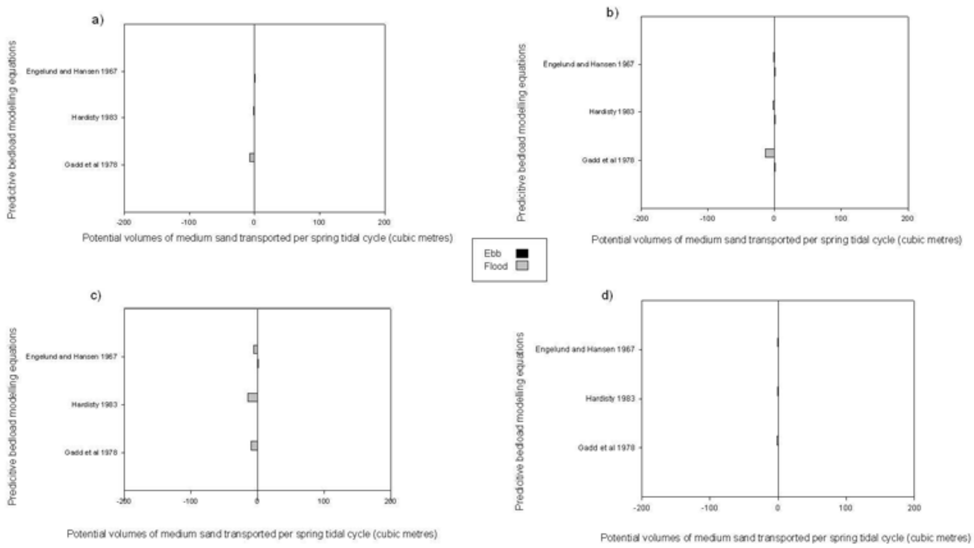

Figure 4.20 a-d. Predicted volumes of medium sand potentially transported landwards and seawards of the Haughton River Estuary per spring tidal cycle. Note: The scale of the x-axis is an order of magnitude smaller than the volumes of fine sand presented in figure 4.21.

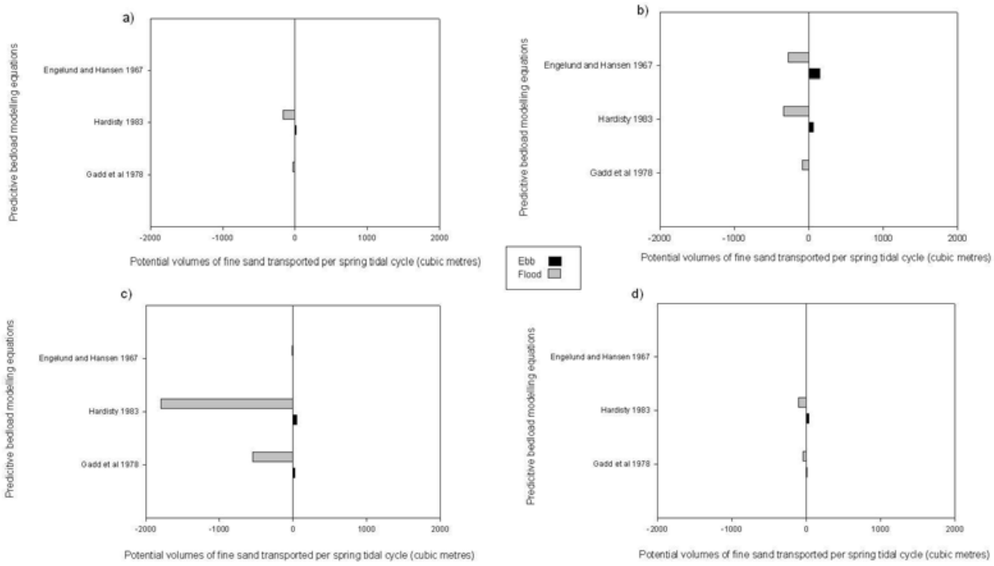

Figure 4.21 a-d. Predicted volumes of fine sand potentially transported landwards and seawards of the Haughton River Estuary per spring tidal cycle. Note: The scale of the x-axis is an order of magnitude larger than the volumes of fine sand presented in figure 4.20.

4.5 CONCLUSIONS

A conceptual model of the spatial and temporal patterns of coastal sand transfer in the Haughton River Estuary was developed based on the sedimentological, stratigraphic and hydrodynamic data collected.

4.5.1 COASTAL CHANGE

The results from aerial photo analysis revealed the dominance of tidal processes on sand transfer in the Haughton River Estuary. Previous work by Hopley and Rasmussen (1995) attribute the rapid changes on the western side of the estuary identified in section 4.2.1, to a localised cycle of erosion and deposition of coastal deposits as a consequence of the secondary tidal channel migrating across the estuary. This theory is supported by predicted volumes of fine sand transport out of the estuary. Erosion has yielded 54,000 m^3 from the Cungulla coast in the last 24 years and 60,000 m^3 of fine sand has been added to the spit between 1995 – 2000. This suggests that even though the secondary tidal channel is a flood-dominated tidal channel, ebb tidal currents are still capable of moving volumes of fine sand seawards. Predictions by Hardisty (1983) using a sediment transport threshold of 0.16 $m.s^{-1}$, suggest that ebb tides have the potential to transport 10,674 $m^3.y^{-1}$ of fine sand. This transport rate equates to 53,372 m^3 over 5 years. The remarkably similar volumes being eroded from the coast and deposited on the spit suggest that reworked coastal deposits are contained within the Bowling Green Bay coastal compartment. There is little evidence of change in other parts of the estuary with location of the eastern bank of the estuary remaining stable and the mangrove fringe becoming more established over the 60 year record.

4.5.2 BEDFORMS

The investigation of bedforms supported the conclusion that sand transfer in the Haughton River Estuary was dominated by tidal processes. Landward facing dunes and ripples flood-dominated) consistently persist at low tide, suggesting that the direction of net sand transfer is into the estuary. Bryce *et al.'s* (1998) observations of landward facing bedforms in the Normanby River Estuary were also indicative of net landward transfer of sand.

4.5.3 SEDIMENTS

The results of sedimentoligcal investigations provide further evidence that sand transfer in the Haughton River Estuary is dominated by tidal processes which results in the net landward transfer of sand. Rounded grains and low proportions of feldspars (< 5%) in the majority of samples taken from the estuary suggest the sands are mature and probably of marine origin (Friedman, 1961; Roy *et al.*, 1980). The similarities of sand characteristics throughout the estuary and the adjacent beach ridge complex suggest that a likely source for this sand is offshore reserves (Hopley, 1970a). Belperio (1978) identified large sand reserves in Bowling Green Bay which were relict deposits from when the Burdekin River discharged into the bay prior to 6 ka BP. The original source of the coarse sediment found in the upper reach of the estuarine channel seemed likely to be fluvial. However on closer inspection, the angularity of the grains and the isolation of the bar within a widened section of the channel, suggests that it was not transported there from upstream but is locally derived from scouring of the adjacent banks. This is similar to the shoals Woodroffe *et al.* (1986) identified in the tidal rivers of the Northern Territory.

Comparisons of grain size, sorting, skewness and kurtosis have failed to distinguish between sediment sampled from different environments within the Haughton River Estuary (see figure 4.13 part a-d). The outliers are commonly samples 42, 44, 45 that were taken from the discrete coarse sediment bar in the upper reaches of the estuarine channel which as discussed previously is the result of localised bank erosion. Moreover a discriminant analysis of the sediment characteristics and sampling location revealed that only 38.9% of samples were correctly classified to their environmental setting by sorting and kurtosis characteristics. The textural characteristics of the majority of the samples (> 60%) do not match their environmental setting. This supports Visher's (1969) comment that the use of grain size distributions to determine environment is problematic because the same sedimentary processes occur within a number of settings and the consequent textural response is similar. The lack of variation between samples also suggests the majority of sediments in the Haughton River Estuary may also be derived from the same source. Similarly the comparison to beach ridge sediments collected by Hopley (1970a) revealed distinct similarities between modern and past sediments, suggesting that modern surficial sediments may be the result of reworked previously deposited sediments. No fluvial sand could be identified in the sub-surface samples retrieved from the Haughton River Estuary. Bryce *et al.* (1998) results show less than 1% terrigenous sand in the cores from the Normanby River Estuary, suggesting that both estuaries have been infilling with marine sand.

Sub-surface sediments (up to 2.6 m below AHD) collected from the river mouth revealed a similar pattern of marine sedimentation over at least the last 1 ka. The results of a conventional radiocarbon date from mangrove peat 1035±105 years BP CAL at 2.6 m below AHD (Wk10904, atmospheric data from Stuiver *et al.*, 1998; OxCal v3.5 Bronk Ramsay, 2000) suggest that the estuary has been infilling with medium to fine marine sand at an average rate of 2.5 $mm.y^{-1}$ over the last 1 ka. While the shells dated at 0.8 m below AHD were dated at more than twice that of the peat at 2378±73 years BP CAL (Wk10905, marine data from Stuiver *et al.*, 1998; Delta_R 10±7; OxCal v3.5 Bronk Ramsay, 2000), this date must be interpreted in context. The age was derived from a bulk sample of a number of different shell fragments indicating reworking. Therefore, while the organisms may have died over 2 ka BP their shells were probably buried many years after. However it is reasonable to believe that the mangrove peat is in situ and evidence of minimal bioturbation through all the cores provides further assurance that this date is reliable. Consequently average sedimentation rates are inferred from the mangrove peat date rather than the shells.

4.5.4 TIDAL SAND TRANSFER

Measurements of near bed tidal currents during spring tides show that both ebb and flood currents have the competency to transport medium to fine sand (0.32 - 0.20 mm). However, maximum near bed flood currents are five times more competent to move sediment than the ebb currents, suggesting that the direction of net sand transfer is into the estuary. Larcombe and Ridd (1995) compared predictions from these same equations with actual measurements of bedload transport in a tidal mangrove creek, Gordon Creek near Townsville, and found that overall the predictions of sediment transport were good. The large disparity between the predictions of the three equations is common to other studies (Larcombe and Ridd, 1995). The predicted volumes in this study showed a similar pattern to the results from Larcombe and Ridd (1995) with the volumes predicted, using Gadd *et al*.'s, (1978) equation, several orders of magnitude larger than that predicted by the other two equations. The predictions derived from Hardisty's (1983) equation were considered the most accurate, given the results of Larcombe and Ridd's (1995) experiments. Predictions using Engelund and Hansen (1967) equation were much lower than the volumes predicted using the other equations, probably due to the relatively low tidal current velocities occurring in the Haughton River Estuary compared to those upon which the equation was originally derived. In this study the calculation of Gadd *et al's.* (1978) and Hardisty's (1983) equations were based on sediment thresholds from Guy *et al.* (Guy *et al.*, 1966) which are derived from flume measurements of bedload transport (0.16 m.s^{-1} for fine sand and 0.19 m.s^{-1} for medium sand) and agree with the widely used Hjulstrom (1935) curve. However Larcombe and Ridd (1995) use a much higher threshold velocity for medium sand of 0.4 m.s^{-1} based on a regression analysis of the results from actual measurements of megaripple migration in Gordon Creek. Recalculation of Gadd *et al.* (1978) and Hardisty (1983) formulas for medium sand using the threshold velocity of 0.4 m.s^{-1} still shows a net landward transfer of medium sand into the estuary but at much lower volumes (see table 4.6). Using the higher sand transport threshold resulted in predictions of no seaward transfer of medium sand as ebb tide velocities did not reach the sediment transport threshold of 0.4 m.s^{-1}.

Table 4.6. Results of sand transport modelling for medium sand using equations from Engelund (1967), Gadd *et al*. (1978) and Larcombe and Ridd (1995).

	Upper Estuary Site (kg per spring tide)	Mid Estuary Site (kg per spring tide)	Lower Estuary Site (kg per spring tide)	Secondary Tidal Channel (kg per spring tide)
Gadd *et al*. (1978) using sand (0.45 mm) transport threshold of 0.19 m.s^{-1} (Guy, 1966)	12081.85	20931.36	151137.56	13489.00
Gadd *et al*. (1978) using sand (0.45 mm) transport threshold of 0.4 m.s^{-1} (Larcombe and Ridd, 1995)	166.35	115.03	4617.96	2779.56
Hardisty (1983) using sand (0.45 mm) transport threshold of 0.19 m.s^{-1} (Guy, 1966)	1734.07	3337.66	22791.68	885.85
Hardisty, (1983) using sand (0.45 mm) transport threshold of 0.4 m.s^{-1} (Larcombe and Ridd, 1995)	820.80	822.38	8143.20	812.70
Engelund (1967) for mean grain size of 0.45 mm (no transport threshold data was used in the equation)	492.10	754.65	8236.00	64.80

Like Larcombe and Ridd (1995) the predictions derived from the Hardisty (1983) equation were chosen as the most likely representation of sand transfer volumes in the Haughton River Estuary, however the lower sediment transport thresholds of Guy *et al.* (1966) were used. Potential volumes of annual sand transfer into the estuary were extrapolated from the predictions for one tidal cycle and are used in the following conceptual model. Extrapolating the predictions from one tidal cycle over 12 months compounds the error already associated with these predictions. For example Larcombe and Ridd (1995) found a strong diurnal inequality in tides measured close to Townsville. However as this data is not available in this study, the estimated volumes of sand that could potentially be transported into the estuary are presented to indicate the order of magnitude rather than absolute figures.

Hydrodynamic and bedload modelling investigations suggest that the secondary tidal channel in the Haughton River Estuary is flood dominated. Tide-dominated estuaries in the literature are often reported as having mutually exclusive tidal channels (one flood and one ebb dominated) (Dalrymple *et al.*, 1992; Heap *et al.*, 2001), however in the Haughton River Estuary both tidal channels are flood dominated. Hopley and Rasmussen (1995) previously identified this channel as ebb dominated based on morphological evidence. As previous classifications of tide-dominated estuaries have been derived from studies of macro-tidal estuaries, the meso-tidal range of the Haughton River Estuary may contribute to this anomaly. Other variations from the literature description of a tide-dominated estuary have been noted in the Haughton River Estuary, for example the lack of a well-developed funnel-shaped mouth commonly associated with tide-dominated systems in macro tidal settings (Wright and Coleman, 1973; Woodroffe *et al.,* 1986). Indeed, Bryce (2001) attributed the lack of a well-developed funnel-shaped mouth in other tide-influenced systems of tropical north-east Queensland to their meso-tidal setting.

4.5.5 CONCEPTUAL MODEL OF SAND TRANSFER

The resultant conceptual model (Figure 4.22) incorporates these findings over contemporary and evolutionary time scales. The sand delivery rates used in this model were calculated for the Haughton River using discharge data from the Powerline gauge and modelling software (MIKE II) based on Ackers and White (1973) equations (Kinhill *et al.*, 1996). The use of these figures are far from ideal due to the error associated with using yearly averages in highly variable discharge rivers, like the Haughton River (Hean and Nanson, 1987). Thus, these figures must be taken as 'potential' amounts of bedload transport given that the availability of sand is limited and that the short duration of flooding and morphology of the channel are not conducive to transporting sand into the estuary (see section 4.3), even during flood events (ARI > 20 years). Indeed only 2% of the estimated potential sand load at Powerline Gauge is modelled to reach the estuary. That any sand is delivered to the estuary may be an overestimate considering that deposits of fluvial sand could not be identified downstream of the tidal limit, with the only coarse sand derived from local bank scour and not transported from upstream (see section 4.3.3). Despite the questionable accuracy of these figures, they demonstrate that a relatively minor proportion of fluvial sand is potentially delivered to the estuary from upstream compared to the potential influx of marine sand by flood tide currents.

Indeed the dominance of tidal processes is further evidenced by the comparison of tidal and fluvial discharges. The exchange of over 30 million cubic metres of water at maximum spring tide (range of 3.8 m, see table 4.5), which occurs three times a year, produces a discharge of 2936 $m^3.s^{-1}$ over a 3 hour flood tide phase. Only four fluvial events (1971/2 – 3964 $m^3.s^{-1}$, 1977/8 – 3865 $m^3.s^{-1}$, 1990/1 – 3547 $m^3.s^{-1}$ recorded at the Powerline Gauge) have exceeded that discharge since 1971.

While tidal sand transport figures are also predictions of the ‘potential’ volume of medium to fine sand that could be moved into the estuary by flood tidal currents, given that the sand supply is unlimited and energy is only partially limited, these figures could be quite conservative. The two most likely sources of the fine to medium marine sand that dominates the estuary are relict reserves of Burdekin River sand or adjacent beach ridge deposits. Belperio (1978) identified major reserves of terrestrial sand offshore of the Haughton River and interpreted them as deposits from the Burdekin River when it discharged in to Bowling Green Bay prior to 6 ka BP (Hopley, 1970a). Additional sources of sand include the reworking of coastal deposits. For example increased significant wave heights associated with tropical cyclones may increase erosion of the lower Haughton Estuary as reported during Cyclone Althea, December 1971 (Hopley and Rasmussen, 1995). The frontal dunes of the adjacent beach ridge complex are showing signs of erosion with notable scarping (Figure 4.23). Truncation of the southern end of the beach ridge complex indicates reworking of these coastal deposits by tidal and perhaps wave processes in the past and present (Hopley and Rasmussen, 1995).

Predictions of contemporary sand transfer processes must be interpreted in the context of the evolution of the estuary. Sub-surface sediment analysis and radiocarbon dating (see section 4.3.3) suggest that the estuary has been infilling with medium to fine sand at an average rate of ~2.5 $mm.y^{-1}$ for the last 1 ka. Over the area of the lower estuary that rate equates to an average influx of 20,650 m^3 per year, which is four times the volume predicted using Hardisty’s (1983) equation (sediment transport threshold of 0.19 $m.s^{-1}$) and similar to the predictions using Gadd *et al.’s* (1978) equation (sediment transport threshold of 0.19 $m.s^{-1}$) for medium sand. Predictions of the annual influx of fine sand into the lower estuary are nine and 28 times greater than this using Gadd *et al.’s* (1978) (sediment transport threshold of 0.19 $m.s^{-1}$) and Hardisty’s (1983) (sediment transport threshold of 0.19 $m.s^{-1}$) equations respectively. However predictions using Engelund and Hansen’s (1967) equation were an order of magnitude lower than the estimated annual influx of 20,625 m^3. Predictive bedload modelling in the Normanby River estuary suggest a landward influx of medium sand at a similar rate of 17,500 $m^3.y^{-1}$ (Bryce *et al.*, 1998). Predictive bedload modelling together with the lack of coarse, poorly-sorted, angular sediments within the estuary suggests that the relative proportion of sediment derived from the Haughton River is minor compared to the influx of marine sediment. The data suggests that the modern Haughton River Estuary is a sink for marine sediment. The conceptual model fits Dalrymple *et al.* (1992) model for estuaries as long-term sediment sinks infilling with sediment since drowning following the Holocene marine transgression (chapter 2, see section 2.2).

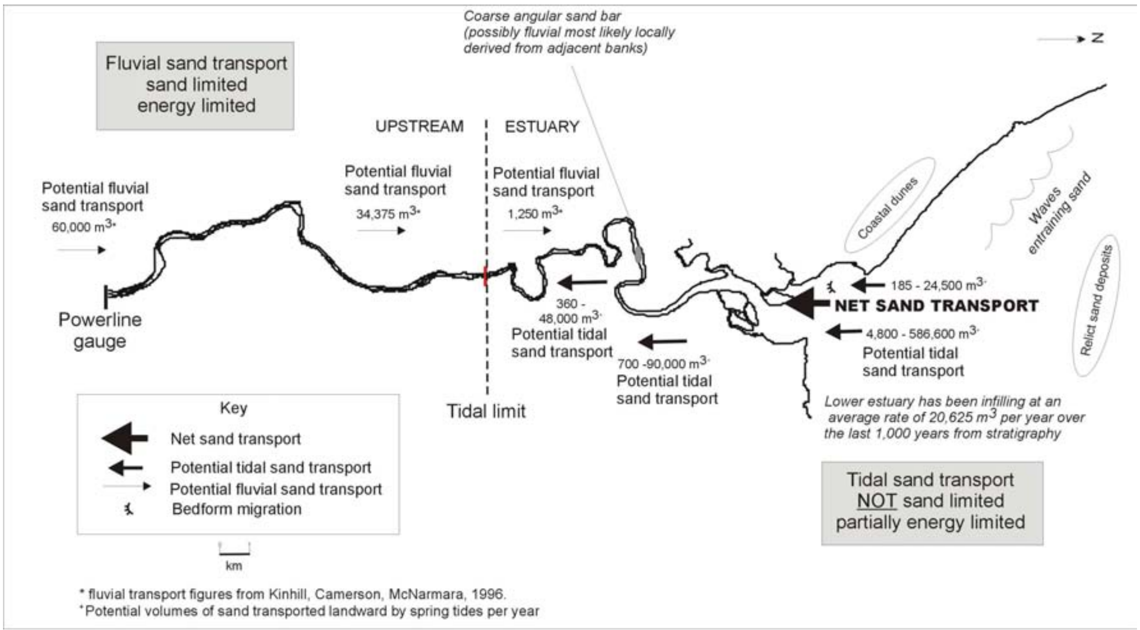

Figure 4.22. Summary diagram of net sand transport trends at the Haughton River Estuary as indicated by bedform orientations, grain size patterns and dominant current directions. Flood tide currents are the most dominant, hence net estuarine sand transport direction is into the estuary.

Figure 4.23. Erosion scarp (~2m high) on frontal dunes of beach ridges adjacent to the Haughton River Estuary (07/03/01).

CHAPTER 5 – ADDING WAVES TO THE EQUATION: THE ELLIOT RIVER ESTUARY.

5.1 INTRODUCTION

The Elliot River Estuary is a good example of coastal system influenced by waves and tides. The results of the aerial photograph analysis, sedimentological and hydrodynamic studies of the Elliot River Estuary are presented and briefly discussed in this chapter (see chapter seven for a more detailed discussion). Contemporary and evolutionary patterns and processes of sand transfer are inferred from the results and presented in a conceptual model. Comparisons are drawn with the results from the Haughton River Estuary (chapter four).

5.2 GEOMORPHOLOGY

The Elliot River is located ~200 km south of Townsville (Figure 5.1). The physical attributes of the system are summarised in Table 5.1. The Elliot River is 40 km long and drains a catchment area of 478 km^2. Compared to the Haughton River, the Elliot River has a comparatively gentle descent to the coast (fluvial reach 0.0064; estuarine reach 0.0025). The mouth of the Elliot River estuary is constricted by the rapid growth of sand spits from the north-west and a 4.25 km long sand barrier complex to the south east. The estuary is dominated by sandy sediments with large flood and ebb tidal deltas. Directly adjacent to the mouth of the Elliot River is Cape Upstart, a sub-circular granitic outcrop joined to the mainland by a tombolo that consists of a double barrier complex. The Elliot River is thought to have contributed large volumes of sand to the tombolo in the past (see appendix G) (Hopley, 1970a). The creation of the tombolo changed the hydrodynamic conditions in both Abbot and Upstart Bay.

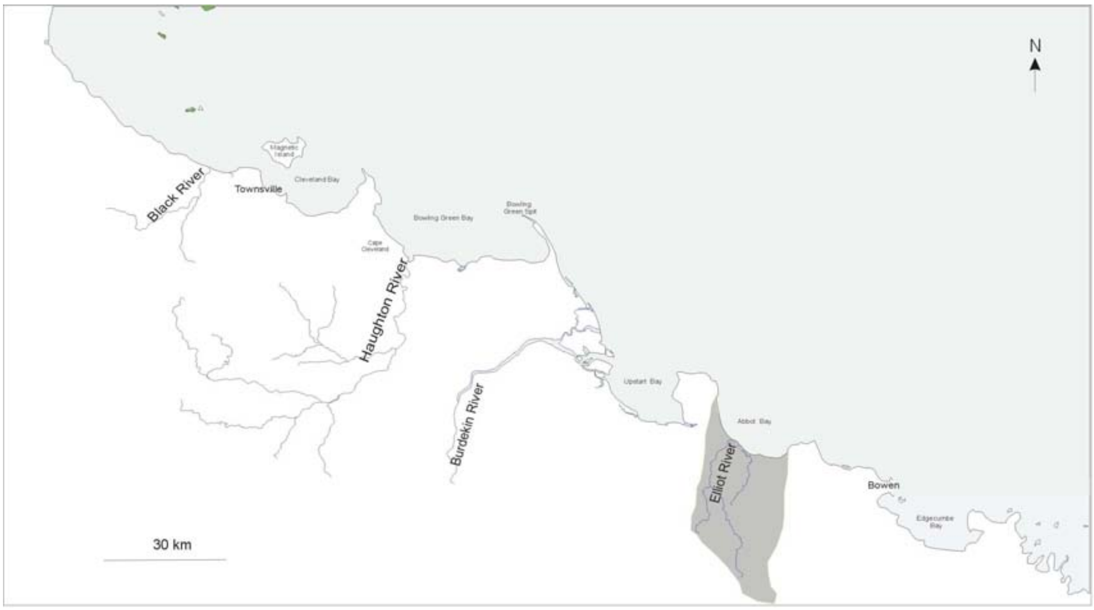

Figure 5.1. The Elliot River catchment.

Table 5.1. Physical characteristics of the Elliot River Estuary

Catchment area	478 km^2
Channel length	40 km
Channel width	100-375 m
Slope	Fluvial reach: 0.0064 Estuarine reach: 0.0025
Sinuosity	1.3
Percentage of channel estuarine	5%
Mean annual rainfall	1022 mm
Modifications	Nil

5.3 SETTING

Like the Haughton River, the Elliot exhibits the typical characteristics of an extremely variable discharge stream (chapter 2, section 2.3). Table 5.2 summarises the flood gauge data used in Figure 5.2 which illustrates the marked intra and inter-annual variability of stream flow in the Elliot, with ~93% of total stream flow occurring between December and April. Seventy-nine percent of annual stream discharges registered below a quarter of the maximum annual flow with several years recording almost no flow at all. Typical of other SWT streams, floods are episodic and flashy (Figure 5.3) and result in over bank flooding.

Table 5.2. Summary of stream flow characteristics for the Elliot River Estuary.

Gauging station	Guthalungra
Distance from stream mouth	7.5 km
Catchment area at gauging station	273 km^2
Gauged area/catchment area	94%
Available records	1973-2001
Maximum annual flow volume	360,000 ML in 1991
Minimum annual flow volume	2,200 ML in 1987
Maximum instant discharge	1430 $m^3.s^{-1}$ in March 1988
Maximum period of no flow	7 months in 1995/96

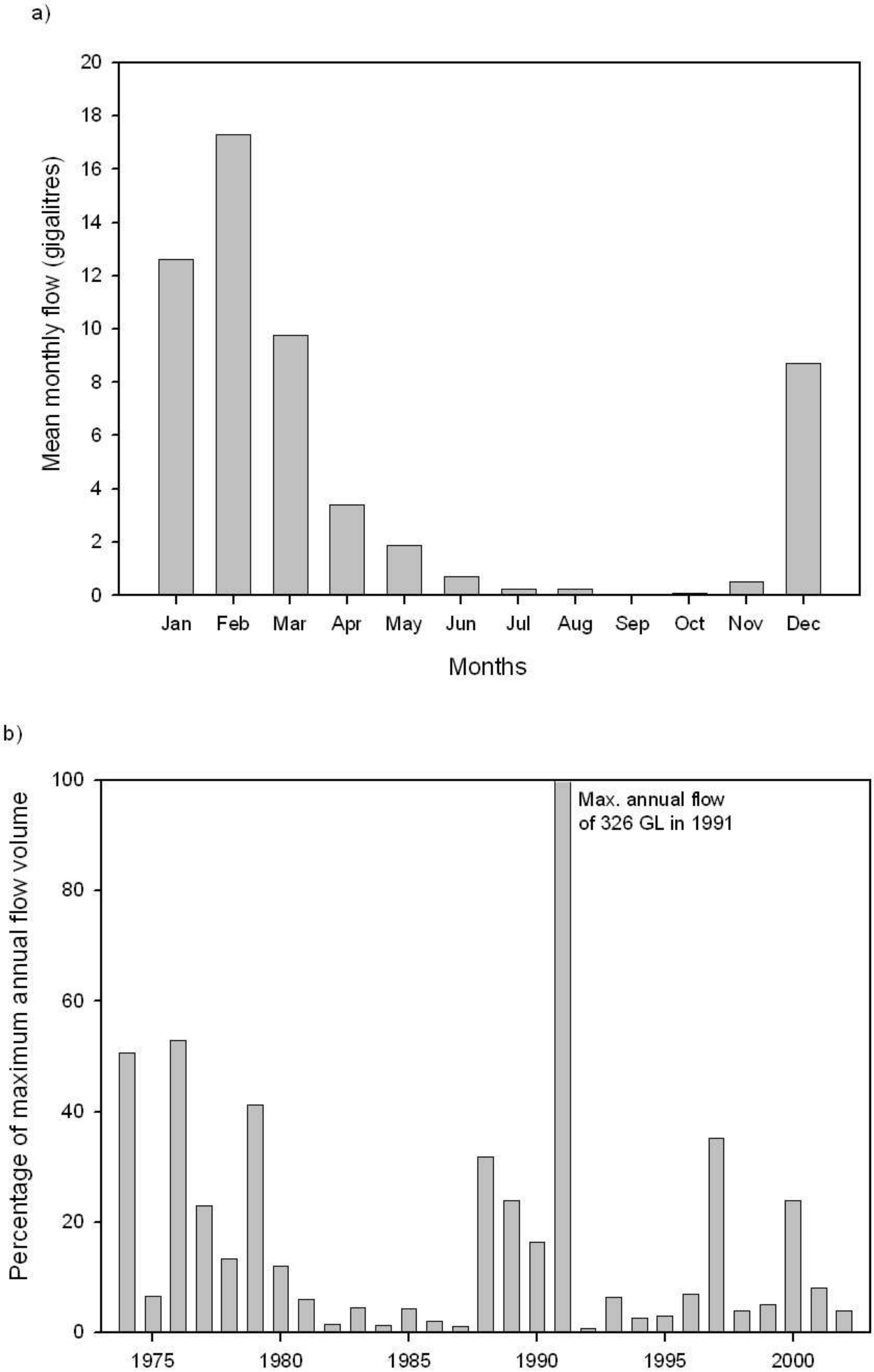

Figure 5.2. Stream flow characteristics for the Elliot River recorded at the Guthalungra gauge from 1974-2002 (DNR, 2002), mean monthly flow volumes (a) and annual flow volumes shown as a percentage of the maximum flow volume (b).

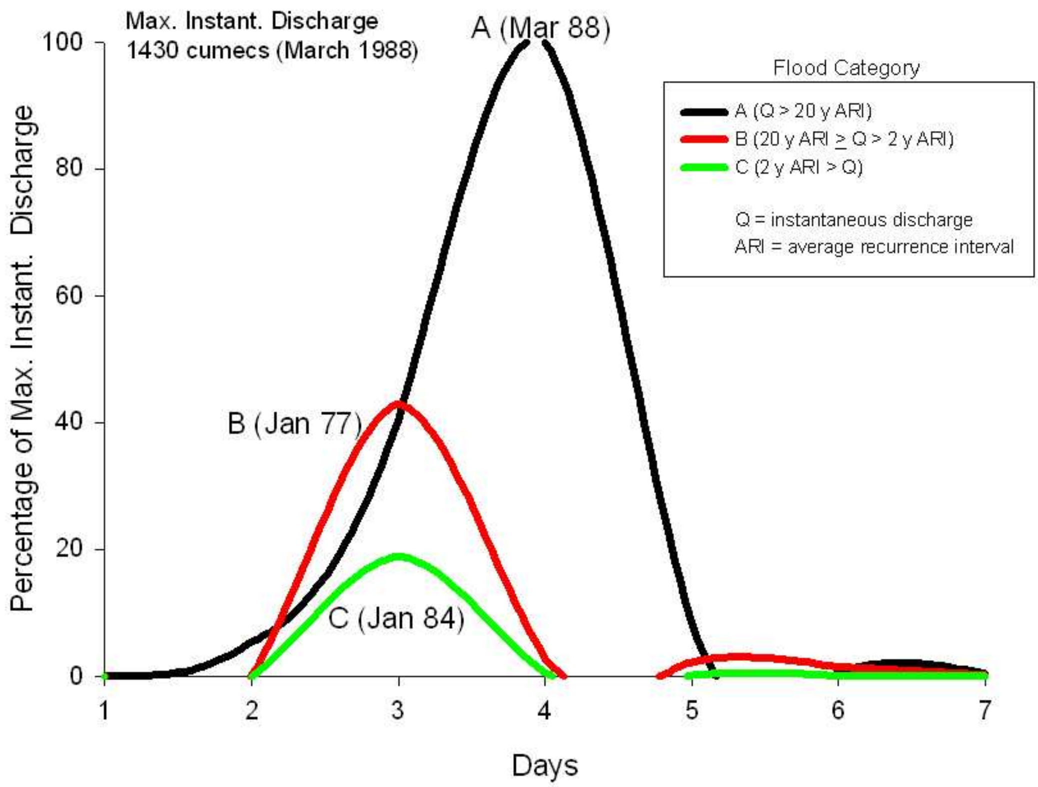

Figure 5.3. Flood hydrograph for the Elliot River recorded at the Guthalungra gauge.

Waverider buoy data collected off Abbot Point represents wave conditions offshore of the Elliot River Estuary. Modal significant wave height ranges from 0.2 - 0.4 m. However for 75% of observations significant wave height ranged from 0.2 – 0.8 m (BPA, 1996a), creating higher energy wave conditions than experienced in Bowling Green Bay. Though still classed as meso-tidal, the Elliot is subject to a smaller maximum spring tide range than the Haughton, of 3 m (Queensland Transport, 2003).

5.4 RESULTS

5.4.1 COASTAL CHANGE

Figure 5.4 shows the position of the coastline from Cape Upstart to Mt Curlewis recorded on aerial photographs taken in 1942, 1974 and 1998. The coastline was taken as the high tide mark. For a discussion of the errors associated with photogrammetry see chapter 3, section 3.4.1. The coastline north west of the mouth has been relatively stable, however rapid progradation and retreat has occurred in other areas. Measurements of coastline position at transects 250 m apart (Figure 5.5) adjacent to the river mouth indicate a complex pattern of retreat and progradation over the 56 years between 1942 and 1998. Measurements of progradation and retreat along each transect from 1942 - 1974 and 1974 - 1998 are illustrated in figure 5.6.

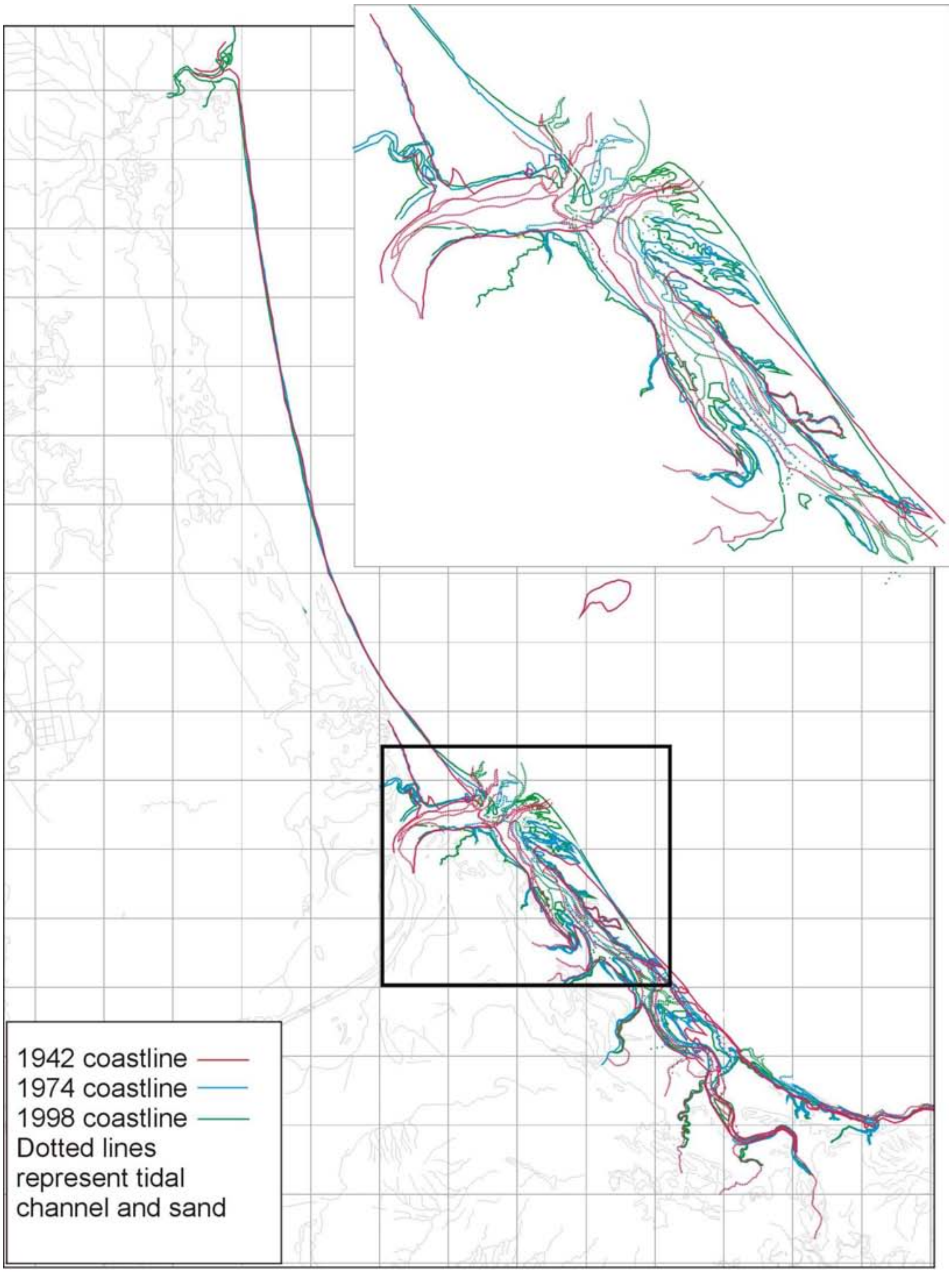

Figure 5.4. Changes in the position of the coastline from Cape Upstart to Mt Curlewis from 1942-1998. Each square on the grid represents 1 km^2 and the vertical lines indicate north.

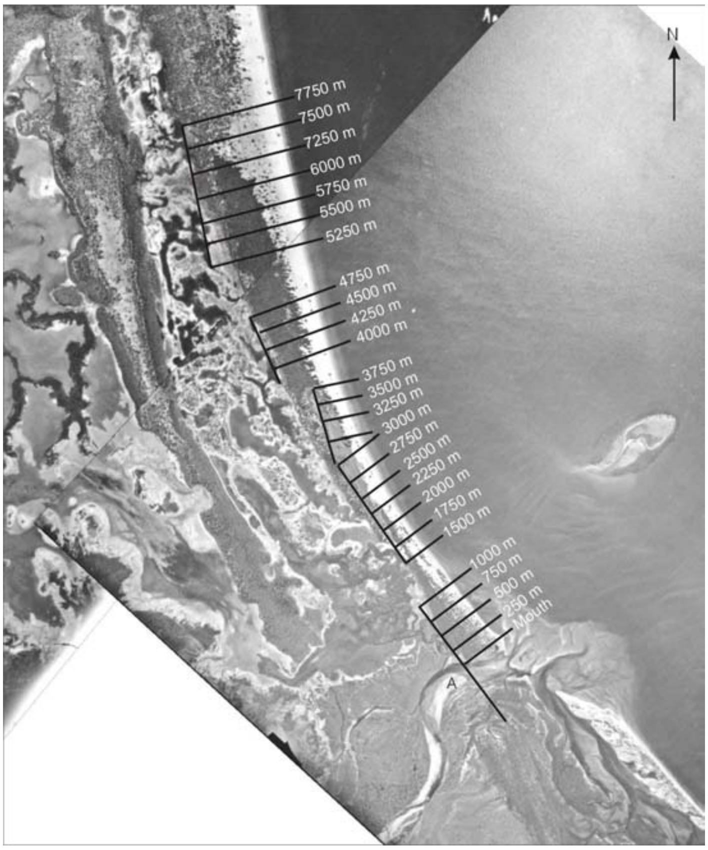

Figure 5.5. Location of transects from which coastal change measurements were derived. 1942 aerial photograph of the Elliot River Estuary. 'A' indicates the location of bedforms shown in figure 5.9.

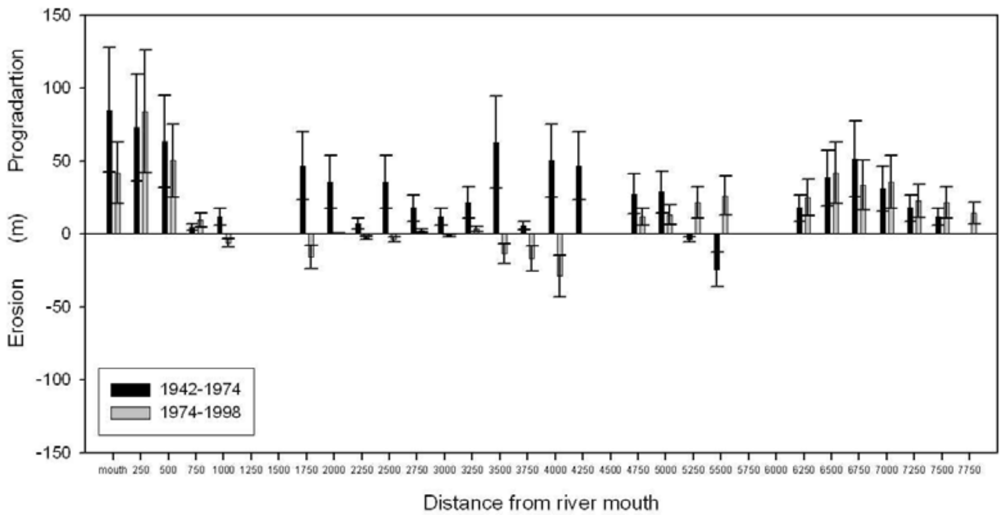

Figure 5.6 Shoreline progradation and retreat along the Elliot River Estuary measured from 1974 and 1998 aerial photographs. Standard error of measurement estimated at 6 m for 1:12,000 scale photography. (See figure 5.5 for locations of transects).

The highest rates of coastline advance occur directly adjacent to the mouth of the Elliot River. This section of coast prograded an average of 59 m from 1974 - 1998, an average annual rate of 2.4 m between 1974 - 1998. The mid section of the coastline between the mouth and Cape Upstart (from 2 - 5 km) is very dynamic and has prograded an average of 32 m or at a rate of 1 $m.y^{-1}$ between 1942 - 1974. This rapid advance was followed by a retreat along this whole 3 km stretch of coast in more recent years (1974 - 1998). The area 5.5 km north of the river mouth eroded 24 m from 1942 - 1974 and has since recovered, prograding 26.4 m during the subsequent 24 years to 1998. The rest of the coast close to the Cape (6-7.5 km from the mouth) has steadily prograded from 1942 - 1998, advancing an average of 50 m from 1942 - 1998 or at a rate of 0.9 $m.y^{-1}$ adding to the Holocene barrier system which has accumulated over the last 5 ka.

The north-west bank of the estuary mouth has eroded an average of 60 m since 1942. Approximately 11,300 m^3 (calculated by assuming a conservative height value of 1 m, see chapter 3, section 3.4.1) of sand has been added to the coastline directly adjacent to the river mouth from 1974–1998, building the coast out to 84 m. A small recurved spit extending from this coastline appears in the 1974 photograph and has continued to grow across the mouth until the 1998 photograph.

The position and morphology of the barrier spit at the mouth of the estuary has changed rapidly since it was completely detached from the coast in 1991. Local residents believe that this is associated with a flood in February 1991, estimated to be a 1 in 60 year event, however it is also possible that wave action caused the breach. This breach led to the erosion of an estimated 36,360 m^3 of sand from the end of the spit between 1991 and 1998, as well as the addition of an estimated 38,736 m^3 of sand to the front of the spit since 1991. Comparison of aerial photographs (Figure 5.7 part a-c) reveals the impact of the February 1991 flood event on the estuary. Pre-flood photographs available from 1985 were compared with post flood photographs taken five months after the February 1991 event. The post-flood 1991 photographs show the sand barrier detached from the shore (Figure 5.7 part b). In the main channel little change was noticed initially but in subsequent photographs sand is building up in the mouth and an ebb tidal delta formed at the breach. The 1998 photograph shows accretion at the front of the barrier extending across the estuary mouth (Figure 5.7 part c). Figure 5.8 part a-c is a schematic model showing the impact of the February 1991 flood on the estuary. It is likely that sand from the breached end of the barrier is the source of the sand added to the front of the barrier.

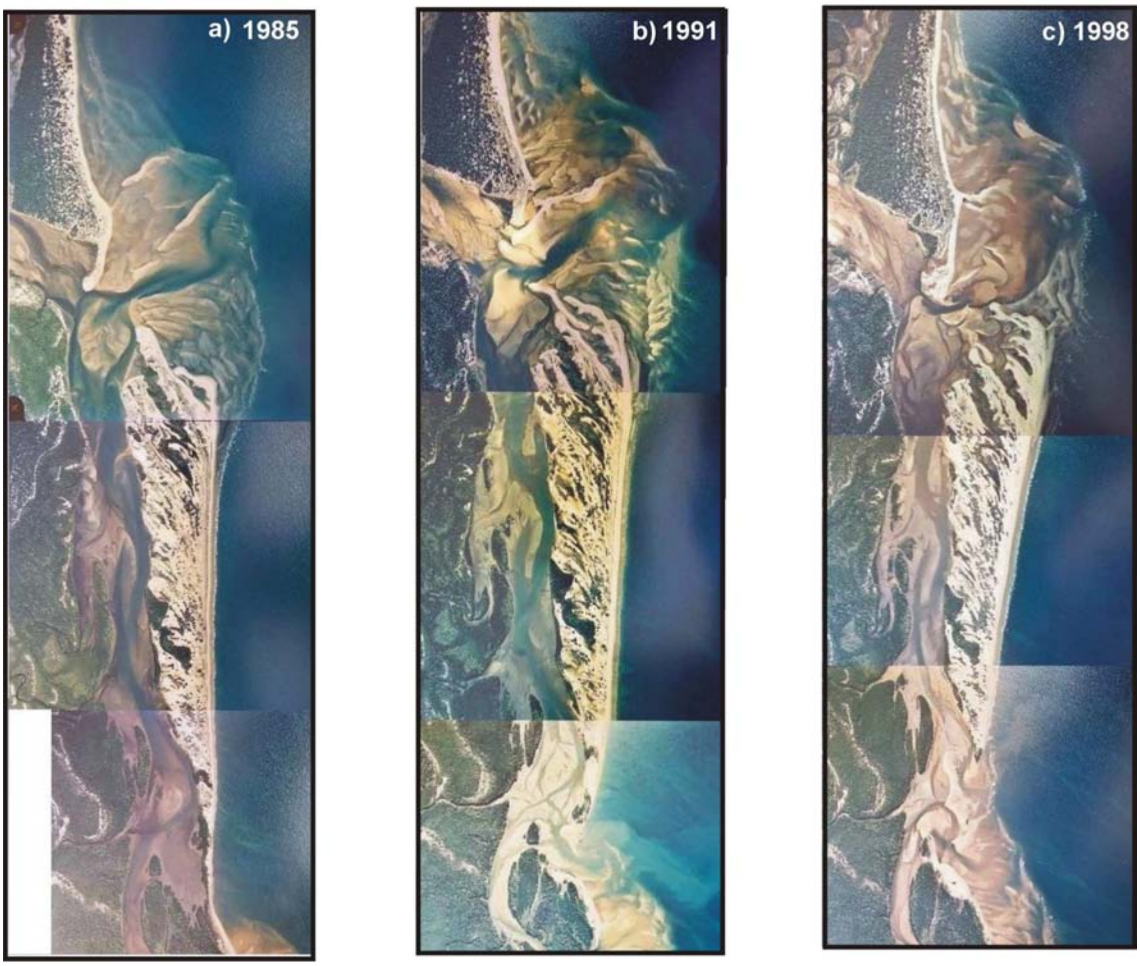

Figure 5.7 a-c. Vertical aerial photographs of the Elliot River Estuary which were used to develop figure 5.8 a-c. Copyright: The State of Queensland (Department of Natural Resources and Water) 1985 (a), 1991 (b), 1998 (c).

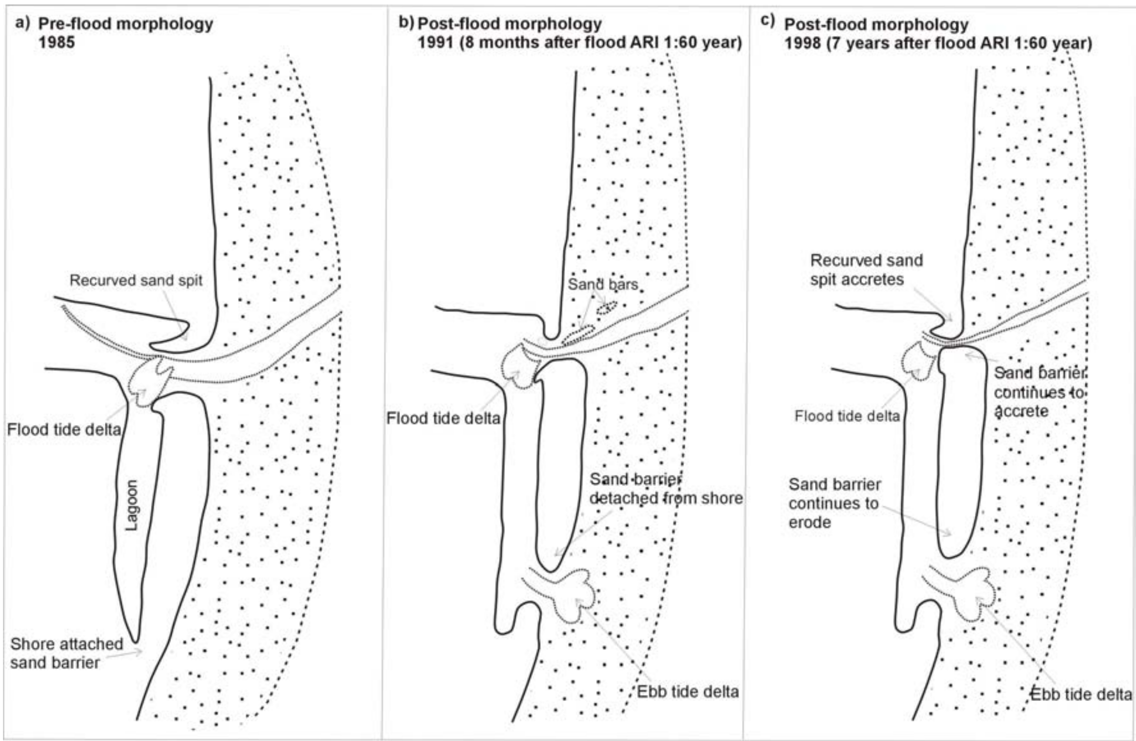

Figure 5.8 a-c. Schematic model illustrating the impact of a flood (ARI 1:60 year) on the morphology of the Elliot River Estuary.

5.4.2 BEDFORMS

Shoreward facing ripples averaging 5 cm in height with wavelengths of 40 cm were observed at low tide in the lower estuarine channel (Figure 5.9). Megaripples up to 0.2 m in height with wavelengths of 5 m were observed at low tide along the landward side of the barrier. These megaripples were orientated to the south east towards the end of the barrier.

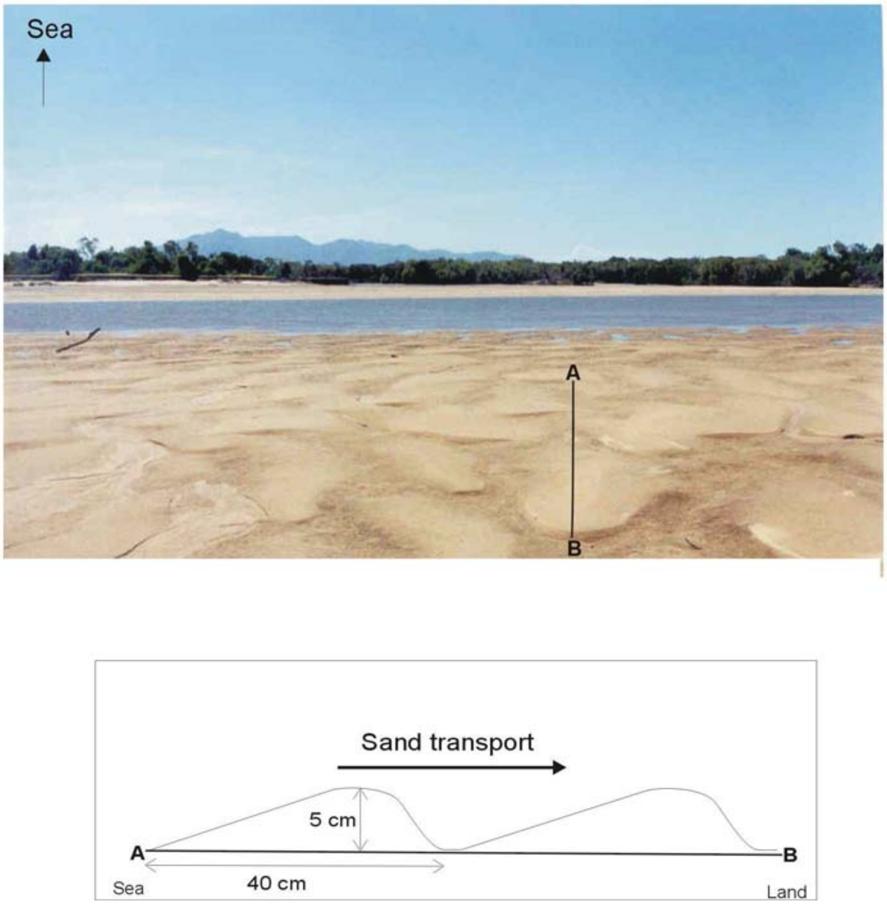

Figure 5.9. Current ripples observed at low tide at the Elliot River Estuary indicate sand transport into the estuary. Location marked as 'A' on figure 5.5.

5.4.3 SEDIMENTOLOGY

Ninety-nine surficial sediment samples and four vibrocores which penetrated 3.2 m below AHD, were collected from the Elliot River Estuary and the adjacent coastline. The locations of surficial samples and vibrocores are shown in figure 5.10. Figure 5.11 provides a summary of the results of textural analysis of the surficial samples (see Appendix D) showing the spatial distribution of facies. Sediment within the study area ranges from very coarse sand (grain size of 1 - 2 mm) to fine sand (grain size of 0.125 - 0.25 mm) with silty fine sand offshore (Figure 5.11). Silty sand deposits appear universally associated with dense seagrass meadows and thus likely to reflect the effect of baffling and binding (Perry, 1999). Moderately sorted very coarse (1.138 mm) – coarse sand (0.769 mm) is predominant in the fluvial and estuarine reaches of the channel, the barrier spit and occurs offshore of the adjacent coast. Angular very coarse gravel (~32 mm) densely overlies the very coarse sand (1.138 mm) in the fluvial reaches (Figure 5.12) and then intermittently throughout the estuarine channel (Figure 5.13). An isolated deposit of very coarse sand (1.226 mm sample 48) is found about 500 m offshore from the middle of the coastline (3.5 km transect). Onshore sediment deposits become finer and better sorted on the adjacent coast with well sorted medium (0.357 mm) to fine (0.208 mm) sands up to Cape Upstart. However, an isolated section of coarse sand (0.559 mm sample 30) was found on the shore about 7.25 km north of the estuary mouth. Despite a northward fining trend in the nearshore sediments <500 m further off the coast, coarse sediment is consistently found along the coast until just south of Cape Upstart. Concentrated wave energy on this section of coast may explain the anomalous presence of coarse and very coarse sediment deposited in the nearshore area (Figure 5.14). Sub-angular to sub-rounded grains were found in all size ranges.

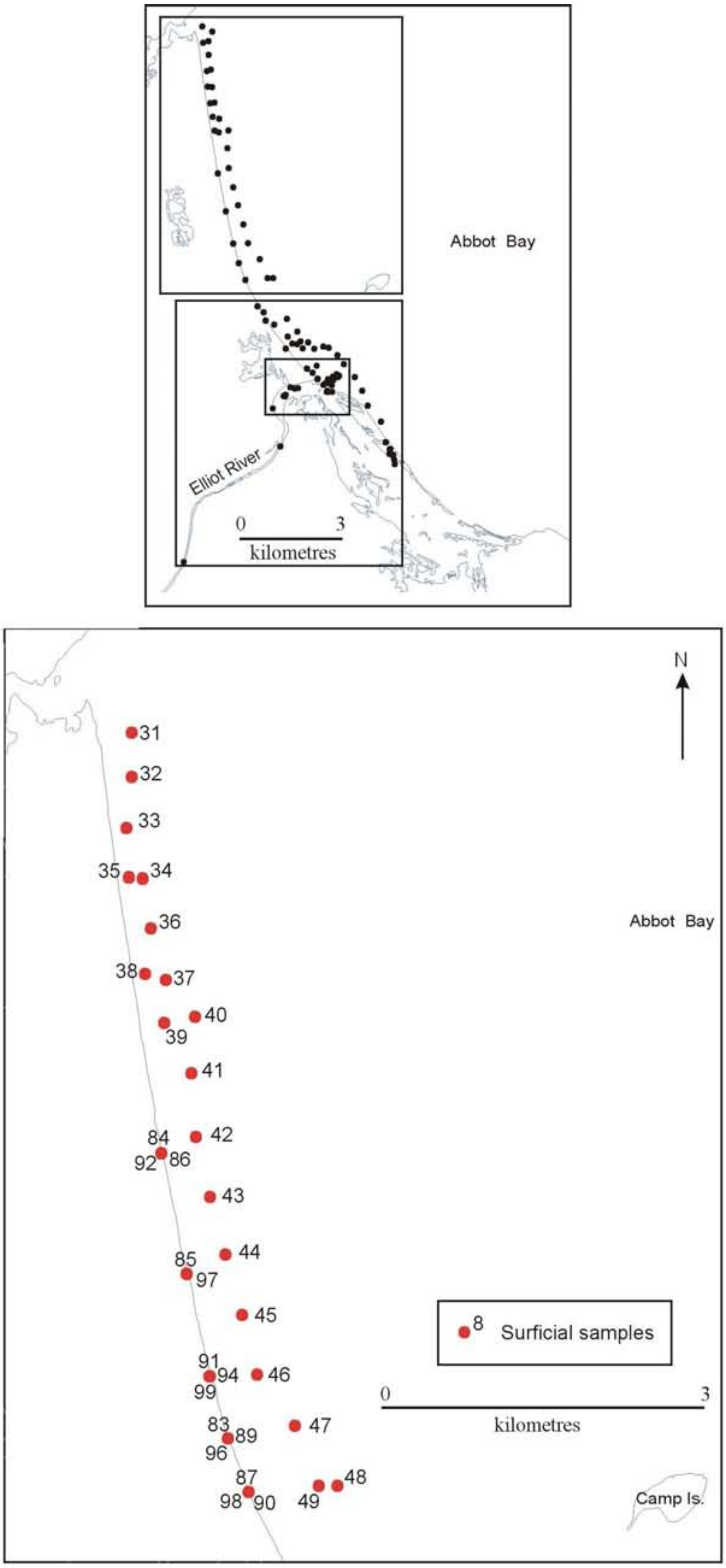

Figure 5.10 a. Locations of surficial and subsurface sediment samples taken at the Elliot River Estuary. (See Appendix D for the results of the textural analysis of samples).

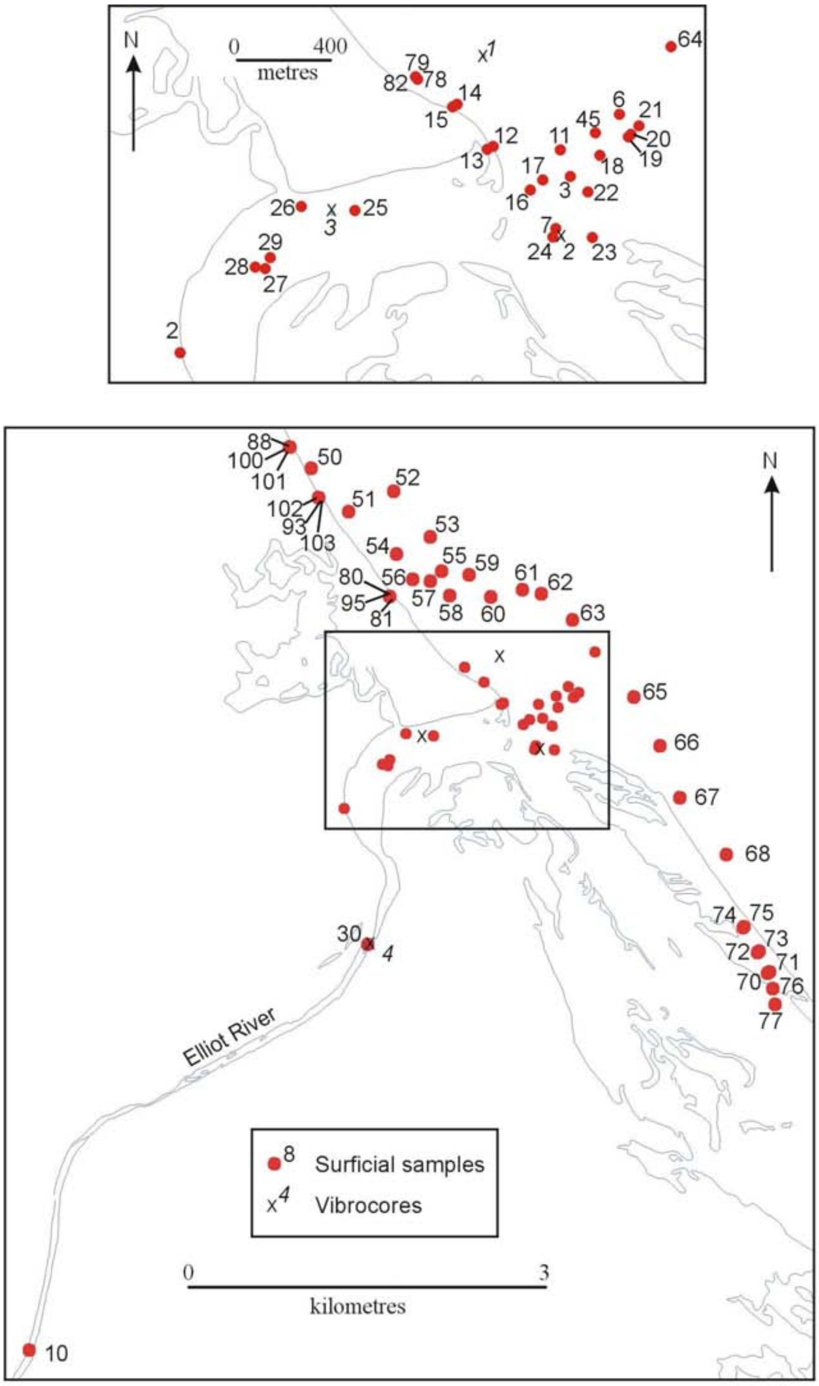

Figure 5.10 b. Locations of surficial and subsurface sediment samples taken at the Elliot River Estuary. (See Appendix D for the results of the textural analysis of samples).

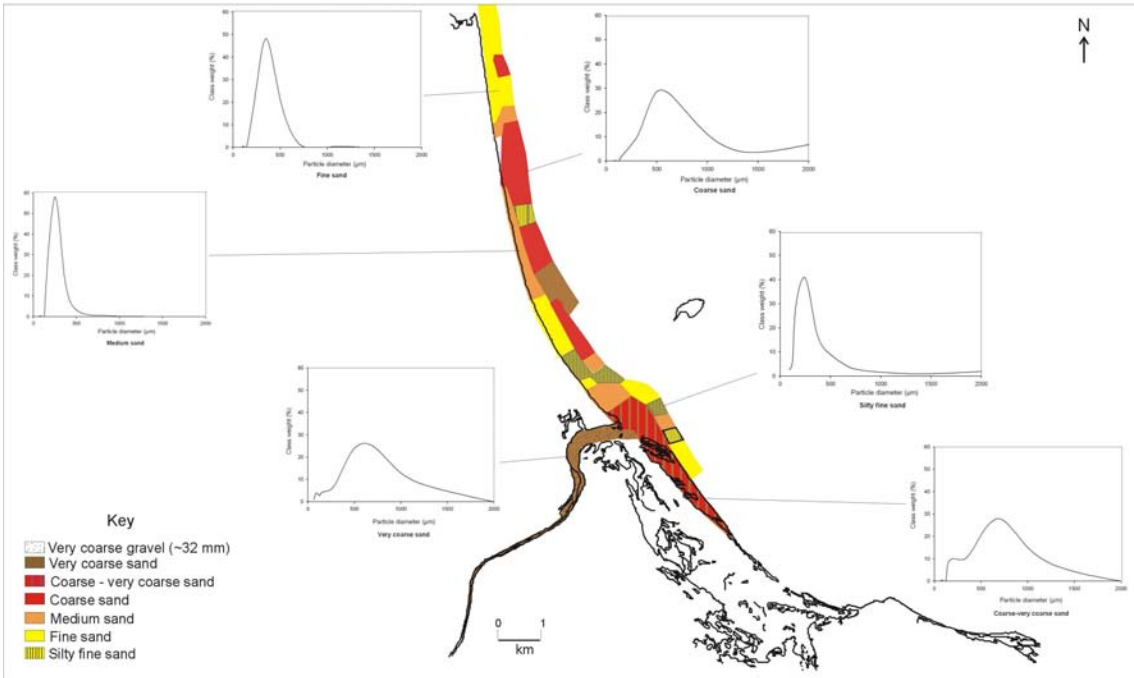

Figure 5.11. Summary of the results of textural analysis of surficial samples from the Elliot River Estuary. Histograms show the distribution of a typical example of each sediment class.

Figure 5.12. Angular coarse gravels densely overlay the very coarse sands in the fluvial reaches of the Elliot River. Photograph taken (07/03/02) looking downstream from the Bruce Highway Bridge.

Figure 5.13. Angular very coarse gravels overlay very coarse sand to a lesser extent in the estuarine reaches of the channel. Photograph taken (07/03/02) looking seawards.

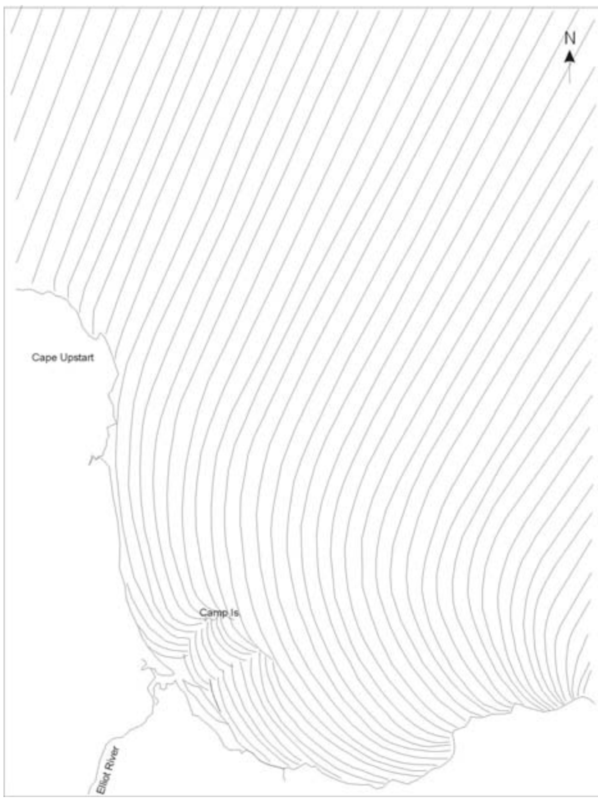

Figure 5.14 a. Wave refraction pattern for 5 second wave intervals and 20 wave crest spacing generated by south easterly winds.

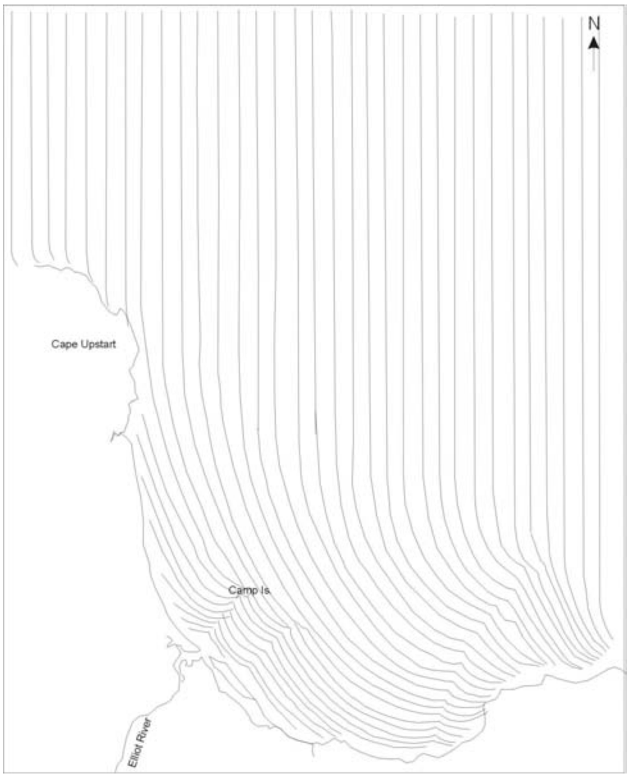

Figure 5.14 b. Wave refraction pattern for 5 second wave intervals and 20 wave crest spacing generated by easterly winds.

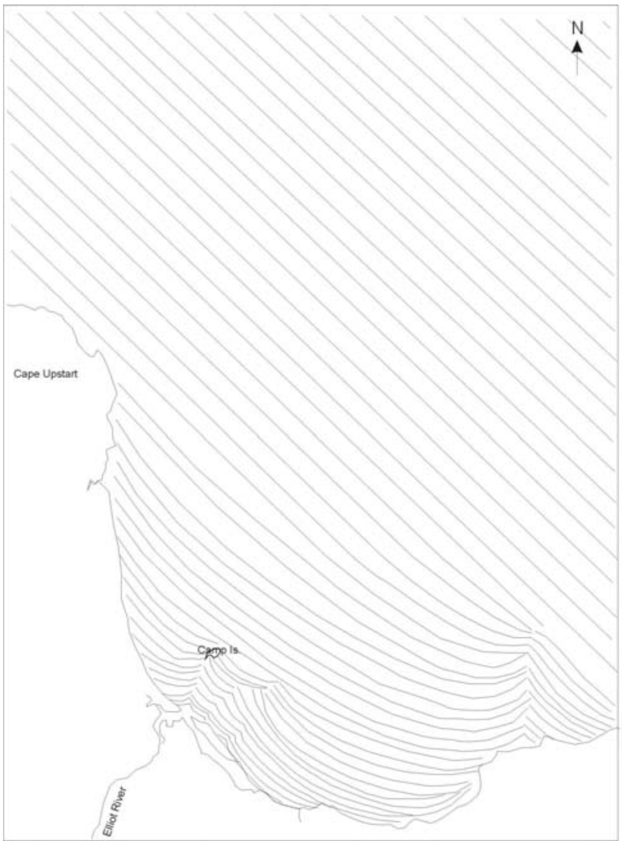

Figure 5.14 c. Wave refraction pattern for 5 second wave intervals and 20 wave crest spacing generated by north easterly winds.

All four vibrocores have similar stratigraphies and are composed of very well to moderately well-sorted very coarse sand, with shells, mud clasts and even coarse gravel interspersed throughout (Figure 5.15). Only one core (ERVC 1) contained units of medium sand ~ 3.2 m below AHD. ERVC 3 and ERVC 4 contain very coarse gravel identical to that observed on the estuary floor today. The lack of organic material in the cores prevented an investigation into the chronology of sedimentation using radiocarbon dating. While some shells were present in the cores, they were fragmented and interspersed throughout, thus not suitable for even a bulk radiocarbon date.

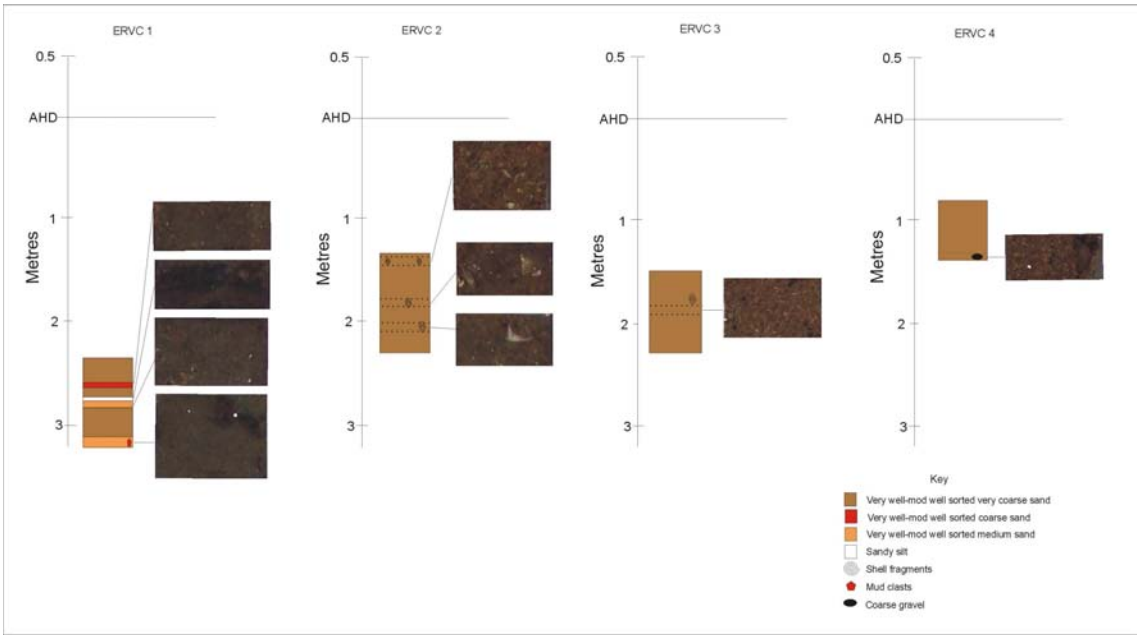

Figure 5.15 Stratigraphy of vibrocores from the Elliot River Estuary including photographs of selected beds.

Figure 5.16 part a-d compares the surficial and sub-surface sediment samples according to mean grain size, sorting, skewness and kurtosis characteristics after Friedman (1961) (see chapter 3, section 3.4.3). There is little consistent separation according to setting across all four plots. Table 5.3 shows the results of a discriminant analysis preformed on the data to determine how well the descriptive parameters distinguish between environmental settings. Kurtosis (0.499) was the most significant variable within function one, while both mean grain size (0.879) and kurtosis (-0.617) are the most significant variables in function two. The results of the discriminant analysis are plotted (Figure 5.17) according to these functions with sorting on the x-axis and mean grain size and kurtosis on the y-axis, illustrating minimal separation of samples according to their environment.

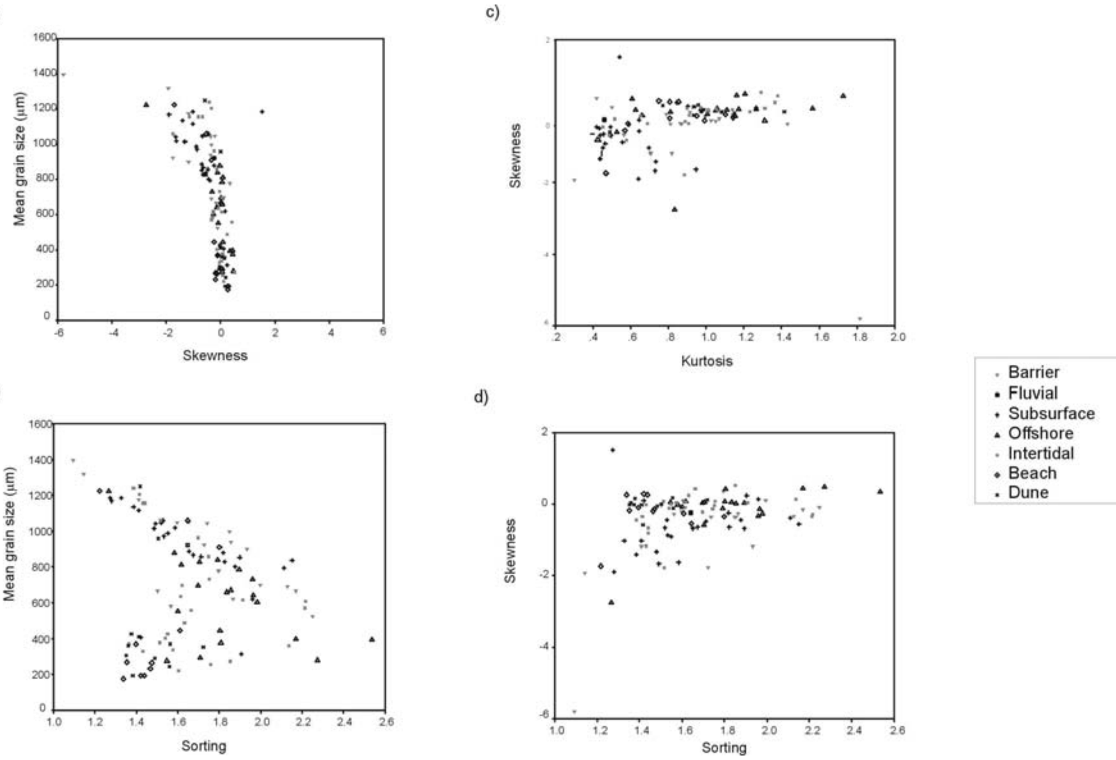

Figure 5.16 a-d. A comparison of the surficial and subsurface sediment samples according to their mean grainsize, sorting, skewness and kurtosis characteristics for the Elliot River Estuary.

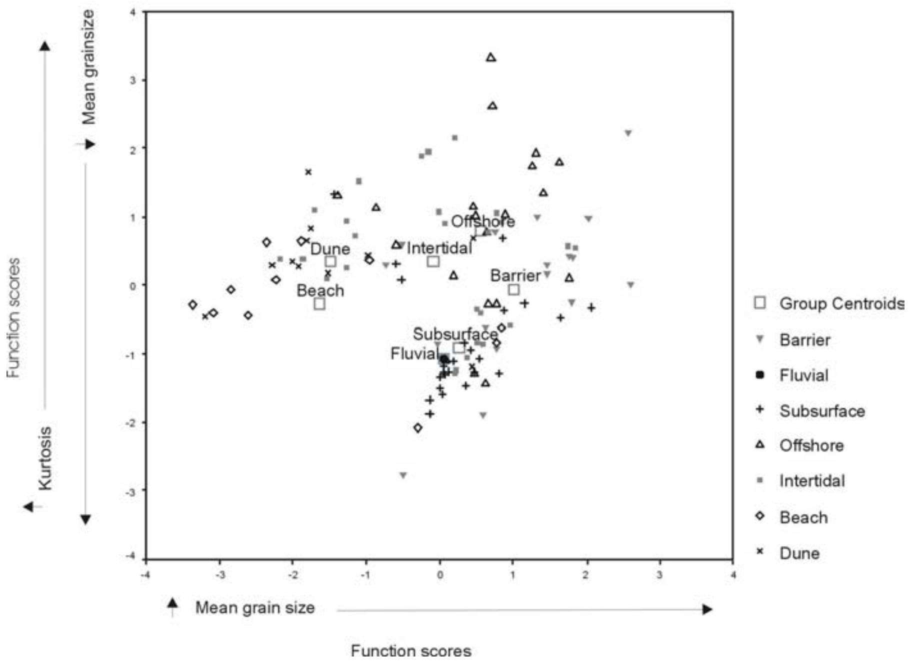

Figure 5.17. Scatter plot showing the results of discriminant analysis using all descriptors fro the Elliot River Estuary.

Table 5.3. Structure matrix from the discriminant analysis for Elliot River Estuary.

Variables	Function			
	1	**2**	**3**	**4**
Mean grain size	-0.063	0.879*	-0.380	0.281
Kurtosis	0.499	-0.617*	0.180	0.581
Skewness	-0.251	-0.476	0.700*	-0.469
Sorting	0.481	0.302	0.067	-0.821*

* indicates the largest absolute correlation between each variable and any discriminant function.

5.5 CONCLUSIONS

A conceptual model of the spatial and temporal patterns of coastal sand transfer in the Elliot River Estuary was developed based on the aerial photographic, sedimentological and hydrodynamic data collected.

5.5.1 COASTAL CHANGE

The dynamic nature of the section of coast directly adjacent to the mouth is probably a result of wave refraction around Camp Island (Figure 5.14). Aggradation and erosion of beaches has been related to slight changes in wind patterns in many locations (e.g. in Byron Bay, northern New South Wales, Hopley, 1967). Analysis of wind data for Bowen 1969 - 1998, reveals significant changes in the wind regime beginning in the late 1970's. There is a strong (R^2 = 0.8713) decrease in the frequency of winds from all directions between 1-10 km.h^{-1} from 1969 – 1998 (Figure 5.18). Similarly there is a trend (R^2 = 0.4949) towards an increase in the frequency of winds over 30 km.h^{-1} during that same period (Figure 5.19). While the winds have increased in velocity from 1969 – 1998, the frequency of winds from each direction has remained constant over time, with dominant south easterlies (occurring 38% of the time) (Figure 5.20) and easterlies (occurring 22% of the time) (Figure 5.21). However, there have been significant increases in the velocity of these dominant south east and east winds since 1969 with R^2 values of 0.9053 and 0.457 respectively (Figures 5.20 & 5.21). Also while the frequency of strong north-east winds over 21 km.h^{-1} has remained constant (Figure 5.22), the frequency of north-east winds of all speeds has decreased significantly (R^2 = 0.7999) from 1969-1998 (Figure 5.23).

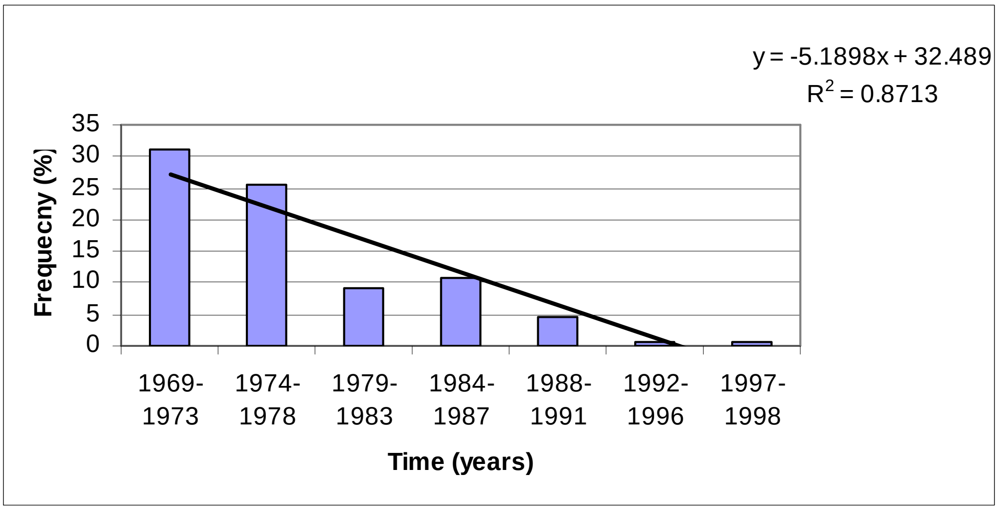

Figure 5.18. Significant decrease in the frequency of winds from all directions between 1-10 km.h^{-1} from 1969-1998. Bowen wind data 1969-1998 from the Bureau of Meteorology.

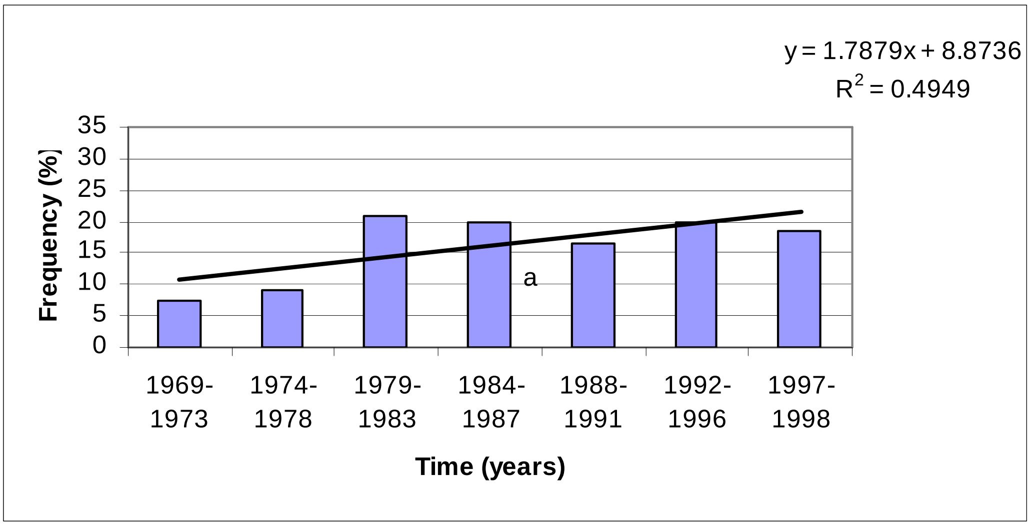

Figure 5.19. Significant increase in the frequency of winds over 30 km.h^{-1} from 1969-1998. Bowen wind data 1969-1998 from the Bureau of Meteorology.

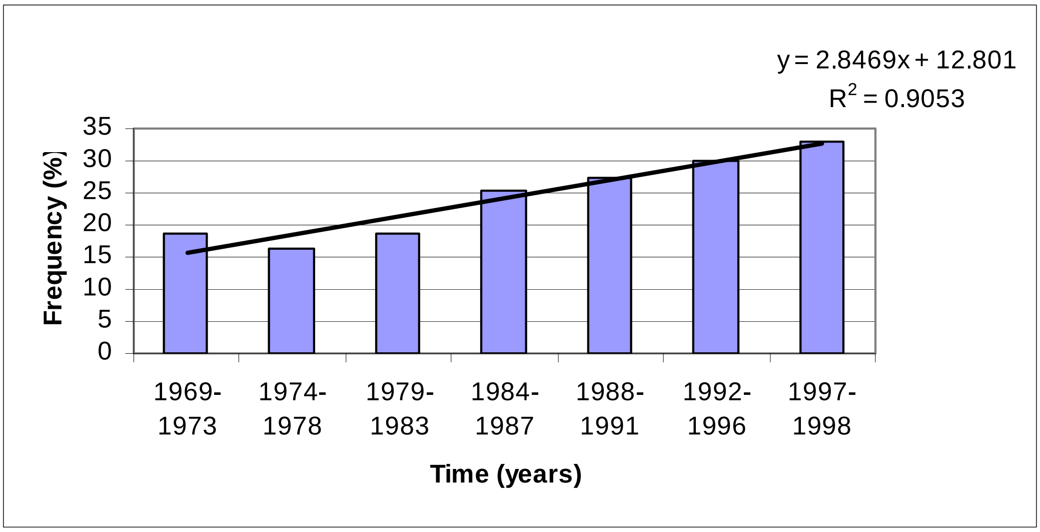

Figure 5.20. Significant increases in the velocity of south-easterly winds over 21 km.h^{-1} from 1969-1998. Bowen wind data 1969-1998 from the Bureau of Meteorology.

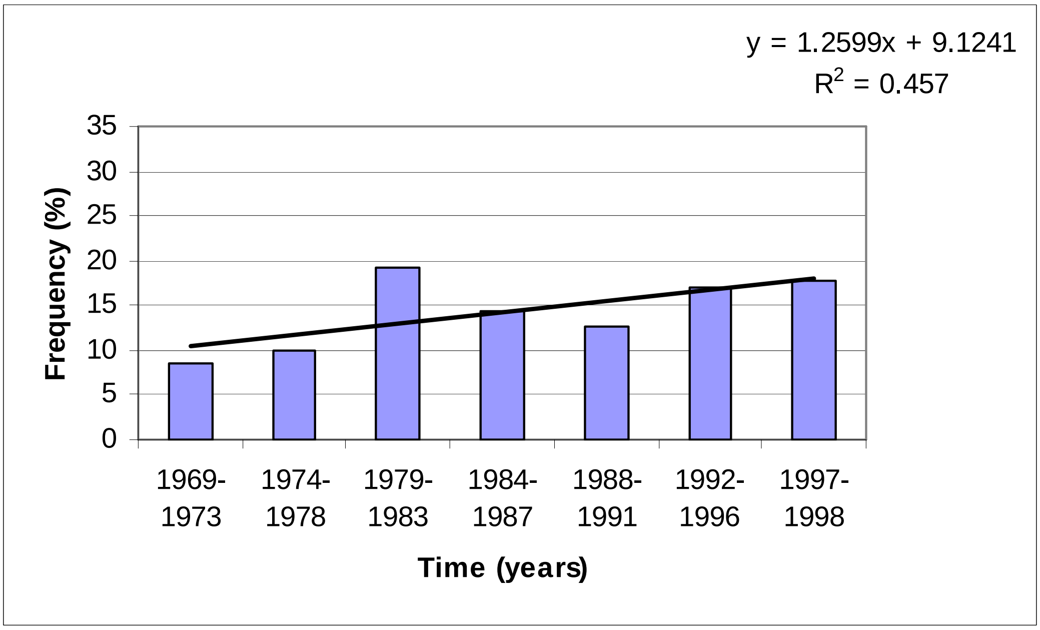

Figure 5.21. Significant increases in the velocity of easterly winds over 21 km.h^{-1} from 1969-1998. Bowen wind data 1969-1998 from the Bureau of Meteorology.

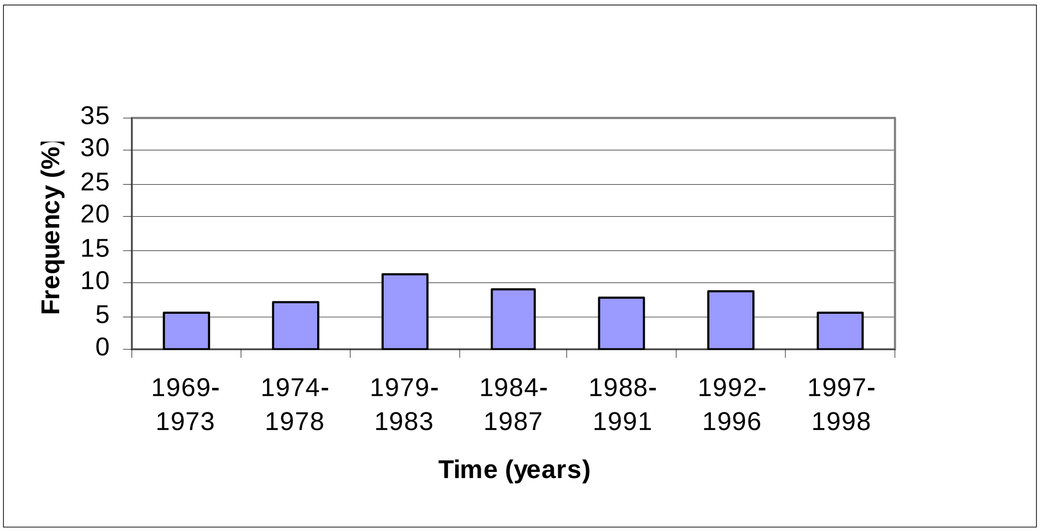

Figure 5.22. The frequency of strong north-easterly winds over 21 km.h^{-1} have increased by up to 5% in 1979-83 and then decreased again by 1998. Bowen wind data 1969-1998 from the Bureau of Meteorology.

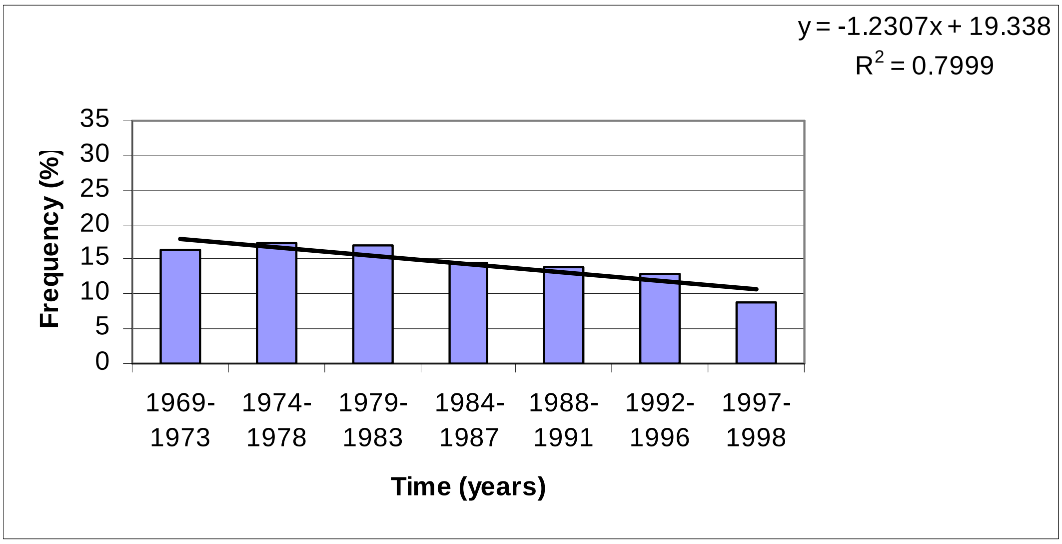

Figure 5.23. The frequency of north-easterly winds of all speeds has decreased significantly from 1969-1998. Bowen wind data 1969-1998 from the Bureau of Meteorology.

It can be seen from Figures 5.14, that wave refraction around Camp Island will direct wave energy at the mainland coastline, with the area of concentration responding sensitively according to wind direction i.e. moving south when winds are more northerly and moving north when winds are more southerly. This adds to the dynamic nature of this section of coast and is superimposed upon the more general south to north movement of sediments along the beach. Figures 5.14 show the different patterns of wave refraction that are formed by the three most common wind directions south easterly, easterly and north-easterly. During south-east winds wave energy is concentrated along the coastline, which may bring sediment on to the shore. Easterly winds produce a more dispersed pattern of wave energy on the shore, however wave energy is still concentrated on the mid sections of the coastline. North-easterly winds create a convergence of wave energy along the coast causing the transfer of sand towards the estuary mouth. Modelling using Automated Coastal Engineering Software (ACES) (Leenknecht *et al.*, 1992)(see chapter 3, section 3.4.4.1) suggests that north-easterly waves (approaching at 10° angle and occurring for 5% of year) can transport ~4,900 m^3 of sand south per year, which explains the build-up of sand on the northern bank of the estuary. This may result in erosion along the coastline and accretion near the river mouth. If the trend shown in the 1969 - 1978 wind data is representative of the previous 25 years, it is possible that the wind regime was weaker from 1942 - 1978, which may account for the widespread coastal progradation between 1942 - 1974. Subsequent erosion around the middle of the coastline and continued progradation at the northern and southern ends from 1974 - 1998 may reflect the strengthening of winds during this period.

The shift from a constructional phase (1942-1974) to an erosional phase (1974-1998) suggests a 30-year cycle of progradation and retreat along the coastline adjacent to the Elliot River. If this is occurring, it is likely that erosion would continue at the same pace (0.9 $m.y^{-1}$) for the next few years and then perhaps a recovery of ~1.5 $m.y^{-1}$ over the next few decades. This cyclic pattern is probably related to changes in the dominant wave pattern, in response to changes in the dominant wind direction. For example, in the Torres Strait Rasmussen & Hopley (1997) have documented a significant change in wind patterns in the late 1970’s. Greater predominance of southerly winds over the last 20 years has changed patterns of sand transfer leading to greater erosion along the southern beach of Warraber Island (Rasmussen and Hopley, 1997). A 20 - 30 year wind cycle has also been reported in the southern Great Barrier Reef by Flood (1986) where a change from dominant south-south-easterly winds in the early 1960’s to dominant east-south-easterly winds in the late 1970’s, has reversed patterns of sand transfer around Heron Island. Therefore the patterns of sand movement in Abbot Bay, including longshore drift, may well reflect changes in wind patterns.

Dominant south-easterly winds produce ambient wave conditions averaging significant wave heights of 0.5 m (BPA, 1996a). Modelling using ACES (Leenknecht *et al.*, 1992) (chapter 3, section 3.4.4.1, Appendix C) suggests that these south-easterly waves, which occur for 38% of the year and approach shore at an 80° angle, produce a potential longshore drift of 100,000 m^3 of sand per year to the north. Similar rates of longshore drift are predicted to occur to the south suggesting that sand from the Don River may be transported into the Elliot River system. Aerial surveys in 2000 and 2003 revealed sand bodies aligned northwards along shore from the Don River to the Elliot (Figures 5.24-5.27). The Don River is estimated to contribute an average of 40,900 m^3 of sand to the coast per year (Horn *et al.*, 1998). The recent construction of a coal loading jetty off Abbot Point may interrupt this movement of sand. However large subaqueous sand waves observed northwards of Abbot Point and orientated northwards suggest sand is still moving towards the Elliot River Estuary via longshore drift and that the jetty is essentially transparent to sand movement.

Figure 5.24. Northward facing sand bars at the Don River looking south towards Bowen. Photograph taken at low tide May 2003.

Figure 5.25. Northward facing sand bars at the mouth of the Don River. Photograph taken at low tide May 2003.

Figure 5.26. Subaqueous sand waves in Abbot Bay orientated north towards the Elliot River. Photograph taken at low tide May 2003.

Figure 5.27. Northward facing sand bars just south of the Elliot River Estuary. Photograph taken at low tide May 2003.

5.5.2 BEDFORMS

A flood tide delta has formed at the river mouth and an equivalent ebb tidal delta is present at the southern opening behind the barrier. Well-formed megaripples were observed on these tidal deltas and indicate strong tidal currents capable of transporting bed material. Surface current velocities to a maximum of 0.7 $m.y^{-1}$ have been recorded at the river mouth during flood phases of spring tides (Sinclair Knight Merz, unpublished data). However the strength of tidal currents is likely to be enhanced due to constriction at the mouth. The south-east facing megaripples observed along the inner side of the barrier suggest strong ebb tidal currents capable of transporting bed material out of the estuary. The orientation of bedforms and tidal deltas suggests an exclusive flood tide inlet at the estuary mouth and ebb outlet at the end of the barrier spit.

5.5.3 SEDIMENTOLOGY

The northward fining of sand deposits suggests the alongshore transport of sand from the mouth of the estuary to the adjacent coast. The presence of coarse sand offshore from the medium to fine sand onshore deposits may be ‘lag’ winnowed by the removal of finer sediments. Most sub-surface and many of the other intertidal and offshore samples were bimodal compromising the reliability of the descriptive statistics (Blott and Pye, 2001). Like the results from the Haughton (see chapter 4, section 4.3.3) there is a lack of consistent separation of samples according to their environmental setting. A discriminant analysis of the sediment characteristics and sampling location revealed that only 39.5% of original grouped cases (35.1% of cross-validated) were correctly classified. Unlike the Haughton this result is not due to a lack of variation in textural characteristics of sediments throughout the estuary. Rather, it is that the distribution of the broad range of sediments within the Elliot, are unrelated to their setting indicated by the significant kurtosis value in the discriminant analysis (Table 5.3).

Similar to the Haughton (see section 4.3.3, chapter 4) there was a lack of sediment interpreted as immature fluvial deposits in either the surficial or sub-surface samples. Even samples from the fluvial reaches of the channel were very similar to the very coarse – to coarse, sub-angular to sub-rounded sands that dominate the estuarine reaches on the surface and up to 3 m below AHD. However fine-medium sands are found on the adjacent coast with coarse to very coarse deposits found in the nearshore areas. Interpretation of these results in the context of previous investigations on the system suggest complex scenarios of sand transfer in the Elliot River Estuary over Holocene and contemporary timescales.

Hopley (1970a) suggested that the Elliot River supplied sand to the double barrier system, Pleistocene aged inner barrier and Holocene aged outer barrier, that link the granitic outcrop of Cape Upstart to the mainland. However these barriers are composed of medium sand (0.375 mm) (Hopley, 1970a) while very coarse to coarse sand dominates the estuary up to 3 m below AHD. The only medium sand found in the estuary was at 3.2 m below AHD at the bottom of ERVC 1. The volumes of sand in the Holocene barrier and barrier spit is approximately 8.39 x 10^6 m^3 of sand so over 6.5 ka that the Elliot would have supplied an average of ~1,300 m^3 of sand per year (assuming no losses or gains to the system). Hopley (1970a) observed erosion on the adjacent coast and attributed it to diminishing fluvial sediment supply from the Elliot. However from the aerial photograph record (see section 5.4.1) the coastline adjacent to the Elliot has been relatively stable since 1942. Further investigation suggests the coastal change that has occurred is more likely the result of varying wind patterns and wave refraction than changes in fluvial sediment supply. However, given the significance of sand waves in wave-dominated coasts further south (Short, 1999), these are likely to influence patterns of coastal change in the Elliot River Estuary. Also the lack of immature fluvial sands in the estuary up to

3.2 m below AHD suggest that the modern Elliot is not contributing significant amounts of sand to the coast. Indeed, considering that the Pleistocene and Holocene barriers are composed of medium sand, and the Elliot River Estuary is dominated by very coarse sands, prompts doubt that the Elliot River supplied the sand for these barriers in the past. However it is possible that the medium sand has been preferentially transported south via longshore currents and the coarse sand remains as a lag deposit (Bird, 2000). It is common for armouring to occur on beds subject to high velocity in fluvial settings (Knighton, 1984). Therefore it is likely that armouring could also occur in high velocity coastal settings and when armoured beds are disturbed, for example by a storm event, a reserve of finer sand is available beneath.

The sand for the outer barriers and the large spit off the mouth of the estuary and adjacent coast may have been supplied, via longshore drift, from the larger Don River (see section 5.5.1). However, even if the Don River was not the sole supplier of sediment for the barriers in the past, the influx of sand via longshore drift would explain the presence of medium to fine well sorted sand in the estuary today.

Similarly the low kurtosis value of the sediment indicates that part of the sediment achieved its sorting in a higher wave-energy environment and that it was transported with its size characteristics unmodified, into another environment where it is mixed with other material (Folk and Ward, 1957; Taylor and Stone, 1996). This suggests the Pleistocene barrier was formed by the onshore movement of marine sediment when sea level rose at 125 ka BP. The truncation of the Pleistocene barrier (2.4 km from the Elliot River) and Holocene alluvial deposits at the end of the barrier, suggest the river channel migrated over the low relief flood plain eroding the end of the Pleistocene barrier. Finer sediments have since been transported out sea and deposited onto the adjacent coast contributing to the Holocene barrier, with the coarse sand remaining in river channel. Additional sand from the Don River may have contributed to the coastline and barrier spit.

5.5.4 CONCEPTUAL MODEL

The interpretation of aerial photographs, sedimentological and hydrodynamic investigations in the Elliot River Estuary are summarised in a conceptual model of contemporary sand transfer processes (Figure 5.28). The Elliot is a mixed estuary, with relatively strong wave and tide processes dominating sand transfer patterns during ambient conditions.

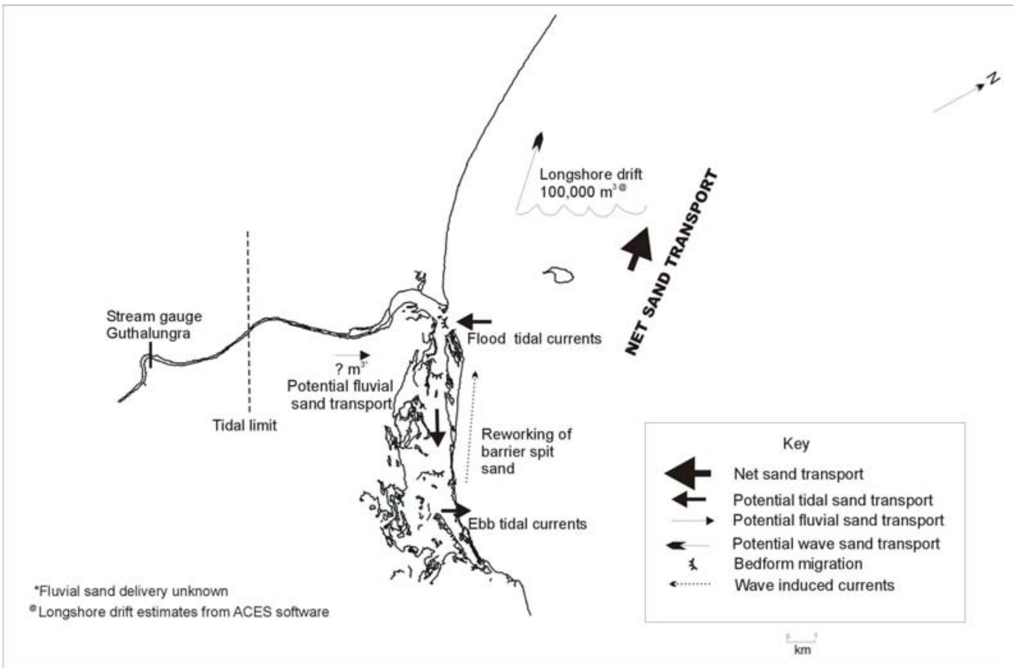

Figure 5.28. Summary diagram of net sand transport trends at the Elliot River Estuary as indicated by bedform orientations, grainsize patterns and dominant current directions. Tide and wave-induced currents are the most dominant, hence net estuarine sand transport direction is north west along the shore.

The most dynamic coastal feature is the barrier spit at the mouth of the Elliot River estuary. Initiated by a major flood event strong ebb tidal currents have led to the rapid erosion of the barrier spit and dominant south easterly wave action combined with strong flood tidal current have lead to subsequent accretion of similar volumes of sand at the northern end of the barrier spit. Strong longshore drift currents in the estuary have the potential to transport 100,000 m^3 of sand northwards alongshore every year into the Elliot system provided it is available. Seismic data offshore from Bowen reveal incisions in the pre-Holocene surface that are infilled with deltaic gravel, sand and mud up to 17 m below sea level (Johnson *et al.*, 1982). These deposits may indicate palaeochannels of the larger Don River to the south of the Elliot River and are a reservoir of marine sand that may be transported northwards.

Before the breach in the barrier inlet strong tidal currents would have been transporting sand into and out the mouth of the estuary and this may have lead to a removal of finer material and lag coarse material in the lower reaches the estuary. Dominant south-easterly wave action would have transported this finer material northwards long the coast. The wind, sedimentological and historical coastal change analysis presented in this chapter suggest that while large-scale coastal change may be initiated by flooding events in some cases (e.g. breach of the barrier spit), sand transfer is dominated by everyday wave action and tidal currents.

The lack of sediments that could be interpreted as immature fluvial sand and the bimodal nature of many of the sediments suggest the coarse – very coarse sand found in the estuary comes from the reworking of the truncated Pleistocene dune and the finer fraction of the deposit (fine – medium sands) have been removed by high discharge events and tidal currents. Therefore, this suggests that the modern Elliot River is not a significant contributor of sand to the coast. Despite significant effort it was not possible to obtain quality and quantity data required to calculate the average volume of sand that could be delivered to the coast by the Elliot River, and unlike the Haughton and the Black Rivers previous estimates were not available. However the relatively coarse sand in the fluvial and estuarine reaches compared to Haughton and the Black suggest relatively high amounts of energy would be need to transport this sand to the coast. The duration of fluvial flooding is brief (see figure 5.3 hydrograph), which is not conducive to transporting large volumes of very coarse sand downstream. Therefore like the Haughton River (see chapter 4, section 4.6), the modern Elliot is not contributing significant amounts of sand to the coast. Wave and tide processes dominate sand transfer throughout the system and the sources of sand are most likely the reworking of previously deposited sediments and the influx of sand via longshore drift.

CHAPTER 6 – THE POWER OF WAVES: THE BLACK RIVER DELTA.

6.1 INTRODUCTION

The Black River coastal system differs from the proceeding systems as it classified as a delta rather than an estuary. The results of the aerial photograph analysis, sedimentological and hydrodynamic studies of the Black River Delta are presented and briefly discussed in this chapter. As with the Haughton and Elliot Estuaries, a more detailed discussion of the results follows in chapter seven. Contemporary and evolutionary patterns and processes of sand transfer are similarly inferred from the results and presented in a conceptual model. Comparisons are drawn with the results from the Haughton River Estuary (chapter four) and the Elliot River Estuary (chapter five).

6.2 GEOMORPHOLOGY

The Black River is located ~20 km west of Townsville see Figure 6.1. Table 6.1 summarises the physical characteristics of the system. The Black River is 42 km long and drains a catchment of 260 km^2, discharging into Halifax Bay. Similar to the Haughton, the Black River descends steeply until the estuarine section of the channel where the slope reduces by an order of magnitude (Fluvial reach: 0.019; Estuarine reach: 0.004). The Black River delta protrudes from the coastline, with sand spits forming across the river mouth. The delta is dominated by sandy sediments (see appendix H) (Hopley, 1970a). Closely spaced beach ridges to the north of the river are indicative of the large quantities of sand originating from weathered granites and diorites of the Hervey Range (Holmes, 1992).

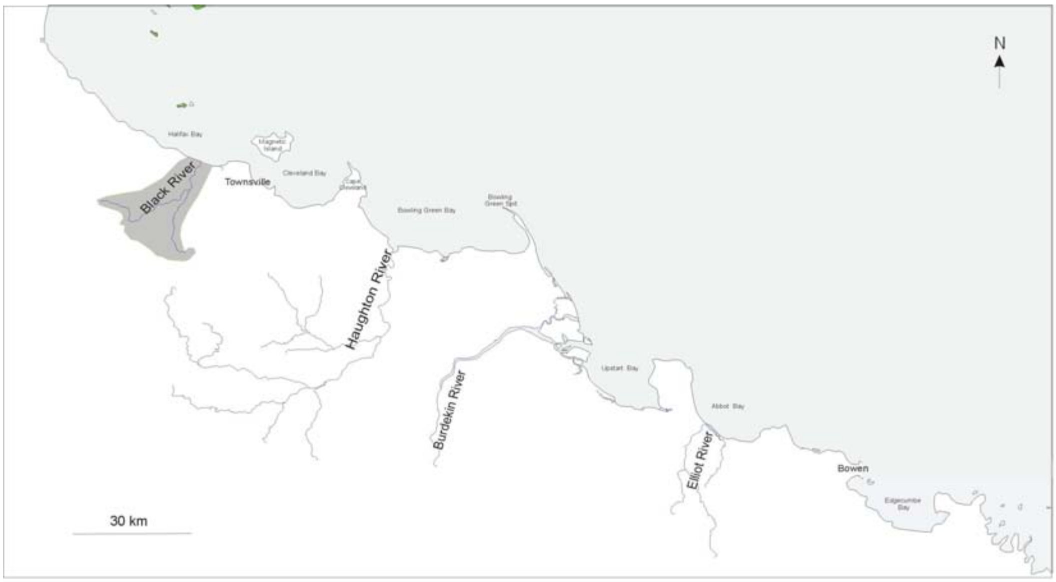

Figure 6.1. The Black River catchment.

Table 6.1. Physical characteristics of the Black River Delta

Catchment area	260 km^2
Channel length	42 km
Channel width	36-100 m
Slope	Fluvial reach: 0.019 Estuarine reach: 0.004
Sinuosity	1.7
Percentage of channel estuarine	3%
Mean annual rainfall	1538 mm
Modifications	• 49% of catchment cleared for grazing and small areas of agriculture • Sand extraction (>1,000,000 m^3 since 1972)

6.3 SETTING

Figure 6.2 illustrates the marked intra and inter-annual variability of stream flow in the Black River (see table 6.2 for a summary of flood gauge data). Similar to the Haughton and Elliot Rivers, ~92% of total annual stream flow occurs between December and April. Discharge also varies between years, with 72% of annual stream discharge registering below a quarter of the maximum flow, with several years recording almost no flow at all. Episodic and flashy floods (see figure 6.3), results in over bank flooding or as observed in the 1998 flood (maximum instantaneous discharge of 2236 $m.s^{-1}$; estimated ARI 1:100 years) the diversion of the river mouth.

Table 6.2. Summary of stream flow characteristics for the Black River Delta.

Gauging station	Bruce Highway
Distance from stream mouth	8.9 km
Catchment area at gauging station	256 km^2
Gauged area/catchment area	24%
Available records	1973-2001
Maximum annual flow volume	395,000 ML in 1974
Minimum annual flow volume	46 ML in 1985
Maximum instant discharge	2236 $m^3.s^{-1}$ in January 1998
Maximum period of no flow	7 months in 1986/87

Similar to the Haughton River Estuary, waverider buoy data from off Cape Cleveland represents offshore wave energy for the Black River Delta. Modal significant wave height ranges from 0.2-0.4 m (BPA, 1996b), but for 66% of observations significant wave height ranged from 0.2-0.8 m (BPA, 1996b). Unlike the Haughton, the Black River Delta is not sheltered from south-easterly winds by Cape Bowling Green leaving it more exposed to south-easterly winds. The Delta experiences a diurnal tidal regime with a maximum spring tide range of 3.8 m (Queensland Transport, 2003).

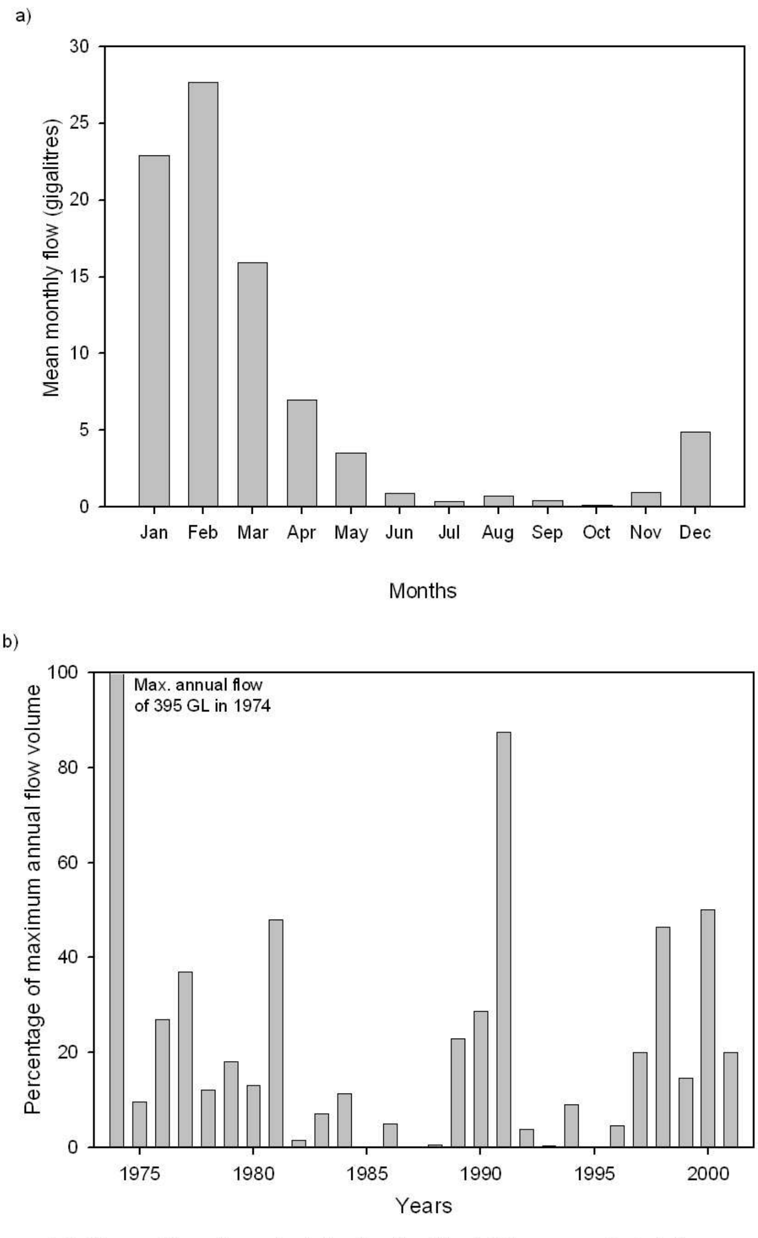

Figure 6.2. Stream flow characteristics for the Black River recorded at the Bruce Highway gauge from 1974 -2001 (DNR, 2002), mean monthly flow volumes (a) and annual flow volumes shown as a percentage fo the maximum flow volume (b).

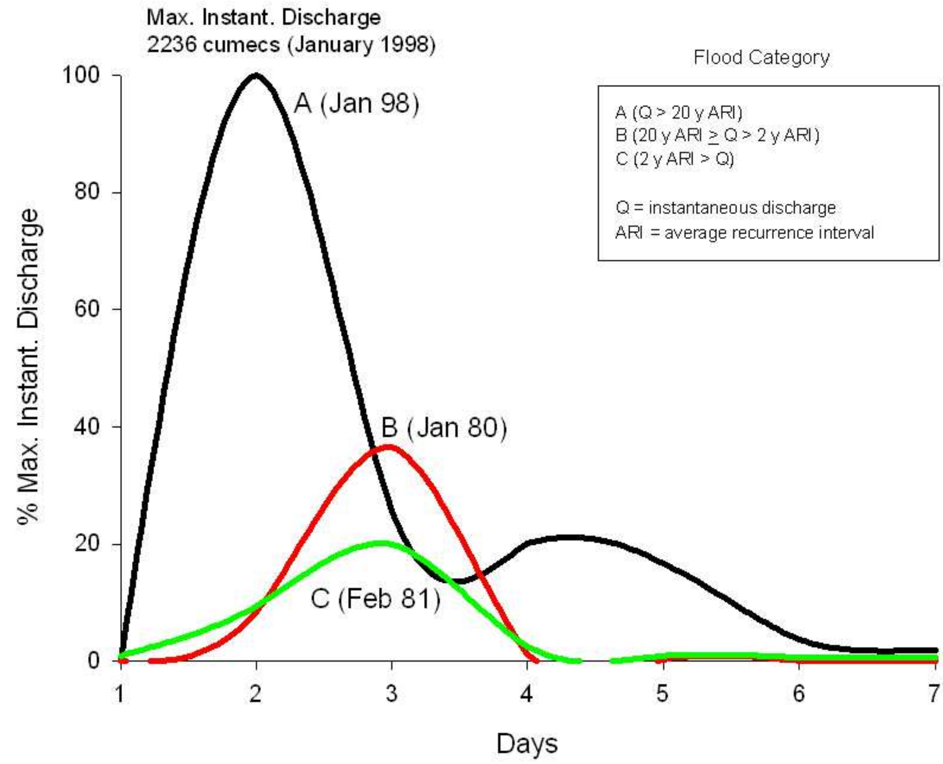

Figure 6.3. Flood hydrograph for the Black River recorded at the Bruce Highway gauge.

6.4 RESULTS

6.4.1 COASTAL CHANGE

Coastline position was recorded from aerial photographs of the Black River Delta from 1942, 1985 and 2000 (see chapter 3, section 3.4.1). The measurements of coastal change along each transect (see figure 6.4) from 1942 - 1983 and 1983 - 2000 are illustrated in Figure 6.5. Analysis of the coastline adjacent to the Black River north to Bluewater Creek revealed a general trend of progradation, with an average of 41 m or 1 $m.y^{-1}$ linear coastline advance between 1942-1983. Between 1983-2000 progradation continued close to the river mouth (2 km north along the coast) at a rate of 1 $m.y^{-1}$, with frequent occurrences of erosion (average of 18 m at each transect or at a rate of 1 $m.y^{-1}$) and some stability from 2.25 km – 5.25 km up the coast towards Bluewater and Althaus Creek.

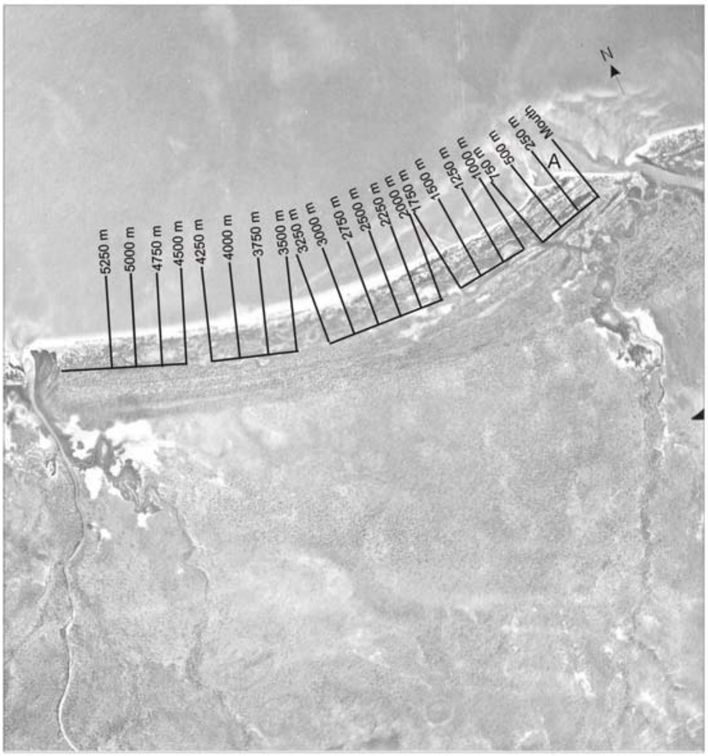

Figure 6.4. Location of transects from which coastal change measurements were derived shown on the 1940 aerial photograph of the Black River Delta. 'A' indicates the location of bedforms shown in figure 6.8.

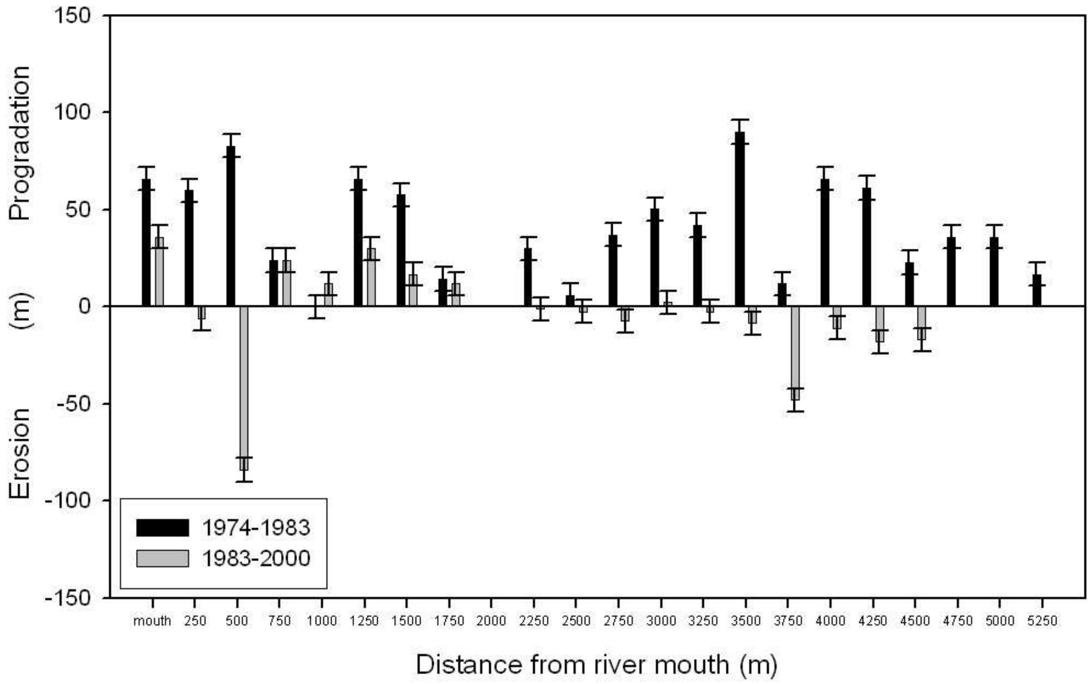

Figure 6.5. Shoreline progradation and retreat along the Black River Delta measured from 1974 and 2000 aerial photographs. Standard error of measurement estimated at 6 m for 1:12,000 scale photography. (See figure 6.4 for locations of transects).

The movement of sand bars explains much of the coastal change, due to a recurring pattern of moving close to shore and welding on to the shoreline and then detaching as described by Pringle (Pringle, 1984; Pringle, 2000) for the Burdekin Delta. For example along the transect 500 m north of the river mouth has prograded 84 m between 1942-1983 and then eroded 80 m in the subsequent 17 years to 2000. Analysis of intervening aerial photographs revealed that this progradation occurred rapidly over a period of five years between 1979-83. Along the 500 m transect there was only 8.4 m of progradation between 1942-1974, then a retreat of 4.8 m to 1979 followed by an advance of 80 m between 1979-1983. Over the following 8 years, this same section of coast retreated 66±6 m, eroding a further 16.8 m to 1995.

The dynamic nature of this coastline was first documented in 1880 (Coastal Engineering Solutions, 1998). The continual build up and erosion of the sand spit on the eastern side of the river mouth has been observed in the earliest surveys and in the most recent aerial photos, seemingly in response to major flood events. For example, the January 1998 flood (ARI 1:100) caused the erosion of the ~100 m long sand spit which extended across the delta mouth (Figure 6.6). A schematic model was produced from comparisons of aerial photos of the delta taken in 1995 and 2000 to illustrate the effect of the flood on its morphology (Figure 6.7).

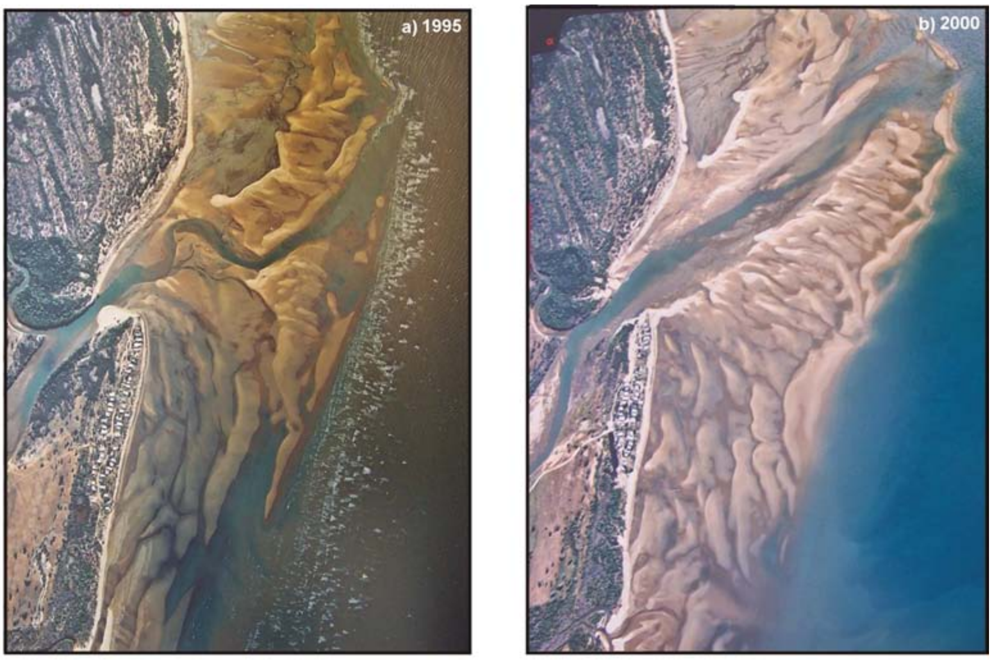

Figure 6.6 a-b. Vertical aerial photographs of the Black River Delta which were used to develop figure 6.7 a-b. Copyright: The State of Queensland (Department of Natural Resources and Water) 1995 (a), 2000 (b).

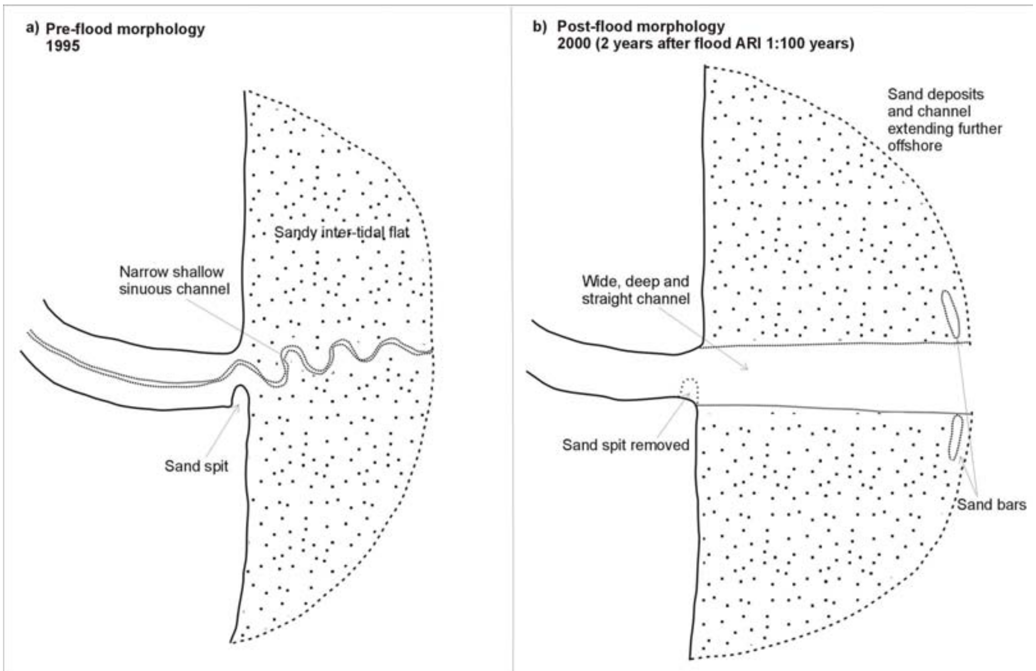

Figure 6.7 a-b. A schematic model illustrating the impact of a ARI 1:100 year flood on the morphology of the Black River Delta.

A comparison of the Black River pre-flood (1995) and post-flood (2000) photographs revealed distinct changes within the delta and adjacent coastline indicative of a major flood event. For example, the narrow (36±6 m) and sinuous main channel captured in the 1995 photograph had widened to 100±6 m, straightened and extended another 400±6 m offshore to 1.89 km, by the 2000 photograph (Figure 6.7). The tidal delta had also extended further offshore and the sand spit in the estuary mouth has been removed to leave a wider inlet in 2000. Tides and waves have started to move the sand bodies into the estuary and further along shore, however recovery to its pre-flood morphology is slow. A recent aerial survey (2003) revealed that the delta is still in the post-flood morphology yet to recover to the pre-flood state over five years after the event. Despite changes in the spatial arrangement of sand bodies within the delta, the flanking coastlines have remained stable from 1995-2000.

6.4.2 BEDFORMS

As noted in section 3.4.2, chapter 3, instantaneous patterns of sand transfer in estuaries can be inferred from studying bedforms. Small current ripples 1 cm in high with a 5 cm wave length, were observed at low spring tide orientated towards the sea (Figure 6.8). No megaripples were observed on the intertidal flats.

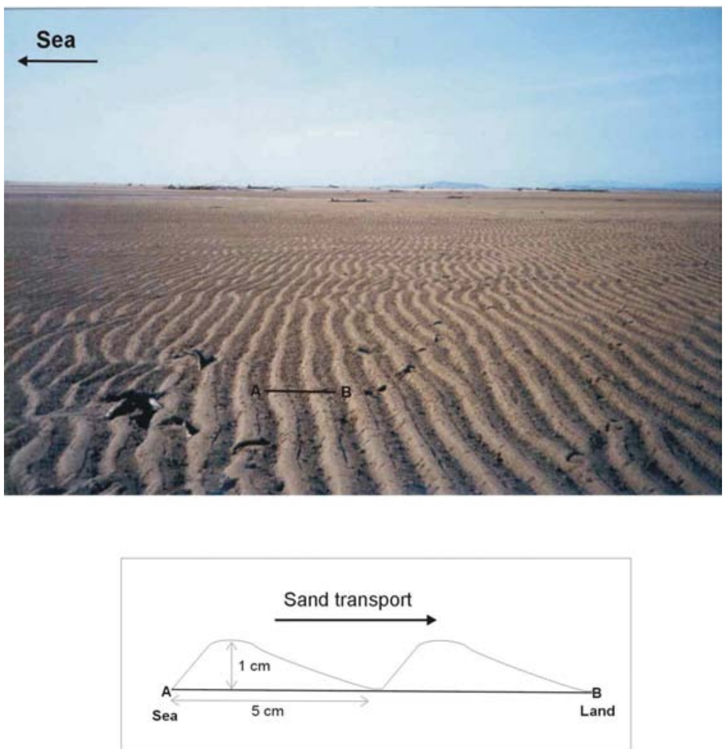

Figure 6.8. Seaward orientated current ripples 1 cm high and 5 cm wavelength observed in the Black River Delta at low spring tide.

6.4.3 SEDIMENTOLOGY

Unfortunately detailed pre-flood sedimentological surveys are not available for the study site. Post-flood fieldwork occurred in January 2001, three years after the January 1998 flood (ARI 1:100 year). Sixty-eight surficial sediment samples were collected from the Black River Delta and adjacent coastline (Figure 6.9). Figure 6.10 summaries the results of textural analysis of the surficial samples (see Appendix D) illustrating the spatial distribution of facies. The tidal reaches and mouth of the delta are dominated by moderately sorted coarse sand with some patches of medium sand. The intertidal areas encompass a broad range of sediment types from coarse silt (0.020 mm) to coarse sand (0.788 mm), moderately well sorted (0.001) to very poorly sorted (0.005), symmetrical (-0.015) to very finely skewed (-0.664). Beach sands also vary in grain size from fine (0.199 mm) to coarse sand (0.640 mm), but are all moderately well sorted (1.65) and symmetrical (-0.018) to coarsely skewed (0.339). Dune sands are generally finer ranging from fine (0.160 mm) to medium sand (0.347 mm) however two of the samples are coarse sand (0.507 mm and 0.550 mm). Further offshore from the delta the sediments become finer and more poorly sorted with mixtures of fine sand and coarse silt. Over half of Black River sediments have leptokurtic kurtosis values and are finely skewed. Coarse (0.510 mm) and moderately sorted (0.89), symmetrical (-0.09) with a feldspars content of 18% and low carbonate content (>1%) sand was interpreted as fluvial.

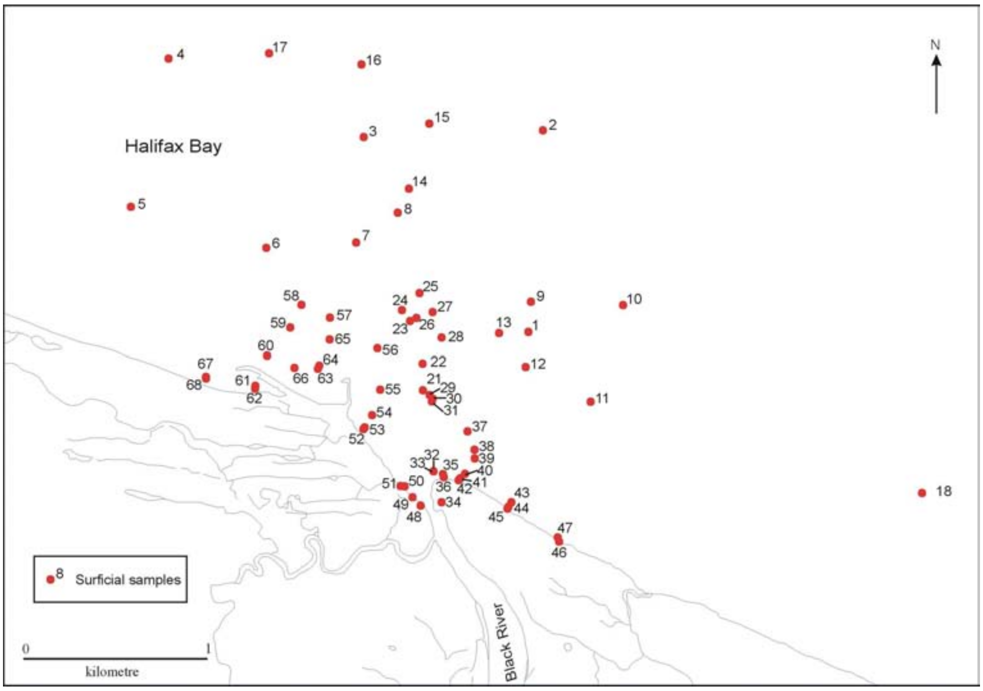

Figure 6.9. Locations of surficial sediment samples taken at the Black River Delta. (See Appendix D for the results of the textural analysis of samples).

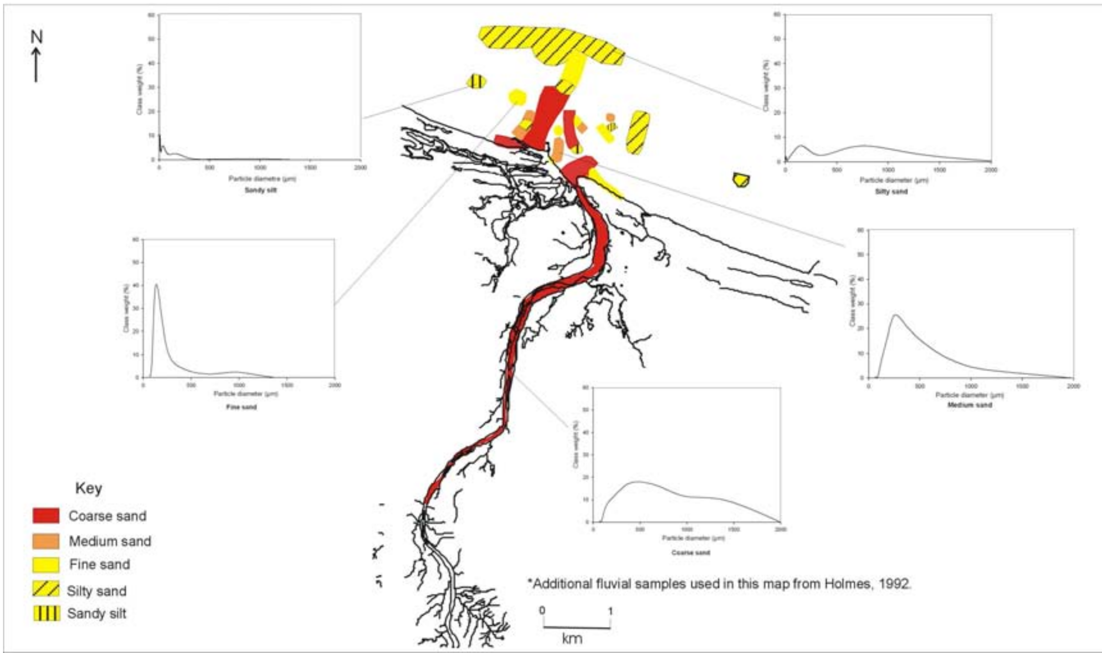

Figure 6.10. Summary of the results of textural analysis of surficial samples from the Black River Delta. Histograms show the distribution of a typical example of each sediment class.

Figure 6.11 part a-d compares the surficial samples according to mean grain size, sorting, skewness and kurtosis characteristics after Friedman (1961) (see section 3.4.3, chapter 3). In all graphs the samples are loosely correlated to their sampling location. The results of a discriminant analysis (Table 6.3) revealed that mean grain size (0.514 mm) was the most significant variable in the first function, with both sorting (0.814) and skewness (-0.638) most significant in the second. Plotted according to these functions (Figure 6.12) the samples loosely cluster according their environmental setting.

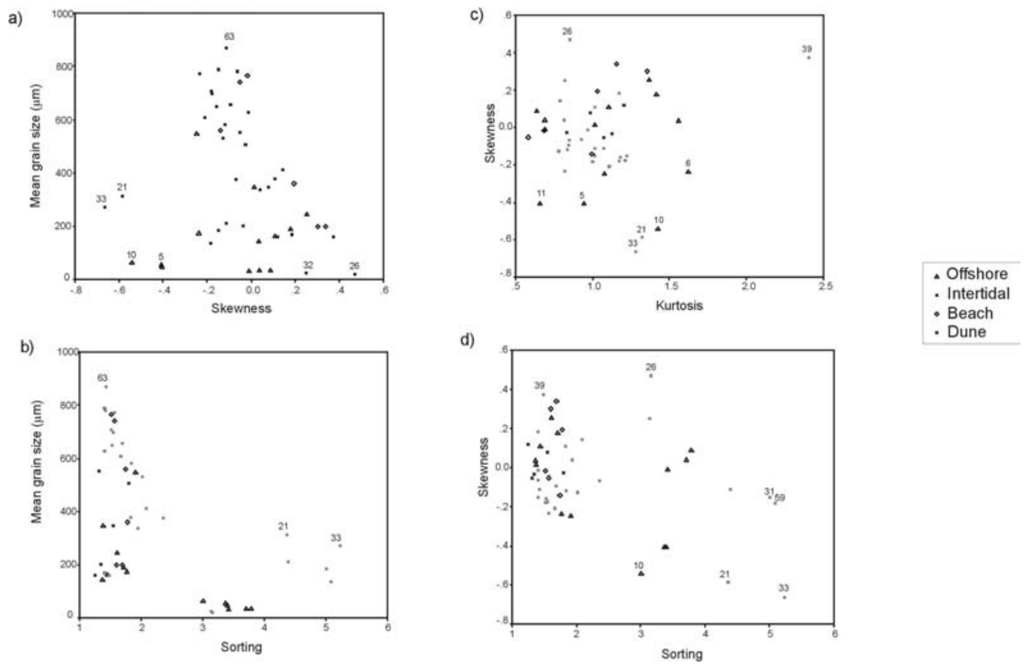

Figure 6.11 a-d. A comparison of the surficial and subsurface sediment samples according to their mean grainsize, sorting, skewness and kurtosis characteristics for the Black River Delta after Friedman 1961.

Table 6.3. Structure matrix from the discriminant analysis for Black River Delta.

Variables	Function		
	1	2	3
Sorting	0.022	0.814*	0.513
Skewness	0.037	-0.638*	0.593
Mean grain size	0.514	-0.369	0.715*
Kurtosis	-0.052	0.231	-0.325*

* indicates the largest absolute correlation between each variable and any discriminant function.

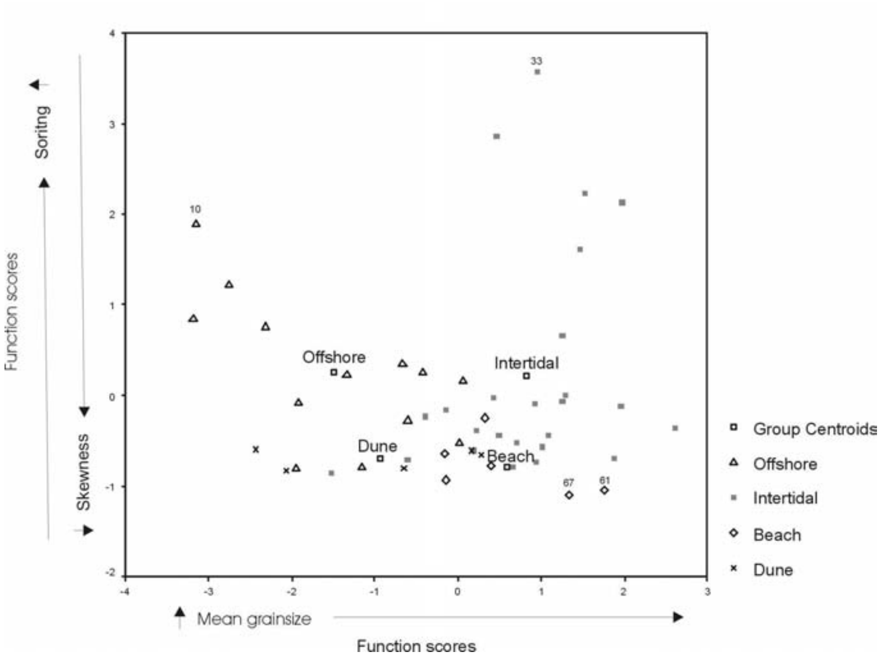

Figure 6.12. Scatter plot showing the results of discriminant analysis using all descriptors for the Black River Delta.

6.5 CONCLUSIONS

Aerial photographic, sedimentological and hydrodynamic data was used to develop a conceptual model of sand transfer in the Black River Estuary.

6.5.1 COASTAL CHANGE

Wave refraction around Magnetic Island probably contributes to the pattern of sand bar movement observed in the Black River Delta. Figures 6.13 a-c show wave refraction patterns for the most common wind directions south-easterly, easterly, and north-easterly. During south-easterly winds the resultant wave pattern indicates sand moving northwards up the coast and perhaps moving sand onshore. The easterly winds create a wave pattern, which targets the most dynamic section of coast (500 m adjacent to the river mouth) which may account for the erosion of the sand bar. Refraction of north-easterly waves creates an overlapping of wave trains on this section of coast directly adjacent to the river mouth. It is likely that this wave pattern would create erosion on the same section of coast and perhaps the movement of sand to the south.

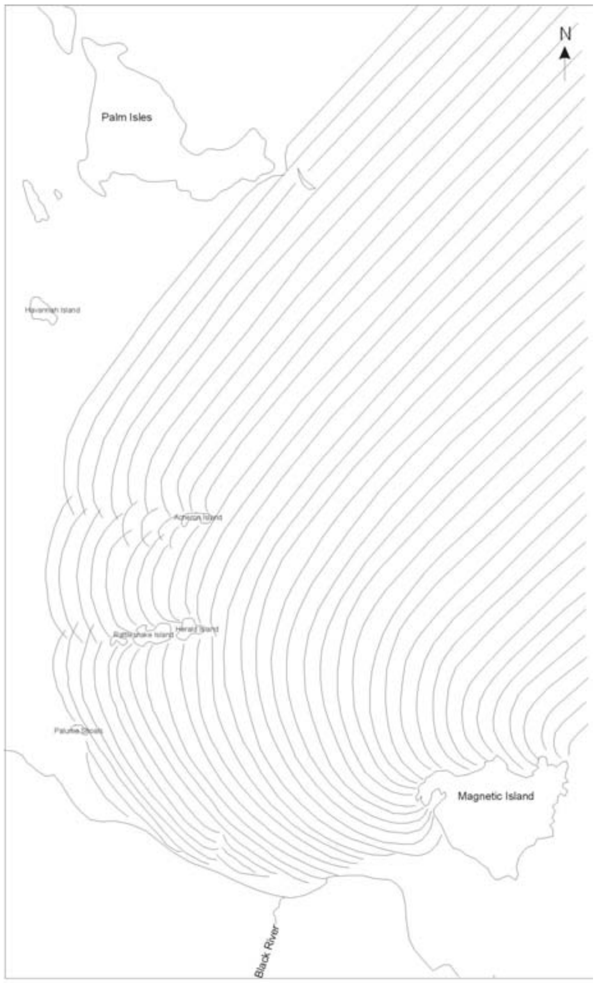

Figure 6.13 a. Wave refraction pattern for 5 second wave intervals and 20 wave crest spacing generated by south easterly winds.

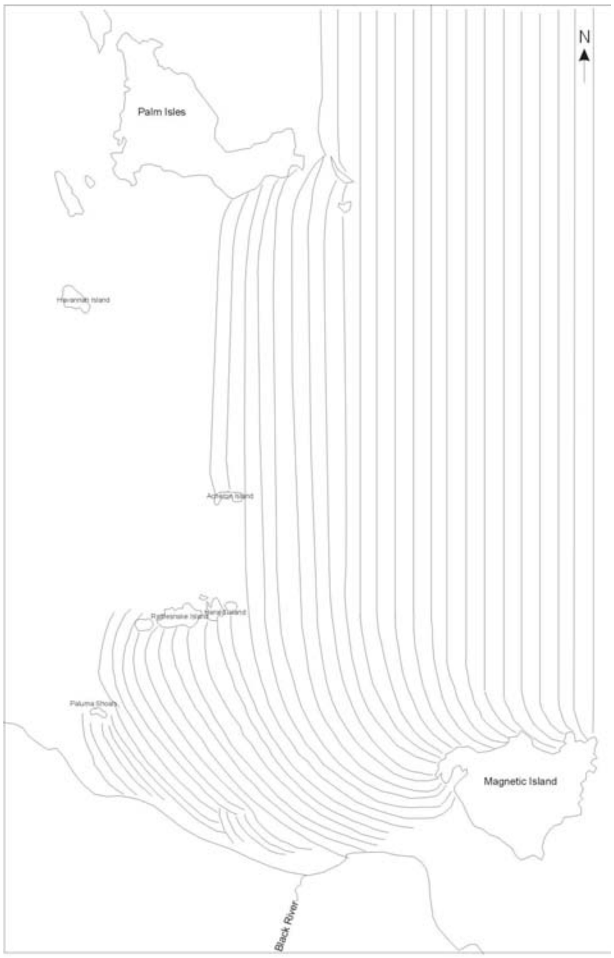

Figure 6.13 b. Wave refraction pattern for 5 second wave intervals and 20 wave crest spacing generated by easterly winds.

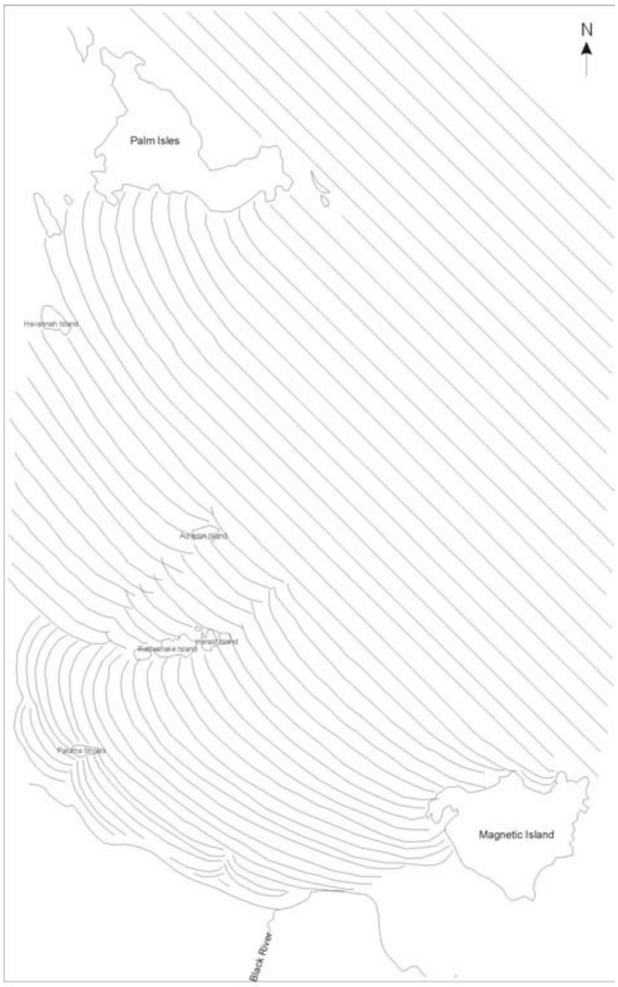

Figure 6.13 c. Wave refraction pattern for 5 second wave intervals and 20 wave crest spacing generated by north easterly winds.

Wind data analysis for Townsville has revealed a significant (both R^2 = 0.47) increase the frequency of south-easterly and easterly winds at all speeds since 1950 (Figures 6.14 and 6.15). This may have increased the movement of sand to the north west – indicated by spits orientated to the north west. There is also a marked increase in the frequency of south-easterly and easterly winds <21 $km.h^{-1}$ from 1980-1984 which decreased again from 1985-1989. The frequency of north-easterly winds has dropped off significantly (R^2 = 0.59) between 1965 and 1985 (Figure 6.16). The frequency of north-easterly winds has increased again in the subsequent 15 years, which may account for recent coastal erosion.

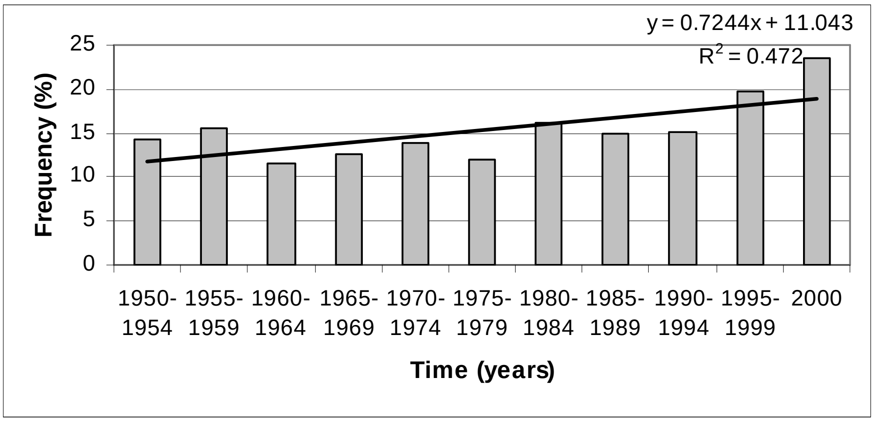

Figure 6.14. The frequency of south easterly winds at all speeds has increased from 1950-2000. Townsville wind data from the Bureau of Meteorology.

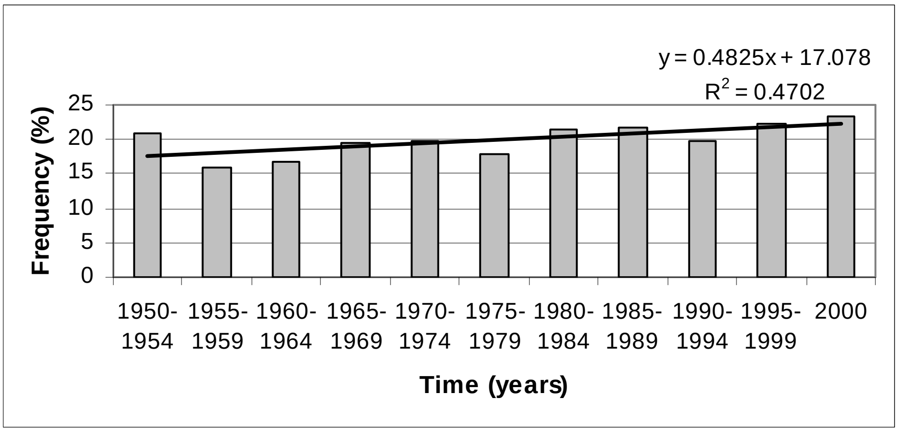

Figure 6.15. The frequency of easterly winds at all speeds has increased from 1950-2000. Townsville wind data from the Bureau of Meteorology.

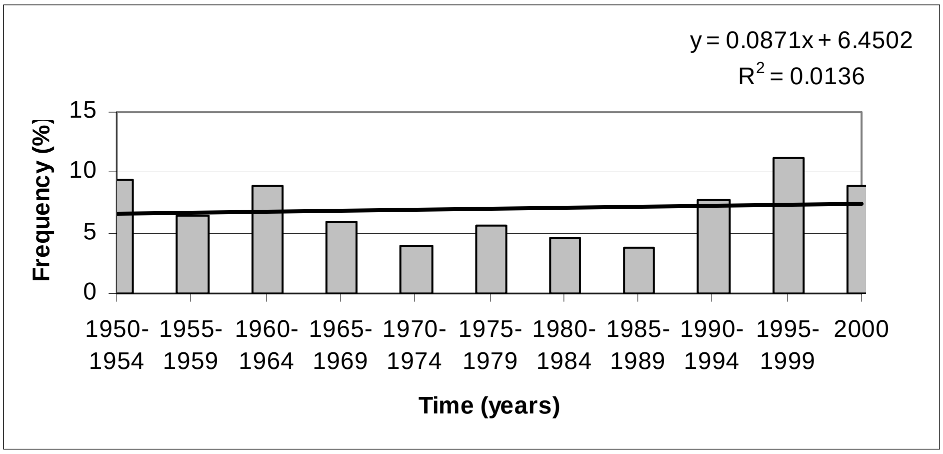

Figure 6.16. The frequency of north easterly winds over 21 km.h-1 has dropped off between 1965-1985. Townsville wind data from the Bureau of Meteorology.

The increase of south-easterly and easterly winds during 1980-84 correlated with the movement of the sand bar onshore 500 m from the mouth and the massive 80 m progradation of the shoreline. An increase in the frequency of north-easterly winds post-1985 is correlated with the sand bar moving offshore again.

6.5.2 BEDFORMS

The lack of larger bedforms (megaripples) suggests that tidal currents are short in duration and weak in the Black River Delta. This is because the size of the estuary is smaller compared to the Haughton and the Elliot River Estuaries. With a maximum bed velocity of 0.2 $m.s^{-1}$ during spring tidal currents (Kinhill, 1998) both ebb and flood currents are insufficient to transport bed material larger than fine sand (0.02 mm) in or out of the delta. Small ebb tide current ripples were observed on the intertidal flat indicating the seawards movement of sand.

6.5.3 SEDIMENTOLOGY

Many of the intertidal and offshore samples from the delta are bimodal, trimodal and even polymodal, therefore interpretations from the statistics must be made with caution. Sediments close to their source are characteristically leptokurtic and finely skewed (Folk and Ward, 1957). Over half of the samples from all locations within the delta are leptokurtic and finely skewed which suggests they are close to their source, which is most likely, the Black River. River and delta mouth sediments are angular and poorly sorted and interpreted as immature fluvial sands. Beach and dune sands are slightly more rounded (sub-angular to sub-rounded) and better sorted however still in the same size range. The angularity of the grains, relatively high feldspars content and low carbonate content (12-24%) suggests that the delta is composed of Black River sands. The presence of magnetite in both fluvial sediment from the Black and sand on the adjacent coast supports the conclusion that the Black River supplies significant volumes of sand to the coast today and in the past.

The Black River delta protrudes from the coastline. The river cuts through approximately 1 km of closely spaced beach ridges from 1 to 4 m in height, which have developed over the last 6,000 years. The most likely source of this sediment is the Black River (Hopley, 1970a) (Holmes, 1992). Belperio (1978) assumed that the original source of this sand was from the Burdekin when it was positioned at the Barrattas, as the tombolo to Cape Cleveland was yet to be completed and sand moved between the compartments. Holmes (1992) tried to establish a definite link between the Black River sediments and adjacent coast deposits by the presence of magnetite. However, magnetite has been found in sand accumulations around the Whitsunday Islands (Heap *et al.*, 2002) therefore cannot be linked exclusively to the Black River.

6.5.4 CONCEPTUAL MODEL

The results of the aerial photograph, sedimentological and hydrodynamic investigations suggest that the Black is a wave-dominated delta. The Delta is a net exporter of sediment, which is in contrast to the Haughton and the Elliot River coastal systems which were classified as estuaries, and are net importers of sediment (chapter 2, section 2.2). The contemporary processes of sand transfer occurring in the Delta are illustrated in figure 6.17.

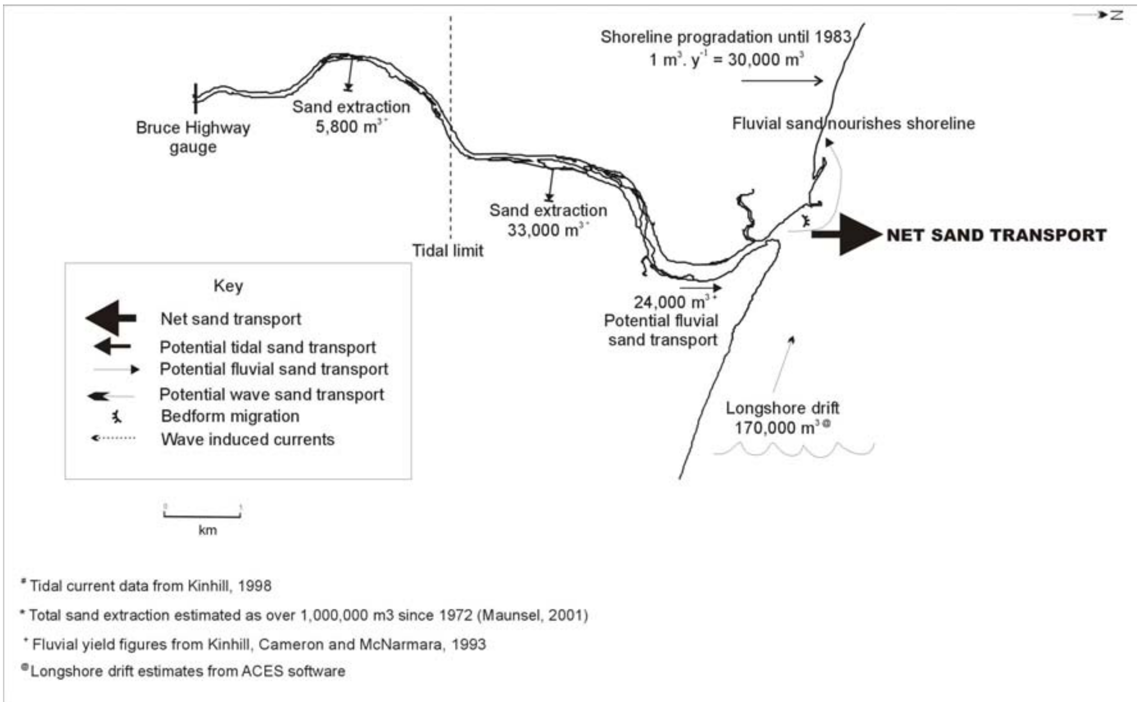

Figure 6.17. Summary diagram of net sand transport trends at the Black River Delta as indicated by bedform orientations, grain size patterns and dominant current directions. Fluvial energy and wave-induced currents are the most dominant, hence net sand transport direction is seawards.

Coastal change can be attributed to the movement of sand spits and bars in association with changes in wave action due to cycles of wind speed, frequency and direction. However, the aerial photograph analysis revealed the impact of flooding on the morphology and spatial arrangement of sand bodies within the delta (section 6.4.1). Modelling suggests that the Black River has the potential to deliver an average of 24,000 m^3 of bedload to the coast every year (Kinhill *et al.*, 1993) (section 7.3, in the following chapter for a discussion of the assumptions associated with modelling fluvial sediment yield). As in the Haughton, reference to yearly estimates of fluvial supply in this highly variable discharge system is not ideal, however it is all that is available. Also similar to the Haughton and the Elliot short duration of high discharge events in the Black River is not conducive to large amounts of sand transfer. However the shorter estuary, i.e. only 3% of the channel is under tidal influence creates a different situation in the Black, and despite geomorphically ineffective flooding (Costa and O'Connor, 1995) (see chapter 2, section 2.4.1) fluvial sediment is still delivered to the coast.

Holmes (1992) identified the Black River Delta as the source of sediment for the adjacent coast. Aerial photograph analysis (see section 6.4.1) reveals that this coast has continued to prograde at a rate of 1 m per year in recent years (1942-1983). Strong longshore currents driven by dominant south-easterly waves act as a mechanism to transport sand at the delta mouth to the adjacent coast and also provide additional sand imported into the system from further south. Modelling using ACES (Leenknecht *et al.*, 1992) (chapter 3, section 3.4.4.1, Appendix C) suggests that longshore currents have the potential to transport 170,000 m^3 of sand north per year. While large-scale coastal progradation has been linked to changes in wind patterns, erosion along the adjacent coast indicated from analysis of the most recent 20 years of aerial photographs (section 6.4.1 and 6.5.1) implies a reduction in the supply of sand. Reduction in sand availability in the delta possibly due to The extraction of over 1,000,000 m^3 of sand from the Black River channel for commercial purposes (Kinhill, 1998) (equivalent to ~30 years of average sediment delivery to the coast) may be a contributing factor to reduced sand availability in the delta.

CHAPTER 7 – HOLOCENE SAND BUDGET FOR THE SWT COAST

7.1 INTRODUCTION

The results of aerial photograph, sedimentological and hydrodynamic investigations at the Haughton River Estuary, Elliot River Estuary and the Black River Delta (see chapters 4, 5 and 6) suggest that SWT streams have not been delivering the volume of sand to the coast predicted by recent modelling e.g. Prosser *et al.*, (2001a) who support an average of 400,000 $m^3.y^{-1}$. These findings must be interpreted within a Holocene context to incorporate multi-cyclic processes of coastal evolution. This chapter presents a Holocene sand budget for the SWT coast. Sand stored onshore and on the inner shelf within the SWT is quantified and compared with modelled estimates of sand delivery to the coast extrapolated over the last 7 ka. The spatial extent of sand that has contributed to the modern SWT coast is largely restricted to sand deposits on the present inner shelf, which at -5 m sea level (~7 ka BP) could have been reworked by waves and transported on shore.

7.2 ESTIMATING THE VOLUME OF SAND IN THE COASTAL ZONE

The SWT coast is dominated by sand with extensive beach ridge plains, sand-choked inlets and sandy nearshore deposits (Figure 7.1). Sedimentological, stratigraphic and seismic investigations were reviewed to quantify the volumes of sand deposited on the SWT coast (4 m to L.A.T.), nearshore (subtidal) (0 to -5 m L.A.T.) and continental shelf (inner shelf -5 to -20 m L.A.T.) during the Holocene. Sand deposits were quantified using the following equation:

$$\mathbf{x = (a \times t)\, s}$$

where

x = the volume of sand contained in a deposit

a = area of deposit

t = estimated or established thickness

s = the proportion of sand-sized material in the deposit.

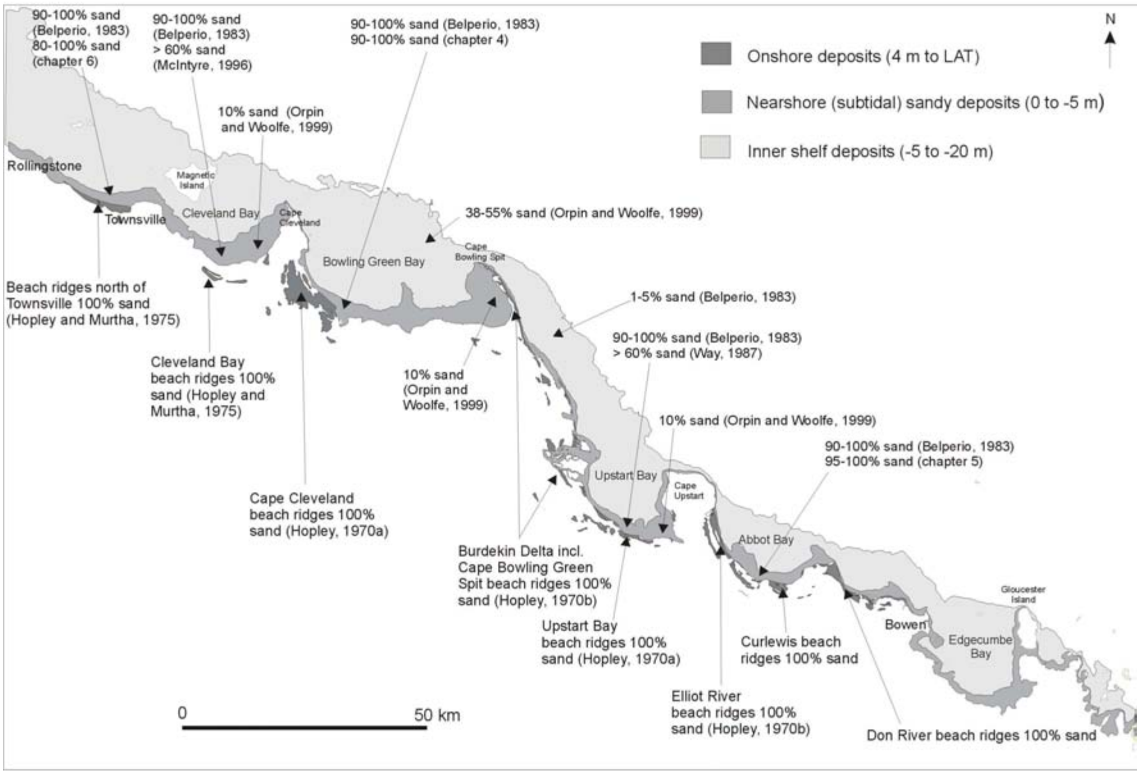

Figure 7.1. Location of onshore, nearshore and inner shelf deposits for the SWT coastal zone and the percentage of sand reported in the literature.

7.2.1 ONSHORE DEPOSITS

Hopley (1970a) and Hopley and Murtha's (1975) detailed studies established that the SWT coastal plain is dominated by sand. Extensive beach ridge complexes of both Pleistocene and Holocene age have been identified and mapped (Hopley, 1970a). The Cape Cleveland beach ridge complex has been most intensively studied and is the largest complex in the region, with over 100 individual ridges covering an area of 15.3 km^2 (Hopley, 1970a). The ridges range from 2.6 m to over 10 m in height and are entirely composed of sand (Hopley, 1970a). Fourteen cores taken in the swales of the Cape Cleveland beach ridge plain revealed a sand thickness of 0.9 m – 3 m (McIntyre and Associates, 1985). Bird's (1973) method was used to calculate the volume of sand stored in the Cape Cleveland beach ridge plain. Bird's (1973) method was considered most appropriate as it accounts for the topographic highs (crests) and lows (swales) characteristic of beach ridge plains unlike other methods (e.g. Holmes, 1992). It was assumed from topographic survey data (McIntyre and Associates, 1985) that 50% of the area is comprised of the ridge crests with an average height of 6 m above L.A.T (Hopley, 1970a) and that 50% of the area is comprised of swales with sand to an average depth of 1.95 m beneath. Using this approach it was calculated that the Cape Cleveland beach ridges contain approximately 6.1×10^7 m^3 of sand.

This methodology was applied to quantify the volume of sand contained in onshore deposits along the entire SWT (Table 7.1). Typically, these coastal deposits comprise a beach foredune and beach ridge plain or open coast and a chenier plain on more sheltered north facing bays (see chapter 2, section 2.5) (Hopley and Murtha, 1975). Previous attempts by Holmes (1992) have overestimated the amount of sand stored onshore by failing to take into account swales in calculations of sand stored in beach ridge plains in the Townsville region, (termed collectively in on figure 7.1 as 'north of Townville beach ridges'). Bird's (1973) method is more realistic as it assumes that 50% of the area is comprised of ridge crests at an average of 4 m above L.A.T. and 50% of the area is swales with sand thickness taken as a minimum thickness of 0.9 m based on the Cape Cleveland cores (McIntyre, 1996). Cheniers are storm deposits and are not commonly homogenous sand deposits like beach ridges (see chapter 2, section 2.5 for more details). Cheniers will be considered separately in the calculations. Chenier ridges, adjacent to the Bohle River, are 1.8 m in height, composed of between 68 and 87% sand and occupy an area of 1.27 km^2 (Hopley and Murtha, 1975). The sum of estimates from individual onshore deposits indicates that ~1.28×10^8 m^3 of sand is stored in onshore deposits on the SWT coast (Table 7.1).

7.2.2 NEARSHORE (SUBTIDAL) DEPOSITS

Sandy nearshore (subtidal) deposits extend out from the SWT coast to a depth of about 5 m below L.A.T. (Johnson and Searle, 1984) and cover ~750 km^2 (Figure 7.1). Seismic investigations reveal an average thickness of Holocene nearshore sediment of 2 m along the SWT coast usually overlying Pleistocene clay (Searle *et al.*, 1981; Johnson *et al.*, 1982; Johnson and Searle, 1984). Textural analyses indicate that sand comprises 60-100% of most of the surficial sediments collected from the nearshore zone along the SWT coast (Table 7.2), however in more sheltered bays such as Bowling Green Bay, sampled sediments may contain only 6-14% sand (Orpin and Woolfe, 1999). Orpin and Woolfe (1999) suggest that the increased deposition of fine fraction muds and silts in northward facing bays is due to generally lower ambient hydrodynamic energy as a result of sheltering from south easterly waves and northerly currents. Therefore the volume of sand in the sheltered areas of the northward facing bays: Cleveland Bay (73 km^2); Bowling Green Bay (72 km^2); Upstart Bay (38 km^2) were calculated separately with an average thickness of 2 m and an estimated proportion of 10% sand (see Table 7.3). A total of 3.7×10^7 m^3 (Cleveland Bay 1.5×10^7 m^3; Bowling Green Bay 1.4×10^7 m^3; Upstart Bay 7.7×10^6 m^3) of sand contained in sheltered areas of the bays.

The remaining nearshore deposits cover an area of 567 km^2 with an average thickness of 2 m. The volume of sand ranges from 2.3×10^8 m^3 at 60% sand to 1.1×10^9 m^3 at 100%. It was conservatively estimated that the remaining majority of nearshore sand deposits would contain approximately 70% sand - slightly above the minimum result from sampling (Table 7.2). These figures provide an estimate of 7.9×10^8 m^3 of sand. With an additional 3.7×10^7 m^3 of sand contained in the sheltered areas of the bays, this approximates 8.3×10^8 m^3 of sand deposited in the nearshore (subtidal) areas during the Holocene.

Table 7.1 Estimated volume of sand stored in SWT onshore deposits.

Onshore deposit	Area km^2 (source)	Height of deposit m (source)	Average thickness of sand (m)	Percent sand (source)	Estimated volume of sand (m^3)
Rollingstone Creek beach ridges*	0.65 (Hopley and Murtha, 1975)		2.45 (50% 4 m; 50 % 0.9 m)	100% (Hopley and Murtha, 1975)	1,592,500
Saltwater Creek beach ridges*	0.08 (Hopley and Murtha, 1975)		2.45 (50% 4 m; 50 % 0.9 m)	100% (Hopley and Murtha, 1975)	196,000
Leichhardt Creek beach ridges*	0.53 (Hopley and Murtha, 1975)		2.45 (50% 4 m; 50 % 0.9 m)	100% (Hopley and Murtha, 1975)	1,298,500
Sleeper Log Creek beach ridges*	0.46 (Hopley and Murtha, 1975)		2.45 (50% 4 m; 50 % 0.9 m)	100% (Hopley and Murtha, 1975)	1,127,000
Bluewater Creek beach ridges*	0.45 (Hopley and Murtha, 1975)		2.45 (50% 4 m; 50 % 0.9 m)	100% (Hopley and Murtha, 1975)	1,102,500
Black River beach ridges*	1.20 (Hopley and Murtha, 1975)		2.45 (50% 4 m; 50 % 0.9 m)	100% (Hopley and Murtha, 1975)	2,940,000
Bohle River chenier ridges	1.27 (Hopley and Murtha, 1975)	1.80 (Hopley and Murtha, 1975)	1.8	77% (Hopley and Murtha, 1975)	1,760,220
Shelly Beach ridges	0.37 (Hopley and Murtha, 1975)	3.50 (Hopley and Murtha, 1975)	2.45 (50% 4 m; 50 % 0.9 m)	100% (Hopley and Murtha, 1975)	899,150
Many Peaks Range beach ridges	2.70 (Hopley and Murtha, 1975)	6.86 (Hopley and Murtha, 1975)	2.45 (50% 4 m; 50 % 0.9 m)	100% (Hopley and Murtha, 1975)	6,165,000
Cleveland Bay beach ridges	1.82 (Hopley and Murtha, 1975)		2.45 (50% 4 m; 50 % 0.9 m)	100% (Hopley and Murtha, 1975)	4,459,000
Cape Cleveland beach ridge plain	15.3 (Hopley, 1970a)	2.6- 10.3 (Hopley, 1970a)	3.98	100% (Hopley, 1970a)	60,894,000
Burdekin Delta incl. Bowling Green Spit	4.60 (geology maps)		2.45 (50% 4 m; 50 % 0.9 m)	100% (Hopley, 1970b)	11,270,000
Upstart Bay (RM point)	2.53 (Hopley, 1970a)		2.45 (50 % 4 m; 50 % 0.9 m)	100% (Hopley, 1970a)	6,198,500
Elliot River beach ridges Barrier spit	3.85 (Hopley, 1970b) 0.34 (see chapter 5)	4.57 (Hopley, 1970b) 2.00 (see chapter 5)	2.45 (50 % 4 m; 50 % 0.9 m) 2.00	100% (Hopley, 1970b)	9,432,500 686,000
Curlewis Bay beach ridges	2.37 (geology maps)		2.45 (50% 4 m; 50 % 0.9 m)		5,806,500
Don River beach ridges	4.80 (geology maps)		2.45 (50% 4 m; 50 % 0.9 m)		11,760,000
TOTAL	**43.32**				**127,587,370**

* these individual deposits appear grouped on figure 7.1 and are referred to as 'North of Townsville' beach ridges.

Table 7.2 Estimated volume of sand stored in SWT nearshore deposits (0 to –5 m L.A.T.)

Sampling Location	Area km^2	Average thickness (m)	Percent sand (source)	Maximum (100% sand) volume of sand (m^3)	Minimum (60% sand) volume of sand (m^3)	Conservative (70% sand) volume of sand (m^3)
Halifax Bay	59	2	80-100 (this study see chapter 5) 90-100 (Belperio, 1983)	118,000,000	70,800,000	82,600,000
Cleveland Bay	106	2	> 60 (McIntyre, 1996) 90-100 (Belperio, 1983)	212,000,000	127,200,000	148,400,000
Bowling Green Bay	198	2	90-100 (this study see chapter 4) 90-100 (Belperio, 1983)	396,000,000	237,600,000	277,000,000
Upstart Bay	89	2	> 60 (Way, 1987) 90-100 (Belperio, 1983)	178,000,000	106,800,000	124,600,000
Abbot Bay	115	2	95-100 (this study see chapter 5) 90-100 (Belperio, 1983)	230,000,000	138,000,000	161,000,000
TOTAL	**567**			**1,134,000,000**	**680,400,000**	**793,600,000**

Table 7.3. Estimated volume of sand stored in SWT nearshore deposits (0 to –5 m L.A.T.) on the leeward side of northward facing bays.

Sampling Location	Area km^2	Average thickness (m)	Percent sand (source)	Conservative (10% sand) volume of sand (m^3)
Leeward side of Cleveland Bay	73	2	10 (Orpin, 1999)	15,000,000
Leeward side of Bowling Green Bay	72	2	10 (Orpin, 1999)	14,000,000
Leeward side of Upstart Bay	38	2	10 (Orpin, 1999)	7,700,000
TOTAL	**183**			**36,700,000**

7.2.3 INNER SHELF

The inner shelf extends from the 5 m isobath to the 20 m isobath (Figure 7.1) and covers an area of approximately 2922 km^2 offshore of the SWT coast. During the 1970's and early 1980's the Queensland Geological Survey conducted an extensive program of Continuous Seismic Profiling (CSP) of the sea bed along the continental shelf between Cairns and Bowen (reviewed in Searle *et al.*, 1981). These seismic records together with later offshore sedimentological studies (e.g. Belperio, 1983; Way, 1987; McIntyre, 1996; Orpin and Woolfe, 1999; Dunbar *et al.*, 2000; Lambeck and Woolfe, 2000; Heap *et al.*, 2002) identified the extent of Holocene sand deposits on much of the inner continental shelf.

Constraining the inputs and outputs of sand on the inner shelf over the Holocene is complicated by rising sea levels altering the position of the coast and varying rates of sea-level rise due to shelf topography. The onset of sea-level rise and the subsequent flooding of the inner shelf (~9 ka) almost certainly caused the onshore movement of sand stored on the shelf (Hopley, 1970a; Thom and Roy, 1985). However the sources of the sand that moved onshore with the marine transgression must be determined to constrain the inputs of this sand budget. Dunbar *et al*. (2000) and Heap *et al*. (2002) suggest that early Holocene sediment deposits have remained on the mid-shelf and were not moved onshore with the transgression. Rather Dunbar *et al.* (2000) found increased rates of deposition of siliciclastic sediments into the Queensland trough during the transgression and Heap *et al.* (2002) found that mid-shelf siliciclastic sediments have been accumulating around the Whitsunday Islands for the last 10 ka. This occurrence can be explained by the altered capacity for the onshore transport of sand as rates of sea-level rise varied with shelf topography. Sea level reached the mid-shelf at ~12 ka rapidly flooding the low gradient shelf at a rate of ~10 $m.\ ka^{-1}$ or a shoreline change rate of as much as 250 $m.y^{-1}$ (Hopley, 1970a; 1984). The capacity of sand to be moved onshore would have been reduced by rapid flooding of the shelf. However once sea level reached the steeper slope of the inner shelf at around 9 ka the rate of sea-level rise halved to ~5 $m.ka^{-1}$ or a shoreline movement of 125 $m.y^{-1}$. Flooding of the inner shelf coincided with the 'open window' phase of the Holocene 'high energy window' and it is likely that sand deposits were reworked and pushed shorewards (Hopley, 1984). This was investigated by Graham (1993) to explain the large sand ridge sequence at Cowley Beach in the wet tropics 100 km north of the study area. Graham's (1993) results were inconclusive but in this analysis the Holocene sand budget includes deposits on the inner shelf and excludes deposits stranded by rapid inundation on the mid and outer shelf due to submergence below the active wave transport zone.

The veneer of Holocene sediment on the inner shelf has been estimated at between 0.5 m (Belperio, 1983) and 1 m (Johnson and Searle, 1984) thick. Sedimentological investigations off the Burdekin Delta have found that muddy deposits on the inner shelf contain minimum values of 1-5% sand (Belperio, 1983). More recent sampling by Orpin and Woolfe (1999) in Cleveland, Bowling Green and Upstart Bay suggests much sandier inner shelf deposits with proportions of sand ranging from 38-55%. The range of estimated volumes of sand on the inner shelf using sand proportions from Belperio (1983) and Orpin and Woolfe (1999) and thickness from Belperio (1983) and Johnson and Searle (1984) are compared in table 7.4. The marked variation of sand content may be explained by sampling locations. Orpin and Woolfe's (1999) sampling regime was concentrated within the bays while Belperio's (1983) sampling regime incorporated more areas of the inner shelf. Therefore there is a high potential to over estimate the amount of sand contained on the entire inner shelf by using Orpin and Woolfe's (1999) results for sampling within the bays. Inner shelf deposits are assumed to be an average of 0.75 m thick given Belperio's (1983) estimate of 0.5 m thick and Johnson and Searle's (Johnson and Searle, 1984) estimate of 1 m thick. Applying a proportion of sand of 5% from Belperio's (1983) comprehensive sampling regime of the SWT inner shelf, yields a conservative and best available estimate of 1.1×10^8 m^3 of sand contained on the inner shelf.

Table 7.4. Estimated volume of sand stored in SWT inner shelf deposits from Rollingstone to Bowen (-5 m to -20 m L.A.T.)

Area km^2 of inner shelf	Average thickness (source)	Percent sand (source)	Estimated volume of sand (m^3) (38-55% sand @ 1 m thick)	Estimated volume of sand (m^3) (1-5% sand @ 0.5 m thick)	Conservative (5% sand @ 0.75 m thick) volume of sand (m^3)
2,921	0.5 m (Belperio, 1983) 1 m (Johnson and Searle, 1984)	1-5% (Belperio, 1983) 38-55% (Oprin and Woolfe, 1999)	1,110,217,500 – 1,606,893,750	14,608,125 – 73,040,625	109,560,938

Sediment deposits trapped in definable palaeochannels on the inner shelf are also included. The longest Burdekin palaeochannel extends 25 km over the inner shelf, is greater than 1000 m wide and contains 5.5 - 14 m thick sediment deposits (Fielding *et al.*, 2003). An average thickness of 9.75 m over the area of the channel (25 km^2) is sufficient for this quantification and equals ~2.4 $\times 10^8$ m^3 of sediment. Fielding *et al*. (2003) describe the channel fill as mud-dominated therefore applying a conservative estimate of 5% sand (Belperio, 1983) equates to 1.2×10^7 m^3 of sand contained in the Burdekin palaeochannel on the inner shelf. Adding the palaeochannel sand deposits (1.2×10^7 m^3) with the above estimate of sand deposited on the rest of the inner shelf (1.1×10^8 m^3) gives a total of ~1.2×10^8 m^3 of sand.

The total volume of sand contained on the SWT coast as onshore deposits (~1.3×10^8 m^3), in the nearshore area (~8.3×10^8 m^3) and the inner shelf (~1.2×10^8 m^3) is ~1.1×10^9 m^3. If this amount of sand was supplied to the coast by SWT fluvial systems over the last 7 ka, this equates to an average annual delivery rate from all SWT catchments of 156,625 m^3 of sand to the coast.

7.3 ESTIMATING FLUVIAL INPUTS OVER THE LAST 7 KA

Quantifying fluvial inputs of SWT streams during the Holocene relies heavily on numerical models estimating current sand delivery rates to the coast. Two methods have been used to model bedload delivered to the coast by streams: 1) calculating the volume according to the energy available, for example, Ackers and White formula (Ackers and White, 1973) which assumes sediment is available to be transported; and 2) estimating erosion rates for the catchment based on the standardised estimates such as the Revised Universal Soil Loss Equation (RUSLE) or the Fournier curve (Stoddart, 1969) which assumes that energy is available to transport the sediment to the coast. The second assumption is particularly relevant to this analysis that SWT streams have highly variable intra and inter annual discharges which has varied markedly throughout the Holocene evidenced by coral records (Isdale *et al.*, 1998) (see section 7.4.2.1). Table 7.3 summarises and compares previous estimates of fluvial bedload inputs for SWT streams between the Don River and Rollingstone Creek.

Streams in the SWT have highly variable stream flow (chapter 2). Therefore the estimates used in this study are based on bedload delivery rates according to energy availability and suggest a potential of 424,525 $m^3.y^{-1}$ supplied to the SWT coast. Application of the Fournier curve method (Belperio, 1978) yields bedload delivery rates of 8.5×10^6 – 1.7×10^7 $m^3.y^{-1}$, which is

20 to 40 times larger than those derived using the RUSLE equation and its derivatives. While reliance on modelled estimates is still problematic, they are the best figures available. For example, contention exists over Belperio's (1978) estimate of average annual bedload yield from the Burdekin River of 281,000 m^3. Neil *et al.* (2002) suggest that Belperio's use of mean monthly flow rather than daily flow results in the underestimation of sediment yield for the Burdekin by a factor of two. However as bedload transport is not just influenced by the magnitude of the flood but also the duration (see chapter 2 section, 2.4), Belperio's (1978) figures are still considered to be the most accurate. Therefore Belperio's (1978) estimate for the Burdekin and estimates for the other SWT streams also derived using the Ackers and White (1973) formula is used to quantify fluvial inputs in the SWT over the last 7 ka. Assuming fluvial sand supply to the SWT coast has averaged 424,525 $m^3.y^{-1}$ over the last 7 ka gives a total of ~2.95×10^9 m^3. However as previously mentioned, stream discharge and other environmental conditions have varied throughout the Holocene which may have impacted on sand delivery rates to the coast over the last 7 ka and will be discussed in the following sections. As indicated in section 7.2.3, only the inner shelf sediment deposits are included in the sand budget for the present coast. At the beginning of the Holocene transgression sea level was at ~-20 m and began to inundate the continental shelf off the SWT at ~9 ka (Thom and Chappell, 1975; Thom and Roy, 1985). At about 7 ka sea level had reached –5 m below present and the sand deposited on the inner shelf is still within the active wave zone and able to be transported onshore (Hopley, 1984). Therefore inner shelf deposits, which are most likely fluvial deposits from previous low sea level stands (Johnson *et al.*, 1982), are also incorporated into the coastal sand budget.

7.4 THE SAND BUDGET

Comparison of mid-late Holocene fluvial sand inputs (2.95×10^9 m^3) with the volume of sand contained in onshore deposits, nearshore areas and the inner shelf (1.1×10^9 m^3), suggests that there should be 62% (1.85×10^9 m^3) more sand deposited within the SWT coastal zone. While this may be the product of inaccurate models, there are other possible explanations for the apparent deficit of sand.

7.4.1 OTHER EXPLANATIONS FOR THE APPARENT DEFICIT OF SAND

Other possible explanations for the apparent deficit that must be considered include:

1. Fluvial sediment supply has varied in the past, perhaps due to climate change, and in the shorter term, the influence of anthropogenic activities such as land use change, sand extraction, and flow regulation;

2. Fluvial sediment supply has also varied spatially, as river mouth locations have changed, creating variations and/or lags between reserves and processes;

3. Longshore drift has lead to net gains or losses of sand to various parts of the SWT coast, with net sediment possibly varying though time.

7.4.2 CHANGE IN FLUVIAL SAND SUPPLY COMPARED TO MODERN DAY RATES

Environmental conditions have varied throughout the Holocene which are likely to have affected sand delivery rates to the coast over the last 7 ka. Factors that may have influenced sand yield from streams in the SWT during the Holocene include:

- Late Quaternary climate changes - variations in rainfall, vegetation cover and stream flow;

- Anthropogenic activities such as land use change, sand extraction and river regulation.

7.4.2.1 Climate change

The Australian climate has exhibited humid and arid phases during the Late Quaternary period (Nott *et al.*, 2001). As indicated in section 7.2.3 fluvial deposition to the inner shelf began ~9 ka, hence variations of climate since 9 ka are most relevant when predicting variations in supply rate to the inner shelf. Figure 7.2 compares records of climate change derived specifically from within the north Queensland region with records from around Australia and Papua New Guinea dating back to 9 ka BP. The record for north Queensland is compiled from three main data sources: 1. Pollen record of vegetation changes from Lynches Crater, north Queensland (Kershaw, 1975; 1978; 1985; 1986); 2. Slack water and boulder deposits in the Burdekin River

Gorge (Wohl, 1992); and, 3. Burdekin River flood discharges reconstructed from records of freshwater influx preserved in coral skeletons including luminescent bands (Isdale *et al.*, 1998).

Kershaw's record of Quaternary climate change in north-east Queensland is derived from the analysis of 60 m of sediment cores from Lynch's Crater on the Atherton Tablelands (Kershaw, 1985). Palaeoclimatic information was derived from the cores and a best estimate precipitation curve was established, though Kershaw (1985) concedes other important climatic variables (that would influence vegetation distributions) such as seasonality and the degree of cloud cover were not considered in this interpretation. Kershaw's (1985) interpretation suggests that annual precipitation on the Tablelands increased from ~800 to 3000 mm after 18 ka particularly between 11 and 7 ka. The apparent increase in precipitation coincides with the late transgression (11 – 7 ka) which reduced the distance from the Atherton Tablelands to the coast allowing moisture bearing south-easterly trade winds to influence the area (Ash, 1981). Wohl's (1992) investigation of boulder deposits in the Burdekin River Gorge reveal that seven floods have occurred over the last 1.2 ka with sufficient discharge and duration to transport boulders much larger than recent floods. Corals from the Great Barrier Reef suggest that overall the last century was generally drier than the seventeenth and eighteenth century (Isdale *et al.*, 1998). Despite being drier overall, three major flood events in the Burdekin have occurred over the last century (Wohl, 1992).

Inferring the probable effect of such climate variations on fluvial bedload yield and delivery to the coast is difficult (Thomas *et al.*, 2001). Figure 7.2 is a schematic representation of the relationships between fluvial sand supply, fluvial sand transport potential and climate change during the Holocene. There is debate in the literature over the impact of palaeoclimate variations on fluvial bedload yields and delivery to the coast. For delivery to occur sand must be available and streams must be capable of transporting this sand to the sea (Thomas, 2003). Increases in average annual rainfall (e.g. over 2000 mm between 11 – 7 ka in the Atherton Tablelands (Kershaw, 1985) have previously been associated with elevated rates of fluvial sand delivery to the coast in other tropical rivers in the early Holocene (Goodbred and Kuehl, 2000). Higher rainfall increased the streams ability to transport bedload sands. However Neil *et al.* (Neil and Yu, 1996a) argue that for north east Australia higher rainfall is likely to increase vegetation cover reducing sand availability. Conversely drier periods would have reduced vegetation cover increasing sand availability; however lower rainfall may have limited the stream's capacity to delivery the sand to the coast (see figure 7.2). Nott (2001) reported an increased period of alluvial fan development between 27 – 14 ka in the wet tropics region of north Queensland (Cairns). Dry conditions (rainfall less than 800 mm (Kershaw, 1985)), lead to sparse vegetation cover on slopes allowing the liberation of sand to stream network (Nott *et al.*, 2001). Lower rainfall also reduced the capacity of the streams to transport this sand to the coast resulting in the accumulation of extensive alluvial fans (Nott *et al.*, 2001). Page *et al.* (2003) claim the onset of wetter conditions between 11 and 7 ka (based on Kershaw's record (Kershaw, 1985) led to north Queensland streams actively depositing sand out to the shelf, despite higher rainfall improving vegetation cover and thus limiting sand available from the slopes. Page *et al*. (2003) argue that during this period (11-7 ka) streams with increased capacity to transport sand incised into previously deposited alluvial fans as described by Nott *et al*. (2001), delivering sand out to the shelf. While climate change has almost certainly impacted fluvial sand delivery to the coast, given that regional vegetation change may lag shifts in rainfall by up to 1 ka (Thomas, 2003), the direct links between climate change and sand flux to the coast are still contentious.

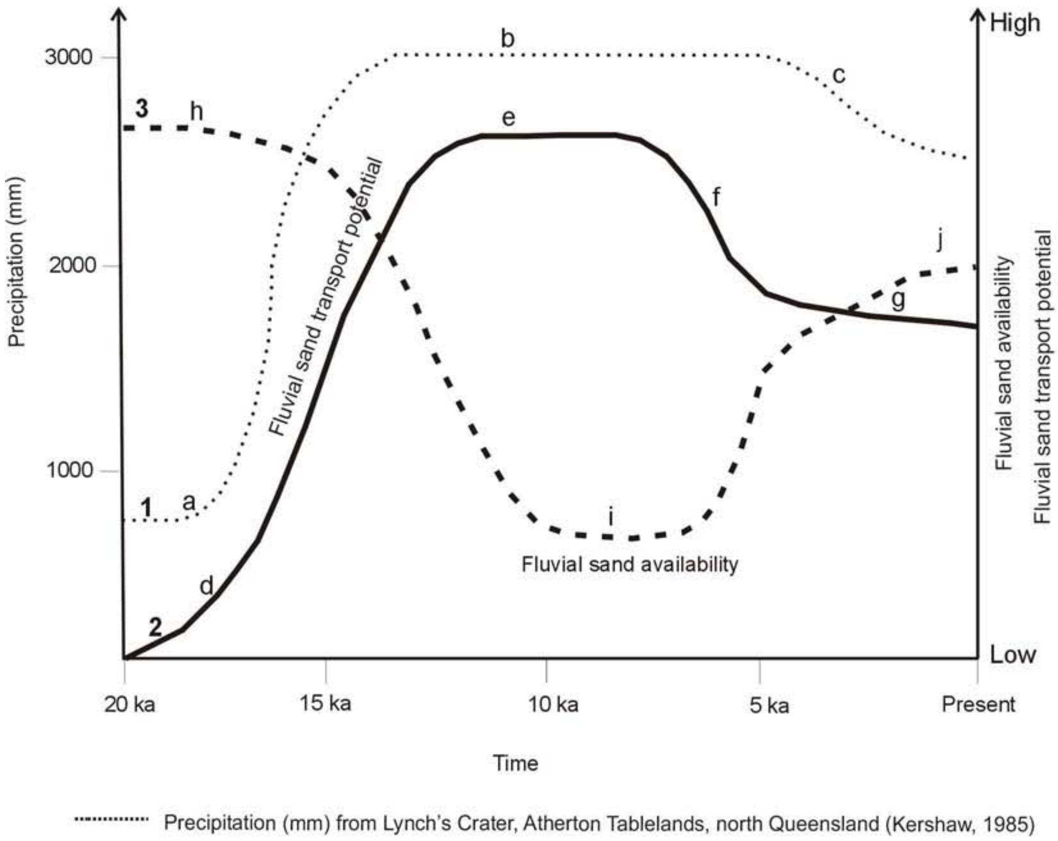

Figure 7.2 This figure portrays the presumed broad relationship between the amount of sand available in the catchments (3) and the stream's ability to transport sand to the coast (2) inferred from variations in precipitation (1) over the last 20 ka. Kershaw (1985) interpreted precipitation levels from pollen samples from Lynch's Crater in north Queensland. From ~20 ka (LGM) until ~14 ka BP was a very dry period, average annual rainfall is estimated at less than 800 mm (1a) (Kershaw, 1985) and would have most likely limited the capacity of stream's to deliver sand to the coast (2d) (Page *et al.*, 2003). The dry conditions from (~20 ka to ~14 ka BP) may have led to sparse vegetation cover in the catchment, consequently a relatively high amount of sand would have been available (3h). The onset of wetter conditions between 11 and 7 ka (1b) (Kershaw, 1985) is likely to have promoted denser vegetation cover in catchments and reduced sand availability (3i) (Neil and Yu, 1996), while higher rainfalls may have increased the stream's ability to transport sand (2e). After 7 ka precipitation reduced slightly to present day levels (~2,500 mm) (1c) (Kershaw, 1985). Drier conditions after 7 ka may have led to sparser catchment vegetation cover, therefore increasing sand availability (3j). Lower precipitation levels may have reduced the potential of streams to deliver sand to the coast after 7 ka (2f) and has remained stable for the last 3 ka (2g).

7.4.2.2 Land use change

While modelling estimates to determine the impact of land use change on SWT catchments are available (see GBRMPA, 2001), the only data derived from actual field experiments is from Wet Tropics catchments. Early work by Douglas (1966) and Gilmour (1971; 1977) to more recent work by Pringle (1991) and Neil *et al.* (2002) have reported four to ten fold increases in suspended sediment concentrations in Wet Tropics rivers after land has been cleared of natural vegetation. Douglas (1967) noted increased erosion rates in the upper Barron catchment after forest clearances from plot experiments. This conclusion was later supported and strengthened by Gilmour's (1971; 1977) findings that logging produced a two-three fold increase and complete clearing up to ten fold increase of suspended sediment loads in Freshwater Creek (a sub-catchment of the Barron River). Clearing for sugarcane and dairy farms in the Barron catchment has been associated with a two to four fold increase in suspended sediment discharged by the Barron River (Pringle, 1991). Vegetation clearing has also been associated with an increase in sand yield from the Barron catchment, empirical models predicting an increase from almost zero in 1916 to 180,000 $m^3.y^{-1}$ in 1979 (Pringle, 1991).

Neil *et al.*'s (2002) review of anthropogenic changes to fluvial sediment yield to the Great Barrier Reef concluded that total sediment delivery to the coast from SWT streams has increased by a factor of four. Vegetation clearing has caused the greatest increases in SWT catchments compared to humid catchments due to the episodic and erosivity of rainfall (Neil *et al.*, 2002). Analysis of Ba/Ca ratios in Great Barrier Reef corals support this theory in part indicating a five to ten fold increase in the delivery of suspended sediments to the inner Great Barrier Reef since European settlement ~1870 (McCulloch *et al.*, 2003).

However, to understand the downstream impacts of land use change, especially sand delivery to the coast, requires information on rates of sediment transfer from catchments to streams rather than rates of erosion on plots, or catchments. Plot-scale experiments give measures of erosion but lack data on the distance the sediment travels which flume experiments have shown may only be a few metres (Wasson *et al.*, 1996). Wasson *et al.* (1996) estimates that sediment yields from Australia streams have only doubled in the last 200 years despite a reported 100-fold increase in hillslope erosion. Indeed it is also thought to be rare for sand-sized sediment eroded due to anthropogenic influences to reach the coast (Roy and Crawford, 1977). The SEDNET model (Prosser *et al.*, 2001a; 2001b) uses the models such as the RUSLE (Revised Universal Soil Loss Equation) which is based on plots measures of erosion. However assumes that there is no input of coarse sediment to the stream from the hillslopes, only 5-10% of the sheet wash and rill erosion and 90% of sediment is trapped in reservoirs. As noted, increased sand yield from cleared catchments is usually inferred from empirical models however the actual delivery of sand to the coast is a complex process (see section 7.6 this chapter). While many authors report strong links between clearing of natural vegetation in catchments and increases in suspended sediment yield to the coast (Brodie, 1996; Isdale *et al.*, 1998; McCulloch *et al.*, 2003; Radlke, 2003), land use change cannot be easily correlated to increased rates of fluvial bedload sediment delivery to the coast (Pringle, 1991; Neil *et al.*, 2002) given that human activities such as dam building and sand extraction may also reduce sand supplies (Pringle, 1986; 1991).

7.4.2.3 Sand extraction and river regulation

Anthropogenic impacts may reduce or interrupt the natural delivery of some sediment fractions to the coast. Reduced sand and gravel delivery to the coast is often attributed to anthropogenic impacts such as sand extraction and dam construction (Kinhill *et al.*, 1993). In the past no limits were imposed on sand extraction from SWT streams and records were not kept, so the total amount of sand that has been removed from the river systems in north Queensland is unknown. Approximately 5,000,000 m^3 of sand is documented to have been extracted from SWT coastal systems since 1972 (Table 7.5).

Table 7.5. Amounts of sand extracted from SWT coastal systems since 1972.

River (Source)	**Sand extracted from non-tidal reaches (m^3)**	**Sand extracted from tidal reaches (m^3)**
Black River (Kinhill, 1998)	100,000	1,000,000
Ross River (Townsville Port Authority, 2002)	1,790,000	4,285,796 of sediment unknown proportion of sand
Haughton River (Kinhill *et al.*, 1996)	560,000	100,000 (since 2001)
Burdekin River (Kinhill *et al.*, 1993)	1,000,000	Figures not available
Don River (Kinhill *et al.*, 1993)	1,000,000	Figures not available

Regulating river flows may diminish the capacity of a river to transport sediment, especially bedload (Pringle, 1986). The Ross River for example, is one of the most highly regulated rivers in the SWT with a dam and three weirs. Coarse sediments are trapped in the upper reaches of the river upstream of the dam (Persson, 1997). Flood frequency analysis based on peak discharges recorded along Ross River shows that the 1 in 10 year flood peak flow rate decreased after dam construction by 89% from 2200 $m^3.s^{-1}$ to 240 $m^3.s^{-1}$ (Persson, 1997), which may reduce the capacity of the river to transport bedload sediments downstream.

Pringle (1986) reports that dams in other north Queensland rivers are trapping coarse sediment. For example the Tinaroo Falls Dam in the Atherton Tablelands, has prevented the downstream movement of all sand-sized sediment. The Burdekin River, the largest river in the SWT region, was dammed in 1986. Pringle suggests (Pringle, 1986) over the longer term (100 years) intertidal and submarine deltas will dwindle and fail to maintain sediment supply to spits and barrier islands further north. This may lead to the destruction of Bowling Green Spit which would alter the hydrodynamics of Bowling Green Bay (Goh, 1992) More recently Pringle (Pringle, 2000) attributed the cessation of the 1 km seaward extension of the northern most spit, Alva Spit observed in 1940-1980 to the impact of the dam. However in the short to medium term, impacts near the contemporary river mouth are likely to be delayed as enhanced erosion of the lower section of the Burdekin River compensates for reduced sand supply (GHD, 2000). Also, the Burdekin Falls Dam is located on the northern tributaries which are draining largely basaltic low sand yielding catchments and make up only one third of the extent of the Burdekin catchment (40,093 km^2). It is the southern tributaries draining mainly sedimentary rocks which produce the most sand-sized sediment, suggesting that impact of the dam on reducing sand supply to the coast has been largely overstated.

The regular release of water from dams for irrigation purposes also has the potential to impact coarse sediment availability in SWT streams. This practice creates elevated dry season base flows which may encourage the growth of instream vegetation and enhance the stability of instream bars (Smithers, 2002). Thus anthropogenic impacts such as sand extraction and river regulation may have contributed to the lack of fluvial sand delivery to the coast, in terms of availability at least in the last 200 years. However from the results of this study it appears that availability of sand is not the restricting factor, rather the competency of SWT streams to deliver this sand to the coast.

7.4.3 CHANGES IN GEOMORPHOLOGY

7.4.3.1 Locations of stream mouths

SWT streams have evolved during the rising sea levels of the Holocene transgression, taking different courses and discharging at different locations (Hopley, 1970b). These variations have affected the spatial distribution of fluvial input over the last 7 ka. For example the Ross and Bohle Rivers were joined at lower sea levels (Hopley, 1970a). The Ross once discharged into Rowes Bay until meander migrations caused it to enter the sea at Ross Creek, and then migrating further south to its present mouth (Hopley, 1970a). The Black and Bohle Rivers used to discharge into a bay that is now the Town Common (Hopley, 1985). The location of the Burdekin River mouth has also varied with changes in sea level (see chapter 8, section 8.4.2). However, the overall effect on sand delivery is purely local and does not affect regional budgets.

7.4.3.2 Pleistocene inheritance

Despite the sand budget for the SWT calculated over the Holocene it is not assumed that all sand contained in Holocene deposits is of Holocene age. Modern landforms are inherited from earlier forms particularly from the last interglacial shorelines which were only a few metres above present sea level (Hopley, 1985). For example, Thom *et al*. (1981) attributed the initial phase of Holocene barrier development in NSW with the landwards movement of sand on the shelf during the post-glacial transgression. This shelf-derived sand almost certainly included material from Pleistocene interglacial barriers (Hopley, 1970a; Belperio, 1978; Pringle, 1983; 2000).

7.4.4 MOVEMENT OF SAND IN AND OUT OF THE SWT

The occurrence of northward extending spits, bars and tombolos along the SWT coast (Hopley, 1970a; Belperio, 1978; Pringle, 1991; 2000) provide geomorphic evidence of the northward movement of sand via longshore currents. Sand movement is restricted in the nearshore to depths of about 5 m as a result of hydrodynamic controls (depth of active wave base). Finer sediments (mud and clay) carried in suspension can be transported further with less energy and the northward transport of these fractions is not restricted by depth like sand (Belperio, 1978; Pringle, 1991). Prevailing south-easterly trade winds promote strong littoral currents (0.25 $m.s^{-1}$) along the SWT coast capable of transporting sand-sized sediment north (Orpin *et al.*, 1999).

Cyclones also cause wind-driven north-directed middle shelf flows (> 130 $cm.s^{-1}$) which erode the sea bed, concentrate the sparse mobile sediment into sand ribbons, and advect suspended load onto the outer part of the nearshore terrigenous sediment prism (Larcombe and Carter, 2004).

In order to quantify the inputs and outputs in a coastal system, Davis (1974) proposed the concept of a coastal sediment compartment. Davies (1974) applied the concept to a hierarchy of compartments of varying size and degrees of exclusiveness. The SWT coastal system can be described as a 'maxi compartment' (Davies, 1974:471) encompassing smaller coastal sediment compartments within it and where the southern limit of the compartment is Gloucester Island and the northern limit in Rollingstone Creek (Figure 7.3). Figure 7.4 is a conceptual model of sand transfer within the SWT maxi compartment. The deeper water (>8 m) around the Whitsunday Islands, Conway Coast, Cape Gloucester and Gloucester Island just south of Bowen, impede sand transfer by longshore drift currents from the south east. Therefore north of Bowen is the start of a partially enclosed sand compartment (Davies, 1974) with net sand movement north of Bowen (see figure 7.3). The presence of northward orientated spits and subtidal sand waves (see chapters 5 and 6) supports sand transport figures derived from models. Longshore drift calculations using ACES (Leenknecht *et al.*, 1992) (chapter 3, section 3.4.4.1; Appendix C) suggest that 100,000 $m^3.y^{-1}$ of sand is potentially driven north from Bowen by south easterly winds to Guthalungra. However, water depths averaging 8 m (below the active sand transport zone) off the granite headland of Cape Upstart impedes the movement of sand further north. Therefore while sand derived from the Don River coastal system could be transported by longshore currents into Abbot Bay it is unlikely to be transported any further north. The low energy wave conditions in Bowling Green Bay produce lower rates of northward sand transfer. However, water depths of over 7 m off Cape Cleveland (Figure 7.5) prevent the transport of sand into Cleveland Bay. Extensive sand bars off Cape Pallarenda (Figure 7.6) indicate the movement of sand northward out of Cleveland Bay. ACES models suggest that 170,000 $m^3.y^{-1}$ of sand could be potentially transported along the coast north of Townsville via longshore currents past Rollingstone Creek and without any impediment until Hinchinbrook Island. This may be producing a potential loss to the SWT system of 170,000 m^3 of sand northwards each year. Indeed continued erosion along the Strand foreshore, Cleveland Bay has lead to the artificial re-nourishment of the foreshore with 400,000 tonnes of sand sourced mainly from the upper reaches of SWT rivers (Kettle *et al*., 2001).

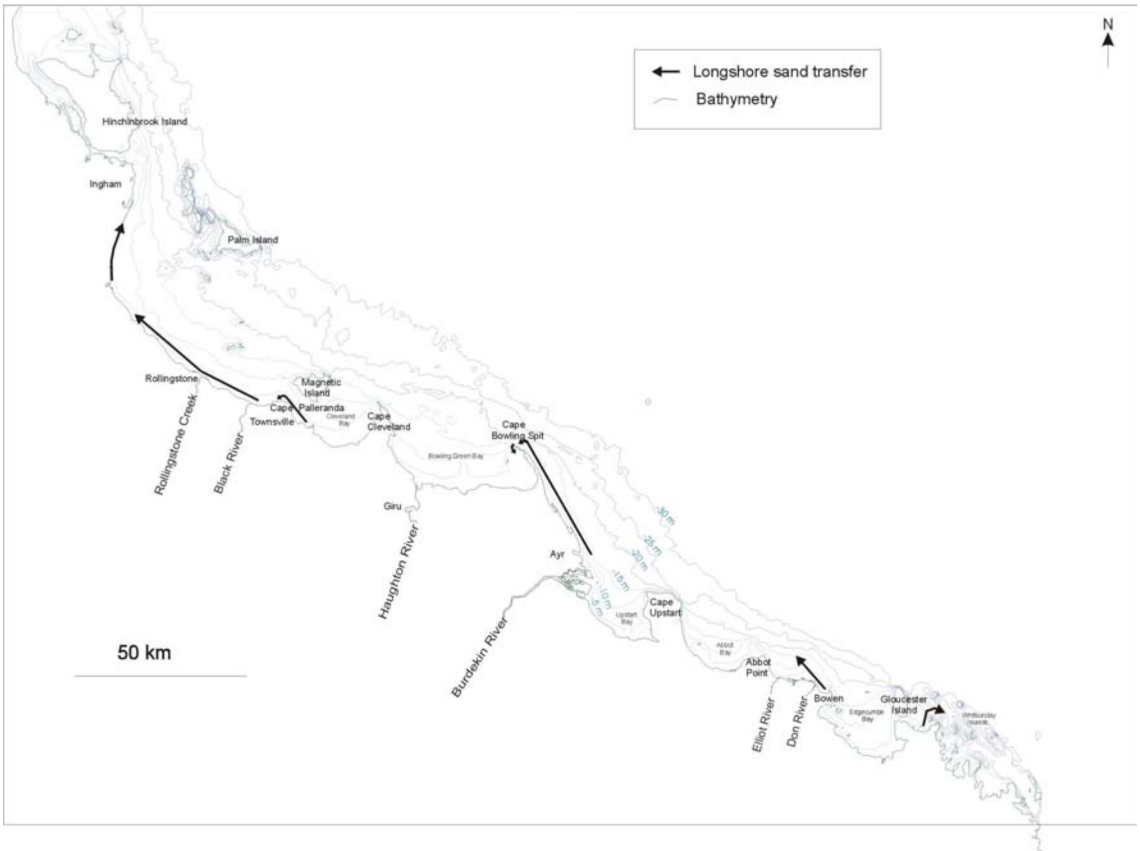

Figure 7.3. The SWT maxi-compartment.

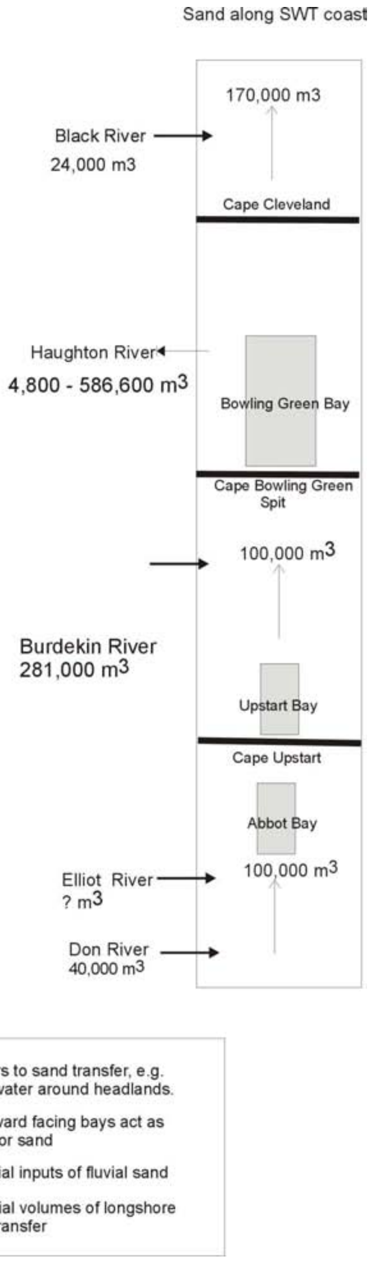

Figure 7.4. Conceptual model of sand transfer in the SWT maxi-compartment (refer to figure 7.3)

Figure 7.5. Oblique aerial photograph of Cape Cleveland. Note the lack of sandy nearshore deposits around the tip of the Cape. (Photograph taken 16/05/03).

Figure 7.6. Oblique aerial photograph of Cape Palleranda. Note the continuation of nearshore (subtidal) sandy deposits around the Cape. (Photograph taken 16/05/03).

The Burdekin Delta is often referred to as the major point source of fluvial sediment to the SWT coast (Belperio, 1978). While this statement is true for the past (see chapter 8, section 8.4), at present suspended sediments from the Burdekin may reach Cleveland Bay, but the northward limit of sand transport is Bowling Green Bay (Belperio, 1978). Northward extending sand spits along the eastern coast of the delta accreted northward at a maximum rate of 375 $m^3.y^{-1}$ in 1991-1993 (Pringle, 2000). The Bowling Green Bay compartment is bounded by Bowling Green Spit to the east and south and Cape Cleveland to the west and north and like other northward facing embayments, is a sink for northward moving sediment (Orpin, 1999). Approximately 76-93% of sediment from the Burdekin is transported north into Bowling Green Bay with only 5-10% retained in Upstart Bay (Orpin, 1999). Way (1987) estimated that 2 x 10^5 t of sediment is retained in Upstart Bay which equates to 12,500 m^3 of sand (assuming 10% bedload after Belperio, 1978). It is feasible that 95,000 – 232,500 $m^3.y^{-1}$ of Burdekin River sand is transported into Bowling Green Bay, either from recent fluvial supply or erosion of the delta. Indeed seismic investigations revealed asymmetrical sand waves approximately 3 m in height and 750 m across along the eastern side of Cape Bowling Green, indicating strong northward movement of sand (Orpin, 1999). From Cleveland Bay north along the SWT coast, sand can be transported northwards with few impediments, until Hinchinbrook Island.

7.5 CONCLUSIONS ON LONG-TERM SAND BUDGETS

Fluvial sediment supply has almost certainly varied during the Holocene in response to climate change, sediment availability, sea level variations and anthropogenic impacts. The onset of wetter conditions (11-7 ka) enabled SWT streams to actively deposit sediment onto the shelf from incision into previously deposited alluvial fans and the erosion of sparsely vegetated slopes (Nott *et al.*, 2001; Page *et al.*, 2003). It is likely that fluvial sand deposited during the late transgression and earlier was pushed shoreward by the strong wave conditions associated with the ‘Holocene High-Energy Window’ (Hopley, 1984). The impact of anthropogenic activities on fluvial sediment yield in more recent times will not affect this quantification as it is difficult to make direct links between increased erosion in catchments and increased delivery of sand to the coast. Results from investigations in the Haughton, Elliot and Black Rivers (see chapters 4, 5, and 6) suggest that SWT streams have not been major contributors of sand to the coast during the late Holocene.

The spatial variability of fluvial sediment discharge due to the changing locations of river mouths along the coast, has little impact on the quantification as the SWT coastal region was treated as a whole. The potential degree of Pleistocene inheritance material in the Holocene deposits does little to explain the sand deficit, in fact it suggests that even larger quantities of sand should be deposited in the coastal zone. However, the loss of a potential 170,000 m^3 of sand northward from the SWT coastal compartment via longshore drift does account for 65% (1.2×10^9 m^3) of the apparent deficit assuming there is no replenishment from the south. However, it still does not account for the rest of the sand - 2.95×10^9 m^3 predicted to have been delivered to the SWT coast by empirical models over the last 7 ka. The answer may lie in the model calculations.

7.6 THE 'SAND DELIVERY PROBLEM'

There is a strong possibility that fluvial sediment delivery models are overestimating the volumes of sand delivered to the coast, especially when applied to SWT streams. Walling (1983) describes the difficulties associated with linking rates of erosion within a catchment to the sediment yield at the catchment outlet as 'the sediment delivery problem.'

Variations in storm magnitude and frequency effect the generation and movement of sediment slugs downstream (Nicholas *et al.*, 1995), making them especially relevant to sediment transfer in the SWT. For example, the sand delivery estimate used from Belperio (1978) for the Burdekin was the average yield 0.45 MT. However, further modelling (Belperio, 1979) shows the substantial variation in delivery rates between flood years (1957/58) estimated yield 3.07 MT and drought years (1968/69) estimated yield of 0.001 MT. The bulk of bedload is thought to be transported through the catchment or delivered to the coast during high magnitude flood events, induced by tropical cyclones. However this is often not the case (refer to chapter 2, section 2.4). The hydrograph from the Black River (see chapter 6, figure 6.3) shows that despite reaching a high maximum instantaneous discharge estimated as having an ARI of 1:100 years the duration of the maximum discharge was less than one day allowing little time for high rates of bedload transport (Costa and O'Connor, 1995)

While globally Australia has high rates of soil erosion, sediment delivery to the coast by streams is inefficient due to the arid, low lying and flat nature of the continent (Wasson *et al.*, 1996). Wasson *et al.* (1996) estimates that the proportion of eroded sediment actually delivered to the coast by streams at 3% in Australia which is a relatively low sediment delivery ratio by global standards. Indeed, Wasson (1997) warns that sediment delivery models like that of Belperio (1983) often result in an overestimation of sediment volumes actually reaching the coast because they rely on measurements of stream discharge and sediment loading collected inland from the coast. The influence of stream power on sediment transport diminishes when it reaches the estuary (Dalrymple *et al.*, 1992; Heap *et al.*, 2001), therefore these estimates must be taken as maximum potential delivery volumes.

Prosser *et al*.'s (2001a) SEDNET quantified sediment storage in river networks including: water reservoir sediment storage; floodplain storage of suspended material; in-channel storage of bedload; and transient in-channel storage. Floodplains are the areas of greatest potential for deposition of both suspended and bedload sediments (Wasson, 1997; Prosser *et al.*, 2001b), particularly in the SWT where streams have downstream decreasing channel capacities (Kapitzke *et al.*, 1998). The channel capacity of the Haughton River decreases by over 90% in the lower 27 km of channel. (Kapitzke *et al.*, 1998) (see chapter 3). Flooding of the Haughton River causes overbank flow and sand remains in-channel rather than being transported to the coast (Kapitzke *et al.*, 1998). In addition, the reduction in channel gradient along the lower reaches in SWT streams results in in-stream storage of sediment common to streams which are transport limited rather than supply limited (Prosser *et al.*, 2001b). The steep descent of streams down the Great Escarpment ends abruptly with the gently sloping coastal plain reducing the capacity of the stream to transport bedload out to the coast, which results in abundant alluvial stores of sand and gravel within the middle fluvial reaches of coastal streams in the region (Hopley and Murtha, 1975). Therefore while the catchment yield modelling may rate SWT streams as having high sediment yielding catchments due to sparse vegetation cover (Neil and Yu, 1996b), the actual sediment delivery ratio is estimated at between 9 and 34% according to the SEDNET model (Prosser *et al.*, 2001a). Even with these refinements the SEDNET model (Prosser *et al.*, 2001a) is still likely to overestimate the rates of sand delivery to the coast because it does not account for the sand that is delivered to the lower reaches of the stream but remains as in channel storage. The lack of recent fluvial sand identified seaward of estuaries from detailed sedimentological investigations in the Haughton, Elliot and Black River Estuaries (see chapters 4, 5 & 6) support this theory.

7.7 CONCLUSIONS

Calculations used in this study have revealed an apparent deficit of sand in the SWT coast budget. The inputs do not equal the outputs with a discrepancy of 0.65×10^9 m^3 of sand, most likely due to an overestimation of the inputs rather than an underestimation of the outputs. Overestimation of the inputs is probably a result of variations in fluvial sediment supply due to:

- climate change, and
- anthropogenic influences including land use change,
- sand extraction and river regulation.

However, the most important factor contributing to the overestimation of sand inputs to the SWT coast is that the morphology of SWT streams is not conducive to delivering the predicted rates of sand to the coast. Detailed investigations on the Haughton, Elliot and Black coastal systems (see chapters 4, 5 & 6) confirm, that these streams have not been delivering predicted quantities of sand to the coast in the recent past and, in the case of the Haughton, for at least the last 1 ka (see chapter 4). The results of the Holocene sand budget suggest an apparent deficit of ~0.65×10^9 m^3 of sand (including loss to the system via longshore drift) suggesting that SWT streams have not been delivering predicted volumes of sand to the coast for at least the last 1.6 ka. Similar conclusions have been drawn in coastal systems in other SWT areas of Australia. For instance, Bryce *et al.* (1998) concluded that the Normanby River is not a significant contributor of sand to the coast despite modelling that suggests it delivers over 100,000 m^3 of sand to the coast per year (Prosser *et al.*, 2001a). Indeed stratigraphic evidence revealed that sand has been trapped in the estuary and has been accumulating over the last 6 ka.

Therefore supposing that the SWT streams have not supplied current estimates of sand at least for the last 1.6 ka, the most likely source for the beach ridges, sand choked inlets and nearshore sediment wedge, characteristic of the SWT coast is the onshore movement of marine sand. The most likely mechanism for placement of the substantial sand deposits that dominate the SWT system is the Holocene transgression (Hopley, 1970a). The slowed rate of sea-level rise when it reached the steeper gradient of the inner shelf at about 9 ka, would have provided ideal conditions for the landward transport of marine sand. The stabilisation of sea level over the last 6.5 ka has then allowed the build up of sand derived landforms on the mainland coast. Thom and Roy (Thom and Roy, 1985) have similarly linked the mass landwards transport of earlier coastal sand deposits in south-east Australia to the Holocene transgression and subsequent stillstand period.

Sedimentological studies in the Haughton Estuary (chapter 4) revealed that the sand-sized sediments that have accumulated in the estuary have very similar characteristics to adjacent beach ridge sands. The well sorted, rounded grains with low feldspar content in the majority of sand sampled from the estuarine and coastal parts of the Haughton system indicate mature marine sands derived from offshore (chapter 4). Orpin and Woolfe (1999) found that the terrigenous component of the inner shelf sand off Bowling Green Bay is quartzose, with only minor feldspar and also concluded they were mature sediments. Similar findings in the Elliot and the Black (chapter 5) further support the theory that the beach ridge plains, sand choked estuaries and thick nearshore sand wedge present in the SWT coastal system are composed of relict sand deposits with little direct input from modern fluvial systems. Contrary to earlier suggestions (e.g. Hopley, 1970a), the sand derived landforms that dominate the SWT coast are the result of multi-cyclic processes – initiated by the landward movement of marine sand during the Holocene transgression.

7.8 IMPACT OF THE HOLOCENE MARINE TRANSGRESSION ON THE COAST

The most recognisable and dominant feature of the SWT coast are the beach ridges. Investigation of these landforms provides an indication of coastal evolution over the Holocene. While it is accepted that the marine transgression between 11-7 ka BP instigated their development (Taylor and Stone, 1996; Otvos, 2000), the dominant source of sand supply to the ridges is debated in the literature. With the exception of the Shoalhaven Delta (Wright, 1970; Young *et al.*, 1996; Umitsu *et al.*, 2001), the majority of research on southern east coast beach ridges and barrier concludes that they were supplied by the onshore movement of marine sand with low sediment yielding rivers having little influence on coastal development (Thom *et al.*, 1981; Bird, 1978). Consistent with literature suggesting SWT region produce high sand yielding streams (Fournier, 1960; Stoddart, 1969), Hopley (1970a) suggested that the beach ridges were formed from sand directly supplied by adjacent streams. However new evidence presented in this thesis suggests that SWT streams have contributed little sand to the coast in the recent past prompting a revision of this theory.

The maturity of the Cape Cleveland beach ridge sands and the recession of the ridges led Hopley (1970a) to consider the possibility that these beach ridges developed in a similar way to those in southern Queensland and New South Wales. The Haughton River was not considered capable of supplying the vast quantities of sand stored in the adjacent beach ridge complex. However there may have been adequate supplies offshore in Bowling Green Bay from the time when the Burdekin discharged there prior to 6 ka BP. Considering that beach ridges form where an abundance of sediment exists and the offshore gradient is low (Taylor and Stone, 1996) waves would have transported marine sand reserves landward when sea level transgressed over the inner shelf. The final part of the transgression and the subsequent stillstand period after ~ 6.5 ka would have seen the rapid progradation of the coast. However this progradation ceased ~3 ka BP and like the rest of the SWT coast the beach ridges are presently eroding. For example the uncovering of mangrove peat on Cape Bowling Green Spit indicates retreating shorelines (chapter 2, section 2.1) (Hopley, 1970a). This suggests that the coast has not been actively supplied with sand in the recent past and implies either a reduction in sand supply or that the mechanism of transporting sand to the beach ridges is no longer occurring. Despite little fluvial sand currently being delivered to the SWT coast, estuaries are continuing to infill with sediment from the landward side and the nearshore and inner shelf are dominated by sand (chapter 7, section 7.2). Thus if the supply of sand is still available it suggests that the mechanism which originally instigated the formation of the beach ridges is no longer occurring or that redistribution has increased. This was a transgressing sea level rising over previously deposited sand. Where and how this sand was deposited as inshore marine, deltaic, estuarine or even lower riverine locations, is irrelevant as once it has been reworked and transported onto the inner shelf the sand becomes part of the coastal sand budget. The onshore movement of marine sand during the transgression has been identified as a major source of sand in other parts of the world, for example the Kennebec River, USA (FitzGerald *et al.*, 2000), and in northern France between the Somme Estuary and Belgium (Anthony, 2000).

The variation in sediment textural characteristics locally between beach ridges along the SWT coast lends some support to the original theory that they were directly supplied by adjacent streams, especially in the Black River where Holmes (1992) established a mineralogical link between Black River fluvial sediments and adjacent beach ridge sediments. However initial origin of the sand is not disputed; the process of delivery is the distinguishing factor. Sand stored in the lower estuarine channels at lower sea levels could be reworked and moved onshore as it was transgressed by rising sea levels. For example sand at the mouth of the Burdekin is very well sorted due to strong longshore currents and wave action. Fine sediments have been dispersed to leave only sand-sized sediment that waves could transport onshore as the shelf is transgressed.

CHAPTER 8 – CONCLUSIONS

8.1 INTRODUCTION

This study set out to address the current gap in knowledge of the spatial and temporal patterns, dominant processes and controlling factors of sand transfer in meso-tidal SWT coastal systems. The aim of this study is to quantify the coastal sand budget for the SWT between Rollingstone and Bowen within a Holocene timeframe. Specifically, the objectives were to evaluate:

- current estimates of sand supply and source to the SWT coastal zone between Rollingstone and Bowen;
- temporal and spatial patterns of sand transfer over contemporary and Holocene timeframes;
- dominant processes associated with these patterns of sand transfer;
- the relative influence of high magnitude low frequency events on sand transfer.

To achieve this aim detailed sedimentological, stratigraphic and hydrodynamic investigations were conducted in the Haughton and Elliot River Estuaries and the Black River Delta to develop a conceptual model of contemporary sand transfer to the coast from both streams and onshore. The second part of the investigation developed a Holocene sand budget for the SWT to interpret the relative volumes of contemporary sand transfer over Holocene time scales. Detailed studies were not conducted in the Burdekin River Delta however its influence was considered in the sand budget for the SWT (see section 8.4). This chapter outlines the main findings of the preceding chapters and discusses these findings within the context of broader issues, that were beyond the direct scope of this study but which have been highlighted by the results. Finally, an alternative scenario of evolution for the SWT coast is proposed, which downplays the direct influence of high sand yielding streams. Predictions of the future evolution of SWT estuaries and coast are discussed in view of potential sea-level rise.

8.2 CONCLUSIONS

8.2.1 CONTEMPORARY SAND TRANSFER PROCESSES IN SWT ESTUARIES

- The modern Haughton is a tide-dominated estuary and the direction of net sand transfer is landward into the estuary. The river has not delivered predicted volumes of sand to the coast for at least the last 1 ka, if at all (chapter 4);

- The modern Elliot is a mixed estuary and the main sand transfer process is the reworking shoreward and alongshore of previously deposited coastal sand by waves and tides, rather than the contribution of fluvial sand to the coast (chapter 5);

- The modern Black River is a wave-dominated delta and while it may deliver predicted volumes of sand to the coast (average of 25,000 $m^3.y^{-1}$) this does not have a major influence on coastal development (chapter 6).

8.2.2 HOLOCENE SAND BUDGET FOR THE SWT

The Holocene sand budget for the SWT is in deficit (chapter 7), in that the volumes of sand identified in the coastal zone as mid-late Holocene are less than models of fluvial input over this same period would suggest that SWT streams do not appear to have been significant contributors of sand to the coast in the past. Cyclone-induced flooding is thought to control fluvial sediment delivery to the SWT (Larcombe *et al.*, 1996a; Larcombe and Carter, 2004). However delivery of the sand fraction to the coast is limited no matter the severity of the cyclone due to:

1. The morphology of SWT streams. Downstream decreasing channel capacities cause overbank flows during floods so the fines are deposited over bank while the coarse sediment (sand) remains in channel rather than transported to the coast.

2. Flooding characteristics of SWT streams. While streams may reach high maximum instantaneous discharges, the duration is short (usually less than one day) limiting the amount of time available to do geomorphic work, in this case transport bedload downstream.

However the strong winds associated cyclones generate high-energy wave conditions which influence coastal sand transfer by reworking previously deposited coastal sand (see chapter 5). The sand derived landforms that dominate the SWT coast today are the result of multi-cyclic processes. Cyclones and flooding can have destructive and constructive impacts over yearly or decadal timeframes while sea-level change has impacted the SWT coast over the Holocene. The Holocene marine transgression is considered to be the most likely mechanism to initiate the onshore movement of marine nearshore sand to the east coast of southern Australia and the subsequent stillstand period allowed the accumulation of marine sand on the coast (Thom and Roy, 1985).

8.2.3 CONCEPTUAL MODEL OF THE HOLOCENE EVOLUTION OF THE SWT COAST

From the findings of this thesis a conceptual model of the Holocene evolution of the SWT coast is proposed (Figure 8.1). Figure 8.1 illustrates the relationship between variations in fluvial and marine sediment supply to the accretion of the SWT coast over the last 10 ka. Marked variations in fluvial sediment supply and transport potential in response to climate change during the Holocene (see chapter 7 section 7.4.2.1) have still resulted in an overall sand deficit for the SWT. Coastal accretion in the SWT during the Holocene has been inextricably linked to fluctuations in marine sediment supply largely controlled by changes in sea level. This process is described in detail later in this chapter (see section 8.5). Cyclones impact the SWT coast over decadal timeframes and could not be depicted in this conceptual model. The influence of low-frequency high-magnitude events is discussed in the following section.

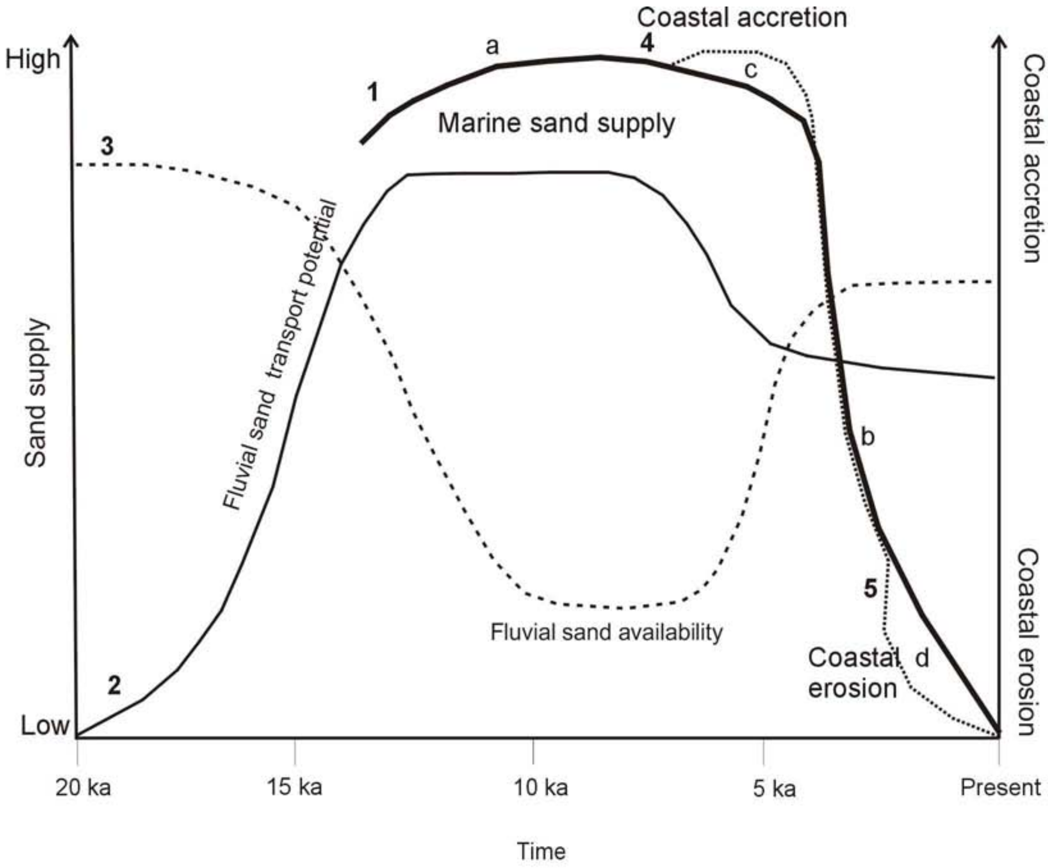

Figure 8.1. Following on from figure 7.2, which illustrated the relationship between amount of sand available in the catchments (3) and the stream's ability to transport sand to the coast (2), this figure includes broad trends of coastal erosion (5) and accretion (4) over the last 20 ka. While sand availability and transport potential fluctuated according to changes in precipitation, the marine sand supply curve (1) and phases coastal accretion (4) and erosion (5) were seemingly unaffected by the interplay between (2) and (3). Rather marine sand supply (1) was linked to sea level change (Thom and Roy, 1985). Marine sand supply would have increased with rapid sea-level rise between ~11 and 7 ka BP (1a) as waves would have transported marine sand landwards as sea level transgressed over the inner shelf. The final phase of the transgression and subsequent stillstand period after ~6.5 ka was associated with the rapid progradation of the coast (4c). Coastal progradation ceased at ~3ka BP, most likely due to a decrease in the shoreward movement of marine sand after sea level stabilised (1b). The SWT coast is presently in an erosional phase (5d) despite fluvial sand supply and fluvial sand transport potential available. Coastal accretion was at the highest levels when fluvial transport potential was high but there was limited sand available to transport, which suggests that patterns of coastal accretion in the SWT are linked to sea level changes and marine sand supply rather than fluvial sand supply and transport potential.

8.3 IMPACT OF LOW-FREQUENCY HIGH-MAGNITUDE EVENTS ON COASTAL SAND TRANSFER

SWT streams have not been delivering predicted volumes of sand to the coast even during low-frequency high-magnitude flooding events which are often induced by cyclones (see chapters 4,5,6,7). However as indicated in chapter two, section 2.4, cyclones do influence coastal sand transfer through direct marine impacts such as storm surge and high-energy waves (Hopley, 1974), which may cause the erosion of previously deposited coastal features. Pringle's (1991) study of the impacts of cyclone induced flooding on the Burdekin River Delta describes both erosive and constructive effects at a local scale (~ 30 km). Major flooding in the Burdekin (maximum instantaneous discharges > 19,000 $m^3.s^{-1}$ recorded at the Home Hill and Clare gauging stations, Queensland Department of Natural Resources and Mines) caused considerable erosion of spits, bars and barrier islands, while the deposition of sand close to the delta front (mainly in subtidal deltas) allows the accretion of spits and the delta (Pringle, 1991). Cyclone Althea (December 1971) also caused erosion along the SWT coast with up to 10 m of erosion at the eastern side of the Burdekin Delta and the south side of Cape Cleveland, between 11.6 and 15.8 m of recession between Rowes Bay and Pallarenda and 10.9 and 12.2 m of erosion at Black River and Saunders Beach, respectively (Hopley, 1974). However within the vicinity (~100m) of the river mouths the overall effect was aggradation – especially on parts of the Burdekin Delta and streams between the Bohle River and Crystal Creek (Hopley, 1974). Hopley (1974) reported an initial accretion of 20 m on the northern end of spits at Alva Beach, east coast of the Burdekin Delta (Figure 8.2). In the subsequent ten months after the cyclone the spits had grown by 200-400 m. However it is not clear whether this is due to the longshore movement of recently delivered fluvial sediment or the redistribution of recently eroded coastal sediments (Hopley, 1974).

Figure 8.2. The Burdekin Delta location map.

Storms and cyclones may be the most important factor controlling short-term (<10 years) coastal change (Morton *et al.*, 1995) (see chapter 2, section 2.4.2) but low-frequency high-magnitude events appear to have a relatively minor impact on large-scale coastal sand transfer and the long-term evolution of the SWT coast. The strong influence of south easterly wind generated waves over coastal sand transport is demonstrated in an analysis of wave data for the central region of the SWT coast. Modelling using ACES (chapter 3, section 3.4.4.1, Appendix C) (Leenknecht *et al.*, 1992) shows that despite relatively low ambient wave energy in north Queensland there is still the potential to move substantial volumes (>100,000 $m^3.y^{-1}$) of sand provided it is available. A waverider buoy located in deep water off Cape Cleveland has recorded modal significant wave height of 0.2 - 0.4 m for the Townsville region (BPA, 1996b). Longshore drift rates were estimated at 812,293 $m^3.y^{-1}$ using the ACES equations, for easterly wind waves approaching the shore at a 70° angle. As easterly winds prevail for 21% of the year (based on records from 1950 to 2001 taken at the Townsville Airport, station 32040) (Bureau of Meteorology, 2003), it is estimated that 170,588 $m^3.y^{-1}$ of sand is potentially moved north (21% of 812,293 $m^3.y^{-1}$). Cyclone Joy (23 December, 1990) produced the highest significant wave heights since 1975 at 2.96 m. North-easterly deep water waves at 2.96 m at a 10° angle to the coast for one day can move 23,000 m^3 of sand alongshore, in this case south. Wind waves associated with Cyclone Joy are estimated to have transported 14% of the amount of sand moved by easterly winds every year. Indeed, while the January 1998 floods associated with Cyclone Sid (estimated ARI of 1:100 years in the Black River see chapter 6) may have delivered sand to the delta it was quickly redistributed along the adjacent coast by ambient wave conditions. Aerial photograph analysis of the Haughton River Estuary failed to show any impact from cyclone or flooding events on the estuarine morphology, and additional stratigraphic analysis also failed to identify any immature fluvial sediments being deposited at the lower estuary for at least the last 1 ka. Modelling of the competency of bedload transport in the Haughton River estuary, further illustrates this point. A flood over ARI 1:3 years with duration over 24 hours has the potential to transport a maximum of 2,000 tonnes of sand into the estuary (Kinhill *et al.*, 1996). This is equivalent to between 2 weeks and 3 months net influx of sand by tidal currents into the lower estuary using Gadd *et al.'s* (1978) and Hardisty's (1983) equations respectively (see chapter 4). Thus the relatively high rates of sand transfer which occur under ambient wave and tidal processes may overshadow the impact of cyclones on coastal sand transfer in SWT estuaries.

The geomorphological impacts of low-frequency high-magnitude events on the SWT coast can persist over longer time frames. Chenier ridges are examples of cyclone/storm deposits which can be found along the SWT coast (Hopley, 1974; Chappell and Grindrod, 1984)(see Chapter 2, section 2.5). More recently, subtidal storm features have been discovered. Shelly gravel megaripples up to 2.5 m high (-8 m AHD) present in Halifax Bay are interpreted as cyclone generated and have been radio-carbon dated at ~2,600±170 y (Kirsch and Larcombe, 1999; Larcombe and Carter, 2004). Heap *et al.'s* (1999) sedimentological study of the Nara Inlet, Whitsunday Islands revealed that bed sediments are too coarse to be remobilised by ambient waves and tides suggesting that bedload sediment transport thresholds are only exceeded in the inlet during cyclones.

Larcombe and Carter (2004) suggest that cyclones are a major control on the supply of sediment to the SWT coast not only by the delivery of terrigenous sediment by river flooding, but by the erosion of the middle shelf seafloor. Their concept of 'The Cyclone Pump' proposes that water motions induced during the passage of a major cyclone introduce 'new' sediment from the middle shelf to the inner shelf (Larcombe and Carter, 2004). This new theory does not discount assumptions made in the 'Holocene sand budget for the SWT coast' (chapter 7) which includes only the inner shelf, as 'cyclone pumping' only results in the finer fraction (mud) being transported northwards and advected towards the coast (Larcombe and Carter, 2004).

8.4 THE BURDEKIN AS A MAJOR POINT SOURCE OF FLUVIAL SAND TO THE COAST

Belperio (1978) identified the Burdekin River as the major point source of fluvial sediment to the SWT coast; modelling suggests it delivers over 70% of the total sand supply (Prosser *et al.*, 2001a). The purpose of this section is to evaluate the Burdekin River's influence on coastal evolution over contemporary and Holocene time scales, especially in relation to sand-sized sediments.

8.4.1 CONTEMPORARY TIME SCALES

Suspended fine sediments discharged from the Burdekin can be dispersed as far north as Cleveland Bay in flood plumes (Orpin and Ridd, 1996; Devlin *et al.*, 2001), however, sands are only deposited over a relatively discrete area between the Burdekin River mouth north to Bowling Green Spit and perhaps some into Bowling Green Bay at contemporary time scales (Belperio, 1978; Pringle, 1983; 1984).

The vertical accretion of 30 m high dunes at the Delta, indicate an alternative sink for fine sand delivered to the coast. Also like other SWT streams, the hydrology of the Burdekin Delta limits the amount of sand actually delivered to the coast. Only a small proportion of flow discharges via the present mouth, with the smaller distributaries with limited sand carrying capacity such as Kalamia Creek dissipating flood waters. Thus floods produce mainly floodplain flow over the Barrattas plain (Queensland Water Resources Commission, 1980) with sand remaining in channel and not delivered to the coast. Therefore, under contemporary time scales, even the Burdekin River is not a major contributor of sand to the SWT coast.

8.4.2 HOLOCENE TIME SCALES

Figure 8.3 a-c is a summary of the previous positions of the Burdekin River channel and an interpretation of the spatial variation of sand supply to the coast during the Holocene after (Hopley, 1970a). Figure 8.2 shows that the Burdekin River would have indirectly supplied sand to a much larger part of the SWT coast in the past influencing the development of the coast. Lambeck and Woolfe (2000) provide evidence of relict sand reserves along the 10 m isobath off the SWT coast with maximum concentrations of sand off Bowling Green Bay and the Burdekin

Delta. This research supports Hopley's (1970a; 1970b) earlier conclusion that large reserves of sand were deposited offshore in Bowling Green Bay when the Burdekin discharged from ~11 to 8 ka.

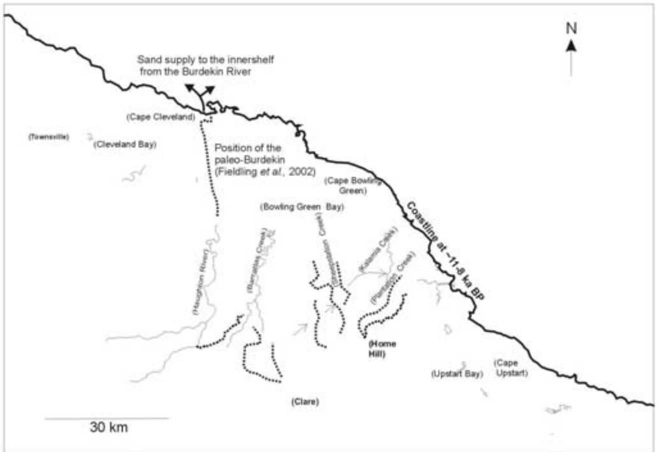

Figure 8.3 a. The influence of the Burdekin River on the SWT coast during the Holocene Transgression (11-8 ka BP).
Sea level was 20 m below present levels. The present coastline position is also shown on this map and the present feature names are in brackets. The Burdekin River channel originally discharged offshore of the modern location of Bowling Green Bay (Fielding et al., 2002). The Burdekin migrated south occupying several positions where Barrattas, Sheepstation, and Plantation Creeks are located today (Hopley, 1970).

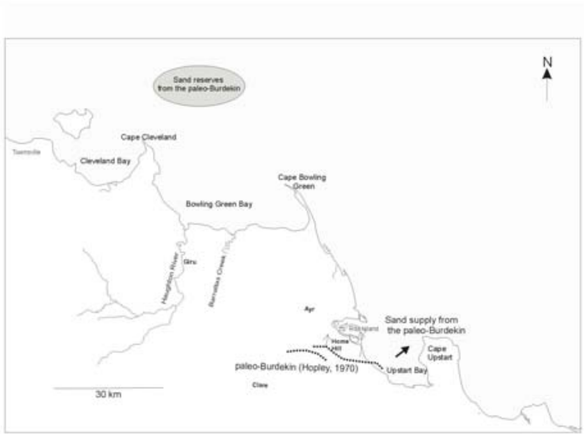

Figure 8.3 b. The influence of the Burdekin River on the SWT coast during the Middle Holocene (8-6 ka BP).
Sea level has reached present levels. The Burdekin River channel is diverted east of the present mouth (Hopley, 1970). Burdekin sand would have been deposited into Upstart Bay. This stage may be the one which found or initiated the large dune ridges found on Rita Island.

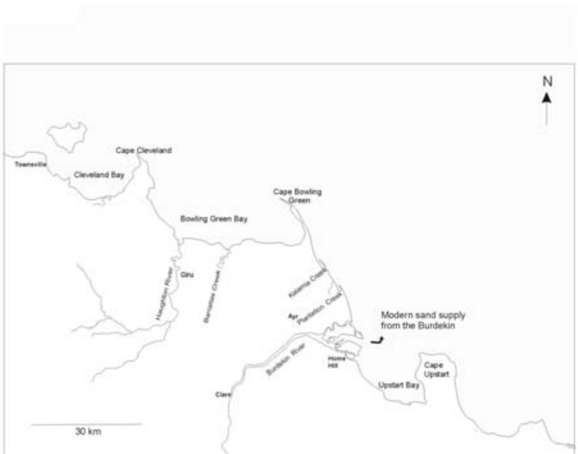

Figure 8.3c. The influence of the Burdekin River on the SWT coast during Late Holocene (6 ka BP - present).
The Burdekin River channel is diverted to its present location. Fluvial sand is only supplied to the east coast of the delta. The rate of delta progradation has slowed compared to the previous 4 ka. Vertical accretion of dunes at the delta mouth suggest an alternative sink for sand supplied to the coast.

8.5 FUTURE EVOLUTION OF SWT COAST AND ESTUARIES

From the evidence presented in this thesis it is apparent that the SWT coast is currently in an erosional phase with little nourishment from modern streams or marine reserves. Figure 8.1 illustrates the relationship between marine sediment supply and sea level change – suggesting that changing sea level has had the greatest influence over coastal accretion in the SWT during the Holocene. The following section will extrapolate these findings to predict the future evolution of the SWT coast under two scenarios: a stable sea level and a rising sea level.

8.5.1 STABLE SEA LEVEL

If sea level and climate remain stable the estuaries that are presently infilling with marine sand, namely the Haughton and the Elliot will continue to infill, while the Black River Delta should retain its present morphology. The Haughton River Estuary is likely to completely infill and become a tide-dominated delta (refer to chapter 2, figure 2.1). The present mouth of the Elliot River Estuary is also likely to be closed off by the continued accretion of the barrier. The lagoon behind the barrier will continue to fill with marine sediment eventually forming a wave-dominated delta (see chapter 2, figure 2.1). There is the potential that once these estuaries become completely infilled, fluvial sand may be delivered to the coast by tidal processes like in the Shoalhaven Delta, NSW (Wright, 1970; Young *et al.*, 1996). However this seems unlikely to occur in the Haughton and the Elliot considering the current deposition of fluvial sands is well above the tidal limit. A more likely scenario, is that complete infilling of these estuaries will reduce tidal currents which may result in increased northward sand transfer via longshore drift. However despite some localised progradation when the former estuaries become deltas, the rest of the SWT coastline will continue to erode.

Graham's (1993) theory of the developing 'maturity' of wet tropical coasts further north could also apply to the SWT. As described in chapter 7 (Figure 7.3), the northward transfer of sand in the SWT is restricted by headlands such as Cape Upstart and Cape Cleveland creating discrete compartments within the region. Progradation in some areas may lead to headlands no longer blocking longshore drift. If this situation was to occur, increasing leakage of sand from the SWT coastal system into other compartments is possible.

8.5.2 IMPACT OF FUTURE SEA-LEVEL RISE ON SWT COAST

The Intergovernmental Panel on Climate Change predict a globally averaged rise in sea level of 0.09-0.88 m by 2070 (2001). The range between the maximum and minium prediction prevents a detailed forecast of the future, however modelling has been conducted and the impacts from most recent sea-level rise may be extrapolated. Wolanski and Chappell (1996) conducted hydrodynamic modelling on the South Alligator River, Northern Territory, the Norman River, and north-west Queensland to predict the impact of a future sea-level rise of 0.1 - 0.5 m. Like the Haughton and Elliot, and the Norman River estuaries are flood-dominated, meso-tidal estuaries. Wolanski and Chappell (1996) predicted that a rise in sea level is likely to enhance the strength of ebb tidal currents in these estuaries. Thus it is likely that a rise in sea level would also increase the strength of ebb tidal currents in the Haughton and Elliot creating more symmetrical tidal currents (rather than flood-dominated) or even reversing the current pattern in the estuary to create an ebb-dominated setting. Further modelling (Wolanski and Chappell, 1996) in the Norman River Estuary predicts an overall increase in tidal current velocities and may cause increased bank erosion which may lead to a widening of the upper estuary channel – a scenario that also seems likely in the Haughton and Elliot estuaries. The direction of net sand transfer is likely to be reversed with more sand being transported seawards than into the estuary. Sea-level rise may increase the tidal prism in the Black producing an overall increase in tidal velocities and tidal range, which may lead to increased erosion and channel widening in the upper estuarine channel like in the Haughton and Elliot. Potential for increased erosion is exacerbated by increased wave set up and storm surge during cyclone events. Increased erosion of stored sand may lead to an increase of sand delivered to the coast.

A sea-level rise of 0.09-0.88 m is likely to accelerate erosion on the SWT coast rather than produce rapid progradation like the rises of 140 m experienced during the Holocene transgression. Submergence will deepen nearshore water allowing larger waves to break upon the shore (Bird, 1993). As the SWT coast is dominated by beach-ridge plains formed as a result of Holocene progradation, a rise in sea level is likely to initiate or accelerate erosion on their seawards margins (Bird, 1993). The Bruun Rule (Bruun, 1962) is a widely used to quantify the impact of sea-level rise on sandy coasts. Bruun (1962) suggests that erosion of the upper beach occurs with removal of this sand to the nearshore zone to restore the previous transverse profile. Erosion of the coast would cease once sea level stabilised at the new higher level (Bruun, 1962). Thus the Bruun Rule predicts that the coastline will retreat 50 – 100 fold the dimensions of the rise in sea level, for example a 9 cm rise (min IPCC) would cause coastal retreat of 4.5 - 9 m while a 88 cm rise (max IPCC) would cause a retreat of 44 – 88 m. Recent studies have evaluated the accuracy of the Bruun Rule predictions (see Kench and Cowell, 2001; Cooper and Pickley, 2004) and have found it tends to overestimate erosion rates in response to sea-level rise, and Bruun (1988) himself warns of the need to apply the ‘rule’ within its’ limitations. However it is clear that if sea level does rise over the next 100 years most sandy coastlines will retreat substantially (in the absence of protective structures and artificial nourishment), (Bird, 1993). However if a rise in sea level also causes estuaries to change from net importers of sand to net exporters perhaps the increased sand delivery to the coast may locally reduce shoreline retreat to some extent. Given that SWT have a maximum tidal range of 4 m an overall sea-level rise of 0.09 – 0.88 m is not likely to have a major impact. For a return to the rapid delivery of sand to the coast and subsequent progradation, a much more substantial rise in sea level would be needed. Only a rise of 10 m or more at a rate of 5-10 $m.ka^{-1}$ would reproduce the early-mid Holocene scenario of transgression over sand deposits of the present coastal plain and the delivery to a newly located coast as 'marine' sediments.

8.6 IMPLICATIONS FOR MANAGEMENT

8.6.1 MANAGEMENT OF SAND RESOURCE

Anthropogenic impacts that reduce the potential amount of fluvial sand reaching the coast, for example sand extraction or river regulation are often linked with coastal erosion (Pringle, 1989; 2000). However in SWT streams the extraction of sand and construction of dams has not altered the delivery of sand to the coast. This research has shown that in SWT streams, namely the Haughton, Elliot and Black Rivers, little sand reaches the coast even under essentially natural conditions. For example investigations revealed that the Haughton River has not delivered significant amounts of sand to the coast for at least the last 1 ka while the weirs have only been in place in the last 27 years (see chapter 4). Therefore artificial reductions in the amount of sand available to transport is not likely to impact the coast, if conditions remain constant. While extraction of sand from the river channel will not cause erosion at the coast, if conducted unsustainably it will have localised impacts on the stability of the river channel most likely accelerating bank erosion as the river attempts to compensate for the missing sediment.

A reduction of sand from the fluvial channel and estuary may have no immediate effect on the adjacent coast, which in the case of the SWT is in a natural erosional phase. However in the longer term the reduction of sand stored in the estuary or river channel may influence coastal evolution. This is especially relevant if there is a substantial rise in sea level. The sand stored in the estuary and river channel is likely to be reworked by marine processes and brought onshore. Reworked river derived 'marine' sand has been a major source of sand for coastal accretion in the SWT in the past (see figure 8.1). Under management timeframes and in terms of determining sustainable rates of sand extraction, the focus should be shifted from the maintenance of coastal sand supply to ensuring the integrity and stability of the river channel.

8.6.2 COASTAL COMMUNITIES

The SWT coast is eroding, and though this erosion may be exacerbated by anthropogenic activities, the process is a natural phase in the coast's evolution. Shoreline retreat is of major concern to residents of coastal communities notably Cungulla (at the mouth of Haughton River), Guthalungra (at the mouth of the Elliot River), Black River and Bushland Beach. Hopley and Rasmussen (1995) were commissioned by the Townsville City Council to review beach erosion in the Cungulla area. Hopley and Rasmussen (1995) concluded that the erosion was a natural processes and it was recommended that the council should adopt the 'do nothing' approach as engineering works would be ineffective and may even exacerbate erosion. Without major engineering works and artificial nourishment like has occurred on Townsville's main beach, The Strand, at a cost of ~$30 million, the SWT coastline will continue to recede impacting the aforementioned coastal communities. Despite the fact that some loss of property would occur, the recession of the coast is a natural process and there is little management agencies can do to prevent it. Large scale engineering works may offer some protection, however the cost is likely to outweigh the value of the property and they are likely to make it far less attractive to residents.

Perhaps more emphasis should be on preventing this unfortunate situation from occurring in the future by incorporating geomorphological timeframes into management decisions, especially with regard to town planning. For example appropriate set-back lines for coastal development need to be established to provide a buffer for the natural dynamism of the coast. These should be in the order of 100-150 m given that Cungulla shoreline has retreated 100 m over the last 60 years (see chapter 4). Planning for coastal change is especially relevant for future development given the predictions of increased rates of erosion under rising sea levels (see section 8.5.2 this chapter). Rising sea levels are also predicted to increase the rate of infilling of SWT estuaries which will impact the Townsville Port, located on the mouth of Ross River. The port is regularly dredged to prevent the infilling, however if the rate of infill increases, an up scaled and more expensive dredging effort will be required by the Townville Port Authority to maintain the channel.

8.7 RECOMMENDATIONS FOR FUTURE RESEARCH

- The fieldwork for this thesis represents an invaluable source of baseline/pre-flood data for SWT estuaries. If a catastrophic flood did occur in the future a similar surficial sampling regime could be undertaken in these systems to test inferences made in this study. For example that sand transfer to the coast in SWT streams is restricted by morphological factors and will be limited irrespective of the magnitude of the flood.

- The impact of cyclones and high magnitude events on sand transfer processes could be investigated further if nearshore wave conditions were monitored during cyclone and storm events.

- The lack of organic material preserved in SWT estuarine deposits limited the detail of the chronology of sedimentation by radiocarbon dating techniques. Application of high resolution Optical Sensor Luminescence (OSL) dating on deeper sand deposits would refine the chronology of sedimentation however the technique would of limited use for reworked surficial sediments. OSL combined with seismic or other techniques such as c-section coring or probing to locate and identify samples for OSL dating could be a better approach.

- This research has reported similar findings to Bryce *et al.'s* (1998) study of the Normanby River Estuary, in a SWT region in far north Queensland, suggesting that other SWT streams may not deliver substantial amounts of sand to the coast Application of the methods used in this study to other SWT regions for example South Africa would provide greater insight into the impact of the SWT climate on fluvial sand supply to the coast.

REFERENCES

2001. Climate change 2001: Synthesis report, Intergovernmental panel on climate change.

Ackers, P. and White, W.R., 1973. Sediment transport: new approach and analysis. Journal of the Hydraulics Division, Proceedings of the American Society of Civil Engineers., 99: 2041-2060.

Anthony, E.J., 2000. Marine sand supply and Holocene coastal sedimentation in northern France between the Somme estuary and Belgium. In: K. Pye and J.R.L. Allen (Editors), Coastal and estuarine environments: sedimentology, geomorphology and geoarchaeology. Geological Society, London, Special Publications. The Geological Society of London, London, pp. 87-97.

Anthony, E.J., Lang, J. and Oyede, L.M., 1996. Sedimentation in a tropical, microtidal, wave-dominated coastal-plain estuary. Sedimentology, 43: 665-675.

Ash, J., 1981. Rainfall patterns in northeastern Queensland. In: J. Chappell and J. Grindrod (Editors), CLIMAZ. Department of Biogeography and Geomorphology, Research School of Pacific Studies, Australian National University, Victoria, Australia, pp. 90.

Baker, V.R. and Costa, J.E., 1987. Flood power. In: L. Mayer and D. Nash (Editors), Catastrophic flooding. Allen & Unwin, Great Britain, pp. 1-21.

Barker, R., Dixon, L. and Hooke, J., 1997. Use of terrestrial photogrammetry for monitoring and measuring bank erosion. Earth Surface Processes and Landforms, 22: 1217-1227.

Barusseau, J.P., Diop, E.H.S. and Saos, J.L., 1985. Evidence of dynamics reversal in tropical estuaries, geomorphological and sediementological consequences (Salum and Casamance Rivers, Sengal). Sedimentology, 32: 543-552.

Belperio, A.P., 1978. An inner shelf sedimentation model for the Townsville region, Great Barrier Reef Province. PhD Thesis, James Cook University, Townsville, 197 pp.

Belperio, A.P., 1979. The combined use of wash load and bed material load rating curves for the calculation of total load: an example from the Burdekin River, Australia. Catena, 6: 317-329.

Belperio, A.P., 1983. Terrigenous sedimentation in the central Great Barrier Reef lagoon: a model from the Burdekin region. BMR Journal of Australian Geology & Geophysics, 8: 179-190.

Bird, E.C.F., 1971. The origin of beach sediments on the north Queensland coast. Earth Science Journal, 5(2): 95-105.

Bird, E.C.F., 1973. Depositional evidence of fluvial sediment yield: an example from north Queensland. The Australian Geographer, 9(3): 250-253.

Bird, E.C.F., 1978. The Geomorphology of the Gippsland Lakes region, Ministry for Conservation, Victoria.

Bird, E.C.F., 1993. Submerging coasts. Coastal Morphology and Research. John Wiley & Sons, Great Britain, 184 pp.

Bird, E.C.F., 2000. Coastal geomorphology: an introduction. John Wiley & Sons, West Sussex, 322 pp.

Blott, S.J. and Pye, K., 2001. Gradistat: a grainsize distribution and statistics package for the analysis of unconsolidated sediments. Earth Surface Processes and Landforms, 26: 1237-1248.

Boyd, R., Dalrymple, R.A. and Zatlin, B.A., 1992. Classification of clastic coastal depositional environments. Sedimentary Geology, 80: 139-150.

BPA, 1996a. Wave data recording program: Abbot Point region 1977-1996., Beach Protection Authority, Brisbane.

BPA, 1996b. Wave data recording program: Townsville region 1975-1996., Beach Protection Authority, Brisbane.

Brodie, J., 1996. River flood plumes in the Great Barrier Reef lagoon. In: P. Larcombe, K.J. Woolfe and R.G. Purdon (Editors), Great Barrier Reef: terrigenous sediment flux and human impact, Townsville, pp. 33 - 39.

Bronk Ramsay, C., 2000. OxCal Program v3.5.

Brown and Root, 2001. Fluvial supply of sediments to the Queensland Coast, Environmental Protection Agency, Brisbane.

Bruun, P., 1962. Sea-level rise as a cause of shore erosion. Journal of Waterways and Harbours Division: Proceedings of the American Society of Civil Engineers., 88: 117-130.

Bruun, P., 1988. The Bruun rule of erosion by sea-level rise: A discussion on large-scale two- and three-dimensional usages. Journal of Coastal Research, 4(4): 627-648.

Bryce, S., 2001. Controlling factors on sediment transport in mangrove creek systems of North-East Queensland. PhD Thesis, James Cook University, Townsville, 192 pp.

Bryce, S., Larcombe, P. and Ridd, P.V., 1998. The relative importance of landward-directed tidal sediment transport versus freshwater flood events in the Normanby River Estuary, Cape York Peninsula, Australia. Marine Geology, 149(1-4): 55-78.

Bryce, S., Larcombe, P. and Ridd, P.V., 2003. Hydrodynamic and geomorphological controls on suspended sediment transport in mangrove creek systems, a case study: Cocoa Creek, Townsville, Australia. Estuarine Coastal & Shelf Science, 56: 415-431.

Carter, R.W.G. and Woodroffe, C.D. (Editors), 1994. Coastal evolution: Late Quaternary shoreline morphodynamics. Cambridge University Press, United Kingdom, 517 pp.

Chapman, D.M., Geary, M., Roy, P.S. and Thom, B.G., 1982. Coastal evolution and coastal erosion in New South Wales, Coastal council of New South Wales, Sydney.

Chappell, J. and Grindrod, J., 1984. Chenier plain formation in Northern Australia. In: T. B.G. (Editor), Coastal Geomorphology In Australia. Academic Press Australia.

Coastal Engineering Solutions, 1998. Black River / Bohle River area: preliminary coastal engineering assessment, Townsville.

Cooper, J.A.G., 1990. Ephemeral stream-mouth bars at flood-breach river mouths on a wave-dominated coast: comparison with ebb-tidal deltas at barrier inlets. Marine Geology, 95: 57-70.

Cooper, J.A.G., 1993. Sedimentation in a river dominated estuary. Sedimentology, 40: 979-1017.

Cooper, J.A.G., 2002. The role of extreme floods in estuary-coastal behaviour: contrasts between river- and tide-dominated micro-tidal estuaries. Sedimentary Geology, 150: 123-137.

Cooper, J.A.G and Pilkey, O.H., 2004. Sea-level rise and shoreline retreat: time to abandon the Bruun Rule. Global And Planetary Change 43: 157

Coppus, R. and Imeson, A.C., 2002. Extreme events controlling erosion and sediment transport in a semi-arid sub-andean valley. Earth Surface Processes and Landforms, 27: 1365-1375.

Costa, J.E. and O'Connor, J.E., 1995. Geomorphically effective floods. In: J.E. Costa, A.J. Miller, K.W. Potter and P.R. Wilcock (Editors), Natural and anthropogenic influences in fluvial geomorphology. American Geophysical Union, USA, pp. 45-55.

Cowell, P., J. and Thom, B.G., 1994. Chapter 2: Morphodynamics of coastal evolution. In: R.W.G. Carter and C.D. Woodroffe (Editors), Coastal Evolution: Late Quaternary shoreine morphodynamics. Cambridge University Press, United Kingdom, pp. 517.

Crowell, M.A., Fletcher, C.H. and Richmond, B.M., 1991. Historical shoreline change: Error analysis and mapping accuracy. Journal of Coastal Research, 7: 839-852.

Dalrymple, R.W., Knight, J., R., Zaitlin, B.A. and Middleton, G., V., 1990. Dynamics and facies model of a macrotidal sand-bar complex, Cobequid Bay-Salmon River Estuary (Bay of Fundy). Sedimentology, 37: 577-612.

Dalrymple, R.W., Zaitlin, B.A. and Boyd, R., 1992. Estuarine facies models: conceptual basis and stratigraphic implications. Journal of Sedimentary Petrology, 62(6): 1130-1146.

Davies, J., L., 1974. The coastal sediment compartment. Australian Geographical Studies, 12: 139-151.

Davis, A.J., 1968. Chiefly fine - A book of weather. Halls Book Store.

Devlin, M., Waterhouse, J., Talyor, J. and Brodie, J., 2001. Flood plumes in the Great Barrier Reef: Spatial and temporal patterns in composition and distribution, Great Barrier Reef Marine Park Authority, Townsville.

Dolan, R., Hayden, B.P., May, P. and May, S., 1980. The reliability of shoreline change measurements from aerial photographs. Shore & Beach, 48(2): 22-29.

Douglas, I., 1967. Natural and man-made erosion in the humid tropics of Australia, Malaysia and Singapore. Publications of International Association of Scientific Hydrology, 75: 17-30.

Dunbar, G.B., Dickens, G.R. and Carter, R.M., 2000. Sediment flux across the Great Barrier Reef shelf to the Queensland Trough over the last 300 ky. Sedimentary Geology, 133: 49-92.

Dyer, K.R., 1995. Sediment transport processes in estuaries. In: G.M.E. Perillo (Editor), Geomorphology and Sedimentology of Estuaries. Elsevier, Netherlands, pp. 423-449.

Engelund, F. and Hansen, E., 1967. A monograph of sediment transport in alluvial streams. Technisk Vorlag, Copenhagen.

Erskine, W.D., 1996. Response and recovery of a sand-bed stream to a catastrophic flood. Zeitschrift fur Geomorphologie, 40(3): 359-383.

Fairbridge, R.W., 1980. The estuary: its defintition and geodynamic cycle. In: E. Olausson and I. Cato (Editors), Chemistry and Biogeochemistry of Estuaries. John Wiley & Sons, pp. 1-35.

Fielding, C.R. and Alexander, J., 1996. Sedimentology of the upper Burdekin River of north Queensland, Australia - an example of a tropical, variable discharge river. Terra Research, 8: 447-457.

Fielding, C.R., Trueman, J.D., Dickens, G.R. and Page, M., 2003. Anatomy of the buried Burdekin River channel across the Great Barrier Reef shelf: how does a major river operate on a tropical mixed siliciclastic/carbonate margin during sea level lowstand? Sedimentary Geology, 157(3-4): 291-301.

FitzGerald, D.M., Buynevich, M.S., Fenster, M.S. and MacKinlay, P.A., 2000. Sand dynamics at the mouth of a rock-bound, tide-dominated estuary. Sedimentary Geology, 131: 25-49.

Flood, P.G., 1986. Sensitivity of coral cays to climatic variations, southern Great Barrier Reef, Austraila. Coral Reefs, 5(13): 13-18.

Folk, R.L. and Ward, W.C., 1957. Brazos River bar: A study in the significance of grain size parameters. Journal of Sedimentary Petrology, 27: 1-19.

Fournier, F., 1960. Climat et erosion: la relation entre l'erosion du sol par l'eau et les precipitations atmospheriques, Paris.

Friedman, G.M., 1961. Distinction between dune, beach and river sands from their textural characteristics. Journal of Sedimentary Petrology, 31(4): 514-529.

Gadd, P.E., Lavelle, J.W. and Swift, D.J.P., 1978. Estimates of sand transport on the New York shelf using near-bottom current meter observations. Journal of Sedimentary Petrology, 48(1): 239-252.

Gagan, M.K., Johnson, D.P. and Crowley, G.M., 1994. Sea level control of stacked late Quaternary coastal sequences, central Great Barrier Reef. Sedimentology, 41: 329-351.

Galgano, F.A. and Douglas, B.D., 2000. Shoreline position prediction: methods and errors. Environmental Geosciences, 7(1): 23-31.

GBRMPA, 2001. Water quality action plan for the Great Barrier Reef Marine Park, Great Barrier Reef Marine Park Authority, Townsville.

GHD, 2000. Burdekin River extraction and sediment management plan. Report for Burdekin Shire Rivers Improvement Trust, Gutteridge Haskins Davey.

Gilmour, D.A., 1971. The effects of logging on streamflow and sedimentation in a north Queensland rainforest catchment. Commonwealth Forestry Review, 50(1): 38-48.

Gilmour, D.A., 1977. Effect of rainforest logging and clearing on water yield and quality in a high rainfall zone of north-east Queensland, Hydrology Symposium, Brisbane, pp. 156-160.

Goh, S., 1992. A morphological prediction of Cape Bowling Green, North Queensland, Australia. Honours Thesis, James Cook University of North Queensland, Townsville, 148 pp.

Goodbred, S.L. and Kuehl, S.A., 2000. Enormous Ganges-Brahmaputra sediment discharge during strengthened early Holocene monsoon. Geology, 28(12): 1083-1086.

Graham, T.L., 1993. Geomorphological response of continental shelf and coastal environments to the Holocene transgression - central Great Barrier Reef. PhD Thesis, James Cook University of North Queensland, Townsville, 191 pp.

Guy, H.P., Simons, D.B. and Richardson, E.V., 1966. Summary of alluvial channel data from flume experiments 1955-1961. Geological Survey Professional Paper U.S. Govt. Printing Office, Paper 462-I: 96.

Hacker, J.L.F., 1988. Rapid accumulation of the fluvially derived sands and gravels in a tropical macrotidal estuary: the Pioneer River at Mackay, North Queensland, Australia. Sedimentary Geology, 57: 299-315.

Hapke, C. and Richmond, B., 2000. Monitoring beach morphology changes using small-format aerial photography and digital softcopy photography. Environmental Geosciences, 7(1): 32-37.

Hardisty, J., 1983. An assessment and calibration of formulations for Bagnold's bedload equation. Journal of Sedimentary Petrology, 53: 1007-1010.

Harris, P.T., 1988. Large-scale bedforms as indicators of mutually evasive sand transport and the sequential infilling of wide-mouthed estuaries. Sedimentary Geology, 57: 273-298.

Harris, P.T., Heap, A., Bryce, S., Porter-Smith, R., Ryan, D. and Heggie, D., 2002. Classification of Australian clastic coastal depositional environments based upon a quantiative analysis of wave, tidal and river power. Journal of Sedimentary Research, 72(6): 858-870.

Harris, T. and Jones, M.R., 1988. Bedform movement in a marine tidal delta: air photo interpretations. Geological Magazine, 125(1): 31-49.

Hean, D.S. and Nanson, G.C., 1987. Serious problems in using equations to estimate bedload yields for coastal rivers in NSW. Australian Geographer, 18(2): 114-124.

Heap, A., Bryce, S., Ryan, D., Radlke, L., Smith, R., Harris, P. and Heggie, D., 2001. Australian estuaries & coastal waterways: A geoscience perspective for improved and intergrated resource management., Australian Geological Survey Organsiation, Canberra.

Heap, A.D., Dickens, G.R., Stewart, L.K. and Woolfe, K.J., 2002. Holocene storage of siliciclastic sediment around islands on the middle shelf of the Great Barrier Reef Platform, north-east Australia. Sedimentology, 49: 603-621.

Heap, A.D., Larcombe, P. and Woolfe, K.J., 1999. Storm-dominated sedimentation in a protected basin fringed by coral reefs, Nara Inlet, Whitsunday Islands, Great Barrier Reef, Australia. Australian Journal of Earth Sciences, 46: 443-451.

Hjulstrom, F., 1935. Bulletin of the Geological Institute, 25.

Holmes, K.H., 1992. Townsville-Rollingstone coastal sector, Marine & Coastal Geology Unit Project Report MA50/2 Department of Minerals and Energy, Brisbane.

Hopley, D., 1967. A statistical approach to the relationship between coastal erosion and changes in wind patterns at Byron Bay, N.S.W. Australian Geographer, 10: 275-285.

Hopley, D., 1970a. Coastal geomorphology of the Townsville region. Ph.D Thesis, James Cook University, Townsville.

Hopley, D., 1970b. The geomorphology of the Burdekin Delta north Queensland. Monograph Series, 1. James Cook University of North Queensland, Townsville, 66 pp.

Hopley, D., 1974. Coastal changes produced by tropical cyclone Althea in Queensland; December 1971. The Australian Geographer, 12(5): 445-56.

Hopley, D., 1980. Sediment movement around a coral cay, Great Barrier Reef, Australia. Pacific Geology, 15: 17-36.

Hopley, D., 1983. Deformation of the north Queensland continental shelf in the Late Quaternary. In: D.E. Smith and A.G. Dawson (Editors), Shorelines and Isostasy. British Geomorphology Research Group, Academic Press, London.

Hopley, D., 1984. The Holocene 'High Energy Window' on the Central Great Barrier Reef. In: B.G. Thom (Editor), Coastal Geomorphology in Australia. Academic Press Australia, pp. 135-150.

Hopley, D., 1985. Geomorphological development of modern coastlines. In: A.F. Pitty (Editor), Themes in Geomorphology. Croon Helm, Great Britain, pp. 56-71.

Hopley, D., 1986. The Queensland coastline: attributes and issues. Queensland Geographical Journal 4th Series, 1: 73-94.

Hopley, D., Harvey, N. and Pye, K., 1980. The eastern coastal plains and continental shelf. In: R.A. Henderson and P.J. Stephenson (Editors), The Geology and Geophysics of Northeastern Australia. Geological Society of Australia, Queensland Division, Townsville, pp. 386-393.

Hopley, D. and Murtha, G.G., 1975. The Quaternary deposits of the Townsville coastal plain. Monograph Series. James Cook University of North Queensland, Townsville, 30 pp.

Hopley, D. and Rasmussen, C., 1995. Cungulla beach erosion review, James Cook University, Townsville.

Hopley, D., Smithers, S.G. and Parnell K.E., 2007. The geomorphology of the Great Barrier Reef: Development, diversity and change. Cambridge University Press, 532 pp.

Horn, A., Joo, M. and Poplawski, W., 1998. Queensland riverine sediment transport rates., Department of Natural Resources, Brisbane.

Isdale, P.J., Stewart, B.J., Tickle, K.S. and Lough, J.M., 1998. Palaeohydrological variation in a tropical river catchment: a reconstruction using flourescent bands in corals of the Great Barrier Reef, Australia. The Holocene, 8(1): 1-8.

Jennings, J.N. and Bird, E.C.F., 1967. Regional Geomorphological Characteristics of Some Australian Estuaries. In: G. Lauff, H, (Editor), Estuaries. American Association for the Advancement of Science, Washington D.C., pp. 121-128.

Johnson, D.P. and Searle, D.E., 1984. Post-glacial seismic stratigraphy, central Great Barrier Reef, Australia. Sedimentology, 31: 335-352.Johnson, D.P., Searle, D.E. and Hopley, D., 1982. Positive relief over buried Post-Glacial channels, Great Barrier Reef Province, Australia. Marine Geology, 46: 149-159.

Kana, T.W., Hayter, E.J. and Work, P.A., 1999. Mesoscale Sediment Transport at Southeastern U.S. Tidal Inlets: Conceptual Model Application to Mixed Energy Settings. Journal of Coastal Research, 15(2): 303-313.

Kapitzke, I.R., Pearson, R.G., Smithers, S.G., Crees, M.R., Sands, L.B., Skull, S.D. and Johnston, A.J., 1998. Stream stabilistation for rehabilitation in north-east Queensland. Land and Water Resources Research & Development Corporation, Canberra, 216 pp.

Kench, P.S., 1999. Geomorphology of Australian estuaries: review and prospect. Australian Journal of Ecology, 24: 367-380.

Kench, P. and Cowell, P., 2001. The Morphological Response of Atoll Islands to Sea-Level Rise. Part 2: Application of the Modified Shoreface Translation Model (STM). *Journal of Coastal Research*, Special Issue 2001.

Kershaw, A.P., 1975. Late Quaternary vegetation and climate in northeastern Australia. In: R.P. Suggate and M.M. Cresswell (Editors), Quaternary Studies. The Royal Society of New Zealand, Wellington, pp. 187-187.

Kershaw, A.P., 1978. Record of last interglacial-glacial cycle from northeastern Queensland. Science, 194: 1121-1132.

Kershaw, A.P., 1985. An extended late Quaternary vegetation record from north-eastern Queensland and its implications for the seasonal tropics of Australia. Proceedings of Ecological Society of Australia, 1985: 179-189.

Kershaw, A.P., 1986. Climatic change and Aboriginal buring in north-east Australia during the last tow glacial/interglacial cycles. Nature, 322(3 July): 47-49.

Kettle, B.T., Dalla Pozza, R. I., Collins, J. 2001. New Directions: A Review of the Impacts of Dredging in Cleveland Bay, and Research Priorities for the Next Decade. A report commissioned by the Townsville Port Authority.

Kidson, C. and Manton, M.M.M., 1973. Assessment of Coastal Change with the aid of Photogrammetric and Computer-aided Techniques. Estuarine and Coastal Marine Science, 1: 271-283.

King, C.A.M., 1972. Beaches and Coasts. Edward Arnold, London, 670 pp.

Kinhill, 1998. Sand supply investigations Black River, Townsville, Kinhill, Milton.

Kinhill, Cameron and McNamara, 1993. Townsville Thuringowa sand and gravel strategy study. BC2403, DPI - Water Resources City of Thuringowa and the Department of Transport, Townsville.

Kinhill, Cameron and McNamara, 1996. Proposed sand extraction operations: Haughton River, Burdekin Shire; environmental impact statement, Boral Resources (QLD) Pty Ltd.

Kirsch, A. and Larcombe, P., 1999. Evidence for the generation of very large dunes generated by cyclones in Halifax Bay, central Great Barrier Reef province, Australia. In: H.A. D. (Editor), North Queensland Sedimentologists' 1st Annual Workshop. James Cook University of North Queensland, School of Earth Sciences, James Cook University, pp. 89.

Knighton, D., 1984. Fluvial forms and processes. Edward Arnold, Great Britain.

Komar, P.D., 1998. Beach processes and sedimentation. Simon & Schuster, U.S.A., 544 pp.

Lambeck, A. and Woolfe, K.J., 2000. Composition and textural variability along the 10m isobath, Great Barrier Reef: evidence for pervasive northward sediment transport. Australian Journal of Earth Sciences, 47(2): 327-335.

Larcombe, P. and Carter, R.M., 1998. Sequence architecture during the Holocene transgression: an example from the Great Barrier Reef shelf, Australia. Sedimentary Geology, 117(1-2): 97-121.

Larcombe, P. and Carter, R.M., 2004. Cyclone pumping, sediment partitioning and the development of the Great Barrier Reef shelf system: a review. Quaternary Science Reviews, 23: 107-135.

Larcombe, P. and Ridd, P.V., 1995. Megaripple dynamics and sediment transport in a mesotidal mangrove creek: implications for palaeoflow reconstructions. Sedimentology, 42: 593-606.

Larcombe, P., Ridd, P.V., Prytz, A. and Wilson, B., 1995. Factors controlling suspended sediment on inner-shelf coral reefs, Townsville, Australia. Coral Reefs, 14: 163-171.

Larcombe, P., Woolfe, K.J., Amjad, N., Barnes, D.J., Brodie, J., Brunskill, G.J., Bryce, S., Carter, R.M., Costen, A., Crook, K.A.W., Crossland, C., Deacon, G.L., Ferland, M.A., Gorrie, A., Grindrod, J., Johnson, D.P., McIntyre, C.M., Neil, D.T., Okubo, C., Orpin, A.R., Purdon, R.G., Pye, K., Ridd, P.V., Shulmeister, J., Talyor, J. and Walker, G.S., 1996a. Terrigenous sediment fluxes and the central Great Barrier Reef shelf: the current state of knowledge. In: P. Larcombe, K.J. Woolfe and R.G. Purdon (Editors), Great Barrier Reef: terrigenous sediment flux and human impact. CRC Reef Research Centre,James Cook University of North Queensland, Townsville, pp. 7 - 23.

Larcombe, P., Woolfe, K.J. and Purdon, R.G. (Editors), 1996b. Great Barrier Reef: terrigenous sediment flux and human impacts. Current Research. CRC Reef Research Centre, James Cook University of North Queensland, Townsville, 174 pp.

Leenknecht, D.A., Szuwalski, A. and Sherlock, A.R., 1992. Automated coastal engineering system, user's guide. ACES version 1.07. U.S. Army Engineer Waterways Experiment Station, Coastal Engineering Research Centre., Mississippi.

Lindholm, R., 1987. A practical approach to sedimentology. Allen and Unwin, London, 276 pp.

Lyons, W.F. and Bonell, M., 1994. Regionalization of daily mesoscale rainfall in the tropical wet/dry climate of the Townsville area of north-east Queensland during the 1988-1989 wet season. international Journal of Climatology, 14: 135-163.

Magilligan, F.J., Phillips, J.D., James, A.L. and Gomez, B., 1998. Geomorphic and sedimentological controls on the effectiveness of an extreme flood. Journal of Geology, 106: 87-95.

Malvarez, G.C., Cooper, J.A.G. and Jackson, D.W.T., 2001. Relationships between wave-induced currents and sediment grain size on a sandy tidal-flat. Journal of Sedimentary Research, 71(5): 705-712.

McCulloch, M.T., Fallon, S., Wyndham, T., Hendy, E.J., Lough, J.M. and Barnes, D.J., 2003. Coral record of increased sediment flux to inner Great Barrier Reef since European settlement. Nature, 421: 727-728.

McIntyre, C.M., 1996. Holocene stratigraphy of Cleveland Bay, Central Great Barrier Reef, Australia. MSc Thesis, James Cook University, Townsville.

McIntyre and Associates, 1985. Cungulla water supply: Groundwater investigations, bore hole cross sections, Townville.

Miles, G., 1991. Transport of sand mixtures. In: R. Soulsby and R. Bettess (Editors), Sand Transport in Rivers, Estuaries and the Sea. A.A. Balkema, Rotterdam, Netherlands, pp. 253-257.

Miller, M.C., Williams, G.D., A., S.J. and Hibler, L.F., 2002. Fox Island laboratory shoreline change evaluation, Battelle Marine Science Laboratory, Washington.

Mitchell, A., W. and Furnas, M., J., 1996. Differences in suspended sediment flux to the Great Barrier Reef shelf between wet and dry catchments of north Queensland. In: P. Larcombe, K.J. Woolfe and R.G. Purdon (Editors), Great Barrier Reef: terrigenous sediment flux and human impact. CRC Reef Research Centre, James Cook University of North Queensland, Townsville, pp. 108-115.

Morton, R., A. , Gibeaut, J., C. and Paine, J., G., 1995. Meso-scale transfer of sand during and after storms: implications for prediction of shoreline movement. Marine Geology, 126: 161-179.

Neil, D.T., Orpin, A.R., Ridd, P. and Yu, B., 2002. Sediment yield and impacts from river catchments to the Great Barrier Reef lagoon. Marine Freshwater Research, 53: 733-752.

Neil, D.T. and Yu, B., 1996a. Fluvial sediment yield to the Great Barrier Reef lagoon: spatial patterns and the effect of land use. In: H.M. Hunter, A.G. Eyles and G.E. Rayment (Editors), Downstream Effects of Land Use. Department of Natural Resources, pp. 281-286.

Neil, D.T. and Yu, B., 1996b. Simple climate models for estimating sediment input to the Great Barrier Reef Lagoon. In: P. Larcombe, K.J. Woolfe and R.G. Purdon (Editors), Great Barrier Reef: Terrigenous Sediment Flux and Human Impacts. CRC Reef Research Centre, James Cook University, Townsville, pp. 122-127.

Nicholas, A.P., Ashworth, P.J., Kirkby, M.J., Macklin, M.G. and Murray, T., 1995. Sediment slugs: large-scale fluctuations in fluvial sediment transport rates and storage volumes. Progress in Physical Geography, 19(4): 500-519.

Nichols, G., 1999. Sedimentology & stratigraphy. Blackwell Science, Great Britain, 355 pp.

Nott, J.F., Price, D.M. and Nanson, G.C., 2002. Stream response to Quaternary climate change: evidence from Shoalhaven River catchment, southeastern highlands, temperate Australia. Quaternary Science Reviews, 21: 965-974.

Nott, J.F., Thomas, M.F. and Price, D.M., 2001. Alluvial fans, landslides and Late Quaternary climatic change in the wet tropics of northeast Queensland. Australian Journal of Earth Sciences, 48: 875-882.

Orpin, A.R., 1999. Sediment transport, partitioning, and unmixing relationships in the mixed terrigenous-cabonate system of the Great Barrier Reef, Burdekin shelf sector, Australia. PhD Thesis, James Cook University, Townsville.

Orpin, A.R. and Ridd, P.V., 1996. Sediment distribution and transport mechanisms, Burdekin region, central Great Barrier Reef lagoon. In: P. Larcombe, K.J. Woolfe and R.G. Purdon (Editors), Great Barrier Reef: Terrigenous Sediment Flux and Human Impacts. CRC Reef Research Centre, James Cook University, Townsville, pp. 128-143.

Orpin, A.R., Ridd, P.V. and Stewart, L.K., 1999. Assessment of the relative importance of major sediment-transport mechanisms in the central Great Barrier Reef lagoon. Australian Journal of Earth Sciences, 46: 883-896.

Orpin, A.R. and Woolfe, K.J., 1999. Unmixing relationships as a method of deriving a semi-quantitiative terrigenous sediment budget, central Great Barrier Reef lagoon, Australia. Sedimentary Geology, 129: 25-35.

Osterkamp, W.R. and Coasta, J.E., 1987. Changes accompaning an extraordinary flood on a sand-bed stream. In: L. Mayer and D. Nash (Editors), Catastrophic flooding. Allen & Unwin, Great Britain, pp. 201-224.

Osterkamp, W.R. and Friedman, J.M., 2000. The disparity between extreme rainfall events and rare floods - with emphasis on the semi-arid American West. Hydrological Processes, 14: 2817-2829.

Otvos, E.G., 2000. Beach ridges - definitions and significance. Geomorphology, 32(1-2): 83-108.

Page, M., Dickens, G.R. and Dunbar, G.B., 2003. Tropical view of Quaternary sequence statigraphy: Siliciclastic accumulation on sloped east of the Great Barrier Reef since the Last Glacial Maximum. Geology, 31(11): 1013-1016.

Perillo, G.M.E. (Editor), 1995. Geomorphology and sedimentology of estuaries. Developments in Sedimentology, 53. Elsevier, Netherlands, 471 pp.

Perry, C.T., 1999. Biofilm-related calcification, sediment trapping and constructive micrite envelopes: a criterion for the recognition of ancient grass-bed environments. Sedimentology, 46(1): 33-40.

Persson, A.C., 1997. Effect of river regulation on sediment supply from the Ross River to Cleveland Bay. Honours Thesis, James Cook University, Townsville, 139 pp.

Pringle, A., W., 1983. Sand spit and bar development along the east Burdekin Delta coast Queensland, Australia. In: D. Hopley (Editor), Monograph Series. Department of Geography, James Cook University of North Queensland, Townsville, pp. 34.

Pringle, A.W., 1984. Evolution of the east Burdekin Delta coast, Queensland, Australia 1940-1980. Z. Geomorph. N. F., 28(2): 129-154.

Pringle, A., W., 1986. Causes and effects of changes in fluvial sediment yield to the north-east Queensland coast, Australia. In: D. Hopley (Editor), Monograph series. Department of Geography, James Cook University of North Queensland, Townsville, pp. 128.

Pringle, A., W., 1989. The history of dredging in Cleveland Bay, Queensland and its effect on sediment movement and on the growth of mangroves, corals and seagrass, Great Barrier Reef Marine Park Authority, Townsville Port Authority, Townsville.

Pringle, A., W., 1991. Fluvial sediment supply to the north-east Queensland coast, Australia. Australian Geographical Studies, 29(1): 114-138.

Pringle, A.W., 2000. Evolution of the east Burdekin Delta coast, Queensland, Australia 1980-1995. Z. Geomorph. N. F., 44(3): 273-304.

Prosser, I., Hughes, A., Lu, H. and Stevenson, J., 2001a. Waterborne erosion - an Australian story: content for the Australian natural resources atlas storyboards, CSIRO Land and Water.

Prosser, I.P., Rutherford, I.D., Olley, J.M., Young, W.J., Wallbrink, P.J. and Maran, C.J., 2001b. Large-scale patterns of erosion and sediment trasnsport in river networks with examples from Australia. Marine Freshwater Research, 52: 81-99.

Puotinen, M.L., Done, T.J. and Skelly, W.C., 1997. An atlas of tropical cyclones in the Great Barrier Reef Region, 1969-1997., CRC Reef Research Centre, James Cook University, Townsville.

Queensland Transport, 2003. The official tide tables and boating safety guide. Queensland Department of Transport, Brisbane.

Queensland Water Resources Commission. 1980. Report on establishment of Burdekin River project undertaking. Queensland Water Resources Commission.

Radlke, L., 2003. Land clearing swells sediment loads in WA estuaries, AUSGEO News, pp. 18-19.

Rasmussen, C. and Hopley, D., 1997. Warraber Island Beach erosion review, James Cook University, Brisbane.

Roy, P.S. and Crawford, E.A., 1977. Significance of sediment distribution in major coastal rivers, Northern NSW., Proceedings of the 3rd Australian Conference on Coastal and Ocean Engineering., pp. 177-184.

Roy, P.S., Thom B.G. and Wright, L.D., 1980. Holocene sequences on an embayed high-energy coast: An evolutionary model. Sedimentary Geology, 26: 1-19.

Roy, P.S., Williams, R.J., Jones, A.R., Yassini, I., Gibbs, P.J., Coates, B., West, R.J., Scanes, P.R., Hudson, J.P. and Nichol, S., 2001. Structure and function of south-east Australian estuaries. Estuarine, Coastal and Shelf Science, 53: 351-384.

Ryan, D.A., Heap, A.D., Radke, L. and Heggie, D.T., 2003. Conceptual models of Australia's estuaries and coastal waterways, Geoscience Australia, Canberra.

Searle, D.E., Harvey, N., Hopley, D. and Johnson, D.P., 1981. Significance of results of shallow seismic research in the Great Barrier Reef Province between 16°10'S and 20°05'S, Proceedings of the Forth International Coral Reef Symposium, Manila, pp. 531-539.

Short, A.D. (Editor), 1999. Handbook of beach and shoreface morphodynamics. John Wiley, New York, 368 pp.

Smith, G.L. and Zarillo, G.A., 1990. Calculating long-term shoreline recession rates using aerial photographic and beach profiling techniques. Journal of Coastal Research, 6(1): 111-120.

Smithers, S.G., 2002. Burdekin basin water resource plan: Current environmental conditions and impacts of existing water resource development, James Cook University, Townsville.

Stafford, D.B. and Langfelder, J., 1971. Air photo survey of coastal erosion. Photogrammetric Engineering, 37(6): 565-575.

Stewart, L.K., Heap, A.D. and Woolfe, K.J., 2000. Evaluating the influence of tidal currents on the distribution of silt in the Nara Inlet, central Great Barrier Reef, Australia. Sedimentary Geology, 136: 59-69.

Stoddart, D.R., 1969. World erosion and sedimentation. In: R.J. Chorley (Editor), Water, earth and man. Methuen & Co., London, pp. 473-485.

Stuiver, M., Reimer, P.J., Bard, e., Beck, J.W., Burr, G.S., Hughen, K.A., Kromer, B., McCormac, G., Van Der Plight, J. and Spurk, M., 1998. INTCAL98 radiocarbon age calibration, 24,000-0 cal BP. Radiocarbon, 40(3): 1041-1083.

Tanner, W.F., 1995. Origin of beach ridges and swales. Marine Geology, 129: 149-161.

Taylor, M. and Stone, G.W., 1996. Beach-ridges: a review. Journal of Coastal Research, 12(3): 612-621.

Thieler, E.R. and Danforth, W.W., 1994. Historical shoreline mapping (I): Improving techniques and reducing positioning errors. Journal of Coastal Research, 10(3): 549-563.

Thom, B.G., Bowman, G., M. and Roy, P.S., 1981. Late Quaternary evolution of coastal sand barriers, Port Stephens - Myall Lakes Area, Central New South Wales, Australia. Quaternary Research, 15: 345-364.

Thom, B.G. and Chappell, J., 1975. Holocene sea levels relative to Australia. Search, 6(3): 90-93.

Thom, B.G. and Roy, P.S., 1985. Relative sea levels and coastal sedimentation in southeast Australia in the Holocene. Journal of Sedimentary Petrology, 55(2): 257-264.

Thomas, M.F., 2003. Late Quaternary sediment fluxes from tropical watersheds. Sedimentary Geology, 162: 63-81.

Thomas, M.F., Nott, J.F. and Price, D.M., 2001. Late Quaternary stream sedimentation in the humid tropics: a review with new data from NE Queensland , Australia. Geomorphology, 39: 53-68.

Umitsu, M., Buman, M., Kawase, K. and Woodroffe, C.D., 2001. Holocene palaeoecology and formation of the Shoalhaven River deltaic-estuarine plains, southeast Australia. The Holocene, 11(4): 407-18.

USACE, 1984. Shore protection manual, U.S. Army Engineer Waterways Experiment Station, Coastal Engineering Research Centre, U.S., Washington.

Visher, G.S., 1969. Grain size distributions and depostional processes. Journal of Sedimentary Petrology, 39(3): 1074-1106.

Walling, D.E., 1983. The sediment delivery problem. Journal of Hydrology, 65: 209-237.

Wasson, R.J., 1997. Run-off from the land to the rivers to the sea. In: N. Turia and C. Dalliston (Editors), The Great Barrier Reef: Science, use and management. Great Barrier Reef Marine Park Authority, Townsville, pp. 23-41.

Wasson, R.J., Olive, L.J. and Rosewell, C.J., 1996. Rates of erosion and sediment transport in Australia. In: D.E. Walling and B.W. Webb (Editors), Erosion and sediment yield: global and regional perspectives. IAHS, pp. 139-148.

Way, A.J., 1987. Post-glacial stratigraphy of Upstart Bay off the Burdekin River, north Queensland. MSc Thesis, James Cook University, Townsville.

Wohl, E.E., 1992. Bedrock benches and boulder bars: Floods in the Burdekin Gorge of Australia. Geological Society of America Bulletin, 104: 770-778.

Wolanski, E. and Chappell, J., 1996. The response of tropical Australian estuaries to a sea level rise. Journal of Marine Systems, 7: 267-279.

Wolman, M.G. and Miller, J.P., 1960. Magnitude and frequency of forces in geomorphic processes. Journal of Geology, 68: 54-74.

Woodroffe, C.D., Chappell, J., Thom, B.G. and Wallensky, E., 1986. Geomorphological dynamics and evolution of the South Alligator Tidal River and Plains, Northern Territory. NARU Monograph,. ANU Press, Canberra, 190 pp.

Woodroffe, C.D., Chappell, J., Thom, B.G. and Wallensky, E., 1989. Depositional model of a macrotidal estuary and floodplain, South Alligator River, Northern Australia. Sedimentology, 36: 737-756.

Woodroffe, C.D., Mulrennan, M.E. and Chappell, J., 1993. Estuarine infill and coastal progradation, southern van Dieman Gulf, northern Australia. Sedimentary Geology, 83: 257-275.

Woolfe, K.J., Larcombe, P., Oprin, A.R., Purdon, R.G., Michaelsen, P., McIntyre, C.M. and Amjad, N., 1998. Controls upon inner-shelf sedimentation, Cape York Peninsula, in the region of 12 degrees S. Australian Journal of Earth Sciences, 45: 611-621.

Wright, L.D., 1970. The influence of sediment availability on patterns of beach ridge development in the vicinity of the Shoalhaven River Delta, NSW. The Australian Geographer, 3: 336-48.

Wright, L.D. and Coleman, J.M., 1973. Variations in morphology of major river deltas as functions of ocean wave and river discharge regimes. The American Association of Petroleum Geologists Bulletin (AAPG), 57(2): 370-398.

Young, R.W., White, K.L. and Price, D.M., 1996. Fluvial deposition on the Shoalhaven Deltaic Plain, Southern New South Wales. Australian Geographer, 27(2): 215-234.

Yu, B., 1998. Rainfall erosivity and its estimation for Australia's tropics. Australian Journal of Soil Research, 36: 143-165.

APPENDIX A - CLASSIFICATION OF SWT COASTAL STREAMS

STREAM NAME	ORIGIN OF STREAM				FLOW		PHYSICAL CHARACTERISTICS										POTENTIAL WAVE ENERGY/WAVE REFRACTION					
	Coast	Hill	Escarp.	Range	Intermittant	Perennial	Valley Length (km)	Channel (km)	Catchment Area (km2)	Sinuousity	Elevation (m) above sea level	Gradient	Mangrove Limit (km)	Tidal Limit (km)	Estuary Length (km)	Estuarine Reach (% of channel)	Distance to 5m depth (km)	Distance to 10m depth (km)	Distance to 5m depth (km)	Distance to 10m depth (km)	Exposure to wind and waves (degrees)	Orientation of the coast (direction)
Don River		*			*		50	60	3985	1.20	0	0.00	3.5	3.5	3.5	5.83	0.7	1.6	1.05	2.4	110	NW
19 57' 148 12'	*				*		2.5	5	18.7	2.00	0	0.00	5		5	100.00	1.6	1.9	2.4	2.85	110	NW
19 57' 148 12'	*				*		0.75	1	3.75	1.33	0	0.00	1		1	100.00	1	2	1.5	3	100	NW
19 57' 148 10'	*				*		1.25	2	15.6	1.60	0	0.00	2		2	100.00	1.1	1.2	1.65	1.8	90	W
Euri Creek		*			*		40	50	365.6	1.25	200	0.00	2.5	2.5	2.5	5.00	1.1	3.4	1.65	5.1	75	W
19 54' 148 01'	*				*		5	10	18.8	2.00	50	0.01	2.5	1.25	2.5	25.00	0.7	3.8	1.05	5.7	0	NE
19 55' 148 05'	*				*		5	10	37.5	2.00	150	0.02	5	1.1	5	50.00	1.2	3.1	1.8	4.65	40	NE
Splitters Creek		*			*		23	25	100	1.09	500	0.02	3.5	1.5	3.5	14.00	2	3	3	4.5	45	W
Saltwater Creek		*			*		18	23	84.4	1.28	40	0.00	4.5	1.3	4.5	19.57	2.3	3.3	3.45	4.95	130	NW
Elliot River		*			*		30	40	290	1.33	250	0.01	2	1.55	2	5.00	2.3	3.3	3.45	4.95	130	NW
19 47' 147 51'		*			*		3	5	11.13	1.67	60	0.01	4	0.65	4	80.00	0.4	0.7	0.6	1.05	170	N
19 47' 147 50'		*			*		3	4	5.25	1.33	160	0.04	2	0.02	2	50.00	0.5	1.7	0.75	2.55	0	N
19 47' 147 46'	*				*		4	6	7.6	1.50	340	0.06	1	0.2	1	16.67	2.7	9	4.05	13.5	0	N
19 48' 147 46'		*			*		1.5	4	1.13	2.67	100	0.03	3	0.3	3	75.00	3.6	10	5.4	15	0	N
19 49' 147 46'	*				*		0.7	4.5	0.6	6.43	0	0.00	4.5		4.5	100.00	3.8	10	5.7	15	0	WNW
19 49' 147 46'	*				*		1	1.5	0.625	1.50	0	0.00	1.5		1.5	100.00	6.1	12	9.15	18	0	WNW
Nobbies Inlet	*				*		3	8	12.75	2.67	50	0.01	7.5	0.85	7.5	93.75	6.1	12	9.15	18	0	WNW
19 51' 147 46'		*			*		3	6	0.625	2.00	20	0.00	5	1.2	5	83.33	6.1	12	9.15	18	0	WNW
Sandy Creek		*					25	30	96.88	1.20	250	0.01	2.75	1.5	2.75	9.17	6.1	12	9.15	18	0	WNW
Cape Creek	*				*		10	16	81.5	1.60	40	0.00	6.25	1.7	6.25	39.06	6.1	12	9.15	18	0	WNW
19 50' 147 44'	*				*		2	4.5	1.88	2.25	0	0.00	4.5		4.5	100.00	4.1	8.1	6.15	12.15	0	W
Armstrong Creek	*				*		20	31	78.12	1.55	150	0.00	5	1.6	5	16.13	4.2	8.2	6.3	12.3	0	W
Molongole Creek		*					25	31	118.17	1.24	100	0.00	1.15	1.15	1.15	3.71	2.6	7.4	3.9	11.1	0	W
R M Creek						*	14	19	81.25	1.36	80	0.00	1.2	1.2	1.2	6.32	1.6	6.5	2.4	9.75	0	NW
Rocky Ponds Creek		*				*	13.5	28	62.5	2.07	240	0.01	3.5	2.5	3.5	12.50	1.6	6.5	2.4	9.75	0	NW
19 44' 147 39'	*				*		5	9	1.25	1.80	0	0.00	2		2	22.22	1.9	3.4	2.85	5.1	70	NNW
Little Sugarloaf Creek							3	5	1.25	1.67	0	0.00	4		4	80.00	1.9	3.4	2.85	5.1	70	NNW
Sugarloaf Creek					*		3	6.5	1.88	2.17	0	0.00	6		6	92.31	1.9	3.4	2.85	5.1	70	NNW
Yellow Gin Creek	*				*		4	11	40.6	2.75	0	0.00	9	1.6	9	81.82	1.9	3.4	2.85	5.1	70	NNW
Saltwater Creek	*				*		8	18	12.5	2.25	0	0.00	10	2	10	55.56	1.9	3.4	2.85	5.1	70	NNW

19 44' 147 34'	*				*		3	5	2.4	1.67	0	0.00	5		5	100.00	1.9	3.4	2.85	5.1	70	NNW
Plantation Creek	*				*		22.5	35	137.5	1.56	0	0.00	18	3.3	18	51.43	1	1.5	1.5	2.25	160	NW
Mud Creek	*				*		3.5	5	36	1.43	0	0.00	5		5	100.00	1	1.5	1.5	2.25	150	NW
19 31' 147 30'	*				*		10	14	37.5	1.40	0	0.00	3		3	21.43	1	1.5	1.5	2.25	150	NW
Alva Creek	*				*		10	12.5	18.7	1.25	0	0.00	3		3	24.00	0.7	1.1	1.05	1.65	140	NW
19 23' 147 27'	*				*		1.25	3	1.5	2.40	0	0.00	3		3	100.00	6.9	10.2	10.35	15.3	0	NE
19 24' 147 27'	*				*		1.75	3	1.7	1.71	0	0.00	3		3	100.00	7.4	10.3	11.1	15.45	0	NE
19 24' 147 27'	*				*		2.25	2	1.88	0.89	0	0.00	2		2	100.00	6.9	10.8	10.35	16.2	0	NE
19 25' 147 27'	*				*		1.5	1.5	0.47	1.00	0	0.00	1.5		1.5	100.00	7	10.7	10.5	16.05	0	NE
19 26' 147 26'	*				*		7.5	10	6.25	1.33	0	0.00	5		5	50.00	7.1	10.8	10.65	16.2	0	NE
19 25' 147 20'	*				*		12.5	15	25	1.20	0	0.00	7		7	46.67	5.6	9	8.4	13.5	0	W
19 25' 147 19'	*				*		3.75	4	3	1.07	0	0.00	3		3	75.00	4.9	7.9	7.35	11.85	0	W
19 25' 147 18'	*				*		3.75	4	4.5	1.07	0	0.00	3		3	75.00	6	6.5	9	9.75	0	W
19 26' 147 17'	*				*		4.25	7	6.25	1.65	0	0.00	7		7	100.00	6.6	6.8	9.9	10.2	0	W
19 26' 147 17'	*				*		2.5	3	3.1	1.20	0	0.00	2.5		2.5	83.33	6.6	6.8	9.9	10.2	0	W
19 26' 147 16'	*				*		23	30	28.13	1.30	100	0.00	3	3	3	10.00	7.2	7.3	10.8	10.95	0	W
Barratta Creek			*		*		70	103	556.25	1.47	460	0.00	24	4.8	24	23.30	7	7.4	10.5	11.1	0	W
19 26' 147 12'	*				*		12.5	6.5	6.25	0.52	0	0.00	6.5		6.5	100.00	4.1	7.3	6.15	10.95	0	W
Barramundi Creek	*				*		10	12	37.5	1.20	0	0.00	12		12	100.00	3.3	7.9	4.95	11.85	0	W
Haughton River			*		*		65	90	3600	1.38	1000	0.01	17	4	17	18.89	2.9	7.2	4.35	10.8	0	W
Burrumbush Creek	*				*		8	19	28.1	2.38	0	0.00	18	2.1	18	94.74	2.9	7.2	4.35	10.8	0	W
Dough Boy Creek	*				*		1.5	2	1.88	1.33	0	0.00	1.5		1.5	75.00	2.9	7.2	4.35	10.8	0	W
Blacksoil Creek	*				*		1	3	1.85	3.00	0	0.00	3		3	100.00	1.6	7	2.4	10.5	80	NW
Salmon Creek	*				*		5	7	2.61	1.40	0	0.00	6		6	85.71	1.2	5.6	1.8	8.4	100	N
19 15' 147 03'		*			*		2.25	5	2	2.22	360	0.07	1.25	0.15	1.25	25.00	1.5	7.5	2.25	11.25	100	N
Cocoa Creek	*				*		3	10	6	3.33	240	0.02	8	0.88	8	80.00	6.2	11.5	9.3	17.25	0	NE
Crocodile Creek	*				*		12	22	56.25	1.83	320	0.01	13.25	1.3	13.25	60.23	6.4	10.5	9.6	15.75	0	NE
19 19' 146 54'	*				*		5.5	11	6.5	2.00	0	0.00	7.75	1.1	7.75	70.45	6.4	10.5	9.6	15.75	0	NE
Alligator Creek		*			*		21	31	175	1.48	1000	0.03	10	1.8	10	32.26	5.9	12.4	8.85	18.6	0	W
19 18' 146 54'		*			*		1.5	3.5	4.25	2.33	60	0.02	2	0.23	2	57.14	5.9	11.6	8.85	17.4	0	W
Sandfly Creek	*				*		2.5	10	18.25	4.00	180	0.02	7	0.9	7	70.00	5.3	11	7.95	16.5	0	NW
Stuart Creek		*			*		16	23	49.87	1.44	230	0.01	4	1.1	4	17.39	3.1	11.1	4.65	16.65	0	NW
Ross River			*		*		45	55	471.9	1.22	400	0.01	4	1.9	4	7.27	3.1	11.1	4.65	16.65	0	NW
Three Mile Creek		*			*		1.5	5	7	3.33	120	0.02	4	0.4	4	80.00	4	12.2	6	18.3	0	NW
Shelly Creek		*			*		1	2.5	1.25	2.50	80	0.03	1	0.12	1	40.00	2.6	6.7	3.9	10.05	0	W
Bohle River		*			*		27	35	306.25	1.30	60	0.00	8	2.25	8	22.86	3.1	8.3	4.65	12.45	0	N
Black River			*		*		25	42	221.88	1.68	720	0.02	1.3	1.3	1.3	3.10	2.2	7.2	3.3	10.8	0	NW
Alick Creek	*				*		6.5	9	13.6	1.38	20	0.00	2.5	0.8	2.5	27.78	2.2	7.2	3.3	10.8	0	NW
Althaus Creek		*			*		16	19	93.75	1.19	220	0.01	2	1.1	2	10.53	1.5	6.5	2.25	9.75	50	NW
Bluewater Creek			*		*		22	35	62.5	1.59	620	0.02	1.28	1.28	1.28	3.66	1.4	6.3	2.1	9.45	50	NW
Two Mile Creek	*				*		8	10	11	1.25	20	0.00	2.5	0.93	2.5	25.00	2.5	8.3	3.75	12.45	50	NW
Sleeper Log Creek*			*		*		12	17	42.2	1.42	320	0.02	1.75	1	1.75	10.29	2.5	8.3	3.75	12.45	50	NW

Christmas Creek*			*		*		12	16	42.2	1.33	460	0.03	1.75	0.6	1.75	10.94	2.5	8.3	3.75	12.45	50	NW
Leichardt Creek			*		*		12	15	35.9	1.25	560	0.04	1.5	0.6	1.5	10.00	2.4	8.3	3.6	12.45	40	NW
Camp Oven Creek		*			*		5	5.5	7	1.10	115	0.02	1	0.4	1	18.18	2.3	8.9	3.45	13.35	45	NW
Saltwater Creek			*		*		11	14.5	37.5	1.32	940	0.06	0.75	0.4	0.75	5.17	1.7	8.9	2.55	13.35	40	NW
Station Creek			*		*		5	7.25	6.75	1.45	460	0.06	1	0.5	1	13.79	2	7.1	3	10.65	30	NW
Wild Boar Creek			*		*		4.5	5.25	3.25	1.17	500	0.10	0.75	0.3	0.75	14.29	2	7.1	3	10.65	30	NW
Surveyors Creek			*		*		5	6.5	9.75	1.30	440	0.07	0.5	0.3	0.5	7.69	1.2	6.4	1.8	9.6	30	NW
Rollingstone Creek			*		*		10	16	78	1.60	760	0.05	0.5	0.5	0.5	3.13	0.9	5.8	1.35	8.7	30	NW
Key																						
Large complex systems				11																		
Small complex systems				22																		
Perrennial systems				2																		
Large coastal inlets				13																		
Small coastal inlets				33																		

APPENDIX B - LIST OF AERIAL PHOTOGRAPHS

Site	Year	Type	Name	Film #	Run #	Photo #	Scale
Haughton River Estuary	1942	Federal	Haughton River			1-733	1:40000
Haughton River Estuary	1961	Federal	Bowling Green	Q 1171	5	129	
Haughton River Estuary	1974	BPA	St Lawrence to Townsville	Qp 3888	74	107	1:12000
Haughton River Estuary	1974	BPA	St Lawrence to Townsville	Qp 3888	74	109	1:12000
Haughton River Estuary	1974	BPA	St Lawrence to Townsville	Qp 3888	75	58	1:12000
Haughton River Estuary	1974	BPA	St Lawrence to Townsville	Qp 3888	75	60	1:12000
Haughton River Estuary	1981	BPA	St Lawrence to Townsville	Qp 3888	74-2	138	1:12000
Haughton River Estuary	1981	BPA	St Lawrence to Townsville	Qp 3888	75	170	1:12000
Haughton River Estuary	1981	BPA	St Lawrence to Townsville	Qp 3888	75	168	1:12000
Haughton River Estuary	1981	BPA	St Lawrence to Townsville	Qp 3888	74 A	181	1:12000
Haughton River Estuary	1985	BPA	St Lawrence to Townsville	Qpc 4460	74 W	119	1:12000
Haughton River Estuary	1985	BPA	St Lawrence to Townsville	Qpc 4460	74 A	112	1:12000
Haughton River Estuary	1985	BPA	St Lawrence to Townsville	Qpc 4460	75	89	1:12000
Haughton River Estuary	1991	BPA	St Lawrence to Townsville	Qpc 5023	75	229	1:12000
Haughton River Estuary	1993	BPA	St Lawrence to Townsville	Qpc 5217	74	169	1:12000
Haughton River Estuary	1993	BPA	St Lawrence to Townsville	Qpc 5217	74 A	97	1:12000
Haughton River Estuary	1993	BPA	St Lawrence to Townsville	Qpc 5217	74 B	82	1:12000
Haughton River Estuary	1993	BPA	St Lawrence to Townsville	Qpc 5217	74 C	7	1:12000
Haughton River Estuary	1993	BPA	St Lawrence to Townsville	Qpc 5217	75	214	1:12000
Haughton River Estuary	1998	BPA	St Lawrence to Townsville	Qpc 5615	74 W	4	1:12000
Haughton River Estuary	1998	BPA	St Lawrence to Townsville	Qpc 5612	75	60	1:12000
Haughton River Estuary	1998	BPA	St Lawrence to Townsville	Qpc 5612	75	62	1:12000
Haughton River Estuary	1998	BPA	St Lawrence to Townsville	Qpc 5612	75	64	1:12000
Haughton River Estuary	1998	BPA	St Lawrence to Townsville	Qpc 5615	74 W	6	1:12000
Haughton River Estuary	1998	BPA	St Lawrence to Townsville	Qpc 5615	74 W	3	1:12000
Haughton River Estuary	1998	BPA	St Lawrence to Townsville	Qpc 5617	59	157	1:12000
Haughton River Estuary	2000	TCC	Townsville City Council		40	2340	1:12000
Haughton River Estuary	2000	TCC	Townsville City Council		40	2342	1:12000
Elliot River Estuary	1942	Federal	Elliot River			1-752v	1:40000
Elliot River Estuary	1942	Federal	Elliot River			1-753v	1:40000
Elliot River Estuary	1942	Federal	Elliot River			1-754v	1:40000
Elliot River Estuary	1942	Federal	Elliot River			1-755v	1:40000
Elliot River Estuary	1974	BPA	St Lawrence to Townsville	Q 2856	63	165	1:12000
Elliot River Estuary	1974	BPA	St Lawrence to Townsville	Q 2856	63	167	1:12000
Elliot River Estuary	1974	BPA	St Lawrence to Townsville	Q 2856	63	169	1:12000
Elliot River Estuary	1974	BPA	St Lawrence to Townsville	Q 2856	64	110	1:12000
Elliot River Estuary	1974	BPA	St Lawrence to Townsville	Q 2856	64	112	1:12000
Elliot River Estuary	1974	BPA	St Lawrence to Townsville	Q 2856	64	114	1:12000
Elliot River Estuary	1974	BPA	St Lawrence to Townsville	Q 2856	64	116	1:12000

Elliot River Estuary	1974	BPA	St Lawrence to Townsville	Q 2856	64	118	1:12000
Elliot River Estuary	1974	BPA	St Lawrence to Townsville	Q 2856	64	114	1:12000
Elliot River Estuary	1974	BPA	St Lawrence to Townsville	Q 2856	65	85	1:12000
Elliot River Estuary	1974	BPA	St Lawrence to Townsville	Q 2856	65	87	1:12000
Elliot River Estuary	1974	BPA	St Lawrence to Townsville	Q 2856	65	89	1:12000
Elliot River Estuary	1974	BPA	St Lawrence to Townsville	unknown	64	116	1:12000
Elliot River Estuary	1982	BPA	St Lawrence to Townsville	Q4033	64	53	1:12000
Elliot River Estuary	1982	BPA	St Lawrence to Townsville	Q4033	64	55	1:12000
Elliot River Estuary	1982	BPA	St Lawrence to Townsville	Q4033	64	57	1:12000
Elliot River Estuary	1981	BPA	St Lawrence to Townsville	Q4033	64	55	1:12000
Elliot River Estuary	1985	BPA	St Lawrence to Townsville	Qpc 4471	64	57	1:12000
Elliot River Estuary	1985	BPA	St Lawrence to Townsville	Q4471	64	59	1:12000
Elliot River Estuary	1991	BPA	St Lawrence to Townsville	Q4892	64	39	1:12000
Elliot River Estuary	1991	BPA	St Lawrence to Townsville	Q4892	64	41	1:12000
Elliot River Estuary	1993	BPA	St Lawrence to Townsville	Qpc5171	64	135	1:12000
Elliot River Estuary	1993	BPA	St Lawrence to Townsville	Qpc5171	64	133	1:12000
Elliot River Estuary	1993	BPA	St Lawrence to Townsville	Qpc5171	63	80	1:12000
Elliot River Estuary	1998	BPA	St Lawrence to Townsville	Qpc 5617	64	65	1:12000
Elliot River Estuary	1998	BPA	St Lawrence to Townsville	Q5617	64	67	1:12000
Black River Delta	1942	Federal	Townsville	3826	13	34166	1:12000
Black River Delta	1974	BPA	Townsville to Cooktown	Q 2996	2	7887	1:12000
Black River Delta	1974	BPA	Townsville to Cooktown	Q 2996	2	7885	1:12000
Black River Delta	1979	BPA	Townsville to Cooktown	Qpc 3677	2	5018	1:12000
Black River Delta	1979	BPA	Townsville to Cooktown	Qpc 3677	2	5019	1:12000
Black River Delta	1979	BPA	Townsville to Cooktown	Qpc 3677	2	5020	1:12000
Black River Delta	1983	BPA	Townsville to Cooktown	Q 4230	2	27	1:12000
Black River Delta	1983	BPA	Townsville to Cooktown	Q 4230	2	29	1:12000
Black River Delta	1983	BPA	Townsville to Cooktown	Q 4230	2	31	1:12000
Black River Delta	1983	BPA	Townsville to Cooktown	Q 4230	2	33	1:12000
Black River Delta	1983	BPA	Townsville to Cooktown	Q 4230	1	17	1:12000
Black River Delta	1983	BPA	Townsville to Cooktown	Q 4230	1	15	1:12000
Black River Delta	1991	BPA	Townsville to Cooktown	Q 4987	2	139	1:12000
Black River Delta	1991	BPA	Townsville to Cooktown	Q 4987	2	137	1:12000
Black River Delta	1991	BPA	Townsville to Cooktown	Q 4987	2	135	1:12000
Black River Delta	1991	BPA	Townsville to Cooktown	Q 4987	2	133	1:12000
Black River Delta	1991	BPA	Townsville to Cooktown	Q 4987	2a	168	1:12000
Black River Delta	1995	BPA	Townsville to Cooktown	Qpc 5268	2	157	1:12000
Black River Delta	1995	BPA	Townsville to Cooktown	Qpc 5268	2	155	1:12000
Black River Delta	1995	BPA	Townsville to Cooktown	Qpc 5268	2A	181	1:12000
Black River Delta	2000	BPA	Townsville to Cooktown	Qap 5829	2	49	1:12000
Black River Delta	2000	BPA	Townsville to Cooktown	Qap 5829	2	51	1:12000
Black River Delta	2000	BPA	Townsville to Cooktown	Qap 5829	2	53	1:12000
Black River Delta	2000	BPA	Townsville to Cooktown	Qap 5829	2	55	1:12000

Black River Delta	2000	BPA	Townsville to Cooktown	Qap 5829	2a	20	1:12000
Black River Delta	2000	BPA	Townsville to Cooktown	Qap 5829	2a	22	1:12000

APPENDIX C - SAND TRANSPORT MODELLING USING ACES (AUTOMATED COASTAL ENGINEERING SYSTEM)

SWT Net Longshore Transport using ACES 1.07

Wind Direction	Deepwater Wave Height (m)	Deepwater Wave Angle Relative to SWT coast (degrees)	Annual Transport Rate ($m^3.y^{-1}$)	Annual Percent Occurrence	Annual Net Transport (m^3)
SE	0.4	90	0	7.3%	0
SE	0.4	89	2,098	7.3%	154.2
SE	0.4	85	15,604	7.3%	1,139.1
E	0.4	60	120,441	10.3%	12,393.4
E	0.4	65	102,150	10.3%	10,521.5
E	0.4	70	812,298	10.3%	83,666.7
NE	0.4	10	56,349	9.3%	5,240.5
NE	0.4	5	28,692	9.3%	2,668.4
NE	0.4	1	5,772	9.3%	536.8
NE	0.4	0	0	9.3%	0
SE	0.7	90	0	2.7%	0
SE	0.7	89	8,499	2.7%	229.5
SE	0.7	85	63,218	2.7%	1,706.9
E	0.7	60	487,941	3.8%	18,444.2
E	0.7	65	413,843	3.8%	15,726.1
E	0.7	70	329,363	3.8%	12,515.8
NE	0.7	10	228,289	3.4%	7,807.5
NE	0.7	5	116,239	3.4%	3,952.1
NE	0.7	1	23,383	3.4%	795
NE	0.7	0	0	3.4%	0

Calculation of Longshore Sediment Transport using ACES 1.07 (Leenknecht *et al.*, 1992)

The longshore transport rate, Q, is the volumetric rate of movement of sand parallel to the shoreline. Much longshore transport occurs in or near the surf zone and is caused by the approach of waves at an angle to the shoreline. Q is expressed in terms of sand volume per unit time (such as cubic yards per year or cubic meters per year). The method used to calculate the longshore transport in this ACES application is based on the assumption that longshore transport rate Q is dependent upon the longshore component of wave energy flux $P_{\iota s}$ entering the surf zone (Equation 4-49 of the Shore Protection Manual, 1984).

$$Q = \frac{K}{(\rho_s - \rho)\, g\, \alpha} P_{\iota s} \quad \text{(unit volume per sec)} \qquad (1)$$

K = dimensionless empirical coefficient (based on field measurements)
= 0.39
ρ_s = density of sand
ρ = density of water
g = acceleration due to gravity
a = ratio of the volume of solids to total volume, accounting for sand porosity
= 0.6

Energy Flux Equation (Deepwater Wave Conditions)

Using deepwater values of wave characteristics (H_{so} significant wave height and α_o angle of approach), Equation 7 becomes:

$$P_{\iota s} = \frac{\rho g}{16} H^2_{s0}\, C_{gb} \sin 2\alpha_0$$

(12)

Again, from linear wave theory:

$$C_{gb} = n C_b \qquad (13)$$

where

$n \approx$ ½ (in deep water)

Again, using solitary wave theory for breaker characteristics:

$$C_b = 8.02\sqrt{H_b} \qquad (14)$$

Local wave height H_b can be related to deepwater height H_o by refraction and shoaling coefficients, where the coefficients are evaluated at the breaker position.

$$\sqrt{H_b} = \sqrt{K_r K_s H_o} \qquad (15)$$

Where

K_r = refraction coefficient

$$\left(\cos \alpha_0 \right.^{1/4}$$

$$\sqrt{K_r} = \left. \frac{\quad}{\cos \alpha_b} \right] \qquad (16)$$

K_s = shoaling coefficient (approximated by the breaker height index) = 1.3

In Equation 16, cos α_b equals 1.0 to a good approximation. For example, if α_b has a high value of 20°, then $(\cos 20^{\circ})^{1/4} = 0.98$.

Substituting the above variables into Equation 11 for $P_{\iota s}$ and simplifying yields the longshore energy flux factor entering the surf zone using deepwater wave conditions (Equation 4-45 of the SPM (1984)).

$$P_{\iota s} = 0.05\, \rho g^{3/2} H_{s0}^{5/2} (\cos \alpha_0)^{1/4} \sin 2\alpha_0 \qquad (17)$$

APPENDIX D - RESULTS OF TEXTURAL ANALYSES

HAUGHTON RIVER ESTUARY SURFICIAL SAMPLES

Sample #	Sample type	Mean	Sorting	Skewness	Kurtosis	Mean	Sorting:	Skewness	Kutosis	MODE 1	MODE 2	MODE 3	D10	D50	D90	(D90 / D10)	(D90 - D10)
11	Unimodal, Moderately Well Sorted	353.0	1.416	-0.001	0.997	Medium Sand	Moderately Well Sorted	Symmetrical	Mesokurtic	317.6			224.5	351.6	556.9	2.481	332.4
12	Unimodal, Moderately Well Sorted	303.1	1.602	0.229	0.988	Medium Sand	Moderately Well Sorted	Coarse Skewed	Mesokurtic	215.0			186.0	283.2	616.6	3.315	430.6
13	Unimodal, Well Sorted	276.3	1.403	0.247	1.031	Medium Sand	Well Sorted	Coarse Skewed	Mesokurtic	215.0			191.6	266.9	459.0	2.396	267.5
14	Unimodal, Well Sorted	189.2	1.319	-0.012	0.986	Fine Sand	Well Sorted	Symmetrical	Mesokurtic	215.0			134.4	193.8	276.2	2.055	141.8
15	Unimodal, Well Sorted	245.2	1.398	0.265	1.277	Fine Sand	Well Sorted	Coarse Skewed	Leptokurtic	215.0			181.9	231.1	399.7	2.197	217.8
16	Unimodal, Moderately Well Sorted	301.4	1.508	0.232	0.942	Medium Sand	Moderately Well Sorted	Coarse Skewed	Mesokurtic	215.0			190.7	288.0	557.9	2.926	367.2
17	Unimodal, Moderately Well Sorted	258.9	1.549	-0.086	1.116	Medium Sand	Moderately Well Sorted	Symmetrical	Leptokurtic	263.0			146.0	261.4	437.0	2.994	291.0
18	Unimodal, Moderately Well Sorted	328.8	1.416	0.014	1.059	Medium Sand	Moderately Well Sorted	Symmetrical	Mesokurtic	317.6			207.8	325.3	507.1	2.440	299.3
19	Unimodal, Moderately Well Sorted	361.9	1.624	0.060	0.934	Medium Sand	Moderately Well Sorted	Symmetrical	Mesokurtic	302.5			196.2	353.4	676.4	3.448	480.3
20	Bimodal, Moderately Sorted	321.6	1.780	0.184	0.987	Medium Sand	Moderately Sorted	Coarse Skewed	Mesokurtic	231.0	327.5		164.0	303.7	752.9	4.592	589.0
21	Unimodal, Very Well Sorted	209.7	1.257	-0.096	1.841	Fine Sand	Very Well Sorted	Symmetrical	Very Leptokurtic	215.0			143.4	209.7	258.4	1.802	114.9
22	Unimodal, Well Sorted	232.5	1.342	0.307	1.975	Fine Sand	Well Sorted	Very Coarse Skewed	Very Leptokurtic	215.0			182.3	220.8	351.0	1.925	168.6
23	Unimodal, Well Sorted	253.6	1.385	0.131	1.119	Medium Sand	Well Sorted	Coarse Skewed	Leptokurtic	215.0			183.7	245.5	398.1	2.167	214.4
24	Unimodal, Well Sorted	310.8	1.400	0.049	1.049	Medium Sand	Well Sorted	Symmetrical	Mesokurtic	302.5			200.2	307.8	478.0	2.387	277.7
25	Bimodal, Very Poorly Sorted	109.4	6.044	-0.606	0.512	Very Fine Sand	Very Poorly Sorted	Very Fine Skewed	Very Platykurtic	468.3	7.930		7.114	273.2	669.1	94.05	662.0
26	Trimodal, Very Poorly Sorted	93.26	5.025	-0.544	0.606	Very Fine Sand	Very Poorly Sorted	Very Fine Skewed	Very Platykurtic	317.6	7.930	45.54	8.033	193.4	490.1	61.01	482.1
27	Unimodal, Moderately Well Sorted	387.5	1.560	-0.024	1.019	Medium Sand	Moderately Well Sorted	Symmetrical	Mesokurtic	385.6			216.2	388.5	683.1	3.160	466.9
28	Unimodal, Poorly Sorted	315.0	2.915	-0.132	1.946	Medium Sand	Poorly Sorted	Fine Skewed	Very Leptokurtic	263.0			113.5	290.4	873.8	7.696	760.3
29	Trimodal, Very Poorly Sorted	40.20	4.174	0.021	0.647	Very Coarse Silt	Very Poorly Sorted	Symmetrical	Very Platykurtic	7.930	177.3	45.54	7.022	41.99	251.3	35.79	244.3
30	Polymodal, Very Poorly Sorted	99.48	5.877	-0.332	0.696	Very Fine Sand	Very Poorly Sorted	Very Fine Skewed	Platykurtic	177.3	568.7	7.930	8.044	163.9	744.1	92.50	736.0
31	Bimodal, Very Poorly Sorted	74.79	4.314	-0.655	0.557	Very Fine Sand	Very Poorly Sorted	Very Fine Skewed	Very Platykurtic	263.0	7.930		7.600	164.5	313.4	41.24	305.8
32	Trimodal, Very Poorly Sorted	42.31	5.054	0.074	0.813	Very Coarse Silt	Very Poorly Sorted	Symmetrical	Platykurtic	7.930	146.0	1236.6	6.977	46.71	340.9	48.86	333.9
33	Trimodal, Poorly Sorted	69.00	3.981	-0.616	0.729	Very Fine Sand	Poorly Sorted	Very Fine Skewed	Platykurtic	177.3	7.930	37.50	7.908	137.7	269.8	34.12	261.9
34	Trimodal, Poorly Sorted	44.67	3.377	-0.254	0.910	Very Coarse Silt	Poorly Sorted	Fine Skewed	Mesokurtic	67.16	7.930	1501.6	8.246	59.59	185.4	22.49	177.2
35	Trimodal, Very Poorly Sorted	154.	6.80	-	0.54	Fine Sand	Very Poorly Sorted	Very Fine	Very	690.5	7.930	37.50	7.86	429	101	129.5	1010.5

		4	7	0.646	0			Skewed	Platykurtic				2	.4	8.3		
36	Bimodal, Poorly Sorted	15.27	2.588	0.576	0.867	Medium Silt	Poorly Sorted	Very Coarse Skewed	Platykurtic	7.930	37.50		6.282	10.61	70.18	11.17	63.90
37	Trimodal, Poorly Sorted	22.06	3.423	0.547	0.745	Coarse Silt	Poorly Sorted	Very Coarse Skewed	Platykurtic	7.930	45.54	146.0	6.488	13.42	158.6	24.44	152.1
38	Unimodal, Moderately Sorted	546.1	1.799	-0.263	1.797	Coarse Sand	Moderately Sorted	Fine Skewed	Very Leptokurtic	568.7			294.4	554.0	916.4	3.113	622.1
39	Unimodal, Poorly Sorted	341.5	2.485	-0.470	2.853	Medium Sand	Poorly Sorted	Very Fine Skewed	Very Leptokurtic	385.6			42.94	370.6	607.0	14.14	564.1
41	Unimodal, Poorly Sorted	223.9	3.058	-0.615	2.320	Fine Sand	Poorly Sorted	Very Fine Skewed	Very Leptokurtic	385.6			24.70	317.1	547.0	22.15	522.3
42	Unimodal, Poorly Sorted	581.4	2.653	-0.513	2.985	Coarse Sand	Poorly Sorted	Very Fine Skewed	Very Leptokurtic	690.5			63.33	646.6	1058.1	16.71	994.8
44	Unimodal, Moderately Sorted	673.3	1.939	-0.348	2.477	Coarse Sand	Moderately Sorted	Very Fine Skewed	Very Leptokurtic	690.5			380.2	687.0	1082.6	2.847	702.4
45	Unimodal, Well Sorted	795.6	1.373	-0.115	1.066	Coarse Sand	Well Sorted	Fine Skewed	Mesokurtic	838.6			520.3	810.4	1158.9	2.227	638.6
46	Unimodal, Poorly Sorted	218.9	2.299	-0.408	2.771	Fine Sand	Poorly Sorted	Very Fine Skewed	Very Leptokurtic	263.0			28.24	231.9	391.8	13.87	363.5
47	Unimodal, Very Well Sorted	317.2	1.065	0.000	0.738	Medium Sand	Very Well Sorted	Symmetrical	Platykurtic	317.6			292.2	317.2	344.3	1.178	52.09
48	Trimodal, Very Poorly Sorted	61.40	5.376	-0.017	0.593	Very Coarse Silt	Very Poorly Sorted	Symmetrical	Very Platykurtic	7.930	263.0	37.50	7.442	65.86	514.6	69.15	507.2
49	Polymodal, Very Poorly Sorted	31.60	4.746	0.507	0.674	Very Coarse Silt	Very Poorly Sorted	Very Coarse Skewed	Platykurtic	7.930	37.50	177.3	6.607	17.82	361.1	54.65	354.5
50	Unimodal, Well Sorted	190.8	1.387	0.152	1.128	Fine Sand	Well Sorted	Coarse Skewed	Leptokurtic	215.0			133.6	191.0	318.2	2.381	184.5
51	Unimodal, Well Sorted	283.0	1.402	0.044	1.051	Medium Sand	Well Sorted	Symmetrical	Mesokurtic	263.0			184.2	279.8	440.9	2.394	256.7
52	Unimodal, Well Sorted	204.2	1.353	0.172	1.107	Fine Sand	Well Sorted	Coarse Skewed	Mesokurtic	181.0			146.9	197.2	311.6	2.122	164.8
53	Unimodal, Well Sorted	162.9	1.287	-0.222	1.302	Fine Sand	Well Sorted	Fine Skewed	Leptokurtic	181.0			110.3	168.1	207.6	1.882	97.29
54	Bimodal, Poorly Sorted	52.74	3.334	-0.477	0.883	Very Coarse Silt	Poorly Sorted	Very Fine Skewed	Platykurtic	120.3	7.930		8.391	83.87	187.1	22.30	178.7
55	Bimodal, Poorly Sorted	26.67	3.337	0.185	0.719	Coarse Silt	Poorly Sorted	Coarse Skewed	Platykurtic	7.930	45.54		6.673	23.63	151.5	22.71	144.9
56	Unimodal, Moderately Sorted	206.9	1.629	0.051	1.086	Fine Sand	Moderately Sorted	Symmetrical	Mesokurtic	177.3			113.2	204.0	392.1	3.465	278.9
58	Bimodal, Poorly Sorted	55.71	3.808	-0.445	0.608	Very Coarse Silt	Poorly Sorted	Very Fine Skewed	Very Platykurtic	177.3	7.930		7.739	91.29	234.4	30.29	226.7
59	Unimodal, Moderately Well Sorted	230.0	1.515	0.021	1.056	Fine Sand	Moderately Well Sorted	Symmetrical	Mesokurtic	263.0			137.0	229.3	396.4	2.894	259.4
60	Unimodal, Well Sorted	187.4	1.338	0.065	0.982	Fine Sand	Well Sorted	Symmetrical	Mesokurtic	215.0			133.0	189.6	290.2	2.181	157.1
61	Unimodal, Moderately Well Sorted	292.8	1.567	0.063	1.067	Medium Sand	Moderately Well Sorted	Symmetrical	Mesokurtic	263.0			167.9	287.7	524.2	3.122	356.3
62	Unimodal, Well Sorted	165.4	1.391	-0.147	1.275	Fine Sand	Well Sorted	Fine Skewed	Leptokurtic	177.3			109.7	167.3	236.7	2.158	127.0
63	Polymodal, Very Poorly Sorted	87.82	5.747	-0.298	0.653	Very Fine Sand	Very Poorly Sorted	Fine Skewed	Very Platykurtic	177.3	7.930	568.7	7.736	140.4	687.4	88.85	679.6
65	Unimodal, Well Sorted	155.6	1.369	-0.123	1.199	Fine Sand	Well Sorted	Fine Skewed	Leptokurtic	177.3			102.4	157.4	225.7	2.203	123.2
66	Bimodal, Poorly Sorted	40.37	3.396	-0.259	0.678	Very Coarse Silt	Poorly Sorted	Fine Skewed	Platykurtic	99.03	7.930		7.569	54.43	167.9	22.18	160.3
67	Bimodal, Poorly Sorted	20.17	3.079	0.507	0.704	Coarse Silt	Poorly Sorted	Very Coarse Skewed	Platykurtic	7.930	55.30		6.490	13.38	117.6	18.11	111.1
68	Trimodal, Poorly Sorted	18.12	2.901	0.534	0.799	Coarse Silt	Poorly Sorted	Very Coarse Skewed	Platykurtic	7.930	37.50	146.0	6.438	12.35	105.3	16.36	98.90

69	Bimodal, Poorly Sorted	41.63	3.272	-0.413	0.613	Very Coarse Silt	Poorly Sorted	Very Fine Skewed	Very Platykurtic	99.03	7.930		7.447	63.04	153.1	20.56	145.7
70	Bimodal, Poorly Sorted	87.92	2.473	-0.537	1.861	Very Fine Sand	Poorly Sorted	Very Fine Skewed	Very Leptokurtic	120.3	7.930		11.35	113.1	190.4	16.78	179.1
71	Trimodal, Very Poorly Sorted	86.25	5.288	-0.457	0.619	Very Fine Sand	Very Poorly Sorted	Very Fine Skewed	Very Platykurtic	263.0	7.930	37.50	7.645	168.9	532.0	69.59	524.3
72	Unimodal, Moderately Sorted	452.4	1.626	-0.026	1.003	Medium Sand	Moderately Sorted	Symmetrical	Mesokurtic	468.3			243.0	453.5	839.8	3.456	596.8
73	Unimodal, Well Sorted	192.7	1.284	0.049	1.187	Fine Sand	Well Sorted	Symmetrical	Leptokurtic	181.0			148.6	190.3	264.6	1.781	116.1
74	Unimodal, Very Well Sorted	212.9	1.222	0.006	1.737	Fine Sand	Very Well Sorted	Symmetrical	Very Leptokurtic	215.0			180.8	212.9	257.9	1.426	77.11
75	Unimodal, Moderately Well Sorted	234.4	1.559	0.355	1.305	Fine Sand	Moderately Well Sorted	Very Coarse Skewed	Leptokurtic	231.0			154.1	217.7	469.1	3.044	315.0
76	Unimodal, Moderately Well Sorted	408.6	1.498	-0.047	0.991	Medium Sand	Moderately Well Sorted	Symmetrical	Mesokurtic	468.3			242.8	412.4	684.5	2.819	441.6
77	Unimodal, Moderately Well Sorted	361.5	1.595	-0.011	1.005	Medium Sand	Moderately Well Sorted	Symmetrical	Mesokurtic	302.5			194.6	358.3	653.2	3.357	458.6
78	Bimodal, Poorly Sorted	404.0	2.828	-0.400	2.481	Medium Sand	Poorly Sorted	Very Fine Skewed	Very Leptokurtic	468.3	7.930		26.66	434.3	849.9	31.89	823.3
79	Trimodal, Very Poorly Sorted	80.07	4.736	-0.335	0.839	Very Fine Sand	Very Poorly Sorted	Very Fine Skewed	Platykurtic	263.0	177.3	7.930	8.570	126.2	473.2	55.22	464.7
80	Unimodal, Poorly Sorted	235.4	2.117	-0.434	2.968	Fine Sand	Poorly Sorted	Very Fine Skewed	Very Leptokurtic	263.0			118.7	245.1	376.4	3.172	257.7
81	Unimodal, Very Well Sorted	167.4	1.250	0.195	0.829	Fine Sand	Very Well Sorted	Coarse Skewed	Platykurtic	152.5			128.7	162.6	231.3	1.797	102.6
82	Unimodal, Well Sorted	258.9	1.405	0.016	1.045	Medium Sand	Well Sorted	Symmetrical	Mesokurtic	263.0			168.3	258.1	403.2	2.396	234.9
84	Bimodal, Poorly Sorted	64.73	3.094	-0.484	1.618	Very Fine Sand	Poorly Sorted	Very Fine Skewed	Very Leptokurtic	99.03	7.930		9.672	97.22	203.9	21.08	194.2
85	Unimodal, Well Sorted	119.7	1.316	0.011	0.976	Very Fine Sand	Well Sorted	Symmetrical	Mesokurtic	120.3			83.52	119.4	172.5	2.065	88.96
86	Unimodal, Moderately Sorted	112.8	1.712	-0.364	2.630	Very Fine Sand	Moderately Sorted	Very Fine Skewed	Very Leptokurtic	120.3			72.05	114.9	162.3	2.252	90.22
87	Bimodal, Poorly Sorted	55.26	3.211	-0.516	1.226	Very Coarse Silt	Poorly Sorted	Very Fine Skewed	Leptokurtic	120.3	7.930		8.785	89.33	183.3	20.87	174.6
88	Unimodal, Poorly Sorted	105.3	2.068	-0.352	2.100	Very Fine Sand	Poorly Sorted	Very Fine Skewed	Very Leptokurtic	120.3			21.83	110.7	189.0	8.656	167.1
89	Bimodal, Poorly Sorted	91.20	2.261	-0.428	1.833	Very Fine Sand	Poorly Sorted	Very Fine Skewed	Very Leptokurtic	120.3	7.930		12.39	103.6	184.1	14.86	171.8
90	Unimodal, Well Sorted	98.21	1.379	0.160	0.942	Very Fine Sand	Well Sorted	Coarse Skewed	Mesokurtic	76.50			67.45	96.05	159.5	2.364	92.03
91	Bimodal, Poorly Sorted	48.39	3.436	-0.438	0.670	Very Coarse Silt	Poorly Sorted	Very Fine Skewed	Very Platykurtic	99.03	7.930		7.864	76.58	184.2	23.42	176.4
92	Unimodal, Moderately Sorted	103.5	1.951	-0.399	2.293	Very Fine Sand	Moderately Sorted	Very Fine Skewed	Very Leptokurtic	120.3			26.99	108.6	170.7	6.324	143.7
93	Unimodal, Well Sorted	121.8	1.407	-0.030	1.144	Very Fine Sand	Well Sorted	Symmetrical	Leptokurtic	120.3			77.87	121.3	185.2	2.378	107.3
94	Bimodal, Poorly Sorted	59.61	3.135	-0.710	1.809	Very Coarse Silt	Poorly Sorted	Very Fine Skewed	Very Leptokurtic	120.3	7.930		8.688	112.1	172.6	19.87	164.0
95	Trimodal, Poorly Sorted	20.19	3.353	0.651	0.867	Coarse Silt	Poorly Sorted	Very Coarse Skewed	Platykurtic	7.930	146.0	37.50	6.355	11.02	146.9	23.11	140.5
96	Bimodal, Poorly Sorted	80.99	3.210	-0.616	2.177	Very Fine Sand	Poorly Sorted	Very Fine Skewed	Very Leptokurtic	146.0	7.930		9.417	135.6	238.7	25.35	229.3
98	Unimodal, Moderately Sorted	215.0	1.996	0.391	1.986	Fine Sand	Moderately Sorted	Very Coarse Skewed	Very Leptokurtic	177.3			118.7	196.4	1102.7	9.292	984.1
99	Unimodal, Poorly Sorted	583.0	2.715	-0.513	3.151	Coarse Sand	Poorly Sorted	Very Fine Skewed	Extremely Leptokurtic	690.5			46.55	643.2	1049.9	22.56	1003.3
100	Trimodal, Poorly Sorted	273.	3.13	-	1.56	Medium Sand	Poorly Sorted	Symmetrical	Very	177.3	690.5	7.930	89.8	238	847.	9.435	758.0

		6	4	0.067	4				Leptokurtic				6	.7	8		
102	Bimodal, Moderately Sorted	615.3	1.997	-0.069	1.678	Coarse Sand	Moderately Sorted	Symmetrical	Very Leptokurtic	568.7	1823.5		295.6	605.1	1476.1	4.994	1180.5
103	Bimodal, Poorly Sorted	363.6	3.058	-0.324	1.868	Medium Sand	Poorly Sorted	Very Fine Skewed	Very Leptokurtic	468.3	7.930		90.62	385.5	914.5	10.09	823.9
104	Unimodal, Moderately Sorted	326.2	1.689	0.043	0.944	Medium Sand	Moderately Sorted	Symmetrical	Mesokurtic	263.0			168.2	321.1	650.6	3.869	482.4
105	Unimodal, Moderately Well Sorted	258.5	1.469	0.036	1.012	Medium Sand	Moderately Well Sorted	Symmetrical	Mesokurtic	263.0			161.6	256.7	424.4	2.627	262.9
106	Unimodal, Well Sorted	168.8	1.347	0.139	1.067	Fine Sand	Well Sorted	Coarse Skewed	Mesokurtic	152.5			120.7	163.5	244.0	2.022	123.3
107	Unimodal, Moderately Well Sorted	170.5	1.460	0.240	1.152	Fine Sand	Moderately Well Sorted	Coarse Skewed	Leptokurtic	152.5			107.9	160.9	304.3	2.820	196.4
108	Bimodal, Moderately Well Sorted	190.7	1.433	-0.206	1.803	Fine Sand	Moderately Well Sorted	Fine Skewed	Very Leptokurtic	215.0	107.5		115.2	205.6	306.0	2.657	190.9
109	Unimodal, Well Sorted	162.8	1.379	0.237	1.461	Fine Sand	Well Sorted	Coarse Skewed	Leptokurtic	152.5			111.8	156.1	243.4	2.178	131.7
110	Unimodal, Well Sorted	154.4	1.288	0.060	1.230	Fine Sand	Well Sorted	Symmetrical	Leptokurtic	152.5			108.8	152.0	218.9	2.011	110.0
112	Unimodal, Very Well Sorted	175.7	1.200	-0.077	1.196	Fine Sand	Very Well Sorted	Symmetrical	Leptokurtic	181.0			134.7	175.7	211.7	1.572	76.99
113	Unimodal, Moderately Well Sorted	259.6	1.441	0.038	1.041	Medium Sand	Moderately Well Sorted	Symmetrical	Mesokurtic	263.0			165.5	257.7	416.1	2.515	250.7
114	Unimodal, Well Sorted	180.8	1.356	0.097	0.962	Fine Sand	Well Sorted	Symmetrical	Mesokurtic	152.5			128.5	178.7	277.9	2.162	149.4
115	Unimodal, Moderately Sorted	241.5	1.808	0.304	0.968	Fine Sand	Moderately Sorted	Very Coarse Skewed	Mesokurtic	152.5			130.2	217.2	589.3	4.527	459.2
116	Unimodal, Moderately Well Sorted	168.4	1.460	0.286	1.390	Fine Sand	Moderately Well Sorted	Coarse Skewed	Leptokurtic	152.5			109.4	159.0	297.0	2.714	187.5
117	Unimodal, Moderately Well Sorted	318.1	1.562	0.077	1.048	Medium Sand	Moderately Well Sorted	Symmetrical	Mesokurtic	263.0			182.9	313.3	579.8	3.171	396.9
118	Unimodal, Well Sorted	267.2	1.398	0.038	1.003	Medium Sand	Well Sorted	Symmetrical	Mesokurtic	263.0			172.9	265.0	412.3	2.385	239.4
119	Unimodal, Very Well Sorted	208.5	1.239	-0.190	1.820	Fine Sand	Very Well Sorted	Fine Skewed	Very Leptokurtic	215.0			140.8	208.5	246.9	1.753	106.1
120	Unimodal, Well Sorted	227.8	1.392	0.169	2.002	Fine Sand	Well Sorted	Coarse Skewed	Very Leptokurtic	215.0			144.8	217.4	343.9	2.375	199.0
121	Unimodal, Very Well Sorted	219.8	1.251	0.284	1.829	Fine Sand	Very Well Sorted	Coarse Skewed	Very Leptokurtic	215.0			183.4	217.4	319.4	1.742	136.0
122	Unimodal, Moderately Well Sorted	315.0	1.513	0.087	1.069	Medium Sand	Moderately Well Sorted	Symmetrical	Mesokurtic	263.0			191.2	309.1	549.2	2.873	358.0
123	Unimodal, Moderately Well Sorted	179.6	1.420	0.234	1.163	Fine Sand	Moderately Well Sorted	Coarse Skewed	Leptokurtic	152.5			127.6	174.0	308.8	2.420	181.2
124	Unimodal, Very Well Sorted	213.0	1.273	0.075	2.091	Fine Sand	Very Well Sorted	Symmetrical	Very Leptokurtic	215.0			169.6	213.0	290.8	1.715	121.2
125	Unimodal, Very Well Sorted	190.2	1.261	0.017	1.032	Fine Sand	Very Well Sorted	Symmetrical	Mesokurtic	181.0			140.6	188.6	249.9	1.778	109.3
126	Unimodal, Moderately Well Sorted	222.1	1.588	0.211	1.109	Fine Sand	Moderately Well Sorted	Coarse Skewed	Mesokurtic	215.0			133.9	215.5	453.7	3.388	319.8
127	Unimodal, Well Sorted	258.0	1.398	0.006	1.026	Medium Sand	Well Sorted	Symmetrical	Mesokurtic	263.0			168.2	257.8	399.8	2.378	231.6
128	Unimodal, Well Sorted	200.8	1.391	0.064	0.937	Fine Sand	Well Sorted	Symmetrical	Mesokurtic	215.0			133.0	199.7	320.0	2.406	187.0
128	Unimodal, Moderately Well Sorted	329.5	1.474	0.012	0.995	Medium Sand	Moderately Well Sorted	Symmetrical	Mesokurtic	317.6			200.5	327.5	547.2	2.730	346.8
129	Unimodal, Very Well Sorted	192.3	1.266	0.036	1.000	Fine Sand	Very Well Sorted	Symmetrical	Mesokurtic	181.0			143.2	190.7	260.8	1.821	117.6
131	Unimodal, Moderately Well Sorted	301.9	1.466	0.021	0.992	Medium Sand	Moderately Well Sorted	Symmetrical	Mesokurtic	263.0			184.5	300.4	495.3	2.685	310.8

132	Unimodal, Very Well Sorted	213.8	1.226	-0.002	1.645	Fine Sand	Very Well Sorted	Symmetrical	Very Leptokurtic	215.0			180.0	213.8	280.8	1.560	100.8
133	Unimodal, Well Sorted	185.0	1.353	0.043	1.265	Fine Sand	Well Sorted	Symmetrical	Leptokurtic	181.0			129.0	183.1	275.8	2.137	146.8
134	Unimodal, Well Sorted	237.7	1.409	0.217	1.505	Fine Sand	Well Sorted	Coarse Skewed	Very Leptokurtic	215.0			162.9	224.5	367.8	2.257	204.8
135	Unimodal, Well Sorted	206.3	1.318	0.117	0.955	Fine Sand	Well Sorted	Coarse Skewed	Mesokurtic	181.0			150.8	201.5	300.0	1.989	149.2
136	Unimodal, Well Sorted	285.2	1.385	0.073	0.857	Medium Sand	Well Sorted	Symmetrical	Platykurtic	302.5			189.7	281.9	447.9	2.362	258.3
137	Unimodal, Moderately Well Sorted	308.0	1.541	-0.062	1.161	Medium Sand	Moderately Well Sorted	Symmetrical	Leptokurtic	317.6			174.9	308.9	514.4	2.941	339.5
138	Unimodal, Moderately Well Sorted	198.1	1.452	0.067	0.978	Fine Sand	Moderately Well Sorted	Symmetrical	Mesokurtic	215.0			128.3	194.5	326.8	2.548	198.5
139	Unimodal, Moderately Well Sorted	315.0	1.563	0.043	1.009	Medium Sand	Moderately Well Sorted	Symmetrical	Mesokurtic	263.0			178.4	311.7	569.4	3.192	391.0
140	Unimodal, Moderately Well Sorted	247.1	1.470	0.027	1.026	Fine Sand	Moderately Well Sorted	Symmetrical	Mesokurtic	263.0			151.9	246.6	408.7	2.690	256.7
141	Unimodal, Moderately Well Sorted	444.4	1.546	-0.015	1.208	Medium Sand	Moderately Well Sorted	Symmetrical	Leptokurtic	427.5			259.8	445.9	762.1	2.934	502.3
142	Unimodal, Well Sorted	324.2	1.366	0.044	1.003	Medium Sand	Well Sorted	Symmetrical	Mesokurtic	317.6			214.1	320.2	487.7	2.278	273.6
143	Unimodal, Well Sorted	246.7	1.392	-0.110	1.044	Fine Sand	Well Sorted	Fine Skewed	Mesokurtic	275.0			158.7	254.2	359.8	2.267	201.1
144	Unimodal, Moderately Sorted	469.9	1.650	-0.040	0.951	Medium Sand	Moderately Sorted	Symmetrical	Mesokurtic	468.3			245.0	475.4	885.3	3.614	640.4
146	Bimodal, Poorly Sorted	68.81	3.881	-0.710	0.734	Very Fine Sand	Poorly Sorted	Very Fine Skewed	Platykurtic	177.3	7.930		7.752	150.0	246.4	31.79	238.7
148	Unimodal, Poorly Sorted	206.3	2.036	-0.414	3.097	Fine Sand	Poorly Sorted	Very Fine Skewed	Extremely Leptokurtic	216.8			117.2	212.4	322.1	2.748	204.9
149	Unimodal, Poorly Sorted	220.8	2.016	-0.187	1.851	Fine Sand	Poorly Sorted	Fine Skewed	Very Leptokurtic	263.0			112.3	220.2	426.7	3.801	314.5
150	Unimodal, Very Well Sorted	191.9	1.245	0.055	1.059	Fine Sand	Very Well Sorted	Symmetrical	Mesokurtic	181.0			151.5	190.6	246.9	1.630	95.48
151	Unimodal, Well Sorted	265.6	1.347	0.015	1.013	Medium Sand	Well Sorted	Symmetrical	Mesokurtic	263.0			179.2	264.7	394.8	2.203	215.6
152	Unimodal, Very Well Sorted	154.1	1.244	0.060	1.302	Fine Sand	Very Well Sorted	Symmetrical	Leptokurtic	152.5			120.4	152.6	211.3	1.755	90.87
153	Unimodal, Very Well Sorted	205.5	1.224	-0.207	1.569	Fine Sand	Very Well Sorted	Fine Skewed	Very Leptokurtic	215.0			144.1	207.2	245.7	1.705	101.6
153	Unimodal, Moderately Well Sorted	236.5	1.532	0.118	1.218	Fine Sand	Moderately Well Sorted	Coarse Skewed	Leptokurtic	216.8			143.3	232.0	413.4	2.885	270.1
154	Unimodal, Well Sorted	161.8	1.356	0.193	1.373	Fine Sand	Well Sorted	Coarse Skewed	Leptokurtic	152.5			110.4	155.5	240.5	2.178	130.1
155	Unimodal, Moderately Well Sorted	246.3	1.515	0.059	1.072	Fine Sand	Moderately Well Sorted	Symmetrical	Mesokurtic	263.0			147.0	243.6	421.7	2.868	274.6
156	Unimodal, Well Sorted	216.6	1.304	0.011	0.931	Fine Sand	Well Sorted	Symmetrical	Mesokurtic	231.0			155.9	218.2	303.9	1.949	148.0
157	Unimodal, Moderately Well Sorted	207.8	1.504	0.225	1.021	Fine Sand	Moderately Well Sorted	Coarse Skewed	Mesokurtic	215.0			132.0	199.6	373.4	2.829	241.4
158	Unimodal, Moderately Well Sorted	240.6	1.441	0.317	1.602	Fine Sand	Moderately Well Sorted	Very Coarse Skewed	Very Leptokurtic	215.0			175.3	225.6	404.1	2.305	228.7
159	Unimodal, Very Well Sorted	211.9	1.265	-0.002	1.839	Fine Sand	Very Well Sorted	Symmetrical	Very Leptokurtic	215.0			152.0	211.9	292.5	1.925	140.5
160	Unimodal, Very Well Sorted	220.8	1.266	0.105	1.703	Fine Sand	Very Well Sorted	Coarse Skewed	Very Leptokurtic	215.0			180.4	216.7	312.7	1.733	132.3
161	Unimodal, Moderately Well Sorted	236.0	1.461	0.031	1.014	Fine Sand	Moderately Well Sorted	Symmetrical	Mesokurtic	263.0			145.1	235.0	390.8	2.694	245.7
178	Unimodal, Well Sorted	244.	1.30	0.373	1.03	Fine Sand	Well Sorted	Very Coarse	Mesokurtic	215.0			186.	232	350.	1.878	164.0

		0	6		7			Skewed					7	.1	6		
179	Unimodal, Very Well Sorted	251. 3	1.25 9	- 0.009	0.75 5	Medium Sand	Very Well Sorted	Symmetrical	Platykurtic	215.0			186. 6	251 .2	338. 5	1.814	151.9
181	Unimodal, Very Well Sorted	210. 2	1.24 3	- 0.117	0.86 4	Fine Sand	Very Well Sorted	Fine Skewed	Platykurtic	231.0			156. 7	215 .6	279. 3	1.782	122.6

Sample #	(D75 / D25)	(D75 - D25) (mm):	% Gravel	% Sand	% Mud	% V.C.Gravel	% C.Gravel	% M.Gravel	% F.Gravel	% V.F.Gravel	% V.C.Sand	% C.Sand	% M.Sand	% F.Sand	% V.F.Sand	% V.C.Silt	% C.Silt	% M.Silt	% F.Silt	% V.F.Silt	% Clay
11	1.607	169.1	0.0%	98.2%	1.9%	0.0%	0.0%	0.0%	0.0%	0.0%	0.0%	16.0%	68.0%	14.1%	0.0%	0.0%	0.0%	1.2%	0.6%	0.0%	0.0%
12	1.925	199.2	0.0%	99.6%	0.4%	0.0%	0.0%	0.0%	0.0%	0.0%	0.0%	15.9%	43.8%	37.8%	2.2%	0.1%	0.1%	0.1%	0.1%	0.1%	0.1%
13	1.565	122.2	0.0%	100.0%	0.0%	0.0%	0.0%	0.0%	0.0%	0.0%	0.0%	6.7%	50.2%	42.6%	0.5%	0.0%	0.0%	0.0%	0.0%	0.0%	0.0%
14	1.475	74.10	0.0%	100.0%	0.0%	0.0%	0.0%	0.0%	0.0%	0.0%	0.0%	0.9%	12.1%	84.3%	2.7%	0.0%	0.0%	0.0%	0.0%	0.0%	0.0%
15	1.493	98.02	0.0%	100.0%	0.0%	0.0%	0.0%	0.0%	0.0%	0.0%	0.0%	4.8%	32.0%	60.0%	3.2%	0.0%	0.0%	0.0%	0.0%	0.0%	0.0%
16	1.781	173.2	0.0%	99.8%	0.2%	0.0%	0.0%	0.0%	0.0%	0.0%	0.0%	12.7%	50.5%	35.0%	1.6%	0.0%	0.0%	0.0%	0.0%	0.0%	0.0%
17	1.736	145.0	0.0%	95.4%	4.6%	0.0%	0.0%	0.0%	0.0%	0.0%	0.0%	5.0%	49.7%	39.0%	1.8%	1.2%	0.5%	1.7%	1.1%	0.0%	0.0%
18	1.581	151.0	0.0%	98.3%	1.7%	0.0%	0.0%	0.0%	0.0%	0.0%	0.0%	10.9%	67.9%	19.4%	0.1%	0.7%	0.1%	0.7%	0.2%	0.0%	0.0%
19	1.969	251.7	0.0%	99.8%	0.2%	0.0%	0.0%	0.0%	0.0%	0.0%	0.0%	26.2%	51.9%	20.9%	0.8%	0.0%	0.0%	0.0%	0.0%	0.0%	0.0%
20	2.173	253.7	0.0%	100.0%	0.0%	0.0%	0.0%	0.0%	0.0%	0.0%	4.1%	18.5%	40.6%	34.6%	2.2%	0.0%	0.0%	0.0%	0.0%	0.0%	0.0%
21	1.251	47.11	0.0%	100.0%	0.0%	0.0%	0.0%	0.0%	0.0%	0.0%	0.0%	0.7%	10.1%	82.7%	6.4%	0.0%	0.0%	0.0%	0.0%	0.0%	0.0%
22	1.270	52.86	0.0%	99.8%	0.2%	0.0%	0.0%	0.0%	0.0%	0.0%	0.0%	3.7%	20.2%	72.8%	3.0%	0.0%	0.0%	0.0%	0.0%	0.0%	0.0%
23	1.539	110.5	0.0%	99.6%	0.4%	0.0%	0.0%	0.0%	0.0%	0.0%	0.0%	3.0%	44.5%	48.9%	3.2%	0.1%	0.1%	0.1%	0.1%	0.1%	0.1%
24	1.531	134.8	0.0%	100.0%	0.0%	0.0%	0.0%	0.0%	0.0%	0.0%	0.0%	6.7%	70.2%	21.2%	1.9%	0.0%	0.0%	0.0%	0.0%	0.0%	0.0%
25	47.95	483.4	0.0%	57.3%	42.7%	0.0%	0.0%	0.0%	0.0%	0.0%	1.2%	23.1%	27.5%	3.9%	1.6%	4.9%	3.8%	20.0%	14.0%	0.0%	0.0%
26	20.55	335.1	0.0%	60.5%	39.5%	0.0%	0.0%	0.0%	0.0%	0.0%	0.4%	8.8%	32.7%	13.8%	4.8%	9.1%	6.2%	15.1%	9.2%	0.0%	0.0%
27	1.814	234.3	0.0%	98.4%	1.7%	0.0%	0.0%	0.0%	0.0%	0.0%	1.3%	27.0%	55.5%	14.5%	0.0%	0.0%	0.1%	1.0%	0.5%	0.0%	0.0%
28	2.628	313.6	0.0%	91.1%	8.9%	0.0%	0.0%	0.0%	0.0%	0.0%	6.8%	18.6%	34.6%	28.8%	2.3%	1.5%	1.0%	3.9%	2.5%	0.0%	0.0%
29	14.20	130.2	0.0%	42.2%	57.8%	0.0%	0.0%	0.0%	0.0%	0.0%	1.7%	2.7%	5.7%	17.9%	14.2%	13.1%	7.4%	22.6%	14.7%	0.0%	0.0%
30	18.25	412.3	0.0%	68.5%	31.5%	0.0%	0.0%	0.0%	0.0%	0.0%	3.8%	17.6%	16.4%	20.5%	10.3%	5.0%	3.3%	14.1%	9.2%	0.0%	0.0%
31	19.02	234.1	0.0%	61.9%	38.1%	0.0%	0.0%	0.0%	0.0%	0.0%	0.0%	0.2%	23.9%	34.2%	3.6%	5.8%	5.0%	16.5%	10.9%	0.0%	0.0%
32	14.80	134.7	0.0%	45.1%	54.9%	0.0%	0.0%	0.0%	0.0%	0.0%	8.6%	1.0%	2.8%	16.7%	15.9%	10.9%	6.3%	22.6%	15.1%	0.0%	0.0%
33	8.682	185.5	0.0%	64.5%	35.5%	0.0%	0.0%	0.0%	0.0%	0.0%	0.0%	0.0%	14.1%	39.6%	10.8%	8.2%	4.3%	13.3%	9.6%	0.0%	0.0%
34	5.247	88.26	0.0%	48.0%	52.0%	0.0%	0.0%	0.0%	0.0%	0.0%	3.7%	0.2%	1.8%	14.7%	27.6%	21.8%	7.4%	14.3%	8.5%	0.0%	0.0%
35	50.76	748.5	0.0%	64.0%	36.0%	0.0%	0.0%	0.0%	0.0%	0.0%	10.8%	35.1%	8.8%	4.7%	4.7%	6.4%	4.2%	15.7%	9.8%	0.0%	0.0%
36	4.201	24.66	0.0%	11.6%	88.4%	0.0%	0.0%	0.0%	0.0%	0.0%	0.0%	0.0%	0.2%	4.4%	6.9%	14.1%	9.1%	39.1%	26.1%	0.0%	0.0%

37	7.342	52.54	0.0%	24.6%	75.4%	0.0%	0.0%	0.0%	0.0%	0.0%	0.4%	1.0%	2.2%	10.4%	10.5%	12.7%	8.8%	32.9%	21.1%	0.0%	0.0%
38	1.756	313.6	0.0%	95.9%	4.1%	0.0%	0.0%	0.0%	0.0%	0.0%	6.9%	52.7%	33.1%	1.5%	1.6%	0.9%	0.8%	1.5%	0.9%	0.0%	0.0%
39	1.854	224.2	0.0%	88.1%	11.9%	0.0%	0.0%	0.0%	0.0%	0.0%	1.4%	21.2%	54.9%	8.4%	2.3%	2.9%	1.1%	4.7%	3.2%	0.0%	0.0%
41	2.111	225.7	0.0%	85.1%	14.9%	0.0%	0.0%	0.0%	0.0%	0.0%	1.8%	12.6%	52.4%	14.8%	3.5%	4.2%	1.8%	5.5%	3.4%	0.0%	0.0%
42	1.891	399.3	0.0%	90.0%	10.0%	0.0%	0.0%	0.0%	0.0%	0.0%	13.2%	56.5%	16.1%	2.5%	1.8%	2.0%	1.7%	3.9%	2.3%	0.0%	0.0%
44	1.665	350.4	0.0%	95.0%	5.0%	0.0%	0.0%	0.0%	0.0%	0.0%	15.0%	63.6%	15.1%	0.4%	0.9%	0.6%	0.6%	2.4%	1.5%	0.0%	0.0%
45	1.512	334.0	0.0%	99.0%	1.0%	0.0%	0.0%	0.0%	0.0%	0.0%	23.6%	67.9%	6.8%	0.3%	0.3%	0.0%	0.0%	0.8%	0.2%	0.0%	0.0%
46	1.789	132.4	0.0%	86.5%	13.5%	0.0%	0.0%	0.0%	0.0%	0.0%	3.1%	1.1%	38.4%	42.1%	1.8%	3.0%	2.0%	5.3%	3.2%	0.0%	0.0%
47	1.108	32.53	0.0%	99.9%	0.1%	0.0%	0.0%	0.0%	0.0%	0.0%	0.1%	2.0%	97.4%	0.5%	0.0%	0.0%	0.0%	0.1%	0.0%	0.0%	0.0%
48	27.02	294.9	0.0%	50.5%	49.5%	0.0%	0.0%	0.0%	0.0%	0.0%	2.9%	7.8%	21.7%	13.5%	4.7%	9.9%	7.7%	20.0%	11.9%	0.0%	0.0%
49	15.84	127.9	0.0%	32.6%	67.4%	0.0%	0.0%	0.0%	0.0%	0.0%	0.7%	5.5%	9.0%	10.8%	6.5%	11.1%	7.9%	29.3%	19.2%	0.0%	0.0%
50	1.528	80.81	0.0%	100.0%	0.0%	0.0%	0.0%	0.0%	0.0%	0.0%	0.0%	2.4%	14.5%	80.5%	2.7%	0.0%	0.0%	0.0%	0.0%	0.0%	0.0%
51	1.550	124.7	0.0%	98.7%	1.3%	0.0%	0.0%	0.0%	0.0%	0.0%	0.4%	4.7%	59.7%	33.7%	0.2%	0.0%	0.0%	0.9%	0.4%	0.0%	0.0%
52	1.469	77.73	0.0%	100.0%	0.0%	0.0%	0.0%	0.0%	0.0%	0.0%	0.4%	1.2%	20.5%	73.6%	4.2%	0.0%	0.0%	0.0%	0.0%	0.0%	0.0%
53	1.336	48.23	0.0%	99.5%	0.5%	0.0%	0.0%	0.0%	0.0%	0.0%	0.4%	1.0%	3.2%	81.1%	13.8%	0.1%	0.1%	0.1%	0.1%	0.1%	0.1%
54	5.027	108.9	0.0%	60.7%	39.3%	0.0%	0.0%	0.0%	0.0%	0.0%	0.0%	0.0%	2.5%	27.1%	31.2%	12.7%	5.3%	13.1%	8.2%	0.0%	0.0%
55	7.686	59.13	0.0%	27.0%	73.0%	0.0%	0.0%	0.0%	0.0%	0.0%	0.4%	1.0%	1.9%	9.9%	13.7%	17.8%	10.0%	27.1%	18.1%	0.0%	0.0%
56	1.881	131.8	0.0%	97.0%	3.0%	0.0%	0.0%	0.0%	0.0%	0.0%	0.9%	3.8%	29.2%	51.9%	11.2%	0.3%	0.8%	1.0%	0.9%	0.0%	0.0%
58	12.46	156.1	0.0%	57.1%	42.9%	0.0%	0.0%	0.0%	0.0%	0.0%	1.3%	0.0%	6.6%	31.9%	17.3%	10.4%	5.7%	16.5%	10.3%	0.0%	0.0%
59	1.730	127.0	0.0%	97.8%	2.2%	0.0%	0.0%	0.0%	0.0%	0.0%	0.9%	3.0%	37.7%	51.5%	4.6%	0.4%	0.3%	0.8%	0.8%	0.0%	0.0%
60	1.511	77.95	0.0%	100.0%	0.0%	0.0%	0.0%	0.0%	0.0%	0.0%	0.0%	1.7%	12.9%	82.4%	3.1%	0.0%	0.0%	0.0%	0.0%	0.0%	0.0%
61	1.795	173.4	0.0%	97.8%	2.2%	0.0%	0.0%	0.0%	0.0%	0.0%	1.6%	10.2%	52.2%	32.9%	1.0%	0.6%	0.1%	0.9%	0.6%	0.0%	0.0%
62	1.467	64.04	0.0%	95.4%	4.6%	0.0%	0.0%	0.0%	0.0%	0.0%	0.0%	0.0%	7.2%	75.4%	12.8%	0.5%	1.1%	1.5%	1.6%	0.0%	0.0%
63	22.07	304.7	0.0%	67.2%	32.8%	0.0%	0.0%	0.0%	0.0%	0.0%	3.5%	13.0%	14.2%	23.2%	13.2%	4.3%	2.6%	15.5%	10.3%	0.0%	0.0%
65	1.454	58.95	0.0%	96.2%	3.8%	0.0%	0.0%	0.0%	0.0%	0.0%	0.0%	0.0%	4.5%	73.4%	18.3%	0.0%	0.0%	2.4%	1.4%	0.0%	0.0%
66	8.770	93.62	0.0%	45.7%	54.3%	0.0%	0.0%	0.0%	0.0%	0.0%	2.3%	1.6%	0.7%	14.1%	27.0%	16.7%	7.8%	18.7%	11.1%	0.0%	0.0%
67	7.047	49.77	0.0%	23.1%	76.9%	0.0%	0.0%	0.0%	0.0%	0.0%	0.7%	0.6%	0.6%	7.1%	14.1%	16.1%	7.3%	32.0%	21.4%	0.0%	0.0%
68	5.497	36.38	0.0%	17.3%	82.7%	0.0%	0.0%	0.0%	0.0%	0.0%	0.0%	0.0%	1.1%	7.0%	9.2%	16.1%	9.8%	34.2%	22.5%	0.0%	0.0%
69	9.438	97.12	0.0%	50.3%	49.7%	0.0%	0.0%	0.0%	0.0%	0.0%	0.0%	0.0%	0.6%	17.6%	32.1%	13.4%	5.3%	19.1%	11.8%	0.0%	0.0%
70	2.082	79.07	0.0%	78.7	21.3	0.0%	0.0%	0.0%	0.0%	0.0%	0.0%	0.0%	1.7%	39.8	37.3%	5.8%	3.0	7.5	5.0	0.0%	0.0

				%	%									%			%	%	%		%
71	22.71	298.8	0.0%	62.8%	37.2%	0.0%	0.0%	0.0%	0.0%	0.0%	1.7%	9.6%	23.2%	23.2%	5.1%	7.1%	3.8%	15.7%	10.7%	0.0%	0.0%
72	1.932	303.0	0.0%	97.4%	2.6%	0.0%	0.0%	0.0%	0.0%	0.0%	4.5%	37.5%	46.8%	8.7%	0.0%	0.2%	0.3%	1.3%	0.7%	0.0%	0.0%
73	1.371	60.83	0.0%	99.9%	0.1%	0.0%	0.0%	0.0%	0.0%	0.0%	0.3%	0.8%	11.1%	82.3%	5.4%	0.0%	0.0%	0.0%	0.0%	0.0%	0.0%
74	1.226	43.52	0.0%	100.0%	0.0%	0.0%	0.0%	0.0%	0.0%	0.0%	0.0%	1.1%	9.5%	85.9%	3.4%	0.0%	0.0%	0.0%	0.0%	0.0%	0.0%
75	1.650	114.2	0.0%	100.0%	0.0%	0.0%	0.0%	0.0%	0.0%	0.0%	2.6%	6.2%	24.3%	64.5%	2.4%	0.0%	0.0%	0.0%	0.0%	0.0%	0.0%
76	1.738	229.3	0.0%	98.7%	1.3%	0.0%	0.0%	0.0%	0.0%	0.0%	0.8%	30.5%	57.1%	10.3%	0.0%	0.0%	0.1%	0.8%	0.4%	0.0%	0.0%
77	1.859	228.2	0.0%	100.0%	0.0%	0.0%	0.0%	0.0%	0.0%	0.0%	0.0%	24.0%	56.0%	19.3%	0.6%	0.0%	0.0%	0.0%	0.0%	0.0%	0.0%
78	2.202	339.7	0.0%	88.4%	11.6%	0.0%	0.0%	0.0%	0.0%	0.0%	5.9%	34.1%	39.6%	8.2%	0.6%	1.4%	0.9%	5.8%	3.6%	0.0%	0.0%
79	9.177	239.2	0.0%	63.9%	36.1%	0.0%	0.0%	0.0%	0.0%	0.0%	1.4%	7.5%	18.7%	22.6%	13.7%	10.3%	5.4%	12.7%	7.7%	0.0%	0.0%
80	1.661	122.0	0.0%	91.1%	8.9%	0.0%	0.0%	0.0%	0.0%	0.0%	0.0%	1.2%	46.4%	41.9%	1.6%	2.0%	0.7%	3.5%	2.8%	0.0%	0.0%
81	1.395	55.44	0.0%	100.0%	0.0%	0.0%	0.0%	0.0%	0.0%	0.0%	0.0%	0.2%	2.8%	92.0%	5.0%	0.0%	0.0%	0.0%	0.0%	0.0%	0.0%
82	1.565	116.8	0.0%	99.0%	1.0%	0.0%	0.0%	0.0%	0.0%	0.0%	0.7%	2.3%	51.3%	43.9%	0.9%	0.0%	0.0%	0.5%	0.5%	0.0%	0.0%
84	2.452	85.23	0.0%	73.0%	27.0%	0.0%	0.0%	0.0%	0.0%	0.0%	0.5%	1.3%	3.6%	28.0%	39.7%	9.2%	1.9%	9.9%	6.0%	0.0%	0.0%
85	1.468	46.16	0.0%	99.1%	0.9%	0.0%	0.0%	0.0%	0.0%	0.0%	0.0%	0.0%	0.2%	43.0%	55.9%	0.9%	0.0%	0.0%	0.0%	0.0%	0.0%
86	1.486	45.38	0.0%	92.4%	7.6%	0.0%	0.0%	0.0%	0.0%	0.0%	0.0%	0.0%	0.1%	37.8%	54.6%	1.2%	1.1%	2.8%	2.4%	0.0%	0.0%
87	3.163	91.14	0.0%	66.4%	33.6%	0.0%	0.0%	0.0%	0.0%	0.0%	0.3%	1.0%	1.6%	26.1%	37.5%	11.3%	3.3%	11.7%	7.3%	0.0%	0.0%
88	1.857	67.93	0.0%	84.2%	15.8%	0.0%	0.0%	0.0%	0.0%	0.0%	0.7%	1.6%	1.0%	35.3%	45.6%	4.8%	2.5%	5.5%	3.1%	0.0%	0.0%
89	2.073	73.74	0.0%	78.4%	21.6%	0.0%	0.0%	0.0%	0.0%	0.0%	0.0%	0.0%	1.5%	33.3%	43.6%	7.4%	2.6%	7.3%	4.4%	0.0%	0.0%
90	1.559	43.04	0.0%	97.7%	2.3%	0.0%	0.0%	0.0%	0.0%	0.0%	0.0%	0.2%	1.8%	18.5%	77.3%	0.4%	0.4%	0.4%	0.4%	0.4%	0.4%
91	8.780	112.3	0.0%	57.5%	42.5%	0.0%	0.0%	0.0%	0.0%	0.0%	0.6%	1.2%	2.0%	22.0%	31.8%	11.9%	4.5%	16.3%	9.8%	0.0%	0.0%
92	1.713	57.60	0.0%	85.8%	14.2%	0.0%	0.0%	0.0%	0.0%	0.0%	0.0%	0.0%	0.5%	34.3%	51.0%	4.2%	1.6%	5.2%	3.2%	0.0%	0.0%
93	1.542	52.98	0.0%	95.2%	4.8%	0.0%	0.0%	0.0%	0.0%	0.0%	0.4%	0.4%	0.9%	44.3%	49.1%	1.2%	1.5%	1.5%	0.7%	0.0%	0.0%
94	2.115	75.30	0.0%	76.0%	24.0%	0.0%	0.0%	0.0%	0.0%	0.0%	0.0%	0.0%	0.4%	38.0%	37.6%	1.5%	3.7%	11.2%	7.6%	0.0%	0.0%
95	5.186	32.86	0.0%	20.7%	79.3%	0.0%	0.0%	0.0%	0.0%	0.0%	1.5%	0.0%	0.7%	11.0%	7.5%	7.9%	7.6%	39.1%	24.6%	0.0%	0.0%
96	1.997	91.35	0.0%	81.9%	18.1%	0.0%	0.0%	0.0%	0.0%	0.0%	1.0%	2.4%	5.2%	47.8%	25.4%	0.6%	2.0%	8.9%	6.5%	0.0%	0.0%
98	1.810	122.7	0.0%	96.8%	3.2%	0.0%	0.0%	0.0%	0.0%	0.0%	10.9%	3.5%	16.2%	57.2%	8.9%	0.4%	0.7%	1.0%	1.1%	0.0%	0.0%
99	1.878	393.7	0.0%	89.7%	10.3%	0.0%	0.0%	0.0%	0.0%	0.0%	12.7%	56.8%	16.6%	2.4%	1.2%	1.0%	1.0%	5.0%	3.2%	0.0%	0.0%
100	3.406	367.8	0.0%	90.7%	9.3%	0.0%	0.0%	0.0%	0.0%	0.0%	5.9%	20.2%	21.7%	35.8%	7.1%	0.7%	1.2%	4.4%	3.1%	0.0%	0.0%
102	1.973	423.1	0.0%	96.1%	3.9%	0.0%	0.0%	0.0%	0.0%	0.0%	18.1%	47.3%	27.3%	2.1%	1.3%	0.0%	0.2%	2.3%	1.3%	0.0%	0.0%

103	2.866	410.8	0.0%	90.3%	9.7%	0.0%	0.0%	0.0%	0.0%	0.0%	8.0%	28.9%	33.4%	17.8%	2.3%	1.2%	0.8%	4.6%	3.0%	0.0%	0.0%
104	2.088	245.4	0.0%	99.2%	0.8%	0.0%	0.0%	0.0%	0.0%	0.0%	1.4%	20.1%	46.7%	29.2%	1.8%	0.0%	0.0%	0.4%	0.3%	0.0%	0.0%
105	1.670	133.6	0.0%	99.2%	0.8%	0.0%	0.0%	0.0%	0.0%	0.0%	0.4%	4.4%	48.1%	44.7%	1.6%	0.0%	0.0%	0.4%	0.4%	0.0%	0.0%
106	1.489	67.21	0.0%	100.0%	0.0%	0.0%	0.0%	0.0%	0.0%	0.0%	0.0%	0.0%	7.9%	81.0%	11.1%	0.0%	0.0%	0.0%	0.0%	0.0%	0.0%
107	1.608	80.97	0.0%	100.0%	0.0%	0.0%	0.0%	0.0%	0.0%	0.0%	0.0%	1.6%	14.3%	67.5%	16.6%	0.0%	0.0%	0.0%	0.0%	0.0%	0.0%
108	1.366	63.37	0.0%	99.9%	0.1%	0.0%	0.0%	0.0%	0.0%	0.0%	0.0%	2.6%	12.6%	71.7%	13.0%	0.0%	0.0%	0.0%	0.0%	0.0%	0.0%
109	1.404	53.89	0.0%	99.9%	0.1%	0.0%	0.0%	0.0%	0.0%	0.0%	0.0%	2.7%	5.8%	76.9%	14.5%	0.0%	0.0%	0.0%	0.0%	0.0%	0.0%
110	1.343	44.99	0.0%	100.0%	0.0%	0.0%	0.0%	0.0%	0.0%	0.0%	0.0%	0.0%	2.3%	80.8%	16.9%	0.0%	0.0%	0.0%	0.0%	0.0%	0.0%
112	1.262	40.98	0.0%	100.0%	0.0%	0.0%	0.0%	0.0%	0.0%	0.0%	0.0%	0.0%	2.0%	92.2%	5.9%	0.0%	0.0%	0.0%	0.0%	0.0%	0.0%
113	1.617	125.5	0.0%	98.9%	1.1%	0.0%	0.0%	0.0%	0.0%	0.0%	1.3%	3.1%	49.4%	44.1%	1.1%	0.0%	0.0%	0.7%	0.5%	0.0%	0.0%
114	1.548	79.74	0.0%	100.0%	0.0%	0.0%	0.0%	0.0%	0.0%	0.0%	0.0%	0.2%	13.5%	79.6%	6.6%	0.0%	0.0%	0.0%	0.0%	0.0%	0.0%
115	2.268	197.6	0.0%	100.0%	0.0%	0.0%	0.0%	0.0%	0.0%	0.0%	0.0%	13.5%	26.8%	53.1%	6.6%	0.0%	0.0%	0.0%	0.0%	0.0%	0.0%
116	1.526	70.38	0.0%	99.4%	0.6%	0.0%	0.0%	0.0%	0.0%	0.0%	0.0%	2.8%	10.7%	71.2%	14.7%	0.1%	0.1%	0.1%	0.1%	0.1%	0.1%
117	1.788	187.8	0.0%	99.4%	0.6%	0.0%	0.0%	0.0%	0.0%	0.0%	1.6%	14.2%	54.8%	28.1%	0.6%	0.0%	0.0%	0.4%	0.3%	0.0%	0.0%
118	1.573	121.5	0.0%	99.5%	0.5%	0.0%	0.0%	0.0%	0.0%	0.0%	0.3%	2.8%	54.3%	41.3%	0.7%	0.0%	0.0%	0.3%	0.2%	0.0%	0.0%
119	1.235	44.14	0.0%	100.0%	0.0%	0.0%	0.0%	0.0%	0.0%	0.0%	0.0%	0.1%	7.0%	85.4%	7.5%	0.0%	0.0%	0.0%	0.0%	0.0%	0.0%
120	1.315	59.67	0.0%	100.0%	0.0%	0.0%	0.0%	0.0%	0.0%	0.0%	0.0%	3.0%	21.4%	69.3%	6.3%	0.0%	0.0%	0.0%	0.0%	0.0%	0.0%
121	1.237	46.27	0.0%	100.0%	0.0%	0.0%	0.0%	0.0%	0.0%	0.0%	0.0%	3.7%	13.4%	80.7%	2.2%	0.0%	0.0%	0.0%	0.0%	0.0%	0.0%
122	1.701	169.5	0.0%	99.1%	0.9%	0.0%	0.0%	0.0%	0.0%	0.0%	1.1%	12.5%	57.9%	27.4%	0.2%	0.0%	0.0%	0.6%	0.3%	0.0%	0.0%
123	1.574	82.27	0.0%	100.0%	0.0%	0.0%	0.0%	0.0%	0.0%	0.0%	0.0%	3.0%	12.6%	77.0%	7.3%	0.0%	0.0%	0.0%	0.0%	0.0%	0.0%
124	1.242	46.33	0.0%	99.8%	0.2%	0.0%	0.0%	0.0%	0.0%	0.0%	0.0%	3.5%	9.6%	83.2%	3.5%	0.0%	0.0%	0.0%	0.0%	0.0%	0.0%
125	1.374	60.45	0.0%	99.9%	0.1%	0.0%	0.0%	0.0%	0.0%	0.0%	0.0%	0.0%	9.9%	85.1%	4.9%	0.0%	0.0%	0.0%	0.0%	0.0%	0.0%
126	1.809	133.1	0.0%	99.9%	0.1%	0.0%	0.0%	0.0%	0.0%	0.0%	0.0%	8.0%	26.8%	60.2%	4.9%	0.0%	0.0%	0.0%	0.0%	0.0%	0.0%
127	1.564	116.3	0.0%	99.2%	0.8%	0.0%	0.0%	0.0%	0.0%	0.0%	0.4%	2.1%	51.6%	44.2%	1.0%	0.3%	0.4%	0.0%	0.0%	0.0%	0.0%
128	1.568	89.08	0.0%	100.0%	0.0%	0.0%	0.0%	0.0%	0.0%	0.0%	0.0%	1.2%	21.8%	72.6%	4.4%	0.0%	0.0%	0.0%	0.0%	0.0%	0.0%
128	1.691	175.0	0.0%	99.4%	0.6%	0.0%	0.0%	0.0%	0.0%	0.0%	0.1%	14.2%	61.8%	23.1%	0.1%	0.5%	0.1%	0.0%	0.0%	0.0%	0.0%
129	1.390	63.49	0.0%	100.0%	0.0%	0.0%	0.0%	0.0%	0.0%	0.0%	0.0%	0.1%	12.1%	84.1%	3.7%	0.0%	0.0%	0.0%	0.0%	0.0%	0.0%
131	1.676	158.6	0.0%	99.5%	0.5%	0.0%	0.0%	0.0%	0.0%	0.0%	0.0%	9.5%	59.6%	30.0%	0.5%	0.0%	0.0%	0.3%	0.2%	0.0%	0.0%
132	1.240	46.10	0.0%	100.0%	0.0%	0.0%	0.0%	0.0%	0.0%	0.0%	0.0%	0.9%	12.7%	83.3%	3.0%	0.0%	0.0%	0.0%	0.0%	0.0%	0.0%
134	1.436	84.69	0.0%	99.6	0.4	0.0%	0.0%	0.0%	0.0%	0.0%	0.0%	4.1%	27.4%	63.7	4.5%	0.1%	0.1	0.1	0.1	0.1%	0.1

				%	%									%			%	%	%		%
135	1.468	78.74	0.0%	99.9%	0.1%	0.0%	0.0%	0.0%	0.0%	0.0%	0.0%	0.3%	23.2%	74.7%	1.7%	0.0%	0.0%	0.0%	0.0%	0.0%	0.0%
136	1.605	133.7	0.0%	99.7%	0.3%	0.0%	0.0%	0.0%	0.0%	0.0%	0.0%	2.9%	60.1%	35.7%	1.0%	0.0%	0.0%	0.0%	0.0%	0.0%	0.0%
137	1.697	166.6	0.0%	95.6%	4.4%	0.0%	0.0%	0.0%	0.0%	0.0%	0.2%	11.5%	59.1%	24.6%	0.2%	0.7%	0.2%	2.2%	1.3%	0.0%	0.0%
138	1.657	98.68	0.0%	99.9%	0.1%	0.0%	0.0%	0.0%	0.0%	0.0%	0.0%	1.0%	23.5%	67.9%	7.5%	0.0%	0.0%	0.0%	0.0%	0.0%	0.0%
139	1.819	191.4	0.0%	99.1%	0.9%	0.0%	0.0%	0.0%	0.0%	0.0%	0.7%	14.8%	54.2%	28.7%	0.8%	0.0%	0.0%	0.5%	0.4%	0.0%	0.0%
140	1.671	128.0	0.0%	98.8%	1.2%	0.0%	0.0%	0.0%	0.0%	0.0%	1.4%	2.8%	44.3%	47.8%	2.5%	0.0%	0.0%	0.6%	0.5%	0.0%	0.0%
141	1.674	238.6	0.0%	100.0%	0.0%	0.0%	0.0%	0.0%	0.0%	0.0%	0.0%	37.5%	54.3%	7.7%	0.4%	0.0%	0.0%	0.0%	0.0%	0.0%	0.0%
142	1.533	138.8	0.0%	99.4%	0.6%	0.0%	0.0%	0.0%	0.0%	0.0%	0.0%	8.4%	71.0%	19.9%	0.0%	0.0%	0.0%	0.5%	0.2%	0.0%	0.0%
143	1.540	109.1	0.0%	100.0%	0.0%	0.0%	0.0%	0.0%	0.0%	0.0%	0.0%	2.2%	49.9%	45.4%	2.5%	0.0%	0.0%	0.0%	0.0%	0.0%	0.0%
144	2.017	337.6	0.0%	99.6%	0.4%	0.0%	0.0%	0.0%	0.0%	0.0%	5.9%	40.2%	43.0%	10.4%	0.1%	0.0%	0.0%	0.4%	0.0%	0.0%	0.0%
146	8.092	176.2	0.0%	68.7%	31.3%	0.0%	0.0%	0.0%	0.0%	0.0%	0.0%	0.0%	9.3%	51.1%	8.3%	4.5%	3.6%	13.0%	10.2%	0.0%	0.0%
148	1.595	98.94	0.0%	92.0%	8.0%	0.0%	0.0%	0.0%	0.0%	0.0%	0.5%	0.1%	30.8%	57.4%	3.2%	0.0%	1.1%	4.4%	2.5%	0.0%	0.0%
149	1.936	148.3	0.0%	94.2%	5.8%	0.0%	0.0%	0.0%	0.0%	0.0%	1.2%	5.2%	33.5%	46.7%	7.6%	0.5%	1.1%	2.5%	1.6%	0.0%	0.0%
150	1.345	56.88	0.0%	100.0%	0.0%	0.0%	0.0%	0.0%	0.0%	0.0%	0.2%	0.9%	7.2%	88.4%	3.3%	0.0%	0.0%	0.0%	0.0%	0.0%	0.0%
151	1.497	107.7	0.0%	99.2%	0.8%	0.0%	0.0%	0.0%	0.0%	0.0%	0.0%	1.7%	56.8%	40.3%	0.4%	0.0%	0.0%	0.6%	0.3%	0.0%	0.0%
152	1.293	39.39	0.0%	99.9%	0.1%	0.0%	0.0%	0.0%	0.0%	0.0%	0.0%	0.2%	1.4%	87.1%	11.1%	0.0%	0.0%	0.0%	0.0%	0.0%	0.0%
153	1.237	44.19	0.0%	99.9%	0.1%	0.0%	0.0%	0.0%	0.0%	0.0%	0.0%	1.0%	4.9%	88.5%	5.5%	0.0%	0.0%	0.0%	0.0%	0.0%	0.0%
153	1.680	122.7	0.0%	97.7%	2.3%	0.0%	0.0%	0.0%	0.0%	0.0%	1.6%	4.6%	36.1%	52.2%	3.2%	0.6%	0.4%	0.7%	0.6%	0.0%	0.0%
154	1.394	52.38	0.0%	99.8%	0.2%	0.0%	0.0%	0.0%	0.0%	0.0%	0.0%	1.0%	6.7%	77.0%	15.0%	0.0%	0.0%	0.0%	0.0%	0.0%	0.0%
155	1.718	133.8	0.0%	97.9%	2.1%	0.0%	0.0%	0.0%	0.0%	0.0%	1.5%	4.3%	41.5%	47.9%	2.7%	0.5%	0.2%	0.7%	0.7%	0.0%	0.0%
156	1.453	80.47	0.0%	100.0%	0.0%	0.0%	0.0%	0.0%	0.0%	0.0%	0.0%	0.8%	27.3%	70.7%	1.3%	0.0%	0.0%	0.0%	0.0%	0.0%	0.0%
157	1.712	109.9	0.0%	99.9%	0.1%	0.0%	0.0%	0.0%	0.0%	0.0%	0.0%	4.1%	23.5%	67.6%	4.7%	0.0%	0.0%	0.0%	0.0%	0.0%	0.0%
158	1.449	87.80	0.0%	100.0%	0.0%	0.0%	0.0%	0.0%	0.0%	0.0%	0.0%	6.2%	25.9%	64.6%	3.3%	0.0%	0.0%	0.0%	0.0%	0.0%	0.0%
159	1.259	48.89	0.0%	99.9%	0.1%	0.0%	0.0%	0.0%	0.0%	0.0%	0.0%	2.2%	11.8%	81.1%	4.7%	0.0%	0.0%	0.0%	0.0%	0.0%	0.0%
160	1.257	49.67	0.0%	100.0%	0.0%	0.0%	0.0%	0.0%	0.0%	0.0%	0.0%	1.8%	16.9%	78.0%	3.3%	0.0%	0.0%	0.0%	0.0%	0.0%	0.0%
161	1.672	121.8	0.0%	98.9%	1.1%	0.0%	0.0%	0.0%	0.0%	0.0%	0.9%	2.2%	40.4%	51.9%	3.4%	0.0%	0.0%	0.6%	0.5%	0.0%	0.0%
178	1.428	86.65	0.0%	100.0%	0.0%	0.0%	0.0%	0.0%	0.0%	0.0%	0.0%	3.1%	33.3%	63.5%	0.1%	0.0%	0.0%	0.0%	0.0%	0.0%	0.0%
179	1.451	94.05	0.0%	100.0%	0.0%	0.0%	0.0%	0.0%	0.0%	0.0%	0.0%	1.2%	49.5%	47.2%	2.2%	0.0%	0.0%	0.0%	0.0%	0.0%	0.0%
181	1.376	66.75	0.0%	100.0%	0.0%	0.0%	0.0%	0.0%	0.0%	0.0%	0.0%	0.1%	20.1%	78.2%	1.5%	0.0%	0.0%	0.0%	0.0%	0.0%	0.0%

RESULTS OF TEXTURAL ANALYSIS ON HAUGHTON RIVER ESTUARY SUBSURFACE SAMPLES

Sample #	Sample type	Mean	Sorting	Skewness	Kurtosis	Mean	Sorting:	Skewness	Kutosis	MODE 1	MODE 2	MODE 3	D10	D50	D90	(D90 / D10)
2: 80 cm	Unimodal, Moderately Well Sorted	165.7	1.495	0.011	1.356	Fine Sand	Moderately Well Sorted	Symmetrical	Leptokurtic	181.0			100.5	170.2	284.5	2.832
2: 104 cm	Trimodal, Very Poorly Sorted	82.53	4.580	-0.575	0.632	Very Fine Sand	Very Poorly Sorted	Very Fine Skewed	Very Platykurtic	263.0	7.930	37.50	8.042	172.2	384.5	47.81
2: 128 cm	Unimodal, Well Sorted	181.7	1.306	0.025	1.576	Fine Sand	Well Sorted	Symmetrical	Very Leptokurtic	181.0			128.8	179.7	254.9	1.979
2: 160 cm	Unimodal, Very Well Sorted	226.3	1.238	-0.160	3.049	Fine Sand	Very Well Sorted	Fine Skewed	Extremely Leptokurtic	231.0			147.8	230.2	288.5	1.952
2: 180 cm	Unimodal, Moderately Well Sorted	194.4	1.450	0.115	1.391	Fine Sand	Moderately Well Sorted	Coarse Skewed	Leptokurtic	181.0			125.9	189.2	321.7	2.555
2: 20 cm	Unimodal, Moderately Well Sorted	185.8	1.433	0.023	1.138	Fine Sand	Moderately Well Sorted	Symmetrical	Leptokurtic	181.0			117.1	184.4	295.5	2.524
2: 20 cm	Unimodal, Well Sorted	189.6	1.395	0.060	1.285	Fine Sand	Well Sorted	Symmetrical	Leptokurtic	181.0			127.6	187.0	294.7	2.309
2: 210 cm	Unimodal, Well Sorted	164.2	1.335	-0.101	1.219	Fine Sand	Well Sorted	Fine Skewed	Leptokurtic	181.0			108.8	168.5	234.2	2.153
2: 240 cm	Trimodal, Very Poorly Sorted	28.82	4.581	0.610	0.593	Coarse Silt	Very Poorly Sorted	Very Coarse Skewed	Very Platykurtic	7.930	263.0	30.88	6.446	13.89	306.7	47.58
2: 259 cm	Bimodal, Well Sorted	187.6	1.385	0.043	1.481	Fine Sand	Well Sorted	Symmetrical	Leptokurtic	181.0	275.0		120.3	179.9	278.8	2.317
2: 40 cm	Bimodal, Moderately Well Sorted	276.7	1.485	0.375	1.502	Medium Sand	Moderately Well Sorted	Very Coarse Skewed	Very Leptokurtic	231.0	137.5		155.3	246.1	478.4	3.081
2: 60 cm	Unimodal, Moderately Well Sorted	188.1	1.477	0.240	2.160	Fine Sand	Moderately Well Sorted	Coarse Skewed	Very Leptokurtic	181.0			129.6	184.1	316.3	2.441
2: 95 cm	Bimodal, Well Sorted	163.3	1.353	-0.029	1.239	Fine Sand	Well Sorted	Symmetrical	Leptokurtic	181.0	275.0		107.9	165.8	272.5	2.526
3: 100 cm	Unimodal, Well Sorted	187.4	1.282	0.063	1.223	Fine Sand	Well Sorted	Symmetrical	Leptokurtic	181.0			136.2	184.7	251.6	1.848
3: 120 cm	Unimodal, Well Sorted	188.0	1.382	0.100	1.263	Fine Sand	Well Sorted	Coarse Skewed	Leptokurtic	181.0			129.6	184.4	294.0	2.269
3: 140 cm	Unimodal, Well Sorted	206.8	1.375	0.054	1.101	Fine Sand	Well Sorted	Symmetrical	Mesokurtic	231.0			138.8	203.0	316.7	2.282
3: 159 cm	Unimodal, Moderately Well Sorted	224.6	1.429	0.164	1.131	Fine Sand	Moderately Well Sorted	Coarse Skewed	Leptokurtic	231.0			153.4	220.2	362.1	2.360
3: 20 cm	Unimodal, Well Sorted	225.1	1.349	0.065	0.966	Fine Sand	Well Sorted	Symmetrical	Mesokurtic	231.0			156.9	225.3	337.5	2.151
3: 40 cm	Unimodal, Well Sorted	195.3	1.346	0.279	1.449	Fine Sand	Well Sorted	Coarse Skewed	Leptokurtic	181.0			149.4	189.4	302.6	2.026
3: 60 cm	Unimodal, Moderately Well Sorted	231.6	1.487	0.291	1.132	Fine Sand	Moderately Well Sorted	Coarse Skewed	Leptokurtic	181.0			154.6	218.8	430.2	2.782
3: 80 cm	Unimodal, Well Sorted	196.2	1.334	0.091	1.108	Fine Sand	Well Sorted	Symmetrical	Mesokurtic	181.0			136.6	192.6	288.6	2.113
4: 100 cm	Unimodal, Moderately Well Sorted	217.5	1.530	0.098	1.174	Fine Sand	Moderately Well Sorted	Symmetrical	Leptokurtic	231.0			127.0	209.2	382.4	3.011
4: 100 cm	Unimodal, Moderately Sorted	287.1	1.640	0.125	1.225	Medium Sand	Moderately Sorted	Coarse Skewed	Leptokurtic	327.5			161.6	282.8	575.5	3.561
4: 130	Unimodal, Moderately Well	158.	1.42	-	1.30	Fine Sand	Moderately Well	Fine Skewed	Leptokurtic	181.0			99.8	168.4	248.	2.487

cm	Sorted	9	6	0.117	2		Sorted						6		3	
4: 155 cm	Trimodal, Very Poorly Sorted	58.19	5.010	-0.004	0.638	Very Coarse Silt	Very Poorly Sorted	Symmetrical	Very Platykurtic	263.0	7.930	37.50	7.739	61.65	462.3	59.73
4: 166 cm	Bimodal, Moderately Sorted	313.4	1.808	0.107	0.900	Medium Sand	Moderately Sorted	Coarse Skewed	Mesokurtic	231.0	327.5		156.4	304.2	713.4	4.562
4: 169 cm	Bimodal, Moderately Well Sorted	203.2	1.444	0.330	1.478	Fine Sand	Moderately Well Sorted	Very Coarse Skewed	Leptokurtic	181.0	327.5		139.0	190.6	345.7	2.487
4: 180 cm	Unimodal, Very Well Sorted	185.1	1.265	-0.018	1.314	Fine Sand	Very Well Sorted	Symmetrical	Leptokurtic	181.0			135.4	183.1	242.5	1.791
4: 20 cm	Unimodal, Well Sorted	192.7	1.303	0.209	1.361	Fine Sand	Well Sorted	Coarse Skewed	Leptokurtic	181.0			150.4	188.7	279.9	1.860
4: 200 cm	Unimodal, Well Sorted	198.9	1.295	0.199	1.078	Fine Sand	Well Sorted	Coarse Skewed	Mesokurtic	181.0			151.8	193.6	289.7	1.908
4: 40 cm	Unimodal, Moderately Well Sorted	201.9	1.502	0.185	1.208	Fine Sand	Moderately Well Sorted	Coarse Skewed	Leptokurtic	181.0			127.7	192.2	350.6	2.745
5: 120 cm	Unimodal, Moderately Well Sorted	329.6	1.509	0.015	1.116	Medium Sand	Moderately Well Sorted	Symmetrical	Leptokurtic	327.5			196.8	330.9	562.8	2.860
5: 140 cm	Unimodal, Moderately Sorted	324.2	1.704	0.078	1.080	Medium Sand	Moderately Sorted	Symmetrical	Mesokurtic	327.5			167.4	320.5	663.3	3.962
5: 20 cm	Unimodal, Well Sorted	190.0	1.312	0.074	1.280	Fine Sand	Well Sorted	Symmetrical	Leptokurtic	181.0			135.7	186.9	269.3	1.984
5: 40 cm	Unimodal, Moderately Well Sorted	210.8	1.426	0.213	1.101	Fine Sand	Moderately Well Sorted	Coarse Skewed	Mesokurtic	181.0			140.3	200.3	344.8	2.458
5: 60 cm	Unimodal, Moderately Well Sorted	226.4	1.589	0.262	1.231	Fine Sand	Moderately Well Sorted	Coarse Skewed	Leptokurtic	181.0			139.2	214.1	442.1	3.175
5: 80 cm	Unimodal, Moderately Sorted	268.8	1.703	0.268	1.146	Medium Sand	Moderately Sorted	Coarse Skewed	Leptokurtic	231.0			155.1	251.2	604.8	3.899
6: 40 cm	Unimodal, Moderately Well Sorted	174.1	1.442	0.067	1.392	Fine Sand	Moderately Well Sorted	Symmetrical	Leptokurtic	181.0			109.6	173.9	284.3	2.593
6: 60 cm	Unimodal, Moderately Well Sorted	192.1	1.444	0.129	1.286	Fine Sand	Moderately Well Sorted	Coarse Skewed	Leptokurtic	181.0			126.7	186.9	317.7	2.508
6: 65 cm	Unimodal, Moderately Well Sorted	181.8	1.445	0.076	1.116	Fine Sand	Moderately Well Sorted	Symmetrical	Leptokurtic	181.0			114.2	178.3	299.0	2.619
6: 85 cm	Unimodal, Moderately Well Sorted	199.8	1.532	0.142	1.134	Fine Sand	Moderately Well Sorted	Coarse Skewed	Leptokurtic	181.0			122.6	192.1	350.3	2.857
6: 92 cm	Trimodal, Very Poorly Sorted	52.22	4.654	-0.058	0.644	Very Coarse Silt	Very Poorly Sorted	Symmetrical	Very Platykurtic	7.930	177.3	37.50	7.485	59.93	363.9	48.62
6: 94 cm	Trimodal, Poorly Sorted	34.50	3.853	0.160	0.630	Very Coarse Silt	Poorly Sorted	Coarse Skewed	Very Platykurtic	7.930	177.3	37.50	7.026	29.80	221.6	31.54
6: 120 cm	Unimodal, Well Sorted	161.7	1.298	-0.203	1.160	Fine Sand	Well Sorted	Fine Skewed	Leptokurtic	181.0			107.8	166.7	209.8	1.947

Sample #	(D90 - D10)	(D75 / D25)	(D75 - D25) (mm):	% Gravel	% Sand	% Mud	% V.C.Gravel	% C.Gravel	% M.Gravel	% F.Gravel	% V.F.Gravel	% V.C.Sand	% C.Sand	% M.Sand	% F.Sand	% V.F.Sand	% V.C.Silt	% C.Silt	% M.Silt	% F.Silt	% V.F.Silt	% Clay
2: 80 cm	184.1	1.551	73.17	0.0%	98.4%	1.6%	0.0%	0.0%	0.0%	0.0%	0.0%	0.0%	2.8%	10.1%	66.4%	19.1%	0.3%	0.3%	0.3%	0.3%	0.3%	0.3%
2: 104 cm	376.4	16.04	257.7	0.0%	63.0%	37.0%	0.0%	0.0%	0.0%	0.0%	0.0%	3.0%	1.5%	26.5%	28.3%	3.9%	6.6%	6.1%	15.1%	9.2%	0.0%	0.0%
2: 128 cm	126.1	1.313	49.14	0.0%	99.6%	0.4%	0.0%	0.0%	0.0%	0.0%	0.0%	0.0%	0.0%	10.6%	80.7%	8.3%	0.1%	0.1%	0.1%	0.1%	0.1%	0.1%
2: 160 cm	140.7	1.136	29.40	0.0%	99.9%	0.1%	0.0%	0.0%	0.0%	0.0%	0.0%	0.0%	0.9%	16.9%	80.9%	1.3%	0.0%	0.0%	0.0%	0.0%	0.0%	0.0%
2: 180 cm	195.8	1.500	78.57	0.0%	99.3%	0.7%	0.0%	0.0%	0.0%	0.0%	0.0%	0.8%	2.3%	16.6%	70.7%	9.0%	0.1%	0.1%	0.1%	0.1%	0.1%	0.1%
2: 20 cm	178.4	1.558	83.41	0.0%	99.8%	0.2%	0.0%	0.0%	0.0%	0.0%	0.0%	0.3%	0.8%	17.8%	69.0%	11.9%	0.0%	0.0%	0.0%	0.0%	0.0%	0.0%
2: 20 cm	167.0	1.471	73.65	0.0%	99.6%	0.4%	0.0%	0.0%	0.0%	0.0%	0.0%	0.2%	1.5%	15.6%	73.9%	8.4%	0.1%	0.1%	0.1%	0.1%	0.1%	0.1%
2: 210 cm	125.4	1.427	59.25	0.0%	99.7%	0.3%	0.0%	0.0%	0.0%	0.0%	0.0%	0.2%	0.6%	6.4%	77.1%	15.4%	0.0%	0.0%	0.0%	0.0%	0.0%	0.0%
2: 240 cm	300.3	18.94	147.8	0.0%	29.5%	70.5%	0.0%	0.0%	0.0%	0.0%	0.0%	0.8%	2.5%	11.7%	12.7%	1.8%	8.5%	9.2%	31.4%	21.5%	0.0%	0.0%
2: 259 cm	158.5	1.350	54.14	0.0%	99.4%	0.6%	0.0%	0.0%	0.0%	0.0%	0.0%	0.1%	0.1%	22.4%	66.5%	10.4%	0.1%	0.1%	0.1%	0.1%	0.1%	0.1%
2: 40 cm	323.1	1.524	115.7	0.0%	99.9%	0.1%	0.0%	0.0%	0.0%	0.0%	0.0%	0.5%	8.1%	37.9%	51.0%	2.5%	0.0%	0.0%	0.0%	0.0%	0.0%	0.0%
2: 60 cm	186.7	1.386	60.84	0.0%	99.3%	0.7%	0.0%	0.0%	0.0%	0.0%	0.0%	2.5%	3.5%	8.8%	76.9%	7.6%	0.1%	0.1%	0.1%	0.1%	0.1%	0.1%
2: 95 cm	164.7	1.455	61.83	0.0%	99.2%	0.8%	0.0%	0.0%	0.0%	0.0%	0.0%	0.1%	1.6%	13.2%	68.9%	15.2%	0.1%	0.1%	0.1%	0.1%	0.1%	0.1%
3: 100 cm	115.5	1.354	56.34	0.0%	99.9%	0.1%	0.0%	0.0%	0.0%	0.0%	0.0%	0.8%	0.3%	9.1%	84.1%	5.6%	0.0%	0.0%	0.0%	0.0%	0.0%	0.0%
3: 120 cm	164.5	1.456	70.66	0.0%	99.7%	0.3%	0.0%	0.0%	0.0%	0.0%	0.0%	0.4%	1.8%	14.7%	75.6%	7.2%	0.1%	0.1%	0.1%	0.1%	0.1%	0.1%
3: 140 cm	177.9	1.500	82.72	0.0%	99.9%	0.1%	0.0%	0.0%	0.0%	0.0%	0.0%	0.0%	1.3%	22.7%	70.2%	5.7%	0.0%	0.0%	0.0%	0.0%	0.0%	0.0%
3: 159 cm	208.7	1.574	101.1	0.0%	99.9%	0.1%	0.0%	0.0%	0.0%	0.0%	0.0%	1.0%	3.4%	28.8%	64.2%	2.4%	0.0%	0.0%	0.0%	0.0%	0.0%	0.0%
3: 20 cm	180.6	1.516	93.79	0.0%	100.0%	0.0%	0.0%	0.0%	0.0%	0.0%	0.0%	0.1%	1.8%	32.4%	64.2%	1.4%	0.0%	0.0%	0.0%	0.0%	0.0%	0.0%
3: 40 cm	153.2	1.385	62.93	0.0%	99.9%	0.1%	0.0%	0.0%	0.0%	0.0%	0.0%	0.3%	3.1%	13.1%	80.6%	2.9%	0.0%	0.0%	0.0%	0.0%	0.0%	0.0%
3: 60 cm	275.5	1.638	112.3	0.0%	99.9%	0.1%	0.0%	0.0%	0.0%	0.0%	0.0%	0.3%	6.5%	27.9%	63.4%	1.9%	0.0%	0.0%	0.0%	0.0%	0.0%	0.0%
3: 80 cm	152.0	1.456	73.48	0.0%	99.9%	0.1%	0.0%	0.0%	0.0%	0.0%	0.0%	0.1%	0.8%	17.1%	76.5%	5.4%	0.0%	0.0%	0.0%	0.0%	0.0%	0.0%
4: 100 cm	255.3	1.687	112.4	0.0%	99.4%	0.6%	0.0%	0.0%	0.0%	0.0%	0.0%	0.0%	3.5%	26.9%	60.2%	8.8%	0.1%	0.1%	0.1%	0.1%	0.1%	0.1%
4: 100 cm	413.9	1.778	166.6	0.0%	99.8%	0.2%	0.0%	0.0%	0.0%	0.0%	0.0%	2.5%	10.9%	47.9%	36.3%	2.2%	0.0%	0.0%	0.0%	0.0%	0.0%	0.0%
4: 130 cm	148.5	1.504	66.86	0.0%	98.9%	1.1%	0.0%	0.0%	0.0%	0.0%	0.0%	0.2%	1.4%	8.1%	69.0%	20.2%	0.2%	0.2%	0.2%	0.2%	0.2%	0.2%
4: 155 cm	454.5	20.07	244.2	0.0%	49.8%	50.2%	0.0%	0.0%	0.0%	0.0%	0.0%	2.0%	6.8%	17.2%	16.9%	7.0%	12.8%	9.1%	18.0%	10.3%	0.0%	0.0%
4: 166 cm	557.0	2.370	274.9	0.0%	99.9%	0.1%	0.0%	0.0%	0.0%	0.0%	0.0%	3.3%	19.4%	37.9%	36.1%	3.1%	0.0%	0.0%	0.0%	0.0%	0.0%	0.0%

4: 169 cm	206.7	1.464	75.09	0.0%	99.6%	0.4%	0.0%	0.0%	0.0%	0.0%	0.0%	1.3%	3.5%	16.1%	74.0%	4.9%	0.1%	0.1%	0.1%	0.1%	0.1%	0.1%
4: 180 cm	107.1	1.317	50.51	0.0%	99.9%	0.1%	0.0%	0.0%	0.0%	0.0%	0.0%	0.0%	0.1%	6.8%	86.0%	6.9%	0.0%	0.0%	0.0%	0.0%	0.0%	0.0%
4: 20 cm	129.4	1.355	58.20	0.0%	100.0%	0.0%	0.0%	0.0%	0.0%	0.0%	0.0%	0.1%	2.2%	11.1%	83.2%	3.3%	0.0%	0.0%	0.0%	0.0%	0.0%	0.0%
4: 200 cm	137.8	1.402	66.89	0.0%	99.7%	0.3%	0.0%	0.0%	0.0%	0.0%	0.0%	0.3%	1.0%	16.3%	80.8%	1.3%	0.0%	0.0%	0.0%	0.0%	0.0%	0.0%
4: 40 cm	222.9	1.621	97.38	0.0%	99.9%	0.1%	0.0%	0.0%	0.0%	0.0%	0.0%	0.8%	2.9%	22.2%	65.4%	8.6%	0.0%	0.0%	0.0%	0.0%	0.0%	0.0%
5: 120 cm	366.0	1.705	179.4	0.0%	99.9%	0.1%	0.0%	0.0%	0.0%	0.0%	0.0%	1.7%	11.3%	63.5%	22.4%	0.9%	0.0%	0.0%	0.0%	0.0%	0.0%	0.0%
5: 140 cm	495.9	1.977	223.6	0.0%	99.6%	0.4%	0.0%	0.0%	0.0%	0.0%	0.0%	3.6%	16.4%	49.0%	28.4%	2.3%	0.1%	0.1%	0.1%	0.1%	0.1%	0.1%
5: 20 cm	133.6	1.385	61.66	0.0%	99.7%	0.3%	0.0%	0.0%	0.0%	0.0%	0.0%	0.1%	1.0%	11.7%	80.9%	6.1%	0.0%	0.0%	0.0%	0.0%	0.0%	0.0%
5: 40 cm	204.5	1.574	94.67	0.0%	99.8%	0.2%	0.0%	0.0%	0.0%	0.0%	0.0%	0.9%	2.2%	24.1%	67.6%	5.1%	0.0%	0.0%	0.0%	0.0%	0.0%	0.0%
5: 60 cm	302.9	1.761	128.0	0.0%	99.8%	0.2%	0.0%	0.0%	0.0%	0.0%	0.0%	2.1%	5.9%	27.9%	58.4%	5.4%	0.0%	0.0%	0.0%	0.0%	0.0%	0.0%
5: 80 cm	449.7	1.925	172.6	0.0%	99.9%	0.1%	0.0%	0.0%	0.0%	0.0%	0.0%	3.2%	10.8%	36.4%	46.9%	2.6%	0.0%	0.0%	0.0%	0.0%	0.0%	0.0%
6: 40 cm	174.7	1.490	69.05	0.0%	99.7%	0.3%	0.0%	0.0%	0.0%	0.0%	0.0%	0.4%	2.2%	11.0%	71.4%	14.8%	0.1%	0.1%	0.1%	0.1%	0.1%	0.1%
6: 60 cm	191.0	1.519	80.26	0.0%	99.9%	0.1%	0.0%	0.0%	0.0%	0.0%	0.0%	0.3%	2.1%	17.6%	70.9%	9.0%	0.0%	0.0%	0.0%	0.0%	0.0%	0.0%
6: 65 cm	184.8	1.592	84.22	0.0%	99.8%	0.2%	0.0%	0.0%	0.0%	0.0%	0.0%	0.0%	1.0%	16.9%	68.9%	12.9%	0.0%	0.0%	0.0%	0.0%	0.0%	0.0%
6: 85 cm	227.7	1.697	106.4	0.0%	99.8%	0.2%	0.0%	0.0%	0.0%	0.0%	0.0%	0.9%	2.8%	23.2%	62.5%	10.4%	0.0%	0.0%	0.0%	0.0%	0.0%	0.0%
6: 92 cm	356.5	17.40	187.7	0.0%	49.4%	50.6%	0.0%	0.0%	0.0%	0.0%	0.0%	1.1%	5.0%	12.1%	20.2%	11.0%	10.9%	8.0%	20.1%	11.6%	0.0%	0.0%
6: 94 cm	214.6	12.09	107.1	0.0%	35.3%	64.7%	0.0%	0.0%	0.0%	0.0%	0.0%	0.3%	1.0%	6.2%	16.2%	11.7%	13.8%	10.3%	25.6%	14.9%	0.0%	0.0%
6: 120 cm	102.1	1.386	53.59	0.0%	99.4%	0.6%	0.0%	0.0%	0.0%	0.0%	0.0%	0.2%	0.6%	3.0%	80.2%	15.4%	0.1%	0.1%	0.1%	0.1%	0.1%	0.1%

RESULTS OF TEXTURAL ANALYSIS ON ELLIOT RIVER ESTUARY SURFICIAL SAMPLES

2	Unimodal, Moderately Sorted	965.0	1.699	-0.225	0.517	Coarse Sand	Moderately Sorted	Fine Skewed	Very Platykurtic	605.0			414.1	924.1	2319.9	5.603
3	Unimodal, Moderately Well Sorted	1061.7	1.517	-1.759	0.885	Very Coarse Sand	Moderately Well Sorted	Very Fine Skewed	Platykurtic	1700.0			393.0	1774.5	7577.7	19.28
4	Bimodal, Moderately Sorted	996.1	1.849	-0.355	0.870	Coarse Sand	Moderately Sorted	Very Fine Skewed	Platykurtic	855.0	200.0		305.2	984.7	2310.2	7.571
5	Bimodal, Moderately Sorted	778.7	1.795	0.354	0.420	Coarse Sand	Moderately Sorted	Very Coarse Skewed	Very Platykurtic	427.5	1200.0		381.0	595.4	2404.2	6.310
7	Unimodal, Moderately Sorted	858.3	1.746	-0.127	0.653	Coarse Sand	Moderately Sorted	Fine Skewed	Very Platykurtic	855.0			384.6	832.7	2057.2	5.350
10	Unimodal, Moderately Sorted	923.0	1.644	-0.231	0.463	Coarse Sand	Moderately Sorted	Fine Skewed	Very Platykurtic	605.0			417.9	899.0	2461.4	5.890
11	Unimodal, Very Well Sorted	1227.0	1.220	-1.718	0.468	Very Coarse Sand	Very Well Sorted	Very Fine Skewed	Very Platykurtic	1200.0			766.4	1505.7	2975.5	3.883
12	Unimodal, Moderately Well Sorted	957.9	1.504	-0.004	0.978	Coarse Sand	Moderately Well Sorted	Symmetrical	Mesokurtic	855.0			560.2	967.8	1732.6	3.093
13	Unimodal, Moderately Sorted	1058.8	1.647	-0.533	0.569	Very Coarse Sand	Moderately Sorted	Very Fine Skewed	Very Platykurtic	1200.0			441.7	1139.6	2354.3	5.330
14	Unimodal, Moderately Well Sorted	1248.9	1.416	-0.581	0.489	Very Coarse Sand	Moderately Well Sorted	Very Fine Skewed	Very Platykurtic	1200.0			692.8	1276.7	2197.2	3.172
15	Unimodal, Very Well Sorted	1317.2	1.145	-1.926	0.300	Very Coarse Sand	Very Well Sorted	Very Fine Skewed	Very Platykurtic	1200.0			941.6	1499.7	2507.5	2.663
16	Unimodal, Moderately Well Sorted	664.1	1.502	-0.039	0.917	Coarse Sand	Moderately Well Sorted	Symmetrical	Mesokurtic	855.0			388.1	679.5	1154.8	2.976
17	Unimodal, Very Well Sorted	1395.6	1.094	-5.799	1.814	Very Coarse Sand	Very Well Sorted	Very Fine Skewed	Very Leptokurtic	1700.0			1005.5	1905.1	3563.7	3.544
18	Bimodal, Poorly Sorted	610.4	2.217	-0.284	0.889	Coarse Sand	Poorly Sorted	Fine Skewed	Platykurtic	855.0	200.0		189.7	729.8	1518.9	8.009
19	Bimodal, Moderately Sorted	698.6	1.996	0.112	0.500	Coarse Sand	Moderately Sorted	Coarse Skewed	Very Platykurtic	427.5	1200.0		279.1	595.4	2204.3	7.899
20	Bimodal, Poorly Sorted	523.5	2.248	-0.104	0.788	Coarse Sand	Poorly Sorted	Fine Skewed	Platykurtic	855.0	200.0		179.4	574.2	1472.2	8.207
21	Bimodal, Poorly Sorted	690.0	2.129	-0.340	0.862	Coarse Sand	Poorly Sorted	Very Fine Skewed	Platykurtic	855.0	200.0		210.1	799.3	1892.7	9.008
22	Bimodal, Moderately Well Sorted	1157.3	1.431	-1.158	0.704	Very Coarse Sand	Moderately Well Sorted	Very Fine Skewed	Platykurtic	1700.0	302.5		533.1	1436.7	3222.5	6.045
23	Bimodal, Poorly Sorted	663.7	2.170	-0.159	0.997	Coarse Sand	Poorly Sorted	Fine Skewed	Mesokurtic	855.0	1700.0		222.4	723.2	1719.9	7.735
24	Unimodal, Moderately Well Sorted	1154.7	1.440	-0.804	0.576	Very Coarse Sand	Moderately Well Sorted	Very Fine Skewed	Very Platykurtic	1200.0			583.5	1288.8	2594.0	4.446
25	Unimodal, Moderately Well Sorted	1016.0	1.607	-0.190	0.746	Very Coarse Sand	Moderately Well Sorted	Fine Skewed	Platykurtic	855.0			514.0	968.5	2079.7	4.046
26	Unimodal, Moderately Well Sorted	1203.8	1.415	-0.331	0.687	Very Coarse Sand	Moderately Well Sorted	Very Fine Skewed	Platykurtic	1200.0			721.9	1194.3	2023.2	2.803
27	Unimodal, Moderately Sorted	911.9	1.802	-0.341	0.585	Coarse Sand	Moderately Sorted	Very Fine Skewed	Very Platykurtic	855.0			363.2	926.9	2420.7	6.664
28	Unimodal, Moderately Sorted	735.4	1.751	-0.034	1.079	Coarse Sand	Moderately Sorted	Symmetrical	Mesokurtic	855.0			350.9	739.7	1473.3	4.199
29	Unimodal, Well Sorted	1242.5	1.387	-0.429	0.453	Very Coarse Sand	Well Sorted	Very Fine Skewed	Very Platykurtic	1200.0			738.5	1211.5	2181.6	2.954
31	Trimodal, Poorly Sorted	396.1	2.536	0.346	0.607	Medium Sand	Poorly Sorted	Very Coarse Skewed	Very Platykurtic	200.0	1200.0	605.0	137.3	300.2	1768.5	12.89
36	Bimodal, Poorly Sorted	281.8	2.273	0.484	1.209	Medium Sand	Poorly Sorted	Very Coarse Skewed	Leptokurtic	200.0	855.0		125.8	211.4	1034.9	8.229
37	Unimodal, Moderately Sorted	446.	1.80	0.077	1.56	Medium Sand	Moderately Sorted	Symmetrical	Very	427.5			226.	441.	975.	4.319

		1	5		6				Leptokurtic				0	7	8	
40	Unimodal, Moderately Well Sorted	812.1	1.619	0.087	1.058	Coarse Sand	Moderately Well Sorted	Symmetrical	Mesokurtic	855.0			445.2	795.9	1568.7	3.523
41	Unimodal, Moderately Well Sorted	878.0	1.582	-0.016	0.813	Coarse Sand	Moderately Well Sorted	Symmetrical	Platykurtic	855.0			479.0	844.2	1889.5	3.945
42	Unimodal, Moderately Sorted	661.0	1.834	0.058	0.974	Coarse Sand	Moderately Sorted	Symmetrical	Mesokurtic	605.0			287.2	597.0	2106.4	7.335
43	Unimodal, Moderately Sorted	695.4	1.697	0.037	1.110	Coarse Sand	Moderately Sorted	Symmetrical	Mesokurtic	605.0			361.4	680.3	1498.7	4.147
44	Unimodal, Moderately Sorted	643.6	1.966	-0.139	1.153	Coarse Sand	Moderately Sorted	Fine Skewed	Leptokurtic	605.0			253.9	662.9	1399.8	5.512
45	Unimodal, Moderately Sorted	786.4	1.896	0.041	0.625	Coarse Sand	Moderately Sorted	Symmetrical	Very Platykurtic	605.0			322.7	675.2	2251.7	6.977
46	Unimodal, Moderately Sorted	671.2	1.855	0.027	1.050	Coarse Sand	Moderately Sorted	Symmetrical	Mesokurtic	605.0			299.7	669.1	1511.8	5.045
47	Bimodal, Moderately Sorted	830.0	1.704	-0.575	0.525	Coarse Sand	Moderately Sorted	Very Fine Skewed	Very Platykurtic	855.0	302.5		319.1	961.4	3774.9	11.83
48	Unimodal, Very Well Sorted	1225.6	1.266	-2.733	0.835	Very Coarse Sand	Very Well Sorted	Very Fine Skewed	Platykurtic	855.0			617.9	1953.1	6921.7	11.20
49	Bimodal, Moderately Sorted	606.2	1.981	-0.260	1.313	Coarse Sand	Moderately Sorted	Fine Skewed	Leptokurtic	855.0	137.5		193.6	652.8	1260.5	6.510
52	Unimodal, Moderately Sorted	617.2	1.911	0.042	1.010	Coarse Sand	Moderately Sorted	Symmetrical	Mesokurtic	605.0			276.0	606.3	1427.1	5.172
53	Unimodal, Poorly Sorted	362.5	2.138	0.155	0.941	Medium Sand	Poorly Sorted	Coarse Skewed	Mesokurtic	302.5			151.8	336.1	1052.6	6.934
69	Unimodal, Moderately Sorted	1044.3	1.739	-0.360	0.812	Very Coarse Sand	Moderately Sorted	Very Fine Skewed	Platykurtic	855.0			433.6	1030.2	2263.2	5.219
70	Unimodal, Moderately Well Sorted	582.0	1.565	-0.282	1.049	Coarse Sand	Moderately Well Sorted	Fine Skewed	Mesokurtic	605.0			290.0	617.0	938.8	3.238
71	Bimodal, Moderately Sorted	939.4	1.855	-0.366	1.432	Coarse Sand	Moderately Sorted	Very Fine Skewed	Leptokurtic	1200.0	200.0		238.0	995.0	1892.7	7.952
73	Bimodal, Poorly Sorted	570.7	2.215	-0.341	0.909	Coarse Sand	Poorly Sorted	Very Fine Skewed	Mesokurtic	855.0	200.0		179.4	720.3	1359.5	7.578
76	Trimodal, Moderately Sorted	897.7	1.932	-0.178	0.819	Coarse Sand	Moderately Sorted	Fine Skewed	Platykurtic	605.0	1700.0	200.0	258.4	815.3	2303.8	8.916
77	Unimodal, Moderately Sorted	622.6	1.865	-0.265	1.027	Coarse Sand	Moderately Sorted	Fine Skewed	Mesokurtic	855.0			253.2	693.3	1267.4	5.006
78	Unimodal, Well Sorted	409.1	1.411	-0.013	0.973	Medium Sand	Well Sorted	Symmetrical	Mesokurtic	427.5			264.3	409.4	644.1	2.437
79	Unimodal, Moderately Sorted	487.1	1.633	0.249	1.367	Medium Sand	Moderately Sorted	Coarse Skewed	Leptokurtic	427.5			278.0	451.0	992.5	3.570
80	Unimodal, Moderately Sorted	273.5	1.852	0.526	1.291	Medium Sand	Moderately Sorted	Very Coarse Skewed	Leptokurtic	200.0			156.1	226.0	797.8	5.112
81	Unimodal, Moderately Well Sorted	371.1	1.562	-0.117	0.935	Medium Sand	Moderately Well Sorted	Fine Skewed	Mesokurtic	427.5			194.0	380.4	640.0	3.298
82	Unimodal, Well Sorted	371.2	1.398	-0.094	1.105	Medium Sand	Well Sorted	Symmetrical	Mesokurtic	427.5			253.1	380.0	580.4	2.293
84	Unimodal, Moderately Well Sorted	635.0	1.615	-0.091	1.140	Coarse Sand	Moderately Well Sorted	Symmetrical	Leptokurtic	605.0			330.0	652.6	1182.0	3.581
85	Unimodal, Moderately Well Sorted	379.3	1.512	0.082	1.312	Medium Sand	Moderately Well Sorted	Symmetrical	Leptokurtic	427.5			247.9	375.7	666.5	2.689
93	Unimodal, Moderately Sorted	356.3	1.722	0.120	0.936	Medium Sand	Moderately Sorted	Coarse Skewed	Mesokurtic	302.5			180.6	341.3	742.0	4.109
95	Unimodal, Moderately Well Sorted	446.8	1.609	-0.248	0.992	Medium Sand	Moderately Well Sorted	Fine Skewed	Mesokurtic	605.0			223.5	484.8	765.4	3.425
96	Unimodal, Well Sorted	426.4	1.376	-0.016	1.086	Medium Sand	Well Sorted	Symmetrical	Mesokurtic	427.5			275.9	426.5	647.6	2.348
97	Unimodal, Well Sorted	269.1	1.353	-0.177	1.143	Medium Sand	Well Sorted	Fine Skewed	Leptokurtic	302.5			176.5	283.4	397.1	2.250

98	Unimodal, Well Sorted	306.8	1.351	-0.014	1.417	Medium Sand	Well Sorted	Symmetrical	Leptokurtic	302.5			196.5	303.3	451.8	2.299
103	Unimodal, Moderately Sorted	314.5	1.905	0.242	0.846	Medium Sand	Moderately Sorted	Coarse Skewed	Platykurtic	200.0			153.4	284.0	813.3	5.300

Sample #	(D90 - D10)	(D75 / D25)	(D75 - D25) (mm):	% Gravel	% Sand	% Mud	% V.C.Gravel	% C.Gravel	% M.Gravel	% F.Gravel	% V.F.Gravel	% V.C.Sand	% C.Sand	% M.Sand	% F.Sand	% V.F.Sand	% V.C.Silt	% C.Silt	% M.Silt	% F.Silt	% V.F.Silt	% Clay
2	1905.9	2.716	1010.6	0.0%	99.9%	0.1%	0.0%	0.0%	0.0%	0.0%	0.0%	45.6%	38.4%	14.2%	1.4%	0.2%	0.0%	0.0%	0.0%	0.0%	0.0%	0.0%
3	7184.7	1.826	660.9	0.0%	99.9%	0.1%	0.0%	0.0%	0.0%	0.0%	0.0%	69.4%	15.7%	12.4%	2.3%	0.1%	0.0%	0.0%	0.0%	0.0%	0.0%	0.0%
4	2005.1	2.371	905.9	0.0%	100.0%	0.0%	0.0%	0.0%	0.0%	0.0%	0.0%	48.9%	35.8%	7.1%	8.0%	0.2%	0.0%	0.0%	0.0%	0.0%	0.0%	0.0%
5	2023.2	3.320	1005.4	0.0%	100.0%	0.0%	0.0%	0.0%	0.0%	0.0%	0.0%	35.6%	22.8%	41.6%	0.1%	0.0%	0.0%	0.0%	0.0%	0.0%	0.0%	0.0%
7	1672.7	2.466	786.0	0.0%	100.0%	0.0%	0.0%	0.0%	0.0%	0.0%	0.0%	38.5%	40.2%	20.3%	1.0%	0.0%	0.0%	0.0%	0.0%	0.0%	0.0%	0.0%
10	2043.5	2.873	1086.6	0.0%	99.9%	0.1%	0.0%	0.0%	0.0%	0.0%	0.0%	44.1%	39.7%	15.3%	0.8%	0.1%	0.0%	0.0%	0.0%	0.0%	0.0%	0.0%
11	2209.1	1.612	640.9	0.0%	100.0%	0.0%	0.0%	0.0%	0.0%	0.0%	0.0%	78.2%	20.9%	0.8%	0.0%	0.0%	0.0%	0.0%	0.0%	0.0%	0.0%	0.0%
12	1172.4	1.744	546.0	0.0%	100.0%	0.0%	0.0%	0.0%	0.0%	0.0%	0.0%	47.0%	48.7%	4.0%	0.1%	0.0%	0.0%	0.0%	0.0%	0.0%	0.0%	0.0%
13	1912.6	2.456	1035.8	0.0%	100.0%	0.0%	0.0%	0.0%	0.0%	0.0%	0.0%	57.9%	29.3%	11.6%	1.1%	0.1%	0.0%	0.0%	0.0%	0.0%	0.0%	0.0%
14	1504.4	1.935	860.4	0.0%	100.0%	0.0%	0.0%	0.0%	0.0%	0.0%	0.0%	70.3%	27.3%	2.2%	0.0%	0.0%	0.0%	0.0%	0.0%	0.0%	0.0%	0.0%
15	1566.0	1.584	667.5	0.0%	100.0%	0.0%	0.0%	0.0%	0.0%	0.0%	0.0%	88.1%	11.8%	0.1%	0.1%	0.0%	0.0%	0.0%	0.0%	0.0%	0.0%	0.0%
16	766.7	1.789	398.0	0.0%	100.0%	0.0%	0.0%	0.0%	0.0%	0.0%	0.0%	15.9%	59.9%	23.7%	0.5%	0.0%	0.0%	0.0%	0.0%	0.0%	0.0%	0.0%
17	2558.2	1.092	122.8	0.0%	100.0%	0.0%	0.0%	0.0%	0.0%	0.0%	0.0%	90.3%	7.6%	2.1%	0.0%	0.0%	0.0%	0.0%	0.0%	0.0%	0.0%	0.0%
18	1329.2	3.127	738.6	0.0%	99.8%	0.2%	0.0%	0.0%	0.0%	0.0%	0.0%	29.2%	36.7%	17.2%	15.5%	1.3%	0.0%	0.0%	0.0%	0.0%	0.0%	0.0%
19	1925.2	3.776	1010.6	0.0%	100.0%	0.0%	0.0%	0.0%	0.0%	0.0%	0.0%	36.2%	19.6%	40.3%	3.7%	0.1%	0.0%	0.0%	0.0%	0.0%	0.0%	0.0%
20	1292.8	3.588	680.4	0.0%	99.9%	0.1%	0.0%	0.0%	0.0%	0.0%	0.0%	21.7%	34.2%	20.8%	22.6%	0.6%	0.0%	0.0%	0.0%	0.0%	0.0%	0.0%
21	1682.6	2.812	778.4	0.0%	100.0%	0.0%	0.0%	0.0%	0.0%	0.0%	0.0%	34.1%	38.0%	13.7%	13.5%	0.6%	0.0%	0.0%	0.0%	0.0%	0.0%	0.0%
22	2689.5	2.005	925.2	0.0%	100.0%	0.0%	0.0%	0.0%	0.0%	0.0%	0.0%	71.8%	19.3%	8.2%	0.5%	0.2%	0.0%	0.0%	0.0%	0.0%	0.0%	0.0%
23	1497.5	2.703	653.5	0.0%	99.9%	0.1%	0.0%	0.0%	0.0%	0.0%	0.0%	26.0%	41.3%	20.1%	12.2%	0.4%	0.0%	0.0%	0.0%	0.0%	0.0%	0.0%
24	2010.5	2.212	1061.3	0.0%	100.0%	0.0%	0.0%	0.0%	0.0%	0.0%	0.0%	67.9%	25.1%	4.3%	2.6%	0.0%	0.0%	0.0%	0.0%	0.0%	0.0%	0.0%
25	1565.7	2.022	739.3	0.0%	100.0%	0.0%	0.0%	0.0%	0.0%	0.0%	0.0%	47.3%	43.9%	7.3%	1.4%	0.2%	0.0%	0.0%	0.0%	0.0%	0.0%	0.0%
26	1301.3	1.721	662.4	0.0%	100.0%	0.0%	0.0%	0.0%	0.0%	0.0%	0.0%	69.8%	26.9%	3.3%	0.1%	0.0%	0.0%	0.0%	0.0%	0.0%	0.0%	0.0%
27	2057.4	2.909	1072.0	0.0%	100.0%	0.0%	0.0%	0.0%	0.0%	0.0%	0.0%	45.9%	34.3%	15.6%	3.7%	0.5%	0.0%	0.0%	0.0%	0.0%	0.0%	0.0%
28	1122.5	2.036	542.3	0.0%	99.8%	0.2%	0.0%	0.0%	0.0%	0.0%	0.0%	28.2%	50.1%	18.8%	2.5%	0.2%	0.0%	0.0%	0.0%	0.0%	0.0%	0.0%
29	1443.1	1.860	788.7	0.0%	100.0%	0.0%	0.0%	0.0%	0.0%	0.0%	0.0%	69.0%	29.7%	1.1%	0.1%	0.0%	0.0%	0.0%	0.0%	0.0%	0.0%	0.0%
31	1631.3	5.609	821.3	0.0%	100.0%	0.0%	0.0%	0.0%	0.0%	0.0%	0.0%	25.0%	15.4%	14.3%	40.2%	5.0%	0.0%	0.0%	0.0%	0.0%	0.0%	0.0%

36	909.1	2.419	223.5	0.0%	99.9%	0.1%	0.0%	0.0%	0.0%	0.0%	0.0%	10.6%	10.4%	14.8%	54.6%	9.6%	0.0%	0.0%	0.0%	0.0%	0.0%	0.0%
37	749.9	1.825	277.8	0.0%	100.0%	0.0%	0.0%	0.0%	0.0%	0.0%	0.0%	9.5%	27.7%	51.3%	9.8%	1.7%	0.0%	0.0%	0.0%	0.0%	0.0%	0.0%
40	1123.4	1.891	517.5	0.0%	100.0%	0.0%	0.0%	0.0%	0.0%	0.0%	0.0%	29.9%	56.3%	13.3%	0.5%	0.0%	0.0%	0.0%	0.0%	0.0%	0.0%	0.0%
41	1410.5	1.971	597.4	0.0%	100.0%	0.0%	0.0%	0.0%	0.0%	0.0%	0.0%	35.0%	54.0%	10.7%	0.4%	0.0%	0.0%	0.0%	0.0%	0.0%	0.0%	0.0%
42	1819.3	2.147	482.4	0.0%	100.0%	0.0%	0.0%	0.0%	0.0%	0.0%	0.0%	20.7%	44.6%	28.3%	5.8%	0.6%	0.0%	0.0%	0.0%	0.0%	0.0%	0.0%
43	1137.3	1.902	454.3	0.0%	100.0%	0.0%	0.0%	0.0%	0.0%	0.0%	0.0%	21.9%	53.7%	22.2%	2.0%	0.2%	0.0%	0.0%	0.0%	0.0%	0.0%	0.0%
44	1145.8	2.298	551.9	0.0%	99.9%	0.1%	0.0%	0.0%	0.0%	0.0%	0.0%	23.5%	44.7%	22.2%	7.1%	2.5%	0.0%	0.0%	0.0%	0.0%	0.0%	0.0%
45	1928.9	2.795	802.3	0.0%	100.0%	0.0%	0.0%	0.0%	0.0%	0.0%	0.0%	31.0%	37.9%	27.4%	3.4%	0.3%	0.0%	0.0%	0.0%	0.0%	0.0%	0.0%
46	1212.1	2.233	543.6	0.0%	100.0%	0.0%	0.0%	0.0%	0.0%	0.0%	0.0%	24.0%	45.1%	26.0%	4.3%	0.6%	0.0%	0.0%	0.0%	0.0%	0.0%	0.0%
47	3455.9	3.156	1198.2	0.0%	99.7%	0.3%	0.0%	0.0%	0.0%	0.0%	0.0%	48.2%	31.6%	15.8%	2.1%	1.9%	0.0%	0.0%	0.0%	0.0%	0.0%	0.0%
48	6303.8	1.448	432.3	0.0%	99.8%	0.2%	0.0%	0.0%	0.0%	0.0%	0.0%	73.7%	21.5%	3.9%	0.5%	0.3%	0.0%	0.0%	0.0%	0.0%	0.0%	0.0%
49	1066.8	2.169	496.7	0.0%	99.8%	0.2%	0.0%	0.0%	0.0%	0.0%	0.0%	19.0%	49.6%	19.2%	7.0%	4.9%	0.0%	0.0%	0.0%	0.0%	0.0%	0.0%
52	1151.2	2.386	548.2	0.0%	99.9%	0.1%	0.0%	0.0%	0.0%	0.0%	0.0%	21.9%	40.1%	31.5%	5.9%	0.4%	0.0%	0.0%	0.0%	0.0%	0.0%	0.0%
53	900.8	2.899	398.5	0.0%	99.6%	0.4%	0.0%	0.0%	0.0%	0.0%	0.0%	10.9%	20.8%	35.2%	27.7%	5.0%	0.1%	0.1%	0.1%	0.1%	0.1%	0.1%
69	1829.6	2.206	861.8	0.0%	100.0%	0.0%	0.0%	0.0%	0.0%	0.0%	0.0%	52.0%	36.1%	7.3%	4.2%	0.5%	0.0%	0.0%	0.0%	0.0%	0.0%	0.0%
70	648.9	1.790	353.6	0.0%	100.0%	0.0%	0.0%	0.0%	0.0%	0.0%	0.0%	4.0%	66.3%	23.5%	6.0%	0.2%	0.0%	0.0%	0.0%	0.0%	0.0%	0.0%
71	1654.6	1.856	623.7	0.0%	100.0%	0.0%	0.0%	0.0%	0.0%	0.0%	0.0%	49.6%	34.9%	4.7%	10.4%	0.5%	0.0%	0.0%	0.0%	0.0%	0.0%	0.0%
73	1180.1	2.974	660.4	0.0%	100.0%	0.0%	0.0%	0.0%	0.0%	0.0%	0.0%	24.6%	43.2%	11.3%	19.3%	1.6%	0.0%	0.0%	0.0%	0.0%	0.0%	0.0%
76	2045.4	2.652	924.5	0.0%	100.0%	0.0%	0.0%	0.0%	0.0%	0.0%	0.0%	37.5%	45.3%	7.5%	9.3%	0.4%	0.0%	0.0%	0.0%	0.0%	0.0%	0.0%
77	1014.2	2.249	526.6	0.0%	100.0%	0.0%	0.0%	0.0%	0.0%	0.0%	0.0%	20.6%	48.8%	20.9%	9.3%	0.3%	0.0%	0.0%	0.0%	0.0%	0.0%	0.0%
78	379.8	1.582	186.8	0.0%	100.0%	0.0%	0.0%	0.0%	0.0%	0.0%	0.0%	0.2%	25.8%	68.4%	5.7%	0.0%	0.0%	0.0%	0.0%	0.0%	0.0%	0.0%
79	714.5	1.698	258.8	0.0%	100.0%	0.0%	0.0%	0.0%	0.0%	0.0%	0.0%	9.8%	27.1%	57.3%	5.7%	0.1%	0.0%	0.0%	0.0%	0.0%	0.0%	0.0%
80	641.7	1.938	168.2	0.0%	100.0%	0.0%	0.0%	0.0%	0.0%	0.0%	0.0%	6.8%	10.8%	21.6%	59.4%	1.5%	0.0%	0.0%	0.0%	0.0%	0.0%	0.0%
81	445.9	1.859	234.1	0.0%	100.0%	0.0%	0.0%	0.0%	0.0%	0.0%	0.0%	0.1%	25.7%	55.3%	18.6%	0.3%	0.0%	0.0%	0.0%	0.0%	0.0%	0.0%
82	327.3	1.560	166.6	0.0%	100.0%	0.0%	0.0%	0.0%	0.0%	0.0%	0.0%	0.3%	15.4%	75.5%	8.8%	0.0%	0.0%	0.0%	0.0%	0.0%	0.0%	0.0%
84	851.9	1.802	394.6	0.0%	100.0%	0.0%	0.0%	0.0%	0.0%	0.0%	0.0%	15.6%	58.7%	22.2%	3.5%	0.0%	0.0%	0.0%	0.0%	0.0%	0.0%	0.0%
85	418.6	1.617	180.2	0.0%	100.0%	0.0%	0.0%	0.0%	0.0%	0.0%	0.0%	3.5%	15.2%	71.1%	10.1%	0.1%	0.0%	0.0%	0.0%	0.0%	0.0%	0.0%
93	561.4	2.118	281.0	0.0%	100.0%	0.0%	0.0%	0.0%	0.0%	0.0%	0.0%	2.1%	25.9%	47.4%	24.3%	0.3%	0.0%	0.0%	0.0%	0.0%	0.0%	0.0%
95	542.0	1.928	302.0	0.0%	100.0%	0.0%	0.0%	0.0%	0.0%	0.0%	0.0%	1.1%	46.8%	39.4%	12.6%	0.1%	0.0%	0.0%	0.0%	0.0%	0.0%	0.0%
96	371.7	1.465	165.6	0.0%	100.	0.0	0.0%	0.0%	0.0%	0.0%	0.0%	0.7%	27.2%	67.7%	4.3%	0.0%	0.0%	0.0	0.0	0.0	0.0%	0.0

					0%	%												%	%	%		%
97	220.6	1.448	102.6	0.0%	100.0%	0.0%	0.0%	0.0%	0.0%	0.0%	0.0%	0.0%	1.4%	68.5%	30.0%	0.1%	0.0%	0.0%	0.0%	0.0%	0.0%	0.0%
98	255.3	1.358	93.28	0.0%	100.0%	0.0%	0.0%	0.0%	0.0%	0.0%	0.0%	0.1%	3.8%	77.6%	18.3%	0.1%	0.0%	0.0%	0.0%	0.0%	0.0%	0.0%
103	659.9	2.634	310.8	0.0%	99.9%	0.1%	0.0%	0.0%	0.0%	0.0%	0.0%	5.0%	20.1%	30.9%	41.7%	2.2%	0.0%	0.0%	0.0%	0.0%	0.0%	0.0%

RESULTS OF TEXTURAL ANALYSIS ON ELLIOT RIVER ESTUARY SUBSURFACE SAMPLES

Sample #	Sample type	Mean	Sorting	Skewness	Kurtosis	Mean	Sorting:	Skewness	Kutosis	MODE 1	MODE 2	MODE 3	D10	D50	D90	(D90 / D10)
1: 1-5 cm	Bimodal, Moderately Sorted	886.1	1.652	-0.686	0.495	Coarse Sand	Moderately Sorted	Very Fine Skewed	Very Platykurtic	605.0	1700.0		381.6	1058.3	3453.9	9.052
1: 10-15 cm	Unimodal, Well Sorted	1116.1	1.409	-1.024	0.695	Very Coarse Sand	Well Sorted	Very Fine Skewed	Platykurtic	1200.0			543.9	1324.2	3182.2	5.851
1: 25-30 cm	Bimodal, Poorly Sorted	794.7	2.112	-0.386	0.589	Coarse Sand	Poorly Sorted	Very Fine Skewed	Very Platykurtic	1700.0	855.0		242.0	859.8	2480.2	10.25
1: 34-40 cm	Bimodal, Moderately Sorted	800.1	1.878	-0.439	0.418	Coarse Sand	Moderately Sorted	Very Fine Skewed	Very Platykurtic	427.5	1200.0		288.8	899.9	2783.8	9.638
1: 45-49 cm	Trimodal, Moderately Sorted	619.6	1.962	0.154	0.905	Coarse Sand	Moderately Sorted	Coarse Skewed	Mesokurtic	427.5	1200.0	137.5	276.2	553.9	1683.9	6.097
1: 50-55 cm	Bimodal, Moderately Well Sorted	986.1	1.551	-0.895	0.464	Coarse Sand	Moderately Well Sorted	Very Fine Skewed	Very Platykurtic	1200.0	605.0		426.3	1233.4	3189.7	7.483
1: 70-75 cm	Bimodal, Moderately Well Sorted	1044.9	1.492	-1.664	0.731	Very Coarse Sand	Moderately Well Sorted	Very Fine Skewed	Platykurtic	1700.0	427.5		419.3	1677.0	5908.0	14.09
1: 80-85 cm	Unimodal, Moderately Well Sorted	407.2	1.422	0.110	1.266	Medium Sand	Moderately Well Sorted	Coarse Skewed	Leptokurtic	427.5			269.5	407.0	655.9	2.433
2: 1-15 cm	Unimodal, Well Sorted	1183.7	1.328	-1.026	0.452	Very Coarse Sand	Well Sorted	Very Fine Skewed	Very Platykurtic	1200.0			704.5	1355.5	2586.9	3.672
2: 25-30 cm	Unimodal, Well Sorted	1134.7	1.386	-1.406	0.733	Very Coarse Sand	Well Sorted	Very Fine Skewed	Platykurtic	1200.0			548.5	1489.3	3713.9	6.771
2: 45-51cm	Bimodal, Moderately Sorted	855.0	1.897	-0.682	0.438	Coarse Sand	Moderately Sorted	Very Fine Skewed	Very Platykurtic	1200.0	302.5		287.1	1097.1	2720.8	9.477
2: 52-57	Bimodal, Moderately Well Sorted	1018.8	1.585	-1.625	0.946	Very Coarse Sand	Moderately Well Sorted	Very Fine Skewed	Mesokurtic	1700.0	427.5		356.1	1734.1	6285.5	17.65
2: 66-71 cm	Bimodal, Moderately Sorted	830.2	1.824	-0.643	0.395	Coarse Sand	Moderately Sorted	Very Fine Skewed	Very Platykurtic	1700.0	427.5		301.1	1034.6	3012.9	10.01
2: 80-85 cm	Bimodal, Moderately Well Sorted	1015.1	1.483	-1.318	0.437	Very Coarse Sand	Moderately Well Sorted	Very Fine Skewed	Very Platykurtic	605.0	1700.0		458.1	1444.4	3935.8	8.592
2: 88-85 cm	Bimodal, Moderately Well Sorted	1015.1	1.483	-1.318	0.437	Very Coarse Sand	Moderately Well Sorted	Very Fine Skewed	Very Platykurtic	605.0	1700.0		458.1	1444.4	3935.8	8.592
2: 95-100 cm	Bimodal, Poorly Sorted	837.4	2.151	-0.551	0.648	Coarse Sand	Poorly Sorted	Very Fine Skewed	Very Platykurtic	1200.0	302.5		226.2	1012.9	2422.6	10.71
3a: 1-5 cm	Unimodal, Moderately Well Sorted	1061.1	1.530	-0.445	0.493	Very Coarse Sand	Moderately Well Sorted	Very Fine Skewed	Very Platykurtic	855.0			531.2	1090.5	2368.4	4.458
3a: 15-20 cm	Unimodal, Well Sorted	1186.0	1.275	-1.514	0.541	Very Coarse Sand	Well Sorted	Very Fine Skewed	Very Platykurtic	1200.0			702.5	1478.9	3062.6	4.360
3a: 30-33 cm	Unimodal, Well Sorted	1169.1	1.279	-1.898	0.643	Very Coarse Sand	Well Sorted	Very Fine Skewed	Very Platykurtic	1200.0			639.5	1596.5	4132.3	6.462
3a: 45-50 cm	Unimodal, Moderately Sorted	879.7	1.819	-0.229	0.645	Coarse Sand	Moderately Sorted	Fine Skewed	Very Platykurtic	855.0			362.9	870.8	2155.6	5.940
3a: 60-65 cm	Unimodal, Moderately Sorted	865.6	1.675	-0.630	0.458	Coarse Sand	Moderately Sorted	Very Fine Skewed	Very Platykurtic	605.0			367.4	1022.8	3324.5	9.048
3: 74-79 cm	Unimodal, Moderately Sorted	860.1	1.713	-0.477	0.436	Coarse Sand	Moderately Sorted	Very Fine Skewed	Very Platykurtic	855.0			365.9	950.9	2904.3	7.938
4: 1-5 cm	Unimodal, Moderately Well Sorted	1155.1	1.442	-0.659	0.485	Very Coarse Sand	Moderately Well Sorted	Very Fine Skewed	Very Platykurtic	1200.0			580.0	1239.3	2396.8	4.133
4: 45-50 cm	Unimodal, Moderately Well Sorted	1049.0	1.518	-0.651	0.488	Very Coarse Sand	Moderately Well Sorted	Very Fine Skewed	Very Platykurtic	1200.0			514.3	1162.9	2566.8	4.991
4: 55-60 cm	Unimodal, Moderately Well Sorted	973.1	1.534	-0.870	0.559	Coarse Sand	Moderately Well Sorted	Very Fine Skewed	Very Platykurtic	855.0			433.4	1192.2	3626.0	8.367

Sample #	(D90 - D10)	(D75 / D25)	(D75 - D25) (mm):	% Gravel	% Sand	% Mud	% V.C.Gravel	% C.Gravel	% M.Gravel	% F.Gravel	% V.F.Gravel	% V.C.Sand	% C.Sand	% M.Sand	% F.Sand	% V.F.Sand	% V.C.Silt	% C.Silt	% M.Silt	% F.Silt	% V.F.Silt	% Clay
1: 1-5 cm	3072.4	3.174	1224.8	0.0%	99.9%	0.1%	0.0%	0.0%	0.0%	0.0%	0.0%	51.7%	28.8%	15.5%	2.8%	0.9%	0.0%	0.0%	0.0%	0.0%	0.0%	0.0%
1: 10-15 cm	2638.3	1.960	865.3	0.0%	100.0%	0.0%	0.0%	0.0%	0.0%	0.0%	0.0%	70.6%	21.0%	6.7%	1.6%	0.2%	0.0%	0.0%	0.0%	0.0%	0.0%	0.0%
1: 25-30 cm	2238.2	3.890	1223.6	0.0%	99.8%	0.2%	0.0%	0.0%	0.0%	0.0%	0.0%	44.2%	25.7%	19.6%	8.9%	1.4%	0.0%	0.0%	0.0%	0.0%	0.0%	0.0%
1: 34-40 cm	2495.0	4.523	1418.2	0.0%	100.0%	0.0%	0.0%	0.0%	0.0%	0.0%	0.0%	48.4%	13.5%	33.2%	4.4%	0.3%	0.0%	0.0%	0.0%	0.0%	0.0%	0.0%
1: 45-49 cm	1407.7	2.634	628.5	0.0%	100.0%	0.0%	0.0%	0.0%	0.0%	0.0%	0.0%	25.4%	30.5%	37.7%	5.6%	0.7%	0.0%	0.0%	0.0%	0.0%	0.0%	0.0%
1: 50-55 cm	2763.5	2.823	1198.3	0.0%	100.0%	0.0%	0.0%	0.0%	0.0%	0.0%	0.0%	60.7%	25.1%	12.9%	1.1%	0.2%	0.0%	0.0%	0.0%	0.0%	0.0%	0.0%
1: 70-75 cm	5488.7	1.900	711.3	0.0%	100.0%	0.0%	0.0%	0.0%	0.0%	0.0%	0.0%	70.5%	14.6%	14.2%	0.6%	0.1%	0.0%	0.0%	0.0%	0.0%	0.0%	0.0%
1: 80-85 cm	386.3	1.486	159.3	0.0%	100.0%	0.0%	0.0%	0.0%	0.0%	0.0%	0.0%	3.7%	17.8%	74.3%	4.0%	0.3%	0.0%	0.0%	0.0%	0.0%	0.0%	0.0%
2: 1-15 cm	1882.4	2.050	999.9	0.0%	99.9%	0.1%	0.0%	0.0%	0.0%	0.0%	0.0%	72.5%	23.0%	2.9%	1.3%	0.1%	0.0%	0.0%	0.0%	0.0%	0.0%	0.0%
2: 25-30 cm	3165.3	1.836	743.7	0.0%	99.9%	0.1%	0.0%	0.0%	0.0%	0.0%	0.0%	70.1%	21.9%	5.5%	2.0%	0.3%	0.0%	0.0%	0.0%	0.0%	0.0%	0.0%
2: 45-51cm	2433.8	4.232	1370.2	0.0%	100.0%	0.0%	0.0%	0.0%	0.0%	0.0%	0.0%	55.9%	12.9%	26.6%	3.9%	0.7%	0.0%	0.0%	0.0%	0.0%	0.0%	0.0%
2: 52-57	5929.4	1.795	669.9	0.0%	100.0%	0.0%	0.0%	0.0%	0.0%	0.0%	0.0%	72.7%	9.9%	14.9%	2.1%	0.4%	0.0%	0.0%	0.0%	0.0%	0.0%	0.0%
2: 66-71 cm	2711.8	4.580	1531.3	0.0%	100.0%	0.0%	0.0%	0.0%	0.0%	0.0%	0.0%	51.1%	17.0%	29.5%	2.3%	0.1%	0.0%	0.0%	0.0%	0.0%	0.0%	0.0%
2: 80-85 cm	3477.7	2.627	1011.8	0.0%	100.0%	0.0%	0.0%	0.0%	0.0%	0.0%	0.0%	60.5%	26.6%	12.8%	0.0%	0.0%	0.0%	0.0%	0.0%	0.0%	0.0%	0.0%
2: 88-85 cm	3477.7	2.627	1011.8	0.0%	100.0%	0.0%	0.0%	0.0%	0.0%	0.0%	0.0%	60.5%	26.6%	12.8%	0.0%	0.0%	0.0%	0.0%	0.0%	0.0%	0.0%	0.0%
2: 95-100 cm	2196.4	3.429	1151.3	0.0%	99.9%	0.1%	0.0%	0.0%	0.0%	0.0%	0.0%	50.7%	23.4%	13.9%	11.0%	0.8%	0.0%	0.0%	0.0%	0.0%	0.0%	0.0%
3a: 1-5 cm	1837.2	2.349	996.4	0.0%	100.0%	0.0%	0.0%	0.0%	0.0%	0.0%	0.0%	55.5%	37.1%	7.1%	0.2%	0.1%	0.0%	0.0%	0.0%	0.0%	0.0%	0.0%
3a: 15-20 cm	2360.1	1.703	695.2	0.0%	100.0%	0.0%	0.0%	0.0%	0.0%	0.0%	0.0%	74.5%	22.4%	2.9%	0.1%	0.0%	0.0%	0.0%	0.0%	0.0%	0.0%	0.0%
3a: 30-33 cm	3492.8	1.616	576.0	0.0%	100.0%	0.0%	0.0%	0.0%	0.0%	0.0%	0.0%	71.9%	23.6%	4.0%	0.2%	0.2%	0.0%	0.0%	0.0%	0.0%	0.0%	0.0%
3a: 45-50 cm	1792.7	2.634	866.3	0.0%	99.9%	0.1%	0.0%	0.0%	0.0%	0.0%	0.0%	42.1%	35.6%	19.5%	2.2%	0.4%	0.0%	0.0%	0.0%	0.0%	0.0%	0.0%
3a: 60-65 cm	2957.1	3.395	1296.5	0.0%	99.9%	0.1%	0.0%	0.0%	0.0%	0.0%	0.0%	50.8%	27.4%	19.3%	2.2%	0.2%	0.0%	0.0%	0.0%	0.0%	0.0%	0.0%
3: 74-79 cm	2538.4	3.698	1431.2	0.0%	99.9%	0.1%	0.0%	0.0%	0.0%	0.0%	0.0%	47.8%	29.7%	20.0%	2.2%	0.3%	0.0%	0.0%	0.0%	0.0%	0.0%	0.0%
4: 1-5 cm	1816.9	2.181	991.9	0.0%	99.7%	0.3%	0.0%	0.0%	0.0%	0.0%	0.0%	65.7%	28.7%	4.7%	0.4%	0.2%	0.1%	0.1%	0.1%	0.1%	0.1%	0.1%
4: 45-50 cm	2052.5	2.527	1143.8	0.0%	99.7%	0.3%	0.0%	0.0%	0.0%	0.0%	0.0%	58.6%	32.5%	7.1%	1.1%	0.4%	0.1%	0.1%	0.1%	0.1%	0.1%	0.1%
4: 55-60 cm	3192.6	2.479	1033.2	0.0%	99.6%	0.4%	0.0%	0.0%	0.0%	0.0%	0.0%	57.9%	29.1%	10.3%	1.8%	0.5%	0.1%	0.1%	0.1%	0.1%	0.1%	0.1%

RESULTS OF TEXTURAL ANALYSIS ON BLACK RIVER DELTA SURFICIAL SAMPLES

Sample #	Sample type	Mean	Sorting	Skewness	Kurtosis	Mean	Sorting:	Skewness	Kutosis	MODE 1	MODE 2	MODE 3	D10	D50	D90	(D90 / D10)
1	Trimodal, Poorly Sorted	34.46	3.783	0.087	0.637	Very Coarse Silt	Poorly Sorted	Symmetrical	Very Platykurtic	7.930	146.0	45.54	6.918	32.71	206.3	29.82
2	Trimodal, Poorly Sorted	33.17	3.421	-0.010	0.691	Very Coarse Silt	Poorly Sorted	Symmetrical	Platykurtic	7.930	45.54	146.0	7.142	34.87	170.1	23.81
5	Bimodal, Poorly Sorted	54.62	3.368	-0.406	0.943	Very Coarse Silt	Poorly Sorted	Very Fine Skewed	Mesokurtic	120.3	7.930		8.750	81.60	202.5	23.14
6	Unimodal, Moderately Sorted	173.2	1.767	-0.237	1.621	Fine Sand	Moderately Sorted	Fine Skewed	Very Leptokurtic	177.3			91.20	176.4	298.3	3.271
7	Unimodal, Moderately Sorted	546.5	1.913	-0.246	1.077	Coarse Sand	Moderately Sorted	Fine Skewed	Mesokurtic	690.5			213.8	589.7	1100.8	5.148
8	Trimodal, Poorly Sorted	60.73	3.763	-0.376	0.722	Very Coarse Silt	Poorly Sorted	Very Fine Skewed	Platykurtic	177.3	7.930	45.54	8.576	90.44	260.2	30.34
9	Unimodal, Well Sorted	347.7	1.383	0.014	1.013	Medium Sand	Well Sorted	Symmetrical	Mesokurtic	317.6			230.7	346.4	524.7	2.275
10	Bimodal, Poorly Sorted	63.19	3.004	-0.542	1.424	Very Fine Sand	Poorly Sorted	Very Fine Skewed	Leptokurtic	120.3	7.930		9.679	97.86	186.7	19.29
11	Bimodal, Poorly Sorted	47.38	3.402	-0.405	0.659	Very Coarse Silt	Poorly Sorted	Very Fine Skewed	Very Platykurtic	120.3	7.930		7.870	71.53	181.0	23.00
12	Unimodal, Moderately Well Sorted	233.3	1.444	0.129	1.165	Fine Sand	Moderately Well Sorted	Coarse Skewed	Leptokurtic	215.0			147.3	228.1	372.9	2.531
12	Unimodal, Well Sorted	143.9	1.368	0.036	1.558	Fine Sand	Well Sorted	Symmetrical	Very Leptokurtic	152.5			98.45	146.7	224.3	2.278
13	Unimodal, Moderately Well Sorted	2.601	0.532	-0.109	1.106	Fine Sand	Moderately Well Sorted	Coarse Skewed	Mesokurtic	152.5			104.4	162.6	263.1	2.521
14	Unimodal, Moderately Well Sorted	245.4	1.613	0.254	1.367	Fine Sand	Moderately Well Sorted	Coarse Skewed	Leptokurtic	215.0			146.6	235.3	485.5	3.311
18	Trimodal, Poorly Sorted	36.20	3.710	0.039	0.690	Very Coarse Silt	Poorly Sorted	Symmetrical	Platykurtic	7.930	45.54	146.0	7.304	36.60	204.1	27.95
19	Unimodal, Moderately Sorted	187.8	1.712	0.178	1.415	Fine Sand	Moderately Sorted	Coarse Skewed	Leptokurtic	177.3			107.3	184.0	375.9	3.504
21	Unimodal, Well Sorted	700.0	1.322	-0.096	1.069	Coarse Sand	Well Sorted	Symmetrical	Mesokurtic	690.5			477.3	709.5	993.5	2.081
22	Unimodal, Moderately Well Sorted	698.4	1.548	-0.177	1.213	Coarse Sand	Moderately Well Sorted	Fine Skewed	Leptokurtic	690.5			390.9	715.5	1116.8	2.857
23	Unimodal, Poorly Sorted	0.911	1.012	0.128	0.779	Coarse Sand	Poorly Sorted	Fine Skewed	Platykurtic	605.0			196.3	540.5	1385.9	7.061
24	Unimodal, Moderately Sorted	0.607	0.758	0.094	0.847	Coarse Sand	Moderately Sorted	Symmetrical	Platykurtic	605.0			310.4	655.9	1319.5	4.252
25	Unimodal, Moderately Sorted	607.6	1.672	-0.209	1.108	Coarse Sand	Moderately Sorted	Fine Skewed	Mesokurtic	690.5			291.3	639.1	1075.2	3.690
26	Trimodal, Poorly Sorted	20.16	3.162	0.470	0.856	Coarse Silt	Poorly Sorted	Very Coarse Skewed	Platykurtic	7.930	37.50	177.3	6.496	14.40	145.5	22.40
27	Bimodal, Moderately Sorted	1.569	0.954	-0.040	0.816	Medium Sand	Moderately Sorted	Symmetrical	Platykurtic	427.5	215.0		147.9	339.2	833.0	5.633
28	Unimodal, Moderately Sorted	1.402	0.874	-0.109	1.015	Medium Sand	Moderately Sorted	Coarse Skewed	Mesokurtic	302.5			186.1	364.2	878.0	4.718
30	Trimodal, Very Poorly Sorted	210.6	4.389	-0.112	1.012	Fine Sand	Very Poorly Sorted	Fine Skewed	Mesokurtic	177.3	838.6	7.930	18.35	205.0	1087.7	59.28
31	Polymodal, Very Poorly Sorted	183.9	5.008	-0.150	1.012	Fine Sand	Very Poorly Sorted	Fine Skewed	Mesokurtic	177.3	690.5	263.0	11.76	203.3	1152.1	97.98
32	Trimodal, Poorly Sorted	24.03	3.140	0.251	0.820	Coarse Silt	Poorly Sorted	Coarse Skewed	Platykurtic	7.930	37.50	177.3	6.859	20.68	143.6	20.94
33	Bimodal, Very Poorly Sorted	271.3	5.229	-0.664	1.281	Medium Sand	Very Poorly Sorted	Very Fine Skewed	Leptokurtic	838.6	7.930		11.37	588.1	1205.1	106.0
34	Unimodal, Well Sorted	0.35	0.49	0.063	0.92	Coarse Sand	Well Sorted	Symmetrical	Mesokurtic	855.0			508.	769	139	2.737

		9	8		8								7	.1	2.4	
35	Unimodal, Moderately Sorted	560.0	1.747	-0.141	0.998	Coarse Sand	Moderately Sorted	Fine Skewed	Mesokurtic	690.5			258.1	584.1	1083.2	4.197
36	Bimodal, Moderately Sorted	0.979	0.848	0.026	0.832	Coarse Sand	Moderately Sorted	Symmetrical	Platykurtic	855.0	427.5		240.1	507.0	1043.4	4.346
37	Bimodal, Poorly Sorted	374.8	2.363	-0.068	0.851	Medium Sand	Poorly Sorted	Symmetrical	Platykurtic	605.0	215.0		125.1	386.6	1096.6	8.766
38	Trimodal, Very Poorly Sorted	313.3	4.361	-0.585	1.322	Medium Sand	Very Poorly Sorted	Very Fine Skewed	Leptokurtic	690.5	177.3	7.930	13.75	523.4	1139.9	82.89
39	Unimodal, Moderately Well Sorted	161.8	1.482	0.373	2.407	Fine Sand	Moderately Well Sorted	Very Coarse Skewed	Very Leptokurtic	152.5			113.3	154.4	253.0	2.234
40	Unimodal, Moderately Well Sorted	649.6	1.525	-0.158	1.184	Coarse Sand	Moderately Well Sorted	Fine Skewed	Leptokurtic	690.5			362.9	665.5	1053.7	2.903
41	Unimodal, Moderately Sorted	360.8	1.778	0.194	1.030	Medium Sand	Moderately Sorted	Coarse Skewed	Mesokurtic	263.0			184.3	337.3	835.9	4.536
42	Unimodal, Moderately Well Sorted	346.9	1.552	0.078	0.989	Medium Sand	Moderately Well Sorted	Symmetrical	Mesokurtic	317.6			201.6	339.7	621.1	3.080
43	Unimodal, Well Sorted	168.3	1.410	0.185	1.172	Fine Sand	Well Sorted	Coarse Skewed	Leptokurtic	152.5			109.9	161.7	265.6	2.416
44	Unimodal, Moderately Sorted	200.2	1.689	0.339	1.158	Fine Sand	Moderately Sorted	Very Coarse Skewed	Leptokurtic	152.5			116.2	181.2	455.9	3.922
45	Unimodal, Well Sorted	202.7	1.348	-0.035	1.126	Fine Sand	Well Sorted	Symmetrical	Leptokurtic	215.0			136.6	206.0	305.9	2.240
46	Unimodal, Very Well Sorted	2.641	0.321	-0.121	1.204	Fine Sand	Very Well Sorted	Coarse Skewed	Leptokurtic	152.5			127.0	156.5	219.5	1.728
47	Unimodal, Moderately Well Sorted	199.7	1.600	0.301	1.357	Fine Sand	Moderately Well Sorted	Very Coarse Skewed	Leptokurtic	152.5			127.7	187.6	397.9	3.115
49	Unimodal, Well Sorted	788.0	1.405	-0.150	1.222	Coarse Sand	Well Sorted	Fine Skewed	Leptokurtic	838.6			514.7	800.6	1151.1	2.236
56	Bimodal, Poorly Sorted	412.8	2.087	0.142	0.791	Medium Sand	Poorly Sorted	Coarse Skewed	Platykurtic	215.0	605.0		174.9	382.3	1147.8	6.563
57	Unimodal, Moderately Sorted	0.782	0.880	0.119	0.836	Coarse Sand	Moderately Sorted	Fine Skewed	Platykurtic	605.0			254.9	592.5	1315.4	5.159
58	Unimodal, Well Sorted	284.1	1.407	-0.037	1.158	Medium Sand	Well Sorted	Symmetrical	Leptokurtic	302.5			186.7	286.7	449.1	2.405
59	Trimodal, Very Poorly Sorted	135.8	5.088	-0.183	1.003	Fine Sand	Very Poorly Sorted	Fine Skewed	Mesokurtic	177.3	838.6	7.930	10.40	159.5	888.5	85.40
61	Unimodal, Moderately Well Sorted	0.387	0.602	0.018	0.685	Coarse Sand	Moderately Well Sorted	Symmetrical	Platykurtic	605.0			419.1	728.1	1448.1	3.455
63	Unimodal, Moderately Well Sorted	870.0	1.433	-0.113	1.073	Coarse Sand	Moderately Well Sorted	Fine Skewed	Mesokurtic	838.6			533.3	881.3	1320.2	2.475
64	Unimodal, Well Sorted	626.8	1.411	-0.015	0.973	Coarse Sand	Well Sorted	Symmetrical	Mesokurtic	690.5			398.5	628.5	980.2	2.460
65	Unimodal, Moderately Well Sorted	708.5	1.515	-0.180	1.174	Coarse Sand	Moderately Well Sorted	Fine Skewed	Leptokurtic	838.6			401.6	729.2	1112.0	2.769
66	Bimodal, Moderately Well Sorted	774.3	1.568	-0.234	0.820	Coarse Sand	Moderately Well Sorted	Fine Skewed	Platykurtic	1200.0	605.0		398.6	817.5	1278.8	3.208
67	Unimodal, Moderately Well Sorted	0.433	0.652	0.052	0.582	Coarse Sand	Moderately Well Sorted	Symmetrical	Very Platykurtic	427.5			393.6	717.6	1477.7	3.755
68	Unimodal, Well Sorted	550.4	1.317	-0.051	1.074	Coarse Sand	Well Sorted	Symmetrical	Mesokurtic	605.0			386.7	566.4	818.7	2.117

Sample #	(D90 - D10)	(D75 / D25)	(D75 - D25) (mm):	% Gravel	% Sand	% Mud	% V.C.Gravel	% C.Gravel	% M.Gravel	% F.Gravel	% V.F.Gravel	% V.C.Sand	% C.Sand	% M.Sand	% F.Sand	% V.F.Sand	% V.C.Silt	% C.Silt	% M.Silt	% F.Silt	% V.F.Silt	% Clay
1	199.4	11.67	101.4	0.0%	37.1%	62.9%	0.0%	0.0%	0.0%	0.0%	0.0%	0.7%	1.7%	4.1%	15.5%	15.0%	13.7%	8.8%	24.7%	15.7%	0.0%	0.0%
2	162.9	8.359	74.27	0.0%	32.8%	67.2%	0.0%	0.0%	0.0%	0.0%	0.0%	0.0%	0.0%	3.2%	13.3%	16.3%	19.9%	10.5%	22.8%	14.0%	0.0%	0.0%
5	193.7	4.769	110.1	0.0%	59.6%	40.4%	0.0%	0.0%	0.0%	0.0%	0.0%	1.4%	1.6%	2.4%	24.9%	29.4%	14.5%	6.1%	12.4%	7.3%	0.0%	0.0%
6	207.1	1.788	103.3	0.0%	94.0%	6.0%	0.0%	0.0%	0.0%	0.0%	0.0%	0.9%	1.0%	18.5%	57.1%	16.5%	1.4%	1.4%	1.8%	1.4%	0.0%	0.0%
7	886.9	2.319	484.2	0.0%	97.1%	2.9%	0.0%	0.0%	0.0%	0.0%	0.0%	15.2%	45.0%	26.8%	8.6%	1.5%	0.6%	0.5%	1.1%	0.6%	0.0%	0.0%
8	251.7	8.520	162.3	0.0%	56.8%	43.2%	0.0%	0.0%	0.0%	0.0%	0.0%	0.0%	0.1%	11.5%	29.9%	15.4%	13.1%	8.4%	14.0%	7.6%	0.0%	0.0%
9	294.0	1.542	151.4	0.0%	100.0%	0.0%	0.0%	0.0%	0.0%	0.0%	0.0%	0.0%	13.0%	71.7%	15.3%	0.0%	0.0%	0.0%	0.0%	0.0%	0.0%	0.0%
10	177.0	2.647	88.19	0.0%	71.3%	28.7%	0.0%	0.0%	0.0%	0.0%	0.0%	0.0%	0.0%	2.0%	31.3%	38.0%	9.5%	3.2%	10.0%	6.0%	0.0%	0.0%
11	173.2	8.767	113.3	0.0%	54.0%	46.0%	0.0%	0.0%	0.0%	0.0%	0.0%	0.0%	0.0%	2.1%	24.0%	27.9%	13.2%	6.9%	16.2%	9.8%	0.0%	0.0%
12	225.6	1.576	108.3	0.0%	99.7%	0.3%	0.0%	0.0%	0.0%	0.0%	0.0%	1.5%	2.8%	33.8%	59.6%	1.9%	0.1%	0.1%	0.1%	0.1%	0.1%	0.1%
12	125.8	1.364	45.78	0.0%	99.6%	0.4%	0.0%	0.0%	0.0%	0.0%	0.0%	1.0%	1.2%	4.3%	69.3%	23.8%	0.1%	0.1%	0.1%	0.1%	0.1%	0.1%
13	158.8	1.609	79.88	0.0%	98.7%	1.3%	0.0%	0.0%	0.0%	0.0%	0.0%	1.5%	2.8%	6.7%	69.6%	18.1%	0.2%	0.2%	0.2%	0.2%	0.2%	0.5%
14	338.9	1.707	133.0	0.0%	100.0%	0.0%	0.0%	0.0%	0.0%	0.0%	0.0%	3.8%	5.5%	34.0%	54.6%	2.1%	0.0%	0.0%	0.0%	0.0%	0.0%	0.0%
18	196.8	9.935	94.07	0.0%	36.7%	63.3%	0.0%	0.0%	0.0%	0.0%	0.0%	2.2%	1.7%	3.0%	14.0%	15.8%	16.9%	11.0%	22.5%	12.8%	0.0%	0.0%
19	268.6	1.817	113.6	0.0%	96.7%	3.3%	0.0%	0.0%	0.0%	0.0%	0.0%	1.7%	5.7%	18.3%	56.6%	14.5%	0.4%	0.9%	0.9%	1.0%	0.0%	0.0%
21	516.2	1.444	260.9	0.0%	100.0%	0.0%	0.0%	0.0%	0.0%	0.0%	0.0%	9.6%	78.6%	10.3%	0.3%	1.2%	0.0%	0.0%	0.0%	0.0%	0.0%	0.0%
22	725.9	1.692	374.5	0.0%	98.2%	1.8%	0.0%	0.0%	0.0%	0.0%	0.0%	18.3%	62.0%	15.0%	1.7%	1.2%	0.0%	0.2%	1.1%	0.5%	0.0%	0.0%
23	1189.6	2.927	600.5	0.0%	99.7%	0.3%	0.0%	0.0%	0.0%	0.0%	0.0%	20.8%	33.1%	29.0%	15.6%	1.2%	0.0%	0.0%	0.0%	0.0%	0.0%	0.1%
24	1009.2	2.174	518.8	0.0%	99.9%	0.1%	0.0%	0.0%	0.0%	0.0%	0.0%	22.4%	46.0%	26.9%	4.0%	0.7%	0.0%	0.0%	0.0%	0.0%	0.0%	0.0%
25	783.8	1.920	410.2	0.0%	98.3%	1.7%	0.0%	0.0%	0.0%	0.0%	0.0%	14.3%	54.3%	24.4%	4.9%	0.5%	0.3%	0.3%	0.6%	0.4%	0.0%	0.0%
26	139.0	5.793	40.00	0.0%	19.4%	80.6%	0.0%	0.0%	0.0%	0.0%	0.0%	1.1%	1.4%	1.9%	7.2%	7.9%	16.9%	11.6%	31.3%	20.8%	0.0%	0.0%
27	685.1	2.798	356.9	0.0%	99.7%	0.3%	0.0%	0.0%	0.0%	0.0%	0.0%	5.5%	24.2%	33.3%	35.5%	1.2%	0.0%	0.0%	0.0%	0.0%	0.0%	0.1%
28	691.9	2.252	317.5	0.0%	99.9%	0.1%	0.0%	0.0%	0.0%	0.0%	0.0%	6.6%	24.2%	45.3%	22.7%	1.2%	0.0%	0.0%	0.0%	0.0%	0.0%	0.1%
30	1069.4	7.656	589.2	0.0%	81.2%	18.8%	0.0%	0.0%	0.0%	0.0%	0.0%	12.6%	19.9%	12.0%	21.5%	15.2%	7.0%	2.2%	5.9%	3.6%	0.0%	0.0%
31	1140.3	8.763	543.6	0.0%	76.9%	23.1%	0.0%	0.0%	0.0%	0.0%	0.0%	12.7%	17.4%	14.8%	18.0%	14.0%	8.1%	2.9%	7.6%	4.6%	0.0%	0.0%
32	136.8	5.949	45.46	0.0%	21.7%	78.3%	0.0%	0.0%	0.0%	0.0%	0.0%	0.4%	0.8%	2.3%	8.1%	10.0%	19.3%	14.0%	28.6%	16.5%	0.0%	0.0%

33	1193.7	5.235	721.5	0.0%	79.9%	20.1%	0.0%	0.0%	0.0%	0.0%	0.0%	18.6%	38.9%	14.0%	5.7%	2.8%	4.3%	3.0%	8.1%	4.7%	0.0%	0.0%
34	883.7	1.597	357.2	0.0%	99.8%	0.2%	0.0%	0.0%	0.0%	0.0%	0.0%	19.8%	71.8%	6.5%	0.5%	1.2%	0.0%	0.0%	0.0%	0.0%	0.0%	0.1%
35	825.1	2.125	438.3	0.0%	99.0%	1.0%	0.0%	0.0%	0.0%	0.0%	0.0%	13.9%	46.9%	30.0%	7.7%	0.4%	0.0%	0.0%	0.6%	0.3%	0.0%	0.0%
36	803.4	2.505	492.5	0.0%	100.0%	0.0%	0.0%	0.0%	0.0%	0.0%	0.0%	11.3%	39.3%	38.5%	10.5%	0.4%	0.0%	0.0%	0.0%	0.0%	0.0%	0.0%
37	971.5	3.679	519.6	0.0%	98.3%	1.7%	0.0%	0.0%	0.0%	0.0%	0.0%	12.4%	28.0%	24.4%	25.3%	8.2%	0.3%	0.3%	0.3%	0.3%	0.3%	0.3%
38	1126.1	4.857	654.9	0.0%	83.7%	16.3%	0.0%	0.0%	0.0%	0.0%	0.0%	15.3%	36.6%	17.2%	9.8%	4.9%	3.7%	1.9%	6.7%	4.0%	0.0%	0.0%
39	139.7	1.338	45.10	0.0%	99.6%	0.4%	0.0%	0.0%	0.0%	0.0%	0.0%	2.3%	3.1%	4.8%	76.2%	13.3%	0.1%	0.1%	0.1%	0.1%	0.1%	0.1%
40	690.8	1.675	343.4	0.0%	98.9%	1.1%	0.0%	0.0%	0.0%	0.0%	0.0%	13.1%	62.9%	19.6%	2.6%	0.8%	0.0%	0.0%	0.9%	0.2%	0.0%	0.0%
41	651.6	2.119	272.8	0.0%	99.2%	0.8%	0.0%	0.0%	0.0%	0.0%	0.0%	6.1%	20.4%	46.4%	25.6%	0.6%	0.0%	0.1%	0.4%	0.3%	0.0%	0.0%
42	419.5	1.822	210.6	0.0%	100.0%	0.0%	0.0%	0.0%	0.0%	0.0%	0.0%	1.2%	19.2%	56.7%	22.7%	0.2%	0.0%	0.0%	0.0%	0.0%	0.0%	0.0%
43	155.6	1.543	73.01	0.0%	100.0%	0.0%	0.0%	0.0%	0.0%	0.0%	0.0%	0.5%	1.7%	9.1%	73.6%	15.1%	0.0%	0.0%	0.0%	0.0%	0.0%	0.0%
44	339.7	1.925	130.7	0.0%	100.0%	0.0%	0.0%	0.0%	0.0%	0.0%	0.0%	1.3%	7.0%	20.0%	59.1%	12.6%	0.0%	0.0%	0.0%	0.0%	0.0%	0.0%
45	169.4	1.428	72.60	0.0%	100.0%	0.0%	0.0%	0.0%	0.0%	0.0%	0.0%	0.1%	0.4%	19.5%	76.0%	3.8%	0.0%	0.0%	0.0%	0.0%	0.0%	0.0%
46	92.47	1.298	40.98	0.0%	99.1%	0.9%	0.0%	0.0%	0.0%	0.0%	0.0%	0.0%	0.2%	1.1%	91.8%	6.0%	0.1%	0.1%	0.1%	0.1%	0.1%	0.1%
47	270.2	1.678	99.78	0.0%	100.0%	0.0%	0.0%	0.0%	0.0%	0.0%	0.0%	2.3%	4.1%	17.4%	68.4%	7.7%	0.0%	0.0%	0.0%	0.0%	0.0%	0.0%
49	636.4	1.504	326.8	0.0%	96.6%	3.4%	0.0%	0.0%	0.0%	0.0%	0.0%	22.5%	68.3%	4.8%	0.6%	0.6%	0.5%	0.5%	1.6%	0.8%	0.0%	0.0%
56	972.9	3.246	510.6	0.0%	99.8%	0.2%	0.0%	0.0%	0.0%	0.0%	0.0%	13.6%	27.2%	28.3%	29.2%	1.3%	0.0%	0.0%	0.0%	0.0%	0.0%	0.0%
57	1060.5	2.469	544.3	0.0%	100.0%	0.0%	0.0%	0.0%	0.0%	0.0%	0.0%	20.0%	40.2%	30.5%	8.5%	0.7%	0.0%	0.0%	0.0%	0.0%	0.0%	0.0%
58	262.4	1.504	115.5	0.0%	100.0%	0.0%	0.0%	0.0%	0.0%	0.0%	0.0%	0.0%	5.0%	63.6%	30.5%	0.9%	0.0%	0.0%	0.0%	0.0%	0.0%	0.0%
59	878.1	7.507	365.8	0.0%	73.8%	26.2%	0.0%	0.0%	0.0%	0.0%	0.0%	6.7%	16.8%	9.3%	26.8%	14.2%	7.4%	4.5%	9.0%	5.3%	0.0%	0.0%
61	1029.0	1.948	512.9	0.0%	100.0%	0.0%	0.0%	0.0%	0.0%	0.0%	0.0%	27.4%	54.4%	18.2%	0.1%	0.0%	0.0%	0.0%	0.0%	0.0%	0.0%	0.0%
63	786.8	1.597	411.0	0.0%	98.3%	1.7%	0.0%	0.0%	0.0%	0.0%	0.0%	35.7%	56.5%	4.0%	1.2%	0.9%	0.1%	0.4%	0.7%	0.4%	0.0%	0.0%
64	581.7	1.606	300.3	0.0%	100.0%	0.0%	0.0%	0.0%	0.0%	0.0%	0.0%	9.1%	65.2%	25.6%	0.2%	0.0%	0.0%	0.0%	0.0%	0.0%	0.0%	0.0%
65	710.4	1.664	367.3	0.0%	97.2%	2.8%	0.0%	0.0%	0.0%	0.0%	0.0%	18.4%	63.2%	14.1%	0.9%	0.6%	0.3%	0.6%	1.2%	0.7%	0.0%	0.0%
66	880.2	2.015	562.3	0.0%	99.4%	0.6%	0.0%	0.0%	0.0%	0.0%	0.0%	37.2%	44.5%	16.0%	1.4%	0.5%	0.1%	0.1%	0.1%	0.1%	0.1%	0.1%
67	1084.2	2.222	597.9	0.0%	100.0%	0.0%	0.0%	0.0%	0.0%	0.0%	0.0%	28.9%	44.6%	26.4%	0.1%	0.0%	0.0%	0.0%	0.0%	0.0%	0.0%	0.0%
68	432.0	1.434	201.7	0.0%	100.0%	0.0%	0.0%	0.0%	0.0%	0.0%	0.0%	2.5%	66.7%	30.7%	0.2%	0.0%	0.0%	0.0%	0.0%	0.0%	0.0%	0.0%

APPENDIX E- RADIOCARBON DATING RESULTS FROM WAIKATO UNIVERSITY LABORATORY

Code	**Wk**	**dC13**	**% Modern**	**Result**
HR2/265-279	10904	-26.8 ± 0.2	87.9 ± 1.1	1035 ± 105 BP
HR4/80-95	10905	-0.4 ± 0.2	74.4 ± 0.7	2378 ± 73 BP

APPENDIX F - GEOMORPHOLOGICAL MAP OF THE HAUGHTON RIVER ESTUARY

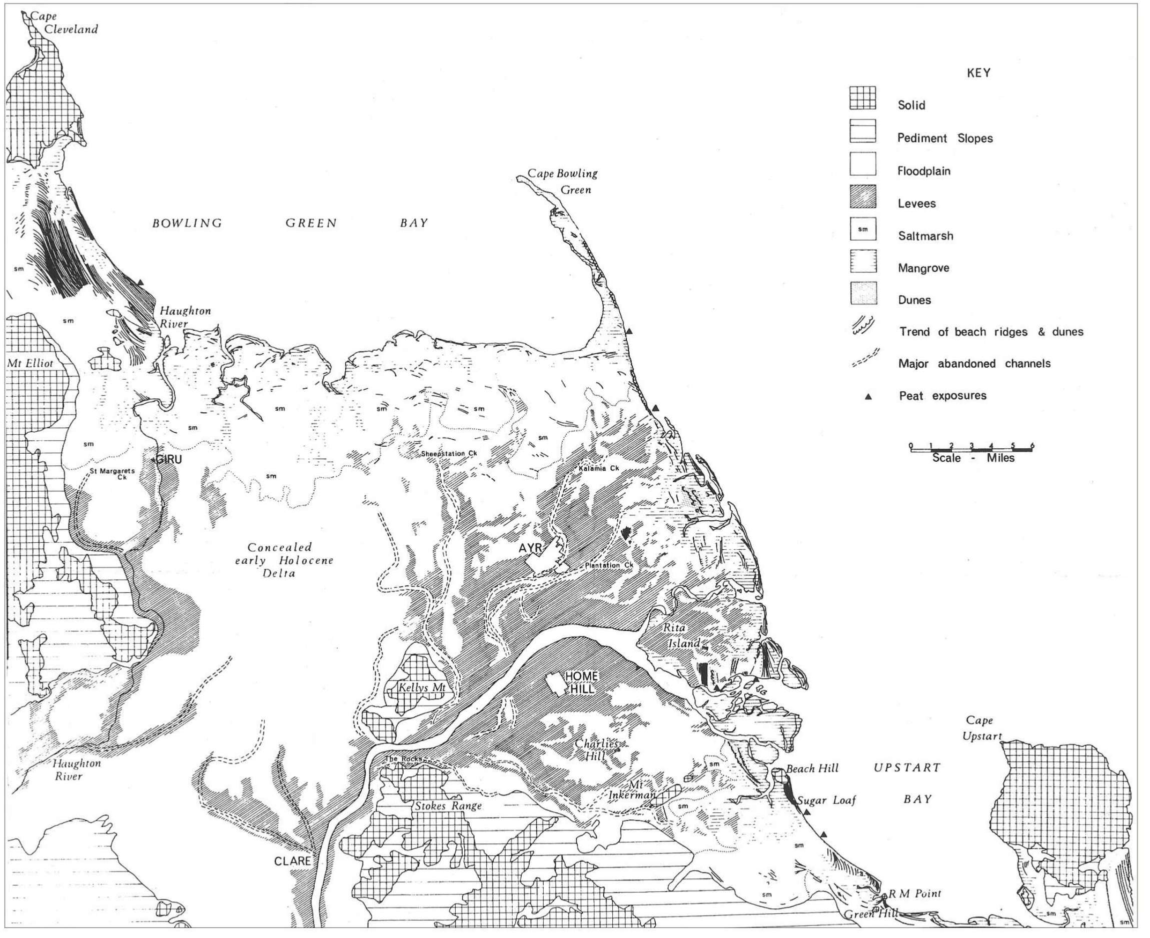

The geomorphology of the Haughton River within the Burdekin Delta from Hopley, 1970a.

APPENDIX G - GEOMORPHOLOGICAL MAP OF THE ELLIOT RIVER ESTUARY

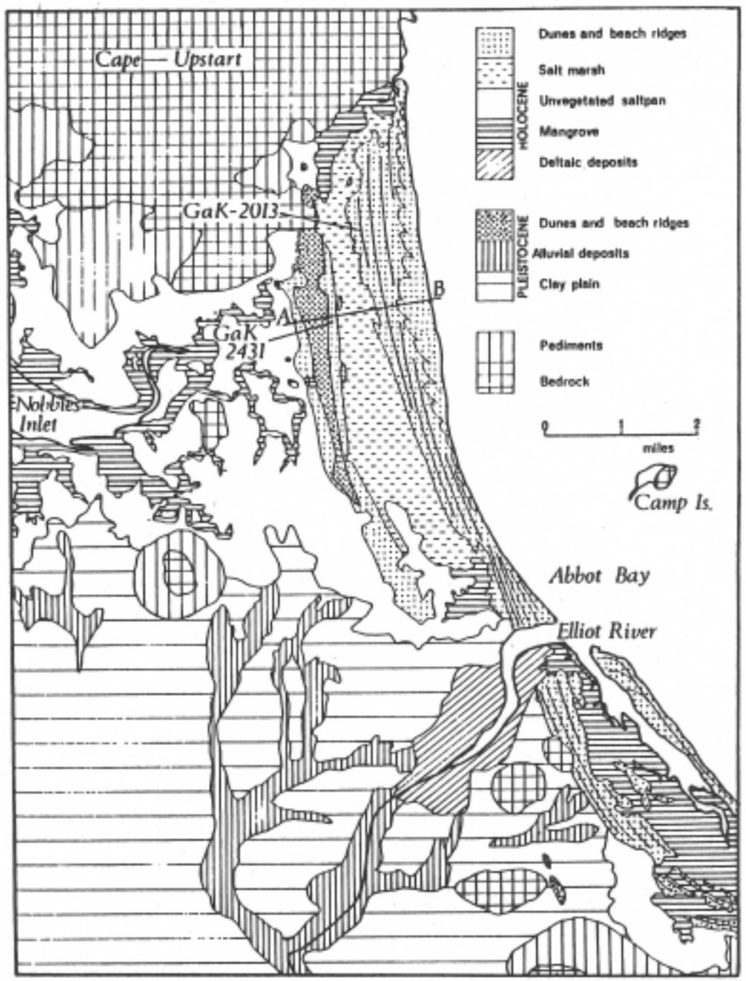

The geomorphology of the Elliot River and surrounding coast from Hopley, 1970b.

APPENDIX H - GEOMORPHOLOGICAL MAP OF THE BLACK RIVER DELTA

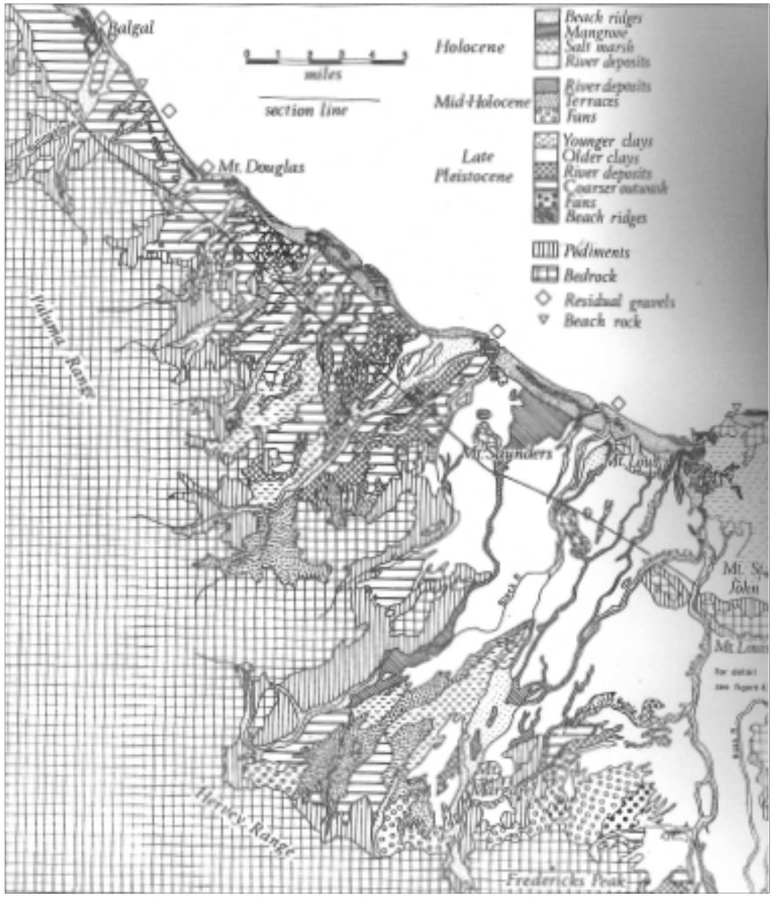

The geomorphology of the Black River Delta and surrounding coast from Hopley, 1970a.